

**Root Water Uptake Under Non-Uniform Transient Salinity
and Water Stress**

Promotor: dr. ir. R.A. Feddes
Hoogleraar in de bodemnatuurkunde, agrohydrologie en
grondwaterbeheer

Copromotor: dr. ir. C. Dirksen
Universitair hoofddocent, departement omgevingswetenschappen

1999-03-05

Root Water Uptake Under Non-Uniform Transient Salinity and Water Stress

Mehdi Homaei

Proefschrift
ter verkrijging van de graad van doctor
op gezag van de rector magnificus
van de Landbouwniversiteit Wageningen,
Dr. C.M. Karssen,
in het openbaar te verdedigen
op vrijdag 5 maart 1999
des namiddags te vier uur in de Aula

The research reported in this dissertation was funded by the Department of Soil Science, Tarbiat Modarres University, Ministry of Higher Education, Tehran, Iran, as a full Ph.D. scholarship.

Mehdi Homaei, 1999

Root water uptake under non-uniform transient salinity and water stress / Homaei, M.
Ph.D. Thesis, Wageningen Agricultural University, -With references - with summaries in English and Dutch.

ISBN 90-5808-022-6

BIBLIOTHEEK
LANDBOUWUNIVERSITEIT
WAGENINGEN

NN08201, 2582

Propositions

1. The macroscopic root water uptake approach is as yet the most feasible and reliable for quantifying the sink term.

This thesis

2. All existing salinity and water stress reduction functions will lead to about the same results if the input parameter values are specified satisfactorily.

This thesis

3. The reduction functions are most sensitive to evaporative demand, and after that to the threshold values.

This thesis

4. The effect of combined water and salinity stress on root water uptake over a large range of stress conditions is neither additive nor multiplicative.

This thesis

5. Under water stress conditions, root water uptake during the night should be included in simulation models.

This thesis

6. Simulation models will not be able to yield satisfactory results as long as water compensation phenomena are not adequately accounted for.

This thesis

7. Our knowledge increases proportional to the diameter of a circle, the questions increase proportional to its periphery.

An old Iranian saying

8. People forget how fast you did a job, but they remember how well you did it.

Howard W. Newton

9. Iran is a country of many resources. The sharp decrease in oil prices provides a golden opportunity to base the country's development on non-oil products.

10. Most saline and sodic soils in Iran occur where there is enough water of good quality. While this water is considered as the main opportunity to improve these soils, any reclamation project must consider the overall environmental impacts.

11. The Dutch experience to use bicycles must be developed in other countries if we are serious to minimize the global warming.

Abstract

Homaei, M. **Root Water Uptake Under Nonuniform Transient Salinity and Water Stress**. Ph.D. thesis, Department of Environmental Sciences, Wageningen University and Research Center, Wageningen, The Netherlands.

The study described in this thesis focuses on the quantitative understanding of water uptake by roots under separate and combined salinity and water stresses. The major difficulty in solving *Richards'* equation stems from the lack of a sink term function that adequately describes root water uptake. From the existing *microscopic* and *macroscopic* sink term functions, the empirical macroscopic approach was chosen because it requires the least number of parameters whose values can readily be determined. All existing reduction functions as well as those newly developed in this study are used in the macroscopic model and tested against experimental data. The experimentally obtained data are used to derive the parameter values needed for the simulation model HYSWASOR. The experiments cover root water uptake by alfalfa under salinity stress, water stress, and combined salinity and water stress. This order is followed with the analysis of the data and the simulation.

Under *salinity stress*, both experimental and simulated results indicate that the well-known linear crop response function can be used as a reduction function. The parameter values available in the literature for different reduction functions cannot provide acceptable agreement with the experimental data. When experimentally derived parameters are used in the simulation model, the agreement becomes much closer, but calibration is still needed. The parameter values obtained by calibration differ slightly from the experiments, because the experimentally derived parameter values are based upon mean soil solution salinity. Both experimental and simulation results indicate that different salinity reduction functions can provide almost the same results if the parameter values are well specified. For practical use the linear reduction function with the least number of parameters appears to be adequate.

Under *water stress*, all existing reduction functions as well as the one developed in this study are tested on the experimental data. Since the trend of the experimental relative transpiration versus mean soil water pressure head is nonlinear, the linear reduction function cannot fit the data. The existing nonlinear reduction functions can fit only half of the data range satisfactorily. The best agreement is obtained with the *newly developed nonlinear two-threshold reduction function*. The parameter values obtained by calibration differ only slightly from those of the experiments. Soil water pressure head heterogeneity over the root zone does not play an important role in water uptake. The roots appear to take up water from the relatively wetter parts of the root zone to compensate for the water deficit in the drier parts. On the first day after irrigation both relative transpiration and relative leaf water head are almost the same for the stressed and non-stressed plants. While the simulated transpiration agrees closely with the experimental data, the main reason for the discrepancy between the simulated and actual water contents appears to be water uptake during the night.

Under *combined water and salinity stress*, the *additive* and *multiplicative* reduction functions are first tested against the experimental data and then inserted in the simulation model. A new combination reduction function is introduced that differs conceptually from the additive and multiplicative functions. Both the experimental and simulated results show that the newly proposed model fits the data best, while the worst results are obtained with the simple additive model.

Key-words: Additive, Alfalfa, HYSWASOR, leaf water potential, macroscopic root water uptake functions, multiplicative, osmotic head, pressure head, reduction functions, Richards' equation, salinity stress, simulation, sink term, transpiration, water stress.

Acknowledgements

This study was conducted under the auspices of a scholarship awarded by the Department of Soil Science, Tarbiat Modarres University, Tehran, Iran. I appreciate Prof. M. J. Malakouti whose help provided me the opportunity to go abroad for obtaining my Ph.D. degree. I acknowledge my indebtedness to Prof. M. Bybordi, for introducing me to my promotor Prof. R. A. Feddes so that I could pursue my study in Wageningen.

The study reported here would never have materialized without the contribution of many people to whom I have the pleasure of expressing my appreciation and gratitude.

First and foremost, my deepest gratefulness is due to my promotor, Prof. R. A. Feddes whose excellent guidance, constructive criticism and regular lengthy discussions have been invaluable to me. His continual willingness during the last four years to listen, discuss and render critical judgments and also to help my family have been of great value to me.

I acknowledge my indebtedness to my co-promotor, Dr. C. Dirksen, for his endless help with designing and establishing the experimental setup, for his valuable guidance, daily discussions, critical reading and comments on the drafts of the thesis, suggestions, and editing the English. I appreciate him for his scientific help that I got from him at any time.

I like to express my special gratitude to Ir. J. C. van Dam for his valuable contribution in all stages of this study, for his help and constructive suggestions. Furthermore, he became my best Dutch friend and together with his family he created me a pleasant atmosphere in Wageningen. I am also grateful to Ir. P. Koorevaar for his excellent guidance in familiarizing me with the HYSWASOR program and his efficient discussions on the related subject.

During the last four years I had the opportunity to discuss my results with several colleagues to whom my especial gratitude is expressed. Dr. S. M. Hassanizadeh, Prof. A. Leijnse, Dr. J. W. van Hoorn, Prof. P. A. C. Raats, Prof. W. H. Van der Molen, Prof. J. Goudriaan, Dr. P. Kabat, Dr. P. A. Leffelaar, Ir. J. G. Wesseling and Ir. R. J. Oosterbaan for their valuable comments and suggestions. Prof. M. Bybordi for visiting the experimental set up, reading the proposal, his comments and suggestions. I am especially grateful to Ir. P. M. W. Warmerdam for his kind helps regarding financial and administrative matters.

Establishment of the experimental setup and growing of healthy plants was impossible without the help of many people to whom I express my thankfulness. Dr. B. Deinum for his continual supervision on plant growing and keeping them in a healthy state, and for his critical reading of the plant related material in the thesis, Dr. W. G. Keltjens for his supervision on fertilizer applications, Dr. M. Nassiri for his help with the plant seeding, Mr. J. Nelemans for chemical analysis of drainage water, Mr. J. C. F. Romelingh, Mr. J. Schuurman, and Mr. H. T. H. Jansen for fabricating the experimental setup. Ing. G. D. Abeele for his frank and endless help on the

electronical problems related to the automated TDR, Ing. R. Dijkma for his help on salinity sensor calibration and helping with the suction pump, Mr. W. J. Ackerman for his help during the soil packing, Mr. H. F. Gertsen for carefully transporting the experimental set up, Mr. G. J. Veerman and Dr. J. H. M. Wosten for their help and assistance to measure the soil hydraulic functions, Mr. A. Van Ommeren and Mr. G. H. Van Dolum for their assistance in the greenhouse, Dr. R. J. Lascano for his quick supply of some parts of his Ph.D. thesis.

My special gratitude is expressed to my Iranian friends Dr. F. Raiesi Gahrooe, Dr. M. Nassiri, Ir. M. Farahpour, and Dr. M. Mesbah, who created a pleasant and friendly atmosphere in Wageningen. Thanks to all of them and their families for helping my family during this period. Also to Ing. R. Dijkma, Ir. E. D. Wietsma and Dr. F. Raiesi Gahrooe for their help at the beginning of my stay in Holland.

Many thanks are due to the secretarial section of the Department, Mrs. H. Van Werven, Mrs. H. L. M. Sijlmans and Mrs. J. M. H. Hofs for their pleasant helps.

During four years I enjoyed the friendly atmosphere in the Department of Water Resources. I like to acknowledge Drs. P. Torfs for his assistance in mathematical issues, Mr. H. Jochems and Ing. G. Bier for computer related matters, Ing. A. Dommerholt for making photographs of the experimental set up, Mr. R. Van Genderen for his quickly assistance in providing books and articles, Ir. A. Sarwar Qureshi, Dr. M. Kuper, Mr. R. K. Jhorar and Mr. J. A. S. Louzada for being pleasant roommates at the Department.

I express my appreciation to my parents and my parents-in-law for supporting my family morally and financially. I could not have attained my desires without their kindness and help. I always be indebted to my brother Ali for his numerous administrative efforts in Tehran.

It is hardly possible to find the appropriate words to express my gratefulness to my wife and my daughter. I am deeply indebted to them for the time I did not spend with them, particularly during the difficult months that I was in the greenhouse from the very early morning until late evening and my wife managed to bring our child in the greenhouse to see me every afternoon. I also express my appreciation to my wife for the period of time she helped me in making some measurements.

... and from water we create everything live

The Quran

CONTENTS

1. Salinity and water stress and plant growth		
1.1	Introduction	1
1.2	Crop response to salinity stress	3
1.3	Crop response to water stress	6
1.4	Crop response to joint salinity and water stress	9
1.5	Salinity and water stress and alfalfa growth	10
1.6	Salinity and sodicity and soil physical properties	12
1.7	Outline of the thesis	14
2. Models for root water uptake under salinity and water stress		
2.1	Introduction	17
2.2	Water movement and solute transport in root zone	18
	2.2.1 Water movement	18
	2.2.2 Solute transport	20
2.3	Root water uptake models	21
	2.3.1 Microscopic models	23
	2.3.2 Macroscopic models	25
2.4	Root water uptake models for salinity stress	31
2.5	Root water uptake models for joint water and salinity stress	33
2.6	Numerical simulation model HYSWASOR	37
2.7	Summary	38
3. Physical experiments		
3.1	Introduction	41
3.2	Experimental setup	43
3.3	Experimental phases	43
3.4	Soil columns	45
3.5	Soil packing	46
3.6	Seeding	47
3.7	Greenhouse conditions	48
3.8	Water application	49
3.9	Fertilizer application	49
3.10	Measurements	49
	3.10.1 Soil water content and bulk electrical conductivity (TDR)	50
	3.10.2 Soil water pressure head	52
	3.10.3 Soil hydraulic functions	53
	3.10.4 Leaf water potential	55
	3.10.5 Soil solution salinity	56
	3.10.6 Transpiration	56
4. Root water uptake under nonuniform transient salinity stress		
4.1	Introduction	57
4.2	Materials and methods	57
4.3	Experimental data	58
4.4	Salt heterogeneity and relative root water uptake	66
4.5	Test of theoretical reduction functions against experimental data	70

4.5.1	Comparison of conceptual soil salinity reduction functions with experimental data	71
4.5.2	A nonlinear two-threshold reduction function for salinity stress	75
4.5.3	Leaf water potentials for nonuniform soil solution salinities	77
4.6	Simulation with HYSWASOR	77
4.6.1	Calibration	79
4.6.2	Comparison of experimental and simulated actual transpiration for different soil solution salinities	81
4.6.3	Quantitative comparison of experimental and simulated actual transpiration	83
4.6.4	Comparison of experimental and simulated water content and salinity distributions	88
4.7	Summary and conclusions	91
5. Root water uptake under nonuniform transient water stress		
5.1	Introduction	93
5.2	Materials and methods	94
5.3	Experimental data	94
5.4	Test of theoretical reduction functions against experimental data	100
5.5	Simulation with HYSWASOR	106
5.5.1	Calibration	107
5.5.2	Comparison of experimental and simulated water content distributions	107
5.5.3	Experimental and simulated actual transpirations for different soil water pressure heads	108
5.5.4	Quantitative comparison of experimental and simulated actual transpiration	112
5.6	Summary and conclusions	114
6. Root water uptake under joint nonuniform transient salinity and water stress		
6.1	Introduction	115
6.2	Materials and methods	116
6.3	Experimental data	116
6.4	Test of theoretical reduction functions against experimental data	123
6.4.1	Theoretical concepts	125
6.4.2	Comparison of separate stress and combined stress data	128
6.4.3	Application of reduction functions to mean soil solution osmotic and pressure heads	129
6.5	Simulation with HYSWASOR	130
6.5.1	Quantitative comparison of experimental and simulated actual transpiration	137
6.6	Summary and conclusions	137
Summary		147
Samenvatting		151
References		157
List of main symbols		171

1. Salinity and water stress and plant growth

1.1. Introduction

Water scarcity and soil salinity are two important limitations for agricultural production in the arid and semi-arid regions. Not only an overall shortage of water resources, but also a poor distribution of precipitation may cause water shortage, even in the winters. Also, the annual precipitation differs significantly from one year to another, causing many difficulties for farmers as well as water managers. The term *drought* or water shortage means a period without appreciable precipitation, during which the soil water content is reduced to such extent that plants suffer from lack of water. Dryness of soil is usually coupled with high evaporation caused by a high level of radiation and high dryness of the air. On a large scale, dryness results from the combination of low precipitation and high evaporation.

In the arid and semi-arid regions, the annual evaporation exceeds total annual precipitation. For instance, in some parts of Iran (*Khuzestan Plain*) the average annual precipitation is about 250 mm, while the annual potential evaporation is about 4000 mm (*Ghassemi, 1995*). About one third of the earth's continental area has a rain deficit, and half of this (about 12 percent of the land area) is so dry that annual precipitation is less than 250 mm, not even a quarter of the potential evaporation (*Larcher, 1995*). In these regions, irrigation is the only reliable way to assure agricultural production. Unfortunately, much of the water available in such regions is brackish, depositing salts in the root zone after each irrigation.

The soil solution salinity increases as water evaporates into the air and plants extract water. Therefore, permanent irrigation with water of relatively good quality still causes excess soluble salts in soils. Accumulation of excess salts in the root zone results in partial or complete loss of soil productivity. Soil salinity is also a serious problem in areas where groundwater of high salt content is used for irrigation. All irrigation waters contain hundreds of parts per million (ppm) of dissolved salts, as compared with 10 ppm in rainwater. In irrigated lands, the concentration and composition of the soil solution are derived from the salinity of irrigation water. The concentration of the soil solution is always greater than that of the irrigation water. Depending on the composition of these soluble salts, the concentrated salts may cause an increase of absorbed sodium, which affects the soil physical properties diversely. Even in humid areas, salinity is a hazard when irrigating with brackish water or treated sewage effluent, or because of sea water intrusion. Recently, interests in

maintenance of the environment, preservation of natural resources, and an awareness toward human health and nutrition have placed new attention on soil and water quality standards (Ghassemi, 1995). Soil is one of the major components of the environment. Soil salinization due to changing agricultural production systems is presently considered a serious environmental hazard and threatens to be even more so in the future. The future need for food will undoubtedly prompt more widespread use of saline water for irrigation. Not only will this water have a higher salinity than much of the irrigation water used in the past, but also the quantity of water available will be less because of the use and degradation by non-agricultural enterprises. Management of these poor quality waters will be more difficult and extensive investigations should be conducted in this regard.

Soil is considered saline when the solute concentration in the water phase causes reduction in crop production. Thus, soil salinity is a plant-dependent concept. For example, an electrical conductivity of the saturated soil extract EC_e of 5 dS/m in the root zone is saline for alfalfa, because crop yields start to decline at about 2.0 dS/m, but for barley it is not saline because its yield starts to decrease at about 6.0 dS/m. Salinity can be defined as the concentration of soluble salts present in water and soil on unit volume or weight basis. The major soluble salts causing salinity are the cations Ca, Mg, Na, and K and the anions Cl, SO_4 , CO_3 , and NO_3 .

During irrigation intervals several mechanisms are involved in the dynamic changes of soil solution salinity. Root water uptake and evaporation from the soil surface concentrate the soil solution and decrease the osmotic potential. The soluble salts in the root zone are left behind at the evaporation sites and the major fraction of dissolved salts is also excluded from water taken up by the roots. The dynamics of solute accumulation due to soil evaporation and root water uptake differs in systems depending on the amount of drainage. If the amount of water from irrigation and rainfall is less than soil evaporation and plant transpiration (arid or semi-arid regions), the soil water deficit is first met by extraction from soil water storage. As the stored soil water is used up and the soil dries, the crop becomes water-stressed, hence soil evaporation and transpiration will be reduced, and salt stored in the root zone concentrates in the remaining volume of water. This increased concentration causes plant osmotic stress, further reducing transpiration. This reduction continues until the plant dies or until water is added to the soil profile and drainage carries salt out of the root zone. In the presence of a groundwater table, deficiencies in irrigation and rainfall may be compensated by upward flow from the groundwater. This situation, however, can not remain indefinitely. Finally, soil salinity will reduce root water uptake to the point that the plant dies.

This chapter deals with some aspects of plant behavior under salinity stress and water stress. In the literature, the plant responses to these stresses are discussed in several ways with different terms. In the physiologically oriented publications, *plant growth* and *yield* are common terms, while in the literature dealing quantitatively with water and salinity, the terms *relative yield*, *crop production functions*, *consumptive use*, *evapotranspiration* and *relative transpiration* are used extensively. The linear relation between the *relative yield* and *relative transpiration* as found by *De Wit* (1958) is generally accepted and is still frequently used in experimental studies. Indeed, any kind of stress on plants will eventually influence the transpiration as well as the *root water uptake*. Since the main emphasis of this research is on root water uptake under salinity and/or water stress, the linear relationship between relative yield and transpiration is followed.

In the following review the concepts of plant response to these stresses, whether considered as yield or growth, can eventually be related to *root water uptake*. In this chapter, after a brief review of plant responses to the separate salinity and water stress, some information on the plant response to joint salinity and water stresses is given. Alfalfa was used in the experimental part of this study, hence, a brief review of alfalfa responses to these stresses is also given. Since salinity and sodicity have a great impact on water and salt movement in the root zone, the soil physical properties under such circumstances are also reviewed.

1.2. Crop response to salinity stress

The adverse effects of salts on plants are generally divided into two categories. The first and most important one is the total salt or osmotic effect on the ability of the plant to take up water from the soil solution. Crop growth reduction due to salinity is generally related to the soil solution osmotic potential of the root zone. All soluble salts contribute to the osmotic effect. When salt is dissolved in water, the potential energy of the water is lowered and the plant must spend more energy to take up water from the same soil water content. The second category consists of specific ion effects, because an excess of specific ions may be toxic to various plant physiological processes. In contrast to the osmotic effect, investigations on specific ion effects are limited to few studies as documented by *Maas* (1990) for several crops and by *Smith* (1994) for alfalfa.

The predominant influence of salinity stress on plants is suppression of root water uptake and growth. This suppression is typically a nonspecific salt effect, depending more on osmotic stress created by total concentration of soluble salts than on the level of specific solutes. Plants under salinity stress show some typical symptoms. Bare spots, poor spotty stands, and severely stunted plants are all signs of

serious salinity stress. Usually, moderate salt stress restricts plant growth without any injury symptoms. Salt-affected plants are stunted in height, have smaller leaves and may have a darker blue-green color than normal plants. Chlorosis, the yellowing or blanching of green plant parts, is not a typical characteristic of salt-affected plants but it appears in many plants as a symptom. Wilting is not a regular characteristic of plants under salinity stress because this typically occurs when water availability decreases rather abruptly. Under salinity stress (but no water stress), moderate soil water potentials are always present and soil water pressure head changes are usually gradual. Thus, plants are hardened by continual salinity stress and are less inclined to exhibit abrupt changes in turgor (*Hoffman, 1981*).

The root zone of all soils naturally contains a mixture of soluble salts. Root water uptake will be reduced when the concentration of soluble salts exceeds the threshold value of the plant. Excess salinity reduces root water uptake, primarily because it increases the energy that the plant must expend to extract water from the soil and make the biochemical adjustment necessary to survive. Actual response of plants to salinity varies with many factors, including climate, soil conditions, water table elevation, agronomic practices, irrigation management, crop variety, stage of growth, and salt composition. Salt sensitivity of the plants changes considerably during the development stages. Three developmental stages can be distinguished with respect to salt tolerance or salt sensitivity: germination, vegetative growth and reproductive growth. The separation between growth stage and duration of salinization is not always clear even in the experimental studies to evaluate the growth stage effect (*Maas and Hoffman, 1977*). Most plants are relatively salt-tolerant during germination and more sensitive during seedling emergence and early stage of seedling growth (*Rhoades, 1990*). A more complex response pattern emerges for germination. However, crops such as corn were found to be more tolerant at germination than at later growth stages, whereas crops like sugarbeet are more salt-sensitive at germination (*Meiri, 1984, Shannon, 1997*). There is much evidence that vegetative growth is particularly salt-sensitive (*Lauchli and Epstein, 1990; Shannon, 1997*). Many crops may be more salt-sensitive at early rather than later growth stages (*Meiri, 1984, Shannon, 1997*). Root growth is often less affected by salinity than shoot growth. In the shoot, reduction of leaf area is then most prominent. Reduced leaf growth may indirectly increase total solute concentration in the leaves, which contributes to osmotic adjustment unless solutes build up toxic concentrations, first in the oldest and then in the younger leaves.

When salinity is a hazard, an effective use of soil and water resources dictates the selection of relatively salt-tolerant plants. Thus, quantifying the yield response to different levels of salinity is of great concern, and hence many field and laboratory

experiments have been conducted for many plant species. The effect of salinity on crop production is determined by crop salt tolerance. Crop salt tolerance can be defined as the ability of plants to survive and produce economic yields under adverse conditions caused by soil salinity. Salt tolerance of agricultural crops is typically expressed in terms of yield decreases associated with soil salinity increases, or as relative crop yield on saline versus nonsaline soils (*Bresler et al.* 1982, *Shannon*, 1997).

The quantitative response of plants to salinity stress is usually described as decreasing yields with increasing electrical conductivity of the soil solution EC_{ss} . *Brown and Hayward* (1956), *Lunin et al.* (1963), *Shalhevet et al.* (1969), and *Maas and Hoffman* (1977) suggested that the reduction in crop yield due to salinity can be linearly related to the electrical conductivity of the soil solution. Until 1977, yield response functions to soil salinity have been either eye-fitted to the data or obtained with linear regression techniques. In an attempt to fit a generalized response function to all salt tolerance data, *Maas and Hoffman* (1977) published a comprehensive analysis based upon an extensive review of the literature. In general, they found that crops tolerate increases in soil salinity up to a threshold value, above which yields show an approximately linear decrease with increasing salt concentration. The analysis of each experiment was based upon a linear least-squares equation for values beyond the threshold salinity value. The response function of *Maas and Hoffman* can be written as:

$$\frac{Y}{Y_m} = 100 - a(EC_e - EC_e^*) \quad EC_e > EC_e^* \quad 1.1$$

where EC_e (dS/m) is the electrical conductivity of the soil saturation extract; EC_e^* (dS/m) is the threshold value of salinity at which relative yield begins to decrease; and a (m/dS) is the slope which indicates the percent yield decrease per unit salinity increase. This equation is valid only when EC_e is higher than the threshold value and less than the value resulting in zero yield.

Maas and Hoffman (1977) and *Maas* (1986, 1990) collected and analyzed data for many crops, and determined the slopes and threshold values. This information is valuable, but the most important limitation of these data is that the data were obtained under uniform salt distributions over the root zone, small changes with time and unrestricted water supply by flood irrigation. Furthermore, Eq. 1.1 assumes that the crop responds primarily to the osmotic potential of the soil solution and that the effect of specific ions or toxicity can be ignored. These tolerance values can change greatly if different water salinity levels are applied at different growth stages.

Equation 1.1 is valid when the irrigation water quantity is considerably in excess of the sum of soil evaporation and plant transpiration, i.e. actual evapotranspiration ET_a . *Bresler et al. (1982)* showed this to be true when the ratio of quantity of water and maximum ET is larger than 1.5. When irrigation water supply is limited to a leaching fraction (LF) of less than 0.3, Eq. 1.1 will not be accurate. Equation 1.1 holds under ideal conditions, but can hardly meet the realities in the field. It is however still useful for approximate purposes.

The main purpose of this dissertation is to find an alternative for Eq. 1.1 that describes the effect of salinity on transpiration under transient, nonuniform and water limited conditions.

1.3. Crop response to water stress

Plant and water relations can be discussed from several points of view. In the agronomic literature, this relation is widely discussed from morphological, physiological and ontogenic points of view, hence main attention is paid to the effect of water deficit on the physiology and morphology of plants. *Begg and Turner (1976)*, *Turner (1986)*, *Kramer and Boyer (1995)*, *Larcher (1995)*, *Boyer (1996)* and *Turner (1997)* extensively discussed and summarized the available literature from agronomic points of view. In this section a summary of these publications is given, followed by a quantitative description of water and plant relations related to the scope of the present study.

Plants consume water essentially for the processes of photosynthesis and transpiration, taking up water through the roots, primarily through their root hairs. Water is transported through the plant and then removed from the leaf surface via transpiration. Transpiration is controlled by the stomatal aperture and by the vapor pressure gradient from the leaf to the air. The amount of water required by plants for their growth depends on a number of factors including the type of plant, its growth stage, soil properties and meteorological conditions.

The demand for water is not equally spread over the growing season. At the beginning of the season, consumptive use is low. It increases as the plant foliage develops and the days become warmer, peaks during flowering and fruit formation and rapidly decreases towards the end of the growing season. The evaluation of water requirements of crops to achieve full production at a particular location is based on the estimation of transpiration or evapotranspiration. Evapotranspiration is an energy dependent process involving a change of water from the liquid to the vapor phase. The rate of ET is a function of the net radiation, the vapor pressure gradient, the

resistance to flow, and the ability of the soil and plant to transport water to the site of evapotranspiration.

It is generally accepted that water moves through the Soil-Plant-Atmosphere Continuum (SPAC) along a gradient of water potential from the soil through the plant to the atmosphere (Philip, 1966; Gardner *et al.*; 1975; Kramer and Boyer, 1995; Turner, 1997). The evaporation of water from the leaf provides the major driving force of water uptake by transpiring plants against the soil water pressure and gravitational potentials, and the frictional resistances in the plant pathways (Begg and Turner, 1976). Low water potentials in the transpiration pathway provide the driving force for water movement out of some tissues such as the leaf mesophyll, cortex and phloem. As a result of this loss, water deficits develop in the leaf, stem and root tissues. Thus, water stress occurs as a result of water flow driven by soil water potential differences along a pathway in which frictional resistances have to be overcome. Water stress does not only occur when the loss of water from the leaves in transpiration exceeds the supply from the roots. For a plant going into water stress, transpiration exceeds the root water uptake as water is drawn out of tissues surrounding the xylem. When the water potential of these tissues has adjusted to the water potential in the xylem, a steady state is reached in which transpiration equals root water uptake. Since the plant can only extract water from the soil when the water potential in the plant is less than that of the soil, a steady state is rarely obtained. The difference between the water potential in the plant and soil depends on the rate of root water uptake and water conducting properties of soil and plant.

Plants are most sensitive to water stress during their period of rapid development. For most plants this is the time of floral initiation, flowering, fruit, and seed development. Plant growth depends basically on continuity of cell division and cell enlargement until the characteristic form of the plant is realized. Cell division is less sensitive to water stress than cell enlargement (Kramer and Boyer, 1995). Leaf enlargement declines rapidly at leaf water potentials (*LWP*) below -2 bars and ceases at *LWP* of -7 to -9 bars (Boyer, 1996). The most important consequence of leaf enlargement decline is a marked reduction in leaf area (*LA*). A reduction in *LA* will reduce the growth rate. This has a permanent effect for which plants cannot compensate by increasing the number of leaves. Water stress can also affect *LA* through its effect of accelerating the rate of leaf senescence. Water stress increases the root/shoot ratio (Hoffman and Rawlins, 1971). There is evidence from a number of crops that at certain growth stages, especially during flowering and formation of fruit, root growth diminishes or ceases completely (Begg and Turner, 1976). By root growth reduction, the root water uptake becomes a function of soil water flow to the root surface. Since the unsaturated hydraulic conductivity at lower water contents is

very low, water stress will soon occur in plants particularly where the roots occupy a relatively small volume of soil.

The influence of water stress on plant physiology is generally attributed to stomatal behavior and photosynthesis. Since stomata act as regulators for CO₂ exchange and water loss, water stress sufficient to close stomata also depresses photosynthesis. It is generally accepted that photosynthesis reduction due to water stress arises from changes in conductance of CO₂ through the stomata (*Kramer and Boyer, 1995*). It is now generally recognized that the stomata do not respond to changes in *LWP* until a critical threshold value is reached. However, even if that threshold is not reached, a reduction in yield may occur owing to the effect of water stress on other physiological or morphological processes (*Turner, 1997*).

In irrigation design and management, the quantitative influence of water on crop production, the so-called *production functions*, are of most interest. Studies on quantitative relationships between water use and crop yield started by several researchers since the beginning of the twentieth century. The term *transpiration ratio* became common and was defined as the ratio (kg/kg) of the amount of water transpired during growth and the dry weight of plants at the time of harvest (*De Wit, 1958*). This ratio was also called the *water requirement* or *consumptive use*. The early work in this field led to the conclusion that the water requirement of plants is proportional to evaporation from a free-water surface, E_0 , and dependent on the plant species, but relatively independent of soil fertility, weather conditions, and the size of the plant (*De Wit, 1958*). *De Wit* (1958) analyzed the findings of the early investigations in an effort to further identify the factors that determine transpiration and yield under field conditions. He concluded that the relationship between yield Y and actual transpiration T_a for arid and semi-arid regions is linear in the following form:

$$Y = f \left(\frac{T_a}{E_0} \right) \quad 1.2$$

where f is a crop parameter. For a given *crop* and *year* for which f and E_0 are constants, the relationship between relative transpiration T_a/T_p and relative yield Y_a/Y_m can simply be written as:

$$\frac{Y}{Y_m} = \frac{T_a}{T_p} \quad 1.3$$

in which Y_m is the maximum yield.

In the early experiments, plants were grown in containers, covered to prevent direct evaporation from the soil surface, and the amount of transpired water was determined by weighing the container. *De Wit* (1958) concluded that this relationship is equally valid for container- and field-grown crops. The validity of *De Wit's* linear relationship in field experiments was confirmed by several researchers in different climates (*Arkerly*, 1963; *Hanks et al.*, 1969; *Stewart et al.*, 1977; *Hanks*, 1974, 1983; *Feddes*, 1971), and hence, can be used as a general relationship. Recent reviews on production functions are given by *Letty and Knapp* (1990, 1995), while world wide data have been collected and evaluated by *Doorenbos and Pruitt* (1977) and *Doorenbos and Kassam* (1979).

1.4. Crop response to joint salinity and water stresses

Both salinity and water stress reduce root water uptake. Under joint salinity and water stress the plants must spend more energy to take up water from the soil, compared with that under salinity stress only or water stress only. In irrigated soils, particularly in arid and semi-arid regions, plants are subjected to both salinity and water stress in different intensities. Evapotranspiration during an irrigation interval reduces osmotic and matric potentials of the soil solution, which in turn strongly reduce root water uptake. Under most conditions, both factors change with time and space and the effective stress will depend on the way in which the plant integrates them. Despite some progress during the last two decades, the question of how plants integrate salinity and water stress remains unsolved. Only few publications are devoted to the symptoms of plants under joint salinity and water stress with the conclusion that all the mentioned symptoms for the separate stresses can occur together. Multiple stress interactions and their impact on plants is the main subject of some publications in the field of environmental stresses. There are two contradictory concepts about stress interactions. The first is *Liebig's* law of the minimum, which states that plant growth is limited by a single stress at any one time; only after the stress limitation is relieved, another stress can influence the plant. If this were true, raising the availability of any other limiting factor would not improve plant growth because the primary limiting factor is still constraining growth. In contrast to *Liebig's* law, one can argue that plants have evolved to compensate for stress imbalances i.e. *compensatory theory* (*Bloom et al.*, 1985), and growth (or root water uptake) should be limited by all stresses simultaneously. Several important implications of the compensatory theory for plants were suggested by *Chapin et al.* (1987). First, if a plant is limited simultaneously by several resources, increases in a number of different resources could increase growth. This improves the chances that growth will be increased because any one of a number of different occurrences would enhance

growth rather than only one type of occurrence. Second, there are many evidences that when plants are limited by several limitations, increases in two or more of them has a synergetic impact on growth (*Lipscomb, 1991*).

It has been known for a long time that in the case of water and salinity stresses there exists a relation between root water uptake reduction and salinity increase. The question is whether under similar climatic conditions, this relationship is identical, additive, or multiplicative with the effect of water stress. It is known that soil water osmotic and pressure potentials are additive in lowering the free energy of the water. It is therefore assumed, that they would also be additive in their effect on transpiration through reduction of the availability of water for plants. A review of this subject and its validity is given in Chapter 2 and quantitatively discussed in Chapter 6.

Despite some obvious similarities, there are some clear differences between plant responses to salt and water stresses. One of the more important observations is the lack of wilting under salt stress at water potentials which cause wilting under water stress. *Wadleigh and Ayers (1945)* and *Sepaskhah and Boersma (1979)* reported no wilting at low osmotic potentials, whereas there was wilting at equivalent low pressure potentials. These observations led to the conclusion that *a decreasing pressure potential is more detrimental than an equivalent decrease in osmotic potential*. Furthermore, there may be a difference in the nature of the solutes that contribute to osmotic adjustment. Osmotic adjustment is a decrease in plant osmotic potential through an increase in solute content in response to a reduction in external water potential to the extent that turgor potential is maintained. Generally, poor osmotic adjustment leads to stomatal closure and turgor loss, which is soon followed by reduced gas exchange and photosynthesis (*Shannon, 1997*). The obvious difference between salinity and water stress is in leaf turgor and the growth processes that are influenced by it. For instance, *Shalhevet and Hsiao (1986)* indicated that the growth rate under water stress was half as large as under salt stress in the leaf water potential range of interest. *Meiri (1984)* indicated that soil water pressure head h had a greater influence on shoot growth and transpiration than osmotic head h_o . However, for root growth the effect of h_o was greater than that of h .

1.5. Salinity and water stress and alfalfa growth

For this study, alfalfa was selected mainly for its moderate tolerance to salinity, its tolerance to water deficit, and its fast postharvest growth. Alfalfa (*Medicago sativa L.*) was one of the first plants cultivated exclusively for use as forage and is now grown on some 35 million ha world-wide (*Smith, 1994*). Relative to other forage crops, alfalfa is frequently favored by farmers for the reasons mentioned

above, as well as its highly nutritious herbage and excellent persistence. Alfalfa also conducts symbiotic N_2 fixation in association with *Rhizobium* bacteria, resulting in a significant carryover of nitrogen in crop rotation. Salinity can limit nodule formation by reducing the population of *Rhizobium* in the soil or by impairing their ability to infect root hairs. However, the direct effect of salinity on the host plant can limit nitrogen fixation independent of the effects of salinity on the *Rhizobium* bacteria and the nodulation process (Keck *et al.*, 1984). Alfalfa may be affected by salinity throughout its growth stages. Increased soil salinity results in smaller plants and a blue-green color in the vegetation, but these effects are greatly dependent upon the timing of the stress. Three developmental stages are recognized due to salinity effects, namely germination, seedling emergence and growth, and mature plant growth from secondary stems.

Considerable research has been conducted to assess the osmotic effects of salts on germination. Smith (1994) reported about very early to recent studies that indicate that alfalfa will not germinate in solutions above 0.5% NaCl. Problems in establishing alfalfa usually start when $EC_e > 8$ dS/m. Little progress has been made in separating the specific ion and osmotic effects on alfalfa. In one study, Smith (1994) indicated that increase in exchangeable sodium percentage (ESP) from 5 to 37.4 decreased seedling establishment. Under salinity stress, alfalfa seedlings exhibit a characteristic set of plant symptoms. At low salinity level, reduced shoot growth is the only obvious evidence of osmotic effect. At higher levels of salinity, reductions in growth are accompanied by bleaching of leaflets in younger plants. This is also associated with increases in leaf and stem succulence, dark green or blue-green color of the foliage, and increases in the leaf-shoot weight ratio. Higher levels of salinity produce marginal leaf necrosis or chlorosis, which may be followed by removal of the oldest leaves. Little progress has been made in separating the effects of specific ion toxicities and osmotic effects on seedling growth for alfalfa (Smith, 1994).

Several studies (Hoffman, 1981; Keck *et al.*, 1984; Shalhevet 1984, 1993, 1994; Meiri 1984, 1992; Smith, 1994) indicate that in mature alfalfa salinity tends to depress shoot growth more than root growth. The effect of salt stress on alfalfa yield has been quantified by Maas and Hoffman (1977) for uniform salinity in the root zone. They concluded that forage yield of alfalfa decreased by about 7.3% (slope) for each dS/m increase above 2.0 dS/m (salinity threshold value) in the saturation soil extract.

In most studies with alfalfa, root zone salinity varies with depth, having low EC near the surface and much higher at the bottom of the root zone (Lonkerd *et al.*, 1979). It is frequently assumed that plants respond to the average root zone salinity under these conditions and some data collected support this idea (Shalhevet and Bernstein, 1968; Bower *et al.*, 1969; Prunty, *et al.*, 1991). This assumption is one of

the main hypotheses of *Maas and Hoffman* (1977) in deriving Eq. 1.1. Since the majority of roots of alfalfa are within the first 50 cm of the root zone, *Bernstein and Francois* (1973) concluded that alfalfa responded to a calculated mean salinity value that is controlled primarily by the salinity of the irrigation water (upper root zone salinity), and hence is less affected by deep root zone salinity. Later research suggested that alfalfa can tolerate high salinity in the lower part of the root zone (at 180 cm) by increasing water uptake from higher regions that are lower in salinity (*Shalhevet and Bernstein* 1968; *Hanks et al.*, 1977). Consequently, overall transpiration and water uptake for the entire plant remains unchanged. *Francois* (1981) reported that significant yield reduction will not occur until after salinity increased in the lower part of the root zone (50-60 cm). *Ingvalson et al.* (1976) suggested that irrigation management, especially the frequency of irrigation, could partially explain these contradictory conclusions. They reasoned that immediately after irrigation, plants would take up water primarily from the less saline upper root zone, and the lower part salinities will affect the plant later in the soil drying cycle. *Raats* (1974a) suggested that the response is determined by a kind of weighted mean salinity, in particular the uptake-weighted mean. *Dirksen* (1985) and *Dirksen et al.* (1994) collected and analyzed some data for alfalfa, which support this suggestion.

1.6. Salinity and sodicity and soil physical properties

The suitability of soils for cropping depends strongly on the permeability for water and air, and on the properties of the aggregates which control the friability of the seedbed. Poor permeability is often a major problem in irrigated lands. Besides salinity, sodicity is also an important problem in semi-arid regions. Sodicity strongly affects the soil physical properties. Sodic soils usually have poor physical properties resulting in restricted water and air movement. The soil is sodic when its *ESP* is 15 or more (*U. S. Salinity Staff*, 1954). For most soils, when the *ESP* reaches more than 15 the soil structure will be destroyed and the aggregation becomes massive.

The soluble salts affect the physical and chemical properties of the soils. Historically, the physical behavior of saline soils has been described in terms of the combined effects of *EC* and *ESP* on flocculation and soil dispersion. Many physical properties of soils are sensitive to the relative composition of exchangeable cations, which in turn depend on the concentration and composition of the soil solution in equilibrium with the solid phase. Divalent cations improve the soil physical properties such as hydraulic conductivity *K*, infiltration rate *I*, aggregate stability, and aeration. High soil solution salinity reduces the unfavorable physical effects of the adsorbed monovalent sodium ions.

The most severe adverse effect of sodium ions on the soil physical properties is on K and I . Soil hydraulic conductivity is a function of the size of the water-filled pores. Therefore, any soil solution salinity that causes a decrease in the size of these water-conducting pores has a marked effect on the soil hydraulic conductivity as well as on the infiltration rate. The size of the water conducting pores is decreased by swelling of clay particles and by dispersion of the colloidal soil material. According to the diffuse double layer theory, both swelling and particle dispersion increase as the soil solution salinity decreases and the sodium to calcium ratio (Na/Ca) increases. Saturated, as well as unsaturated soil hydraulic conductivity behaves accordingly, that is, they are higher at the more saline soil solution and decrease with the high Na/Ca ratio (Oster, *et al.* 1996).

Water flow in unsaturated soil is described well by Darcy's equation. In the Darcy-type water flow equation it is assumed that the hydraulic gradient is the only driving force that causes water flow. Because of mass movement of salt and water content fluctuations, however, dynamic changes of salt concentration may create an additional driving force due to the osmotic gradient. Also, variations in salt concentration and composition may affect the hydraulic conductivity function, $K(\theta)$, because of density, particle swelling, and dispersion (Bresler *et al.*, 1982). Thus, in applying Darcy's flow equation to a given salinity, mutual salt-water flow effects must be considered. Investigations to quantify the mutual salt-water flow effects are limited to the works of Kemper and co-workers (Kemper, 1961; Kemper and Evans, 1963; Kemper and Rollins, 1966; Kemper and van Schaik, 1966; and Porter *et al.*, 1960), providing several complicated coefficients and parameters whose values are difficult to obtain.

Irrigation and leaching of sodic soils with water having too low electrolyte concentrations to maintain flocculated conditions, cause hydraulic conductivity reductions due to clay dispersion, movement, and consequent blockage of water-conducting pores. Clay swelling and dispersion due to high sodicity and low salinity, are two mechanisms that account for changes in hydraulic properties. Swelling that occurs within a fixed soil volume reduces pore radii, thereby reducing both saturated and unsaturated hydraulic conductivities. Swelling results in aggregate breakdown or slaking, and clay particle movement, which in turn leads to blockage of conducting pores. The experimental evidence shows that aggregate dispersion occurs at lower electrolyte concentration than that required to flocculate a clay suspension (Oster *et al.*, 1996). The electrolyte concentration of the soil solution should be above the threshold value that causes dispersion or permeability decrease. The threshold concentration is the concentration in the percolating solution that would give rise to a 10 to 15 percent decrease in the relative permeability at a given sodicity level, as first introduced by Quirk and Schofield (1955). Further investigations indicated that water

with salinity less than 0.3 dS/m causes clays to swell, resulting in swelling-induced effects such as breakdown of aggregates, crusting, and reduced permeability (Bresler *et al.*, 1982; Gupta and Abrol, 1990; Oster *et al.*, 1996).

In the semi-arid regions a great part of soils are both saline and sodic. In Iran, this is due to the dominance of NaCl in these soils, which causes both salinity and sodicity. Since the solubility of NaCl in water is very high, the reclamation of such soils by leaching is relatively easy (Homaei, 1991). Often, the difficulty during improvement is the decreasing infiltration rate during leaching. To avoid this problem, the use of brackish water rather than fresh water, and/or application of gypsum is recommended (U. S. Salinity Lab. Staff, 1954; Oster *et al.*, 1996; Gupta and Abrol, 1990; Homaei, 1991). Infiltration rates are more strongly affected by low soil salinity and high exchangeable sodium levels than hydraulic conductivities because of mechanical impact and stirring action of the applied water and the freedom for soil particle movement at the soil surface (Oster *et al.* 1996). Investigations to quantify the influence of salinity and sodicity on infiltration rate are still empirical. Oster and Schroer (1979) and Kaur (1994) introduced some empirical relationships as function of salinity and sodicity of irrigation water. The relationship proposed by Oster and Schroer (1979) can be written as:

$$I = 6.8 - 1.1 SAR + 0.79 c \quad 1.4$$

in which, I is the infiltration rate in mm/h, SAR is sodium adsorption ratio of the irrigation water ($[\text{meq/lit}]^{1/2}$) in equilibrium with the solid phase of CaCO_3 at a CO_2 pressure of 0.07% based on ion activities corrected for ion pairing, and c is total cation concentration in mol/m^3 . The advantage of this type of relations is that it employs the SAR of the irrigation water rather than the ESP of the soil that is difficult and time consuming to obtain. The slopes as well as the intercept in Eq. 1.4 are only valid for the soil type and the irrigation management for which the equation was derived and must be adjusted for other soils and irrigation methods.

1.7. Outline of the thesis

The thesis deals with root water uptake under separate and joint salinity and water stress conditions. The introductory Chapter 1 presents the interactions of plants under such circumstances, particularly for alfalfa. Chapter 2 presents governing equations for water flow and solute transport and reviews the existing root water uptake models. Chapter 3 describes the experimental setup and program. Chapters 4 to 6 present the analyses of the experimental data and simulation results for salinity stress, water stress, and joint salinity and water stress, respectively.

In Chapter 2, available root water uptake models are reviewed and classified in *microscopic* and *macroscopic* groups. For the joint water and salinity stress conditions, *additive* and *multiplicative* concepts are discussed. The simulation model for hysteretic one-dimensional water flow and solute transport in the root zone, HYSWASOR, with its governing equations is introduced.

Chapter 3 gives a detailed description of the experimental setup specifically designed for growing alfalfa in the greenhouse under water and/or salinity stress conditions and making extensive measurements on soil and plant. Instrumentation and methods are described for measuring soil water content and soil bulk electrical conductivity (TDR), soil solution electrical conductivity (salinity sensors), leaf water potential (pressure chamber), and actual transpiration (weighing).

Chapter 4 deals with root water uptake under saline conditions. In the first part, experimental data are presented and analyzed based on the mean soil solution salinity. The second part reports the results with the numerical simulation model HYSWASOR. The same order of analysis is followed in Chapter 5 for water stress.

Chapter 6 deals with joint salinity and water stress. The parameter values for additive, multiplicative, and a newly proposed combination reduction function are first derived from averaged experimental data for the single stresses in the previous chapters, and then tested in the simulation model.

2. Models for root water uptake under salinity and water stress

2.1. Introduction

Study of plant roots is one of the oldest subjects in plant science, usually dealing qualitatively with several aspects of water uptake. The soil-root-stem-leaf-atmosphere water flow pathway is a major component of the hydrologic cycle. About 70 percent of the water that falls on the soil surface returns to the atmosphere through evapotranspiration. Therefore, vegetated areas constitute an important part of the hydrologic cycle. The boundary between soil and roots is a major hydrologic interface in that over 50 percent of the evapotranspiration crosses the soil-root interface. *Penman* (1970) estimated that in order to produce 1 kg fresh weight of a crop, approximately 100 kg of water must be withdrawn from the soil. Such observations led to the conclusion that an important long term aim of hydrologists should be to extend and develop their understanding of the hydrologic processes involved in the transport of water from soil, into and through plants.

Root water uptake approaches generally serve one of two purposes. Either they produce an estimate of transpired water loss for water budget models or they provide estimates of plant water status for predicting water stress. Root water extraction is a dynamic term influenced by soil, plant, and climate. Root water uptake depends on a number of factors like soil hydraulic conductivity, rooting depth, rooting density, root distribution, soil water pressure head, soil water osmotic head, evaporative demand, the presence of a groundwater table, plant resistances, growth stage of plant, etc. This indicates that an exact physical description of root water uptake is rather complicated. Despite of this, several models have been introduced to quantify the root water uptake, particularly for use in numerical simulation models.

Quantitative concepts of water transport into plants first appeared in publications of *Gradmann* (1928) and *Van den Honert* (1948). *Gradmann* (1928) was the first to suggest that an analogy could be drawn between steady electric current flow in a resistance network and steady water flow through the roots, stem, and leaves of a plant. *Van den Honert* (1948) followed this concept and stated that under steady state conditions the rate of water flow through a plant part is directly proportional to the water potential difference across that part and inversely proportional to the water flow resistance. *Philip* (1958a, b) developed the first detailed quantitative description of water transport in plant tissue, resulting in a diffusion equation. His derivation assumed that water moves primarily from vacuole to vacuole. Subsequent researchers added cell walls and plasmodesmata as possible pathway (*Molz*, 1981).

On the other hand, understanding of soil water status improved by the introduction of quantitative energy concepts of soil water by *Buckingham* (1907) and *Richards* (1931). In another development, introducing the concept of *available water* for plants, *field capacity FC* and *permanent wilting point WP*, *Veihmeyer and Hendrickson* (1927, 1931, 1955) stated that soil water is equally available for plants from *FC* to *WP*. This concept was criticized later by many researchers (*Richards*, 1928, 1960; *Slatyer*, 1957; *Van Bavel and Ahmed*, 1976). *Richards* (1928) pointed out that available water involves both the ability of the plant to take up water and the readiness with which water moves to replace the extracted water, which indicates that soil hydraulic conductivity is an important variable to take into account. Hence, from very early investigations it became clear that both soil and plant resistances are involved in root water uptake. Many investigations have been conducted later to improve and quantify the understanding of the soil-water-root system.

This chapter presents a brief review on these concepts after introducing the governing equations for water flow and solute transport in the root zone. Furthermore, root water uptake models are reviewed and classified into the so-called *microscopic* and *macroscopic* categories. Since in this study the numerical simulation model *HYSWASOR* (*Dirksen et al.*, 1993) has been used, a brief introduction to this model is also given.

2.2. Water movement and solute transport in root zone

2.2.1. Water movement

One-dimensional vertical water flow in soil is well described by *Darcy's* equation:

$$q = -K(h) \frac{\partial (h+z)}{\partial z} \quad 2.1$$

where q is the soil water flux density taken positive upward (LT^{-1}), K is soil hydraulic conductivity (LT^{-1}), h is soil water pressure head (L), and z is gravitational head, as well as the vertical coordinate (L) taken positive upward. Applying the principle of continuity and representing root water uptake as a sink term S depending on h , leads to:

$$\frac{\partial \theta}{\partial t} = -\frac{\partial q}{\partial z} - S(h) \quad 2.2$$

where θ is volumetric water content (L^3L^{-3}), t is time (T), and S is soil water extraction rate by plant roots ($\text{L}^3\text{L}^{-3}\text{T}^{-1}$). Water flow in unsaturated or partly saturated

soils is then traditionally described with *Richards'* equation (*Richards*, 1931) who was the first to combine Eqs. 2.1 and 2.2 as:

$$\frac{\partial \theta}{\partial t} = C(h) \frac{\partial h}{\partial t} = \frac{\partial}{\partial z} \left(K(h) \frac{\partial h}{\partial z} + K(h) \right) - S(h) \quad 2.3$$

where C is the differential soil water capacity (L^{-1}) which is equal to the slope $d\theta/dh$ of the soil water retention curve. Equation 2.3 may also be expressed in terms of the water content if the soil profile is homogeneous, unsaturated, and hysteresis can be neglected:

$$\frac{\partial \theta}{\partial t} = \frac{\partial}{\partial z} \left(D(\theta) \frac{\partial \theta}{\partial z} + K(\theta) \right) - S(\theta) \quad 2.4$$

where D is the soil water diffusivity (L^2T^{-1}), defined as:

$$D = K \frac{dh}{d\theta} \quad 2.5$$

The unsaturated soil hydraulic functions in the above equations are the soil water retention curve $\theta(h)$, the hydraulic conductivity function $K(h)$ or $K(\theta)$, and the soil diffusivity function $D(\theta)$. Several functions have been proposed to describe the soil water retention curve. Among those, the analytical functions of *Brooks and Corey* (1964) and *Van Genuchten* (1980) are most popular. The latter is extensively used particularly in numerical simulation models and can be written as:

$$S_e = \frac{\theta - \theta_r}{\theta_s - \theta_r} = (1 + \alpha |h|^n)^{-m} \quad 2.6$$

where θ_r and θ_s are residual and saturated water contents, respectively; and α (L^{-1}), n (-), and m (-) are shape factors. The latter can be taken equal to:

$$m = 1 - \frac{1}{n} \quad 2.7$$

The soil hydraulic conductivity function can be described by (*Mualem*, 1976; *Van Genuchten*, 1980):

$$K = K_s S_e^{1/2} [1 - (1 - S_e^{1/m})^m]^2 \quad 2.8$$

where K_s (LT^{-1}) is the saturated hydraulic conductivity.

Van Genuchten et al. (1991) developed the program *RETC* to estimate the parameter values of these equations from measured $\theta(h)$ and $K(\theta)$ data. *Wosten et al.* (1994) obtained the above mentioned parameters for more than 600 soil samples in The Netherlands (*Van Dam et al.*, 1997).

2.2.2. Solute transport

In numerical simulation models, the salt concentration as well as the soil solution salinity EC_{ss} at any given depth in the root zone is determined by either deterministic or stochastic solute transport approaches. The rate at which solutes move through the soil is determined by several transport mechanisms. The mechanisms often act simultaneously and may include such processes as *convection*, *dispersion*, *diffusion*, *adsorption*, and *production* or *decay*. In the case of simultaneous movement of solute and water, it is usually assumed that the transport of solute is governed by convection and hydrodynamic dispersion. Convection refers to solute movement due to the bulk motion of the flowing fluid. Hydrodynamic dispersion consists of the two processes of molecular diffusion and mechanical dispersion. The relative contributions of these two phenomena to total hydrodynamic dispersion depend on the average fluid velocity through the porous medium. The total solute flux is obtained by adding the convective flux, diffusive flux, and the flux due to mechanical dispersion.

Considerable research has been conducted to model solute transport in soils. These models vary widely in their conceptual approach and degree of complexity. Among others, *Addiscott and Wagenet* (1985) classified these models as *deterministic* and *stochastic* models.

In deterministic models, individual processes and the interactions between those processes are defined mathematically, with each set of input data leading to a unique and reproducible prediction. These types of models typically account poorly for the spatially variable nature of soil.

Stochastic models presuppose that soil properties vary spatially, so that solute and water movements also vary. Stochastic models place less emphasis on the processes but more on prediction of the statistical distribution or probability of a given characteristic. Common to all stochastic models is the assumption that parameter values are distributed in space. The probability distribution functions at each point in space are usually unknown and cannot be evaluated from only one or few observations within close proximity of the location. Some recent reviews of analytical and numerical modeling on solute transport in soil are given by *Guyen et al.* (1990), *Sudicky and Huyakorn* (1991), *Sardin et al.* (1991) and *Van Genuchten* (1994).

The deterministic convection-dispersion equation is extensively used in numerical simulation models. The convective-dispersive equation of solute transport similar to Eq. 2.4 can be written as:

$$\frac{\partial(\rho s)}{\partial t} + \frac{\partial(\theta c)}{\partial t} = \frac{\partial}{\partial z} \left(\theta D \frac{\partial c}{\partial z} - qc \right) - S_s \quad 2.9$$

where ρ is the soil bulk density (ML^{-3}), s is the solute concentration associated with the solid phase of the soil (ML^{-3}), D is the solute dispersion coefficient (L^2T^{-1}), c is the solute concentration of the fluid phase (ML^{-3}), and S_s ($\text{ML}^{-3}\text{T}^{-1}$) is a sink for solute. The classical Eqs. 2.3 and 2.9 have been solved for a variety of one- and multi-dimensional applications (*Van Genuchten, 1994*). While models based on these equations are important tools, they are also subject to a large number of simplifying assumptions which limit their applicability to many problems in the field. These are discussed in detail by *Van Genuchten (1994)*. One important limitation in the use of Eq. 2.3 involves the sink term S in the flow equation.

As will be discussed in the rest of this chapter, widely different approaches exist for simulating root water uptake, most of them are essentially empirical and contain parameters that depend on specific crop, soil, and environmental conditions. Much research is still needed to derive physically based descriptions of root water uptake as function of water and salinity in the root zone. Another complication arises from the extreme heterogeneity of the subsurface environment. There is ample evidence to suggest that solutions of these classical models fail to describe accurately transfer processes in most natural field soils (*Van Genuchten, 1994*). Besides these facts, deterministic models are still useful to analyze mechanisms involved in flow and transport problems and to perform scenario analyses.

2.3. Root water uptake models

Steady-state water flow through the entire soil-plant system can be described by an analogue of *Ohm's law* as introduced by *Van den Honert (1948)*:

$$T_a = \frac{h - h_{\text{root}}}{R_s} = \frac{h_{\text{root}} - h_l}{R_p} \quad 2.10$$

where h , h_{root} , and h_l are the pressure heads (L) in the soil, at the root surface and in the leaves, respectively; R_s and R_p are the flow resistances (T) in soil and plant, respectively, and T_a is actual transpiration rate (LT^{-1}). Since h_{root} is hardly measurable

(if not impossible), it is convenient to use an equivalent equation rather than Eq. 2.10:

$$T_a = \frac{h - h_1}{R_s + R_p} \quad 2.11$$

The relative importance of R_s and R_p was extensively studied by *Gardner and Ehlig* (1962), *Cowan* (1965), *Newman* (1969), *Feddes* (1971), *Yang and De Jong* (1971), *Feddes and Rijtema* (1972), *Hansen* (1974a,b), *Taylor and Klepper* (1975), *Molz* (1975), *Jarvis* (1975), *Reicosky and Ritchie* (1976), *Herkelrath, et al.* (1977a,b), *Nnyamah et al.* (1977), *Meyer et al.* (1978) and *Blizer and Boyer* (1980). The majority of these authors believe that R_p is dependent on soil water content θ and transpiration rate T_a , while some believe that R_p is independent of them. Furthermore, there is some evidence that the hydraulic resistance of the root system usually dominates the resistance of soil surrounding the roots (*Newman*, 1969; *Molz*, 1975, 1976; *Taylor and Klepper*, 1975; *Nnyamah et al.*, 1978; *Meyer et al.*, 1978; *Blizer and Boyer*, 1980). If this is true, one may draw the conclusion that root water extraction functions expressed in terms of soil hydraulic resistance alone are conceptually wrong. However, there is some controversy concerning the degree of dominance of the root resistance (*So et al.*, 1976; *Faiz and Weatherley*, 1977, 1978). Whether this is true or not, it is now well understood that complete specification of all the resistances encountered in the soil-root-plant system is hardly feasible.

There are two main approaches to quantify root water uptake. The first one considers the convergent radial flow of soil water toward and into a representative individual root, taken to be a line or narrow tube sink uniform along its length. In this approach the root is an infinitely long cylinder of uniform radius and water absorbing properties. The soil water flow equation in this model is written in cylindrical coordinates and solved for the appropriate boundary conditions at the root surface and at some distance from the roots. The most common formulation of this *microscopic* approach is based on the work of *Gardner* (1960, 1964) and describes the microscale physics of water flow from the soil to, and through the plant roots. The most important limitation of this group of models is the unavailability of the required input parameter values. The models of *Gardner* (1964), *Nimah and Hanks* (1973a), *Feddes et al.* (1974), *Hillel et al.* (1976) and *Herkelrath et al.* (1977a) are in this category. The second, *macroscopic* approach assumes that the whole root system is a diffuse sink which permeates each layer of soil uniformly, though not necessarily with a constant density throughout the root zone. In the macroscopic approach, the flow to

individual roots is ignored and the overall root system is assumed to extract water at some rate from each differential volume of the root zone. The advantage of the macroscopic approach is that it does not require complete insight in the physical process of root water uptake and, therefore, eliminates the need for difficult to measure soil and plant parameters. However, some empirical parameters are still needed for different plants, soils, and climates. The models of *Molz and Remson* (1970, 1971); *Raats* (1974); *Feddes et al.* (1976, 1978); *Van Genuchten* (1987); *Dirksen et al.* (1993) and *Schmidhalter et al.* (1994) are in this group.

2.3.1. Microscopic models

The major difficulty in solving Eq. 2.3 (or 2.4), either numerically or analytically stems from the unknown form of the S term. There has been a tendency to describe the root water uptake analogous to *Darcy's* equation, assuming that the rate of uptake is proportional to the soil hydraulic conductivity and the difference between the total pressure head at the root-soil interface and the corresponding pressure head in the soil. In this description, an individual root is considered as a hollow cylinder of uniform radius and infinite length having uniform water absorbing properties. The governing *Darcy* flow equation for the radial flow coordinates can be written as

$$\frac{\partial \theta}{\partial t} = \frac{1}{r} \frac{\partial}{\partial r} \left[rK(h) \frac{\partial h}{\partial r} \right] \quad 2.12$$

where r (L) is the radial distance from the center of the root. Solution of the above equation can be obtained for both steady-and nonsteady-state conditions. For steady-state conditions with water flowing from a distance r_2 to a root with radius r_1 , the solution under the assumption of a constant K is (*Feddes*, 1981):

$$q_{\text{root}} = \frac{2\pi k (h - h_{\text{root}})}{\ln \left(\frac{r_2}{r_1} \right)} \quad 2.13$$

in which q_{root} is the rate of water uptake per unit length of root ($L^3L^{-1}T^{-1}$). For a discrete soil layer of thickness Δz and a rooting length per unit volume of soil of L (LL^{-3}) the water uptake rate ΔV_{root} (LT^{-1}) can be written as:

$$\Delta V_{\text{root}} = L \Delta z q_{\text{root}} \quad 2.14$$

With this soil layer being located at depth Z , equation 2.14 can be written as:

$$\Delta V_{\text{root}} = \frac{2\pi}{\ln\left(\frac{r_2}{r_1}\right)} LK (h - h_{\text{root}} - Z) \Delta z \quad 2.15$$

or

$$\Delta q_r = BKL (h - h_{\text{root}} - Z) \Delta z \quad 2.16$$

where B , equal to $2\pi/[\ln(r_2/r_1)]$, represents a dimensionless geometric and root distribution factor. The soil resistance R_s can then be written as:

$$R_s = \frac{1}{BLK} \quad 2.17$$

By dividing the root water uptake rate by the depth increment Δz , one may describe the sink term as:

$$S = \frac{\Delta V_{\text{root}}}{\Delta z} = BLK (h - h_{\text{root}} - Z) \quad 2.18$$

Equation 2.18 is the general form of the microscopic root water uptake models first introduced by *Gardner* (1960). Indeed, Eq. 2.18 is based upon the assumption that the rate of water flow from the soil into the plant root is proportional to the difference between the free energy of the water that surrounding soil and in the plant root. As pointed out by *Feddes* (1981), Eq. 2.18 can be used to describe water uptake for individual soil layers. Then, summation of the water uptake for all the layers over the entire root zone yields the total uptake rate of the whole root system which is equal to the actual transpiration rate T_a . Thus, this model describes the extraction term as a macroscopic process as well. However, in this chapter we will refer to the single root extraction functions as microscopic models.

Several researchers (*Whisler et al.* 1968; *Nimah and Hanks*, 1973a ,b; *Feddes et al.* 1974; *Childs and Hanks*, 1975; *Hansen*, 1974, 1975; *Van Bavel and Ahmed*, 1976; *Hillel et al.* 1976; *Herkelrath et al.* 1977; *Bresler et al.* 1982; *Rowse et al.*, 1978) followed the same concept as *Gardner* (1960) and made some modifications to make the model practical. Most of them devoted their work to find a direct or indirect way to determine B and h_{root} in Eq. 2.18. These models are partly listed by *Molz* (1981) and extensively reviewed and discussed by *Feddes* (1981). Only a brief review of some of the most important models is given here.

Bresler and Hanks (1969) introduced a model to compute the water and concentration of salts in the soil as a function of time and depth, assuming no precipitation or

dissolution of salts. *Nimah and Hanks (1973)* expanded this analysis by including a root extraction term. The extraction term can be written as:

$$S = \frac{K [h_{\text{root}} + 1.05Z - h - h_0] RDF}{\Delta x \Delta z} \quad 2.19$$

where *RDF* is the proportion of the total active roots in depth increment Δz ; Δx is the distance between the plant roots at the point in the soil where h and h_0 are measured, and h_0 is the osmotic head. The value 1.05 accounts for the frictional loss in the root (0.05) and for the gravitational head within the root at different depths (1.0).

The model predicted significant changes in root extraction, evapotranspiration, and drainage due to the variations in h - θ relations and rooting depth. The model needs information on the effective water potential in the root at the soil surface, the root resistance, and the distribution of active roots with depth.

Among microscopic models only this model deals with salinity. As can be seen in Eq. 2.19, a simple additivity of soil water osmotic and pressure heads is assumed.

Herkelrath et al. (1977) assumed that the rate of flow through the root membrane is proportional to the difference in the water potential across the membrane and the relative saturation θ/θ_s :

$$S = BLK \frac{\theta}{\theta_s} (h - h_{\text{root}} - Z) \quad 2.20$$

2.3.2. Macroscopic models

As has been discussed in the previous section, soil water transport models for which flow to each individual rootlet of a complete root system must be considered are not practical. The detailed geometry of the root system is practically impossible to measure and is time dependent. In addition, the water permeability of a root varies with position along the root. At present, only macroscopic models that simplify the system considerably are able to produce practical results.

In contrast to the microscopic root water uptake concepts, few macroscopic models have been proposed. One reason for this is that in many studies the macroscopic models provided reasonable agreement with the experimental field data, hence, they are satisfactory for practical purposes. The breakthrough for using such a concept came from the assumption made by *Molz and Remson (1970, 1971)* that the root water uptake can be described as *actual transpiration*. The idea in principle was promising, but the major problem was still unsolved: how to obtain the actual transpiration?

Molz and Remson (1970) developed a one-dimensional mathematical model for the macroscopic water extraction and flow process caused by transpiration demands of living plants. They assumed, as a first attempt, that root water uptake depends only on depth and actual transpiration rate, that is:

$$S = -\frac{1.6T_a}{(Z_r)^2}z + \frac{1.8T_a}{Z_r} \quad 2.21$$

where Z_r is the depth of the root zone, and z is depth below soil surface. The constants 1.6 and 1.8 are empirical values to fit a given fixed pattern of water extraction as suggested by *Danielson* (1967). Indeed, the constants came from an empirical rule used by some agricultural workers that 40, 30, 20, and 10 percent of the total transpiration come from successively deeper quarters of the root zone. The numbers of 40, 30, 20, and 10 percent have no special significance and should be regarded only as reasonable quantities. As pointed out by *Molz and Remson* (1970) an expression such as Eq. 2.21, may give reasonable results at higher water contents, but not at lower water contents. As the upper soil layers become drier, more of the transpiration requirement has to come from deeper roots in the wetter parts of soil. Similar to any other extraction term, Eq. 2.21 does not account for soil water hysteresis.

In a second attempt, *Molz and Remson* (1970) developed an extraction term that depends on water content, depth, transpiration rate, and the so-called "effective root distribution function", which can be written as:

$$S = \left(\frac{D(\theta)R}{\int_0^{Z_r} D(\theta)R dz} \right) T \quad 2.22$$

where R is the effective root distribution defined as a relative, spatial measure of the roots effective in soil water uptake at a given time (*Molz*, 1971). *Molz and Remson* (1970) indicated that R could be evaluated from the relationship between soil water flux, flux in the plant roots, and the transpiration rate.

Molz (1971) compared calculated and measured values of effective root distribution for sorghum. The root distribution was calculated from the data of *Gardner and Ehlig* (1962) and *Gardner* (1964), and compared with the measured data in terms of length per unit volume of soil. He found a poor correlation between the calculated and

measured values when the soil was wet, and a somewhat better correlation when the soil dried due to transpiration.

Molz (1981) introduced a third extraction term that depends on transpiration rate, soil water pressure head, water pressure in the root xylem, volumetric soil water content, and length of roots:

$$S = \left(\frac{\theta L(h - h_x)}{\int_0^z \theta L(h - h_x) dz} \right) T \quad 2.23$$

in which h_x is pressure head of the root xylem. Since in practice it is very difficult to obtain the water pressure in the root xylem, no investigation has been conducted to evaluate this model.

Raats (1974) developed a macroscopic root water uptake model based upon an exponential decrease of the rate of water uptake with depth:

$$S = \left(\frac{T_a}{\lambda} \right) \exp \left(-\frac{z}{\lambda} \right) \quad 2.24$$

where λ (L) is an empirical relative root density or activity chosen such that the integral of S over the root zone equals T_a .

A modification of Eq. 2.24 as given by *Schmidhalter et al.* (1994) consists of an exponential and a linear term:

$$S = \frac{f T_a}{\lambda} \exp \left(-\frac{z}{\lambda} \right) + (1 - f) T_a b \quad 2.25$$

in which the parameter f indicates a fraction of the transpiration rate, and b is an empirical parameter representing the non-exponentially distributed part of the transpiration rate, specified for 5-cm increments. The first part of right hand side of this equation is the same as that of *Raats* (1974), multiplied by f . The parameters λ and $b(z)$ in this model are obtained by relating the root water uptake function to the measured chloride distribution. Both parameters were found to be time-invariant and were therefore assumed constant. While *Schmidhalter et al.* (1994) proposed the model for areas with saline soils where upward flow from groundwater is the principal mechanism leading to salinization, there is no specific term in Eq. 2.25 to quantify soil salinity.

Popularity of the macroscopic approach increased when the studies of *Feddes* (1976) and *Feddes et al.* (1978) led to a simple *reduction term* to convert *potential transpiration* to actual transpiration as a function of soil water pressure head only. Based on this model, the extraction term under non-stress conditions is simply equal to potential transpiration over the root zone. As soon as the soil water pressure head reaches a critical value the actual transpiration reduces linearly until the root water uptake ceases completely (wilting point). This reduction is quantified by the so-called *reduction function*.

After encountering the difficulties in quantifying the root water uptake function with the microscopic approach, *Feddes et al.* (1976) developed a macroscopic approach, in which the sink term was considered as function of transpiration rate and the soil water content only. The sink term varies with θ according to the soil water pressure heads generally known to be critical for water uptake by roots. The flow equation is then solved with Eq. 2.4 with the following extraction term:

$$S = \alpha(\theta) \frac{T_p}{Z_r} \quad 2.26$$

in which $\alpha(\theta)$ is a dimensionless reduction term, depending on soil water content only.

In a second attempt, *Feddes et al.* (1978) changed the model of *Feddes et al.* (1976) by making the reduction term dependent on soil water pressure head h only, and assumed the sink term to be a function of h and potential transpiration rate T_p . They assumed that root water uptake is at maximum when the absolute value of the negative soil water pressure head $|h|$ is between h_2 and h_3 , as illustrated in Fig. 2.1a. When $|h|$ is between h_3 and h_4 (soil water pressure head at the wilting point), the water uptake decreases linearly to zero. It was further assumed that root water uptake is equal to zero at values of $|h|$ smaller than h_1 (oxygen deficiency) and larger than h_4 . Similarly to Eq. 2.26, the sink term can then be written as:

$$S = \alpha(h) S_{\max} \quad 2.27$$

in which S_{\max} is the maximum water uptake rate and $\alpha(h)$ is a dimensionless function of pressure head, defined as:

$$\alpha(h) = \frac{S(h)}{S_{\max}} \quad 2.28$$

Integration of $S(h)$ over Z_r gives the actual transpiration rate:

$$T_a = \int_{z=0}^{z=Z_r} S dz \quad 2.29$$

and S_{\max} can be obtained by substituting Eq. 2.27 into Eq. 2.29:

$$S_{\max} = \frac{T_p}{Z_r} \quad 2.30$$

Among the parameters, h_3 and h_4 are most important. The model assumes that the value of h_3 is dependent on evaporative demand and thus varies with T_p as depicted in Fig. 2.1a. This assumption is based on the early investigation by *Denmead and Shaw* (1962), who presented experimental confirmation of the effect of dynamic conditions on water uptake and transpiration. They found that under an evaporative demand of 3-4 mm/d, the actual transpiration rate began to fall below the potential transpiration rate at an average h of about -2 bar. When the evaporative demand was 6-7 mm/d, this drop already began at a soil water pressure of about -0.3 bar. When the evaporative demand was about 1.4 mm/d, no drop in transpiration rate was noticed until the average soil water pressure exceeded -12 bar. Besides these observations, it is still not clear whether the assumption that only h_3 in the *Feddes et al.* (1978) model depends on evaporative demand, is correct or not. If the assumption is true, the reduction term is not a single-dependent variable, as they defined. Even if this is true, the suggestion still remains qualitative, as one cannot quantify the effect of an intermediate transpiration rate on $\alpha(h)$. Hence, an alternative is to introduce the atmospheric demand in the model, and describing the reduction term as $\alpha(h, T_p)$. More studies are needed to quantify such a reduction term.

As can be seen from the above derivation, a constant rate of maximum extraction is assumed for the entire root zone. Such an assumption can hardly meet reality. *Kabat et al.* (1992) stated that for a non-homogeneous root distribution one can incorporate a root distribution function in Eq. 2.30, for example, as a weight fraction of the roots relative to the total weight of roots. Such root distribution functions are extensively used in numerical simulation models. While the root distribution functions can be either linear or nonlinear, *Hoogland et al.* (1981) concluded from many experimental data that in wet soils roots can principally extract water from the moist upper layers leaving the deeper layers untouched. Thus, the upper part of the root zone dominates the root distribution function. *Prasad* (1988) assumed that potential water uptake varies linearly with depth during the vegetation phase. Similar to *Hoogland et al.* (1981), he took care of the fact that in a moist soil, roots prefer to take up water from the upper soil layers without any limitation. He assumed that root water uptake at the bottom of the root zone Z_r is zero and derived:

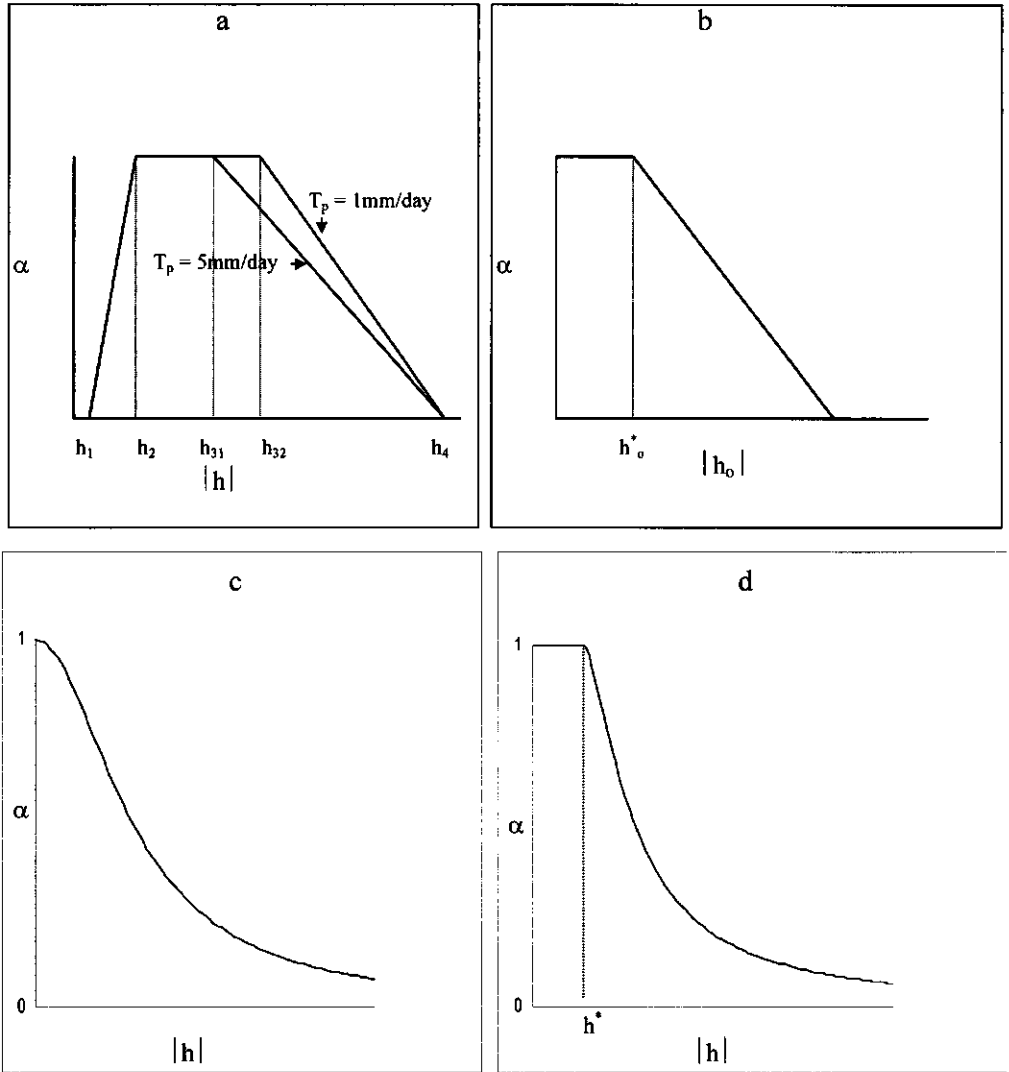


Figure 2.1. Schematic representations of root water uptake reduction functions a: Feddes *et al.* (1978); b: Maas and Hoffman (1977); c: Van Genuchten (1987); and d: Dirken *et al.* (1993). Note that in (a) the reduction function depends not only on the absolute value of the soil water pressure head $|h|$, but also on evaporative demand: at high evaporative demand ($T_p = 5 \text{ mm/day}$) the reduction occurs at lower absolute pressure head (h_{31}) than under low evaporative conditions ($T_p = 1 \text{ mm/day}$), h_{32} .

$$S_{\max} = \frac{2T_p}{Z_r} \left(1 - \frac{z}{Z_r}\right) \quad 2.31$$

Schematic representations of the different water uptake functions under optimal soil water content are depicted in Fig. 2.2.

Belmans et al. (1983) assumed that the root density is constant with depth and time and proposed for S_{\max} :

$$S_{\max} = P - Qz \quad 2.32$$

where P is the maximum uptake rate and Q is the rate of decrease in uptake with depth z . They indicated that the magnitude of Q is very small and could be disregarded. Neglecting Q in Eq. 2.32 implies that S_{\max} at equivalent h is a constant for the entire rooting depth. However, experimental data of *Allmaras* (1975), *Prasad* (1988) and *Rasih et al.* (1992) indicated that S_{\max} couldn't be regarded constant over the root zone. *Rasih et al.* (1992) assessed the influence of parameter estimation of the macroscopic root water uptake functions. They used Eq. 2.32 to simulate root water uptake. According to the fact that S_{\max} is not constant over the root zone, they proposed an independent discontinuous S_{\max} function for each arbitrary compartment. They indicated that in the presence of living roots, volumetric water content could be predicted with high accuracy, using nonlinear and discontinuous estimation techniques. *Rubin and Or* (1993) developed a stochastic-analytical model for unsaturated flow in heterogeneous soils including root water uptake. The best agreement of soil water contents was found when water uptake by plant roots was specified to an exponential decay with depth, as proposed by *Raats* (1974).

2.4. Root water uptake models for salinity stress

Following the assumption of *Feddes et al.* (1978), one may introduce a soil salinity reduction term, $\alpha(h_o)$, into Eq. 2.27 instead of $\alpha(h)$. This salinity function can be put in the form of the *Maas and Hoffman* equation (Eq. 1.1). Written in terms of the soil solution osmotic head h_o , this gives (Fig. 2.1b):

$$\alpha(h_o) = 1 - \frac{a}{360} (h_o^* - h_o) \quad 2.33$$

where h_o^* is the osmotic threshold value and 360 is a factor to convert the salinity-based slope to cm osmotic head (*U.S. Salinity Laboratory Staff*, 1954). To improve the analysis of *Maas and Hoffman* (1977), *Feinerman et al.* (1982) proposed a switching regression method to estimate the coefficients in Eq. 1.1.

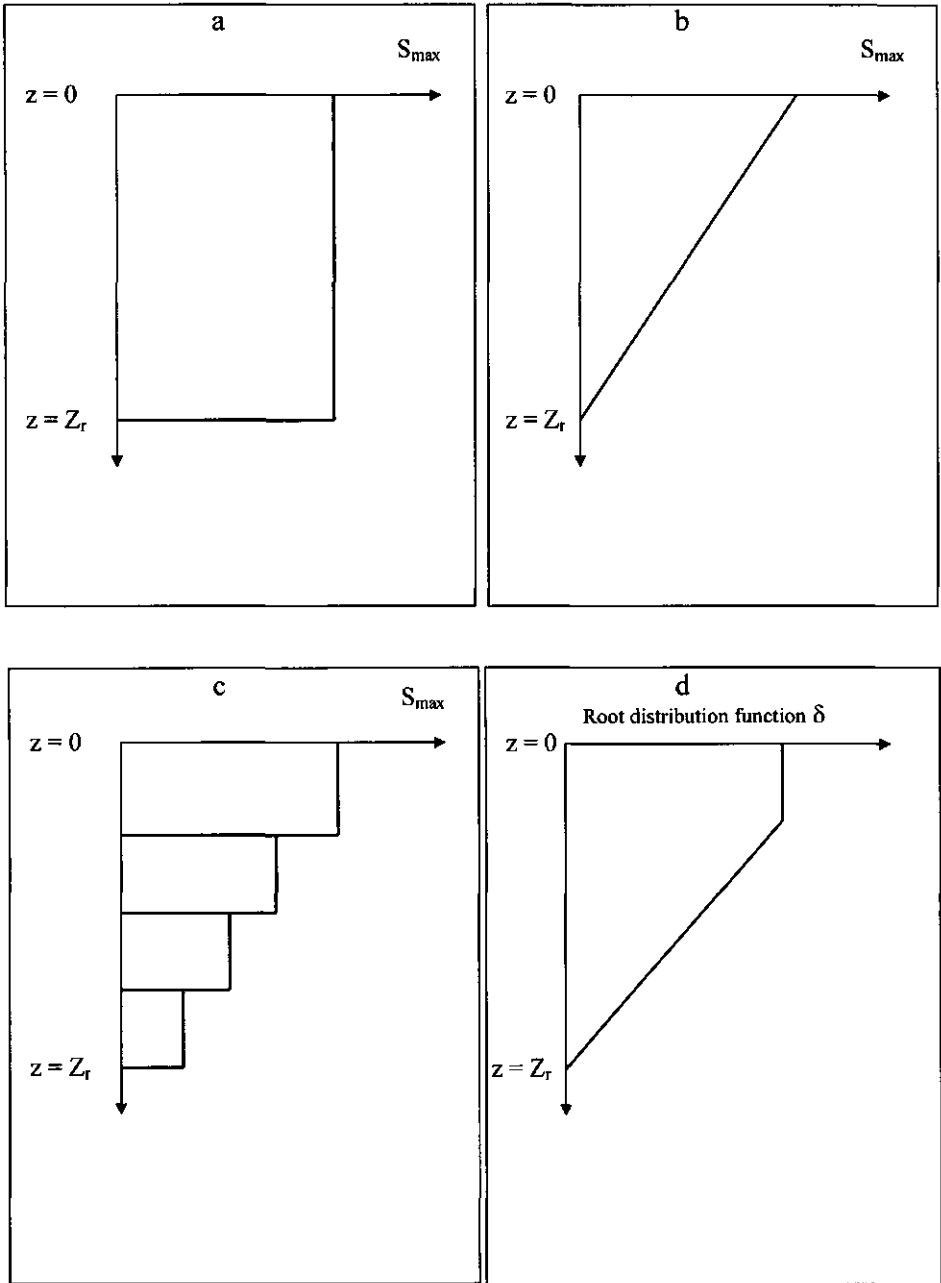


Figure 2.2. Schematic representations of different water uptake distributions under optimal soil water contents. a: Feddes *et al.* (1978); b: Prasad (1988); Danielson *et al.* (1967), and Hoffman and Van Genuchten (1983).

This method requires at least two data points to the left and at least three data points to the right of the fitted threshold value. This makes the method less suitable for experiments with a limited number of data points. Equation 1.1 is a popular model for quantifying salinity effects on crop production because of its linearity and simplicity.

Since the linear assumption does not fully meet real conditions in the field, *Van Genuchten and Hoffman* (1984) proposed two alternative equations for Eq. 2.33. Their proposed exponential equation reads as:

$$\alpha(h_o) = [\exp(\lambda h_o - \beta h_o^2)]^{-1} \quad 2.34$$

in which λ and β are empirical constants. Their S-shape function can be written as:

$$\alpha(h_o) = \frac{1}{\left[1 + \left(\frac{h_o}{h_{o50}}\right)^p\right]} \quad 2.35$$

where h_{o50} is the soil salinity at which $\alpha(h_o)$ is reduced by 0.50, and p is an empirical, presumably crop, soil and climate-specific dimensionless parameter. The value of p was found to be 3 when the S-shaped function was applied to salinity stress data. Equation 2.35 was found to describe crop salt tolerance data equally well or better than Eq. 2.33 (*Van Genuchten*, 1987).

Dirksen et al. (1988, 1993) proposed as modification for Eq. 2.35:

$$\alpha(h_o) = \frac{1}{\left[1 + \left(\frac{h_o^* - h_o}{h_o^* - h_{o50}}\right)^p\right]} \quad 2.36$$

Equation 2.36 is more realistic than Eq. 2.35, incorporating a salinity threshold value in the equation. The most important limitation for Eqs. 2.35 and 2.36 arises from the difficulty involved to obtain h_{o50} . Furthermore, p is not yet defined either physically or empirically.

2.5. Root water uptake models for joint water and salinity stress

Whereas root water uptake is reduced due to low soil water pressure and osmotic potentials, it is not clear how these stresses interact when they occur together, and vary with time and depth. The simple additivity of soil water pressure and

osmotic potentials as proposed by early investigators (*Ayers et al.*, 1943; *Wadleigh and Ayers* 1945; *Wadleigh et al.*, 1946; *U.S. Salinity Laboratory Staff*, 1954) is still questionable. Because soil water pressure and osmotic heads are additive in reducing the free energy of soil water, it was assumed that their effect on transpiration is also additive through reduction in the availability of water for plants. Early studies indicated that yield reduction is a function of integrated osmotic and pressure heads. This observation led to the conclusion that the effect of excess salt on transpiration is similar to that of water stress. *Meiri* (1984) analyzed data of *Meiri and Shalhevet* (1973), *Sepaskhah and Boersma* (1979), *Jensen* (1982), and *Parra and Romero* (1980) by multilinear regression and found that the effects of osmotic and matric potentials are somewhat additive. It is important to keep in mind that in most of these investigations PEG (Poly ethylene glycol) rather than a real drought intrusion was used to create water stress. *Shalhevet* (1984, 1994) referred to the same studies and stated that the bulk evidence suggests that the effects of salinity and water stress are *identical*, and that a unified function may be applied to both stress components. This would imply that h and h_0 are additive in their effect on transpiration, but one unit of h is not equivalent to one unit of h_0 (*Shalhevet*, 1994). Such a conclusion remains useless, however, unless an empirical proportionality coefficient can be determined.

It has been known for many years that crop response to soil water and salinity is a continuous function. Information on the consumptive use of many crops is available for irrigation with nonsaline water. The question is whether this information also applies to saline irrigation water, and if not, what adjustments need to be made. *Stewart and Hagan* (1973) proposed the following production function:

$$\frac{Y}{Y_m} = (1-b) + b \frac{ET_a}{ET_m} \quad 2.37$$

where ET_a and ET_m are actual and maximum evapotranspiration, respectively, and b is an empirical constant. *Shalhevet et al.* (1973) and *Shalhevet* (1984) argued that b may or may not be affected by salinity. Since salinity may affect the rate of canopy development and the eventual leaf area index (LAI), b could indeed depend on soil salinity. Application of the equation to different locations with different soil water osmotic and pressure heads indicated that regardless of the type of stress causing reduction, ET_a decreased proportionally. Where salinity stress was involved, plant water extraction was less than in similar treatments without salinity stress. Using Eq. 2.37, *Katerji et al.* (1998) found that the yield estimate for maize and sunflower was quite accurate, for potatoes somewhat less, but for soybean unsatisfactory. Still, the

relative effect of salinity stress and water stress on transpiration cannot be calculated with this equation.

Among the microscopic extraction functions, only Eq. 2.19 deals both with h and h_0 . In this model, the osmotic head is added to the matric head to establish the water potential gradient from the soil to the root. Furthermore, the influence of salinity is assumed to be only osmotic, and effects of specific ions as well as chemical precipitation-dissolution are ignored. *Nimah and Hanks (1973b)* and *Childs and Hanks (1975)* reported good agreement between the field data for alfalfa under joint water and salinity stresses and computed water contents over the root zone and transpiration. *Wolf (1977)* reported that computed and measured data correlated excellently when salinity was low, but for high salinity the model overestimated. *Hanks (1984)* stated that Eq. 2.19 is quite crude, particularly regarding plant factors. He indicated that attempts to make the model more realistic by including such plant factors as axial and radial root resistance did not improve the predictability when applied to actual problems.

Childs and Hanks (1975) used this model to simulate the effect of root distribution on dry matter yield in saline condition. The result indicated that because of upward water flow, the influence of rooting depth on relative yield was large where the amount of water applied was much less than the water lost through evapotranspiration. *Hanks (1984)* pointed out that the model cannot be applied to the field scale because of considerable spatial variability in the field which the model cannot handle. *Cardon and Letey (1992)* showed that in its calculations of root water uptake Eq. 2.19 is generally inconsistent with plant behavior. The insensitivity of this model is caused by the manner in which the salinity effect is incorporated in the uptake term. The value of S is dominated by the nonlinear changes of h and K with θ . In contrast, h_0 decreases linearly with θ (simple concentration-dilution). Moreover, increasing the salinity of the irrigation water while maintaining high water contents, results in relatively high $K(\theta)$ values and plant water extraction proceeds at or near maximum levels.

Basically, the macroscopic models do not account for saline conditions. One reason for this is the unknown relation between h and h_0 as they vary in time and space. Few attempts have been made to modify the *Feddes et al. (1978)* model for salinity. In a first attempt, *Van Genuchten (1987)* modified Eq. 2.27, using different equations for both the water stress reduction function $\alpha(h)$ and the maximum extraction rate S_{\max} . He assumed that water and salinity stress have similar effects on

yield, and hence on transpiration, and proposed a similar smooth S-shaped relationship for $\alpha(h)$:

$$\alpha(h) = \frac{1}{\left[1 + \left(\frac{h}{h_{50}}\right)^p\right]} \quad 2.38$$

in which h_{50} is the soil water pressure head at which $\alpha(h)$ is reduced by 0.50. It was expected that h_{50} depends on soil, climatic, and management conditions. Except near saturation, a plot of Eq. 2.38 closely resembles the stress part of the *Feddes et al.* (1978) model. This simplification can be justified for relatively short periods of saturation. A schematic representation of Eq. 2.38 is given in Fig. 2.1c.

The reduction function due to joint salinity and water stress is then obtained by summation of h and h_o with undefined empirical coefficients for soil water pressure head (a_1) and osmotic head (a_2):

$$\alpha(h, h_o) = \frac{1}{1 + \left[\frac{(a_1 h + a_2 h_o)}{h_{50}}\right]^p} \quad 2.39$$

Since the assumption of linear additivity is still being questioned, and parameters a_1 and a_2 practically are difficult to obtain, *Van Genuchten* (1987) proposed a simple multiplication of Eqs. 2.35 and 2.38:

$$\alpha(h, h_o) = \frac{1}{1 + \left[\frac{h}{h_{50}}\right]^{p_1}} \times \frac{1}{1 + \left[\frac{h_o}{h_{o50}}\right]^{p_2}} \quad 2.40$$

Dirksen et al. (1988, 1993) multiplied identical reduction terms for water stress and salinity stress, each with their own values for the threshold value h^* , h_o^* and 50% value h_{o50} and h_{o50}^* :

$$\alpha(h, h_o) = \frac{1}{1 + \left[\frac{h^* - h}{h^* - h_{50}}\right]^{p_1}} \times \frac{1}{1 + \left[\frac{h_o^* - h_o}{h_o^* - h_{o50}}\right]^{p_2}} \quad 2.41$$

Schematic view of the pressure head reduction function of Eq. 2.41 is given in Fig. 2.1d.

Van Genuchten (1987) proposed for the maximum extraction term S_{\max} :

$$S_{\max} = T_p \delta(z) \quad 2.42$$

where $\delta(z)$ is a depth-dependent root distribution function. Based on the experimental data documented by Gardner (1983), Hoffman and Van Genuchten (1983) proposed:

$$\begin{aligned} \delta &= \frac{5}{3Z_r} && \text{for } z \leq 0.2Z_r \\ \delta &= \frac{25}{12Z_r} \left(1 - \frac{z}{Z_r}\right) && \text{for } 0.2Z_r < z \leq Z_r \\ \delta &= 0 && \text{for } z > Z_r \end{aligned} \quad 2.43$$

A plot of the relative root distribution function as a function of relative rooting depth (z/Z_r) is presented in Fig. 2.2d.

The most important limitation of Eqs. 2.40 and 2.41 is the difficulties involved in obtaining the required parameter values. Furthermore, there is still no physical or empirical explanation for p_1 and p_2 , which determine the rate at which the water uptake diminishes when the threshold values are exceeded. It is still not clear whether p_1 and p_2 have approximately the same values.

As shown by Dirksen (1985) and discussed by Dirksen *et al.* (1993), leaf water potentials closely reflect the effect of soil water potentials on water uptake integrated over the root zone. Thus, Dirksen *et al.* (1993) derived the parameter values from experimental leaf water potentials of alfalfa, which can be measured easily.

In one study, Cardon and Letey (1992) compared the sensitivity of Eq. 2.19 and Eq. 2.40 to salinity stress. They found that the water uptake term of Eq. 2.19 was insensitive to salinity and generally inconsistent with plant behavior. Equation 2.40 had a broad range of sensitivity for fluctuations in both the pressure and osmotic heads, providing reasonable calculations of transpiration rates.

2.6. Numerical simulation model HYSWASOR

The numerical simulation model for hysteretic water and solute transport in the root zone, HYSWASOR (Dirksen *et al.*, 1993), was designed to study the influence of soil water pressure and osmotic potentials on root water uptake under hysteretic conditions (frequent irrigation). This makes this model ideally suitable for use in this study. Detailed information on this model is given elsewhere (Dirksen *et al.*, 1993; Kool and Van Genuchten, 1991; and Van Genuchten, 1987).

HYSWASOR is a modified version of WORM (*Van Genuchten, 1987*), an efficient mass-lumped, fully implicit Galerkin finite element code for one-dimensional, isothermal transport of water and solute in rigid porous media (*Dirksen et al., 1993*).

The governing one-dimensional water flow equation is Eq. 2.3. The main wetting and drying soil water retention functions are described by the parametric function of Eq. 2.6. Similar equations are used in the algebraic algorithm to generate closed hysteretic scanning curves. The hydraulic conductivity function can be described by Eq. 2.8, or can be given in a table of K as function of θ .

Solute transport is described by the familiar advection-dispersion equation. The only major change in the solute transport module, in comparison with WORM, is the inclusion of *Freundlich's* nonlinear adsorption isotherm. Osmotic potential is expressed as osmotic head which is assumed to be a linear function of solute concentration c and EC_{ss} according to:

$$h_o = -40c = -400 EC_{ss} \quad 2.44$$

in which h_o is in cm, c in $\mu \text{ mol/cm}^3$ and EC_{ss} in dS/m.

Eq. 2.41 is used as the reduction function, multiplied by $\phi_{\text{air}} / \text{MinAir}$ to incorporate the effect of oxygen deficiency on root water uptake reduction under wet conditions. This effect is assumed to vary linearly between the threshold air volume fraction $\phi_{\text{air}} = \text{MinAir}$ and $\phi_{\text{air}} = 0$. The complete extraction term is then:

$$S = \left(\frac{\phi_{\text{air}}}{\text{MinAir}}, \text{ if } < 1 \right) \frac{1}{1 + \left[\frac{h^* - h}{h^* - h_{s0}} \right]^{p_1}} \times \frac{1}{1 + \left[\frac{h_o^* - h_o}{h_o^* - h_{o50}} \right]^{p_2}} T_p \delta \quad 2.45$$

where δ is the relative root density or activity (L^{-1}) defined such that the integral of δ over the root zone equals 1.

2.7. Summary

Historically, two concepts of root water uptake have evolved: microscopic and macroscopic. The microscopic concept considers the radial flow of soil water toward a representative root of infinite length, uniform thickness, and uniform absorptivity. In microscopic models, the soil water flow equation is usually written in cylindrical

coordinates and solved with appropriate boundary conditions at a root surface and at some distance from the root. Because the required input parameters at the soil-root interface are rather difficult to measure, it has not proven practical to test the proposed microscopic models directly.

The macroscopic concept regards the root system as a whole. Because the parameters needed in macroscopic models can be measured, this concept is most widely used in numerical simulation models. The macroscopic concept remains essentially empirical, however, and much research is still needed to derive a physically based description.

3. Physical experiments

3.1 Introduction

Most salt tolerance and water stress studies have been carried out separately and many data are available for either water stress or salinity stress only. There are only few publications in terms of root water uptake under joint water and salinity stresses (*Dirksen et al.*,1994). Even in studies with only salinity stress, most investigations have been conducted at uniform salt distributions over the root zone with soil solution concentrations relatively constant in time. The objective of this study was to investigate the influence of water, salinity, and joint water and salinity stress on root water uptake when both soil water osmotic and pressure heads change in time and space. To facilitate such a study, a specific experimental set up was designed on which alfalfa was grown in densely instrumented laboratory soil columns and harvested at approximately 50-day intervals for one year. Stresses imposed on the plants lasted for about 20 days, while considerable time has been spent for the plants to recover and regrow after each stress period. Different soil water osmotic and pressure head distributions over the root zone have been obtained by varying irrigation water salinities and irrigation quantity and intervals.

The experiments consisted of five major periods. In the first period, information on plant, soil and greenhouse conditions was obtained, which was essential for the measurements during the following four periods. The second and the third period were dedicated to only salinity stress and only water stress, respectively. The joint water and salinity stress data were collected during two different phases, the fourth and fifth period. Each period had its own reference treatment.

Water content and bulk electrical conductivity in the root zone were measured nondestructively with (mostly) automated TDR (Time Domain Reflectometry) instrumentation. This apparatus could measure 36 locations (four columns) fully automatically, the remaining locations were measured semi-automatically. The time intervals for all automated TDR measurements were two hours. In-situ soil solution electrical conductivities were measured manually with salinity sensors once a day at all locations, while the actual transpiration was determined by weighing the columns five times a day (with few exceptions). Leaf water potentials of the treatments were measured twice a day. Details of the experimental set up are discussed in the next part, while Table 3.1 lists detail information on the experimental treatments. An overview of the experimental setup is given in Fig. 3.1a.



Figure 3.1a. An overview of experimental apparatus with automated TDR equipment, salinity and TDR sensors, electronic scale, pressure chamber, and an apparatus to control the suction applied to reach the target leaching fraction. The plants belong to the second growth period and were in flowering stage under no stress condition. Plants in the first 3 columns in the left row were damaged by insects.

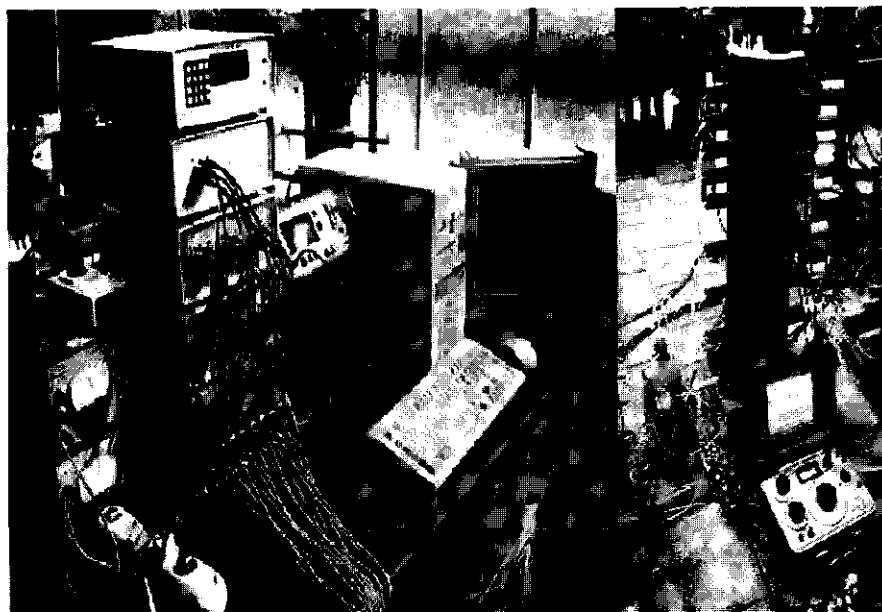


Figure 3.1b. (left): An overview of the automated TDR apparatus with the PC, (right): an experimental column with TDR and salinity sensors and tensiometers. Two glass bottles for collecting suction-drainage via two parallel filter tubes from the bottom of the column, and a salinity bridge to measure soil solution salinity, are also shown.

3.2. Experimental setup

To obtain as accurate experimental data as possible, highly instrumented experiments were carried out by growing alfalfa (*Medicago Sativa L.*) in a greenhouse under controlled environmental conditions. Alfalfa has been chosen because it can be harvested repeatedly for a relatively long period without significant changes in the root system and more importantly, because alfalfa is categorized as moderately tolerant to salinity stress and tolerant to water deficit. This makes alfalfa ideal for this study. Because the alfalfa plants were well developed, the distance between the containers was kept as large as possible (55 cm) to minimize neighboring plants shadowing to each other (Fig. 3.1a). This arrangement caused the plants to transpire large amounts of water compared to field conditions. The experimental measurements covered four periods consisting of 5 salinity stress treatments (S_iW_0), 2 water stress treatments (S_0W_i), and 10 joint salinity and water stress treatments (S_iW_i), respectively. Detailed information on each individual treatment and its replicates is given in Table 3.1. The reference treatment R for each period of measurements was different from the others. Because the joint water and salinity stresses were introduced to the plants in two time periods, the reference treatments were also different and all the collected data were later compared with their own R. The transpired water from R was considered to be equal to potential transpiration T_p .

3.3. Experimental phases

All treatments were carried out in duplicate. Within all experimental phases, the first treatment was always the reference treatment R without salinity or water stress. From this treatment, the required amounts of water for the other treatments were derived. Also, all the data obtained from the other treatments were compared with the data of this treatment. All irrigations of R were with tap water of $EC_{iw} < 0.2$ dS/m. Since no water stress was allowed for R, the irrigation intervals needed to be short; hence, the columns received irrigation water every two days during the entire experiment. The target leaching fraction of the salinity treatments was 0.5. Thus, a large amount of saline water in excess of potential transpiration was applied to the columns, and the same amount of excess water was given to the reference treatment. This provided a relatively similar water distribution over the root zone for all treatments. In the cases of water stress and joint salinity and water stress, no extra water was given to the reference as it was not given to the stressed treatments. At the end of the stress period the plants were harvested, excess salinity was flushed out of all soil columns and the alfalfa was allowed to develop healthy plants under no-stress

Table 3.1. Quantity Q_{iw} , and salinity EC_{iw} of irrigation water, target leaching fraction LF , number of irrigations N , and irrigation time intervals t of experimental treatments.

Experimental Phase	Name	Treatment	EC_{iw}	Q_{iw}	t	N	LF
			dS/m	cm ³	d	-	-
I. Preliminary							
		R	Tap	1.5 R	2	10	0.5
		S ₁ W ₀	1.5	1.5 R	2	10	0.5
		S ₂ W ₀	2.0	1.5 R	2	10	0.5
II. Salinity stress	S _i W ₀	S ₃ W ₀	3.0	1.5 R	2	10	0.5
		S ₄ W ₀	4.0	1.5 R	2	10	0.5
		S ₅ W ₀	5.0	1.5 R	2	10	0.5
III. Water stress	S ₀ W _i	R	Tap	1.5 R	2	10	-
		S ₀ W ₁	Tap	0.7 R	4, 4, 3, 3, 3, 3	5	-
		S ₀ W ₂	Tap	0.5 R	4, 4, 3, 3, 3, 3	5	-
IV. Salinity and water stress	S _i W ₁	R ₁	Tap	1.5 R	2	10	-
		S ₁ W ₁	1.5	0.7 R	4, 4, 3, 3, 3, 3	5	-
		S ₂ W ₁	2.0	0.7 R	4, 4, 3, 3, 3, 3	5	-
		S ₃ W ₁	3.0	0.7 R	4, 4, 3, 3, 3, 3	5	-
		S ₄ W ₁	4.0	0.7 R	4, 4, 3, 3, 3, 3	5	-
		S ₅ W ₁	5.0	0.7 R	4, 4, 3, 3, 3, 3	5	-
V. Salinity and water stress	S _i W ₂	R ₂	Tap	1.5 R	2	10	-
		S ₁ W ₂	1.5	0.5 R	4, 4, 3, 3, 3, 3	5	-
		S ₂ W ₂	2.0	0.5 R	4, 4, 3, 3, 3, 3	5	-
		S ₃ W ₂	3.0	0.5 R	4, 4, 3, 3, 3, 3	5	-
		S ₄ W ₂	4.0	0.5 R	4, 4, 3, 3, 3, 3	5	-
		S ₅ W ₂	5.0	0.5 R	4, 4, 3, 3, 3, 3	5	-

conditions, before the next stress was introduced.

Experimental phase II was carried out under salinity stress without water stress, consisting of five treatments. The soil was salinized by twice saturating and draining all columns, applying appropriate amounts of water and salinity. This salinization as well as the salinity stress was introduced to the columns after developing healthy plants. To avoid toxicity effects and precipitation/dissolution reactions of salts with the soil solid phase, salinities were created by adding equal molar (charge base) quantities of CaCl₂ and NaCl to the irrigation water. The imposed salinity levels were related to the salinity threshold value of alfalfa, $EC_e = 2$ dS/m. Accordingly, the EC of

the irrigation water was 1.5, 2.0, 3.0, 4.0, and 5.0 dS/m for the treatments S_1W_0 , S_2W_0 , S_3W_0 , S_4W_0 , and S_5W_0 , respectively. Similar to R, these treatments were irrigated every two days. To minimize salt accumulation, particularly in the deeper part of the root zone, the target leaching fraction was 0.50 for all saline columns. For this reason and also because no water deficiency was allowed, the applied irrigation water was always in excess of potential transpiration. The excess water was sucked out overnight with a vacuum pump at suctions of 60 to 80 cm.

In experimental phase III, two levels of water stress were introduced to the plants, denoted as S_0W_1 , and S_0W_2 . No salinity stress was allowed for these treatments. The columns were first irrigated twice with tap water at 4-day intervals and thereafter received water at 3-day intervals. The amounts of irrigation water for these treatments were 70% and 50% of their own reference treatment i.e. $W_1 = 0.7R$ and $W_2 = 0.5R$. Since the columns received less irrigation water than needed for potential transpiration, there was no leaching.

Experimental phase IV with salinity stress and first level water stresses consisted of five treatments denoted as S_1W_1 , S_2W_1 , S_3W_1 , S_4W_1 , and S_5W_1 , respectively. Since there was no leaching, after each water application the salinity in the root zone increased particularly in the upper parts. The amount of applied irrigation water for all replicates was about 0.7 of potential transpiration, calculated from the reference treatment ($W_1 = 0.7R$). The first two irrigation intervals of 4 days were followed by 3-day intervals. The columns received the same amount of irrigation water; the only difference between the treatments was the salinity of the irrigation water which varied from 1.5 to 5 dS/m. Since the columns did not receive enough water, no leaching occurred.

In experimental phase V, both salinity stress and the second level of water stress were investigated, having five treatments denoted as S_1W_2 , S_2W_2 , S_3W_2 , S_4W_2 , and S_5W_2 , respectively. The amount of applied irrigation water for all treatments was about 50 percent of the potential transpiration stress ($W_2 = 0.5R$). Irrigation intervals were the same as for the fourth experimental phase. The columns received the same amount of irrigation water; thus the only difference within treatments was the salinity of the applied water which varied from 1.5 to 5 dS/m.

3.4. Soil columns

The soil containers were PVC cylinders, 67 cm high and 21 cm in diameter (Fig.3.1b). The most active part of alfalfa roots is usually located in the top 50 cm of

the root zone (Smith, 1994). Thus, it was decided to study root water uptake of alfalfa in soil columns 15 cm deeper than this active part. Accordingly, the containers were filled up to 65 cm with soil and the remaining 2 cm was filled with coarse sand to reduce evaporation from the soil surface. In the top 30 cm of the columns three parallel ports for TDR sensors, self-made tensiometers, and salinity sensors were made at 5-cm increments. The outside diameter of the tensiometers was made the same as that of the salinity sensors. In the lower 30 cm of the columns the same ports were located at 10 cm intervals. Later, 15 cm of glass wall was added to the top of the columns as a free board to facilitate the flood irrigation. To suck out the excess water, measure the leaching fraction, and make optimal aeration conditions in the root zone, two parallel ports were installed at the bottom of each column. Two filter tubes were installed in these ports to suck out the excess waters with a vacuum pump. To measure actual transpiration, the columns were hung onto an electronic scale. To facilitate attaching a handle to the columns an extra piece of PVC was glued to the top of each column.

3.5. Soil Packing

In laboratory studies of water movement and solute transport, soil packing plays an important role, as it strongly influences the soil water hydraulic functions. Many laboratory studies are based upon the assumption that the packed soil columns are both longitudinally and laterally homogeneous. In most of the studies with multiple columns it is assumed that the packing of the columns is nearly similar. Despite considerable progress in soil physical instrumentation, there still is no standard method for soil packing. In some studies the soil columns are packed with dry soil (Oliviera *et al.*, 1996), while others (Topp and Miller, 1966; Nimmo and Miller, 1986) packed their columns under water. However, the most uniform packing can be achieved by adding an optimal amount of water to the soil. The uniformity of packing is usually evaluated by measuring the soil bulk density (or porosity) along the longitudinal direction. The packing method used in this study consisted of adding some water to the soil, compressing equal mass of soil by dropping a weight an equal number of times from the same height and checking the bulk density for each soil increment.

Wichmond loamy sand soil (14% clay, 31% silt and 55% sand) was chosen to avoid preferential flow as much as possible. The soil was first sieved with a 1-cm sieve. One column was packed with air-dried soil at 5-cm increments. Compressing the air-dried soil by more than 20 hits from 65 cm height with a 1750 g weight did not increase the soil bulk density more than 1.27 g/cm^3 . Using a heavier weight (3100 g) and increasing the number of hits from 20 to 30 did not change the bulk density of air-

dried soil. The same soil packing procedure was then followed with soil mixed uniformly 0.050, 0.075, 0.100, 0.125 and 0.150 gram water per gram of soil. At a water content of 0.125 g/g, 15 hits yielded nearly uniform bulk densities of 1.42 g/cm³. Subsequently, all fourteen columns were packed at this water content by the same procedure. To minimize the variations during packing, the bulk density of every 5 cm packed soil was measured before adding the next soil increment. The remaining small variations in bulk densities are depicted in Fig. 3.2.

After packing, all the sensors were installed and the columns were saturated with tap water and drained twice with a suction pump to reduce remaining differences in the soil packing. During the first irrigation, some ports leaked water. This was controlled by a very thin film of Vaseline at the contact places between the outside of the sensors and the ports. After fixing all the seepage holes the columns were twice irrigated and drained.

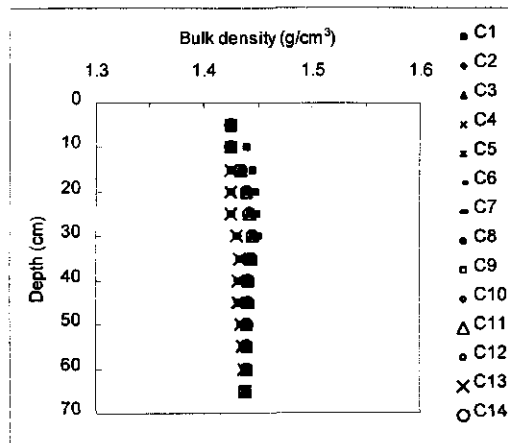


Figure 3.2. Dry bulk density of packed soil at 5-cm increments for 14 experimental columns, denoted as C₁ to C₁₄.

3.6. Seeding

It was very important to grow healthy plants before introducing any kind of stress. To fix nitrogen of air in the roots, the alfalfa seeds were inoculated with *Rhizobium* bacteria. First the suspension of *Rhizobia* was mixed by *Carboxyl MethylCellulose* CMC and later four parts of seeds were mixed by one part of this mixture. CMC was used to fix the *Rhizobial* cells to the seed coat. Finally, the wet seeds were dusted with dry CaCO₃ (1 g CaCO₃ for 2 g seeds). After this inoculation, alfalfa was immediately seeded at a density of four seeds per location and 20 locations

per column. A week later, all locations were thinned to one plant, giving 20 plants per columns.

The seeds received the first irrigation water (tap water) 15 minutes after seeding. The second irrigation was given 4 days after seeding and later on every three or two days, depending on the evaporative demand in the greenhouse; the columns were irrigated by the same amount of tap water. Eight days before the first harvesting, the columns had to be irrigated daily. The first harvest was 11 weeks after the seeding, which was the longest growth period of the experiments. The second harvest was 7 weeks after the first cutting. During this re-growth period the young plants were infested with insects (White fly and Thrips). To prevent any more damage from these insects, a biological control was proposed but for practical reasons a weekly spraying with some selective insecticides was used. After three growth periods when all of the conditions were controlled and healthy plants were established, the target stresses were introduced to the plants and the actual measurements were started.

3.7. Greenhouse conditions

The experimental setup was located in a greenhouse that was originally designed to grow tropical plants. Therefore, both temperature and relative humidity were high. The recorded minimum and maximum temperature during the whole experimental period were 18 and 36 °C, respectively, while the relative humidity was recorded between 34 and 65 percent. The humidity was controlled by regular air circulation. The experimental columns were located in two rows of seven. Above each row 4 artificial lights (Son-T Agro 400, Philips, Belgium) were suspended at 220 cm above the ground (150 cm above top of the columns). The height of mature plants at flowering stage was about 70-75 cm for the nonstressed plant. Thus, the distance of the lamps in this case was about 75-80 cm above the top stems. Therefore, the heating by the artificial lights could not cause any damage to the plants. At the beginning, the light period was 10 hours but that caused horizontal development of stems. In the absence of enough light, plants speed up cell division and the stems tend to grow horizontally due to their weight. This will break the stems after a few days. For this reason the light period was increased to 14-16 hours a day (depending on the season). The re-growth periods depended on the environmental conditions in the greenhouse. They were about 7-10 days longer in the winter than in the spring and summer. Most re-growth periods were 4-6 weeks, and the experimental measurements were accomplished during the last 20 days of each growth period.

3.8. Water application

The electrical conductivity of the applied water and the leaching water were measured for each water application. For practical reasons all irrigations were performed by flooding. In all cases, irrigation water was applied to the soil columns in the evening just before turning off the light, so that the applied water could infiltrate into the soil columns during the night. This allowed the assumption that during the light period soil water pressure heads corresponded to the main drying soil water retention curve. While this is true for the salinity stress treatments (because they were nearly saturated with water with each irrigation), in the case of water stress soil water pressure heads may have differed from the main drying curve.

Water stress was created as function of potential transpiration, obtained experimentally from daily measurement of transpiration of non-stressed treatments. One complete growth period was carried out to find out how much water had to be applied to the column to avoid any water limitation. Also, based on these results the required amounts of water for stress treatments were obtained, but these were modified later due to changes in the evaporative demand in the greenhouse.

3.9. Fertilizer application

Because alfalfa can fix nitrogen in its roots, no nitrogen fertilizer was added to the soil. Early in the second re-growth period some nutrient deficiencies appeared. Chemical analyses of the drainage water indicated that there were not sufficient nutrients in the drainage water as well as in the soil itself. Thus, except N, a complete nutrient mixture (including P, K, Mg, Ca, S, Fe, Zn) was added in solution to the irrigation water. Since the fertilizer solution was dilute, its electrical conductivity was low ($EC < 0.3$ dS/m) and the additional influence on the case of salinity and/or water stress was negligible. However, the additional salinity was directly measured by the salinity bridge and was taken into account.

3.10. Measurements

In-situ measurements were made of soil water content $\theta(t, z)$, soil water pressure head $h(t, z)$, soil solution electrical conductivity $EC_{ss}(t, z)$, and bulk soil electrical conductivity $EC_b(t, z)$. The EC_{ss} was measured manually once a day at each depth and converted to osmotic head. Water contents were measured automatically in 4 columns (32 locations) 12 times a day and the remaining columns were measured semi-automatically 5 times a day. Soil water pressure heads could be measured with self-made tensiometers (flat-shaped ceramics) and pressure transducers that could be

scanned automatically at 16 locations. The remaining locations had to be measured manually. Due to some difficulties the tensiometer measurements were not reliable (for more detail see section 3.10.2).

Actual transpiration T_a and leaf water potential LWP were also measured. To measure transpiration the surface of all columns was isolated uniformly with coarse sand to minimize soil evaporation. Since alfalfa is a heterogeneous plant, the number of stems for each plant, as well as the transpiration rate, was not necessarily the same for all plants. To minimize errors due to this heterogeneity, transpiration was measured eight times a day for four weeks. In this case no stress was allowed and the columns received sufficient tap water. The irrigation intervals were two or three days. Because the young plants were thinned uniformly, 28 days actual transpiration measurements showed only very small (negligible) variation between the columns. At the end of each growth period the plants were harvested to 15 cm above the top of the soil columns.

3.10.1. Soil water content and bulk electrical conductivity (TDR)

Information on the temporal and spatial variation of soil water content is central to understanding root water uptake patterns. The accepted standard technique for measuring soil water content is oven drying at 105 °C to constant mass (*Gardner, 1986*). This inevitably involves destructive sampling. It is also time consuming and thus not suited for in-situ measurements required for this study. For these reasons an indirect method of soil water monitoring was used. Soil water content can be determined indirectly by measuring the effective soil permittivity. In the time domain reflectometry (TDR) technique the permittivity can be derived from the propagation velocity of a very fast rise-time voltage pulse traveling along a wave guide (sensor) imbedded in the soil. The pulse is reflected back at the open end of the sensor. From the down and return travel time of the pulse along the sensor and the length of the sensor, the permittivity of the soil can be derived. *Fellner-Feldegg (1969)* was the first to use TDR to measure the permittivity of liquids, while its use for measuring soil water content was introduced by *Topp et al. (1980)*.

The effective permittivity ϵ of the soil, which is strongly related to θ , determines the propagation velocity v of the electromagnetic waves:

$$v = \frac{c}{\sqrt{\epsilon}} \quad 3.1$$

where $c = 3 \times 10^8$ m/s is the velocity of light in vacuum.

A cable-tester can be used to measure the travel time t_s of the pulse along the TDR sensor. Since the wave travels forth and back along the rods of length l , the mechanical propagation velocity is:

$$v = \frac{2l}{t_s} \quad 3.2$$

By equating Eqs. 3.1 and 3.2, the permittivity can be calculated according to:

$$\varepsilon = \left(\frac{ct_s}{2l} \right)^2 \quad 3.3$$

A calibration relationship is needed to convert ε to volumetric water content θ . *Topp et al.* (1980) found that the following relationship holds for a relatively large number of soils:

$$\theta = (-530 + 292\varepsilon - 5.5\varepsilon^2 + 0.043\varepsilon^3) \times 10^{-4} \quad 3.4$$

This calibration relationship has given satisfactory results for many soils; however, for low bulk densities, specific mineralogical properties, clays, and organic soils, a soil-specific calibration is necessary (*Dirksen and Dasberg*, 1993). For a wide range of porous media $\theta(\varepsilon)$ calibration functions can be obtained by applying a theoretical mixing model originally developed by *Maxwell* and applied by *De Loor* (1990). In this model, components with different ε are thought to be randomly distributed in a homogeneous mixture. *Dirksen and Dasberg* (1993) showed that for many clay soils the theoretical mixing model yields a better calibration than Eq. 3.4. For the soil used in this study Eq. 3.4 proved to be accurate enough and hence was used to convert the TDR wave forms to volumetric water contents.

Dalton et al. (1984), *Dasberg and Dalton* (1985), and *Dalton and Van Genuchten* (1986) proposed that the attenuation of the TDR signal could be used to estimate the bulk electrical conductivity of the soil. *Topp et al.* (1988), *Yanuka et al.* (1988), and *Zegelin et al.* (1989) examined this proposal in detail. The bulk electrical conductivity measured with TDR is the result of different components (*Dirksen*, 1996) and the soil solution electrical conductivity (which influences the root water uptake) is only one of them. Indeed, plant roots take up water through semi-permeable membranes in the cell walls, thus sieving solutes out of the transpiration stream. As a result, root water uptake takes place against the osmotic potential of the soil water. Thus, the electrical conductivity of the soil solution is of most interest rather than the bulk electrical conductivity. For this reason, EC_{ss} was directly measured with a salinity bridge and

some EC_b data were used randomly to check the trend of salinity distributions over the root zone, using the following equation (Dirksen, 1996):

$$EC_b = 1.06 - 3.45\rho_f + 1.75\rho_f^2 - 4.36\rho_f^3 + 12.96\rho_f^4 \quad 3.5$$

where ρ_f (-) is the final reflection coefficient obtained directly from the automatic wave form analysis.

An automated TDR system with 32 probes (Fig. 3.1b) was installed for 4 columns (8 position for each) in the greenhouse to obtain measurement series of ε at different depths in the root zone. Every 2 hours wave forms of all probes were measured, using a *Tektronix 1502B* cable tester and a multiplexer and control system, developed by *Heimovaara and Bouten* (1990). The wave forms were stored in a personal computer. The measurement and storage of 32 wave forms took about 11 minutes. The stored wave forms were analyzed with procedures and programs of *Heimovaara and Bouten* (1990). The wave forms collected for the manual TDR measurements were also analyzed with the same program. All volumetric soil water contents were obtained based on the calibration equation of 3.4.

3.10.2. Soil water pressure head

Soil water pressure heads in the tensiometry range were measured with tensiometers with individual pressure transducers (XCA4-01-150DN, Silicon Pressure Sensors; AE Sensors B.V; Dordrecht, The Netherlands) linked to a computerized control box. This facilitated a fully automated monitoring of soil water pressure heads with 16 tensiometers at the same times as the TDR measurements. Before starting any actual measurements in the soil columns, all tensiometers were filled with de-aired water and checked in water at different elevations. These measurements showed a high accuracy (in water). When the tensiometers were installed in two columns at different depths, they provided reasonable measurements in very wet conditions, but unfortunately, were unsatisfactory in dryer soil. Since the ceramics had a flat shape, the first suspicion was poor contact of the tensiometers with the soil as the soil dries out. If this was true, this problem could be improved by pushing the tensiometers a few centimeters further into the soil to facilitate better contact. By pushing the tensiometers 5 cm (in 2 steps, each step 2.5 cm) more inside the soil, the problem was not solved. Therefore, the readings collected by the control box were checked manually for the same tensiometers at the same depths. The result indicated large differences (55-135 cm) between the fully automated and manual measurements. The readings for both automated and manual measurements from saturation until very dry

conditions never decreased beyond -488 cm. Thus, we concluded that the flat-shaped tensiometers could not make good contact with the soil, and also the automated instruments did not register accurate values. Another attempt was made to use a newly developed osmotic tensiometer (*Dirksen, 1996*). The data collected by a datalogger were not reliable, however, suggesting that here also there was no good contact between the flat-shaped osmotic tensiometer and the soil. Due to these difficulties no tensiometry readings were made during the experimental periods. The water content data were later converted to corresponding soil water pressure heads, using the drying main soil water retention characteristics measured by the evaporation method (*Wind, 1966*).

3.10.3. Soil hydraulic functions

All irrigation waters were applied to the soil during the dark period. Thus, the applied water moved downward and distributed in the soil while there was no water uptake by the plants. The measurements were made in the light period when the plants transpired water and thus, all data were collected during drying periods. For this reason the soil hydraulic functions were determined for drying conditions, using *Wind's* evaporation method. This method was originally proposed by *Wind (1966)* and adapted for fully and semi-automated monitoring by *Halbertsma and Vermin (1994, 1997)*. The advantage of this method is that it can be used to determine both the unsaturated soil hydraulic conductivity and soil water retention characteristics. The range of determination of conductivity depends on the soil type and mostly lies between $h = -50$ cm to $h = -700$ cm. The range of determination of soil water retention characteristic is approximately between $h = 0$ cm to $h = -800$ cm.

Three soil columns were packed in PVC cylinders, 8 cm high and 10.1 cm diameter, with the same bulk density as the experimental columns. The samples were saturated from below by placing them in a few centimeters of water for 48 hours, and then allowed to dry by evaporation from the top surface. Soil water pressure heads were measured with 4 tensiometers (outer diameter 0.2 cm, length 1.5 cm) horizontally installed into pre-bored holes at heights of 1, 3, 5 and 7 cm from the bottom of the soil samples. Each tensiometer was connected to a pressure transducer. Each soil column was placed on an electronic scale (accuracy = 0.1 g). First, the top of the samples was covered and the saturated samples and tensiometers were equilibrated for a few hours. When the top lid was removed, the initial evaporation rate in the controlled environment (temperature = 20 °C, relative humidity = 50 %) was approximately 1.5 mm/h. At regular intervals, the hydraulic heads and total weight of the soil columns were measured and recorded in a personal computer. After the upper tensiometer failed to function due to air entry, the soil was removed from the cylinder, weighed and dried at 105 °C to determine the average water content at the end of the

experiment. From these data and the measured weights the average water content during the experiment was calculated. The method assumes that the soil sample is homogeneous in its hydraulic properties, thus the water content of each compartment can be estimated from the water content of the whole sample and the tensiometer readings. From these data the $K-h-\theta$ relationships were calculated, using an adaptation of *Wind's* method (*Halbertsma and Veerman, 1994*). The nonlinear least-squares optimization program *RETC* (*Van Genuchten et al., 1991*) was used to obtain the values for the parameters in Eqs. 2.6 and 2.8, shown in Table 3.2. The hydraulic functions of soil column 2 are depicted in Fig. 3.3.

Table 3.2. Parameter values of the analytical expressions of *Van Genuchten* (Eq.2.6) and *Mualem* (Eq. 2.8) for three columns packed at a bulk density of 1.42 g/cm^3 , obtained with the nonlinear least-square optimization program *RETC*.

Soil column	θ_r $\text{cm}^3 \text{ cm}^{-3}$	θ_s $\text{cm}^3 \text{ cm}^{-3}$	K_s cm d^{-1}	α -	n -	l -
1	0.010	0.438	20.790	0.0116	1.387	-1.000
2	0.010	0.460	19.528	0.0197	1.584	-1.000
3	0.010	0.460	20.561	0.0146	1.386	-1.000

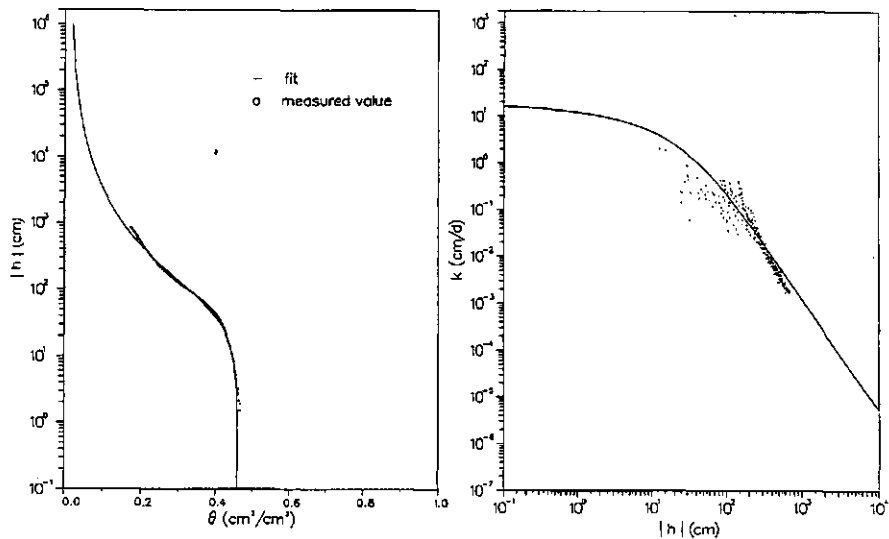


Figure 3.3. Water retention characteristic (left) and hydraulic conductivity characteristic (right) for soil column 2. The *Van Genuchten-Mualem* parameter values are given in Table 3.2.

3.10.4. Leaf water potential

Leaf water potentials (*LWP*) can be considered to reflect the whole soil-root-water-plant-climate system. Therefore, it was important that this be measured as accurately as possible under the nonuniform soil water osmotic and pressure head conditions. *LWPs* were measured with a pressure chamber (Plant Water Status Console, Model 3005, Soilmoisture Equipment Co., Santa Barbara, California, USA). For the same reason as for the actual transpiration, the measurements were made manually twice a day. Before starting actual measurements, from seven days after harvesting until flowering stage, leaf water potentials were measured eight times a day at 6.00 (before turning the light on), 8.00, 10.00, 12.00, 14.00, 16.00, 18.00 and 20.00 hrs. The result of these extensive measurements indicated that for the climatic conditions in the greenhouse there was no considerable difference between 8.00 to 10.00 and 12.00 to 16.00. Thus, all *LWP* measurements were made at 10.00 in the morning and 14.00 in the afternoon. To obtain a complete picture for each experimental phase, *LWP* were measured 8 times a day at 2 hour intervals during one irrigation interval. The effect of growth on the leaf water potentials was considerable during the first three weeks of re-growth; thereafter, they became more stable. Since all stresses were introduced to the plants about 4-5 weeks after harvesting, the data obtained during stress belong to this stable period. All of the reported *LWP* data are the average of at least 5 measurements. The leaves were taken uniformly from the top of common stems that were exposed to direct light. To reduce the experimental error, each leaf was put in the pressure chamber immediately after cutting. Each *LWP* measurement took about 2-3 minutes. A sample of full measurements of *LWP* for 3 days of the first experimental stage is given in Table 3.3.

Table 3.3. *LWP* (bar) variation during one irrigation interval under no stress condition. The data at 6.00 were obtained just before the lights were turned on. The column received irrigation water 10 hours before the first measurements.

Day	Time							
	6.00	8.00	10.00	12.00	14.00	16.00	18.00	20.00
1	-5.4	-9.1	-10.4	-12.1	-12.3	-12.6	-10.8	-7.5
2	-6.3	-10.3	-11.8	-12.2	-12.4	-13.2	-11.5	-8.8
3	-6.8	-11.2	-12.3	-12.5	-12.6	-13.2	-11.8	-9.6

3.10.5. Soil solution salinity

Root water uptake takes place against the osmotic potential of the soil water. Thus, soil solution salinity rather than the bulk electrical conductivity is the appropriate parameter to evaluate the influence of soil salinity on root water uptake. For this reason, soil solution salinities were measured in-situ with salinity sensors (Model 5100) and a salinity bridge (Model 5100, Soilmoisture Equipment Company, Santa Barbara, California, USA). All sensors were installed horizontally into the soil columns in one row at depth intervals of 5 cm in the top 30 cm and 10 cm below that. Since the transpiration of the plants in the greenhouse was high, it was expected that the applied solutes would concentrate in the root zone in a relatively short time. To find out the best time for the salinity measurements, one week monitoring with 2-hour time intervals was carried out. The results indicated that the sensitivity of the Salinity Bridge is not high enough to measure the small changes of EC_{ss} within a day. Thus, EC_{ss} was measured daily at 10.00 am and the values were converted to osmotic head (cm) according to (US. Salinity Laboratory Staff, 1954):

$$h_o = -36c = -360 EC_{ss} \quad 3.6$$

in which h_o is in cm; c is the solute concentration in $\mu \text{ mol/cm}^3$, and EC_{ss} in dS/m.

3.10.6. Transpiration

Both salinity and water deficit strongly influence plant transpiration; thus, actual transpiration measurements were essential for this study. At the beginning of the experiment, daily transpiration measurements were considered. Later, the number of measurements was increased to five per day. The plants needed 4-5 weeks for healthy re-growth after each cutting and had to be harvested a few days after development of secondary stems. Due to optimal conditions in the greenhouse, the secondary stems always appeared about 7-8 weeks after the last harvest. Thus the plant could be held under stress for about 20 days. The actual transpiration was obtained by weighing the columns. The amount of transpired water was converted to mm/h per surface area of the soil columns, rather than that of the plant canopy.

4. Root water uptake under nonuniform transient salinity stress

4.1. Introduction

Many investigations on root water uptake have been conducted under steady-state saline conditions. Most of these studies were carried out in controlled experimental conditions in which uniform salt distributions over the root zone were established and the soil solution changes over time were negligible. A large number of the so-called salt tolerance experiments (*Maas and Hoffman, 1977; Maas, 1990*), which are now accepted as a reference data base for salinity studies, were conducted under such conditions. In contrast, under field conditions such uniformity over the root zone is rare. Thus, the way that plants react to different degrees of salinity along its root system is important for understanding how plants integrate such effects. For instance, it is not yet clear whether under heterogeneous salinity condition plants react preliminary to the salinity of the upper or deeper part of the root zone.

The objective of this part of the study was to investigate the influence of different irrigation water salinities as well as different soil solution osmotic heads on root water uptake patterns, and to investigate which macroscopic model can provide the best agreement with the experimental data. Since the overall reaction of plants on different salinities is of most interest, the actual reaction of the plants in terms of transpiration was central for this study. Also, it was important to check the conceptual salinity approaches when dealing with the numerical simulation models. The concepts available for this purpose are originally based on the work of *Feddes et al. (1978)* in combination with the salinity reduction functions of *Maas and Hoffman (1977)*, *Van Genuchten (1987)*, and *Dirksen et al. (1993)*. These concepts were discussed in Chapter 1 and Chapter 2. This chapter consists of two main parts. First, after illustrating samples of experimental data, the macroscopic root water uptake model of *Feddes et al. (1978)* with the different salinity reduction functions are compared with experimental data. Second, the collected data are compared with results of numerical simulation with the model HYSWASOR.

4.2. Materials and methods

Alfalfa was seeded in packed cylindrical soil columns with a height of 65 cm and a diameter of 21 cm. The measurements started after healthy plants had developed. Since water stress was not allowed, in this part of the experiment the

irrigation intervals were relatively short (48 hours). Assuming no water uptake during the dark period, all irrigation waters were applied to the columns by flood irrigation immediately before turning off the lights in order to allow the applied water to distribute over the root zone in the time that the plants did not transpire water. The excess water was sucked out with a suction pump. This allowed us to assume that all downward water movement occurred at night, and that during the light period no downward water movement took place. To attain the target leaching fractions, the columns were saturated. Thus, it can be assumed that during the measurements hysteresis in soil water did not occur and the main drying curve of the soil moisture retention characteristic can be used. All measurements (with few exceptions) started after switching on the lights. The light period normally was 15 hours per day until 9.00 pm.

Water salinities were varied around the salinity threshold value of alfalfa, i.e. at 1.5, 2.0, 3.0, 4.0, and 5.0 dS/m, denoted as S_1 , S_2 , S_3 , S_4 , and S_5 , respectively. Soil water osmotic heads were obtained by converting the corresponding soil solution salinities according to Eq. 3.6. Since the plants react to the soil solution salinity EC_{ss} , the data were analysed based on EC_{ss} rather than soil bulk electrical conductivity EC_b .

Soil water content θ and EC_b were measured with the TDR equipment. Fully automated TDR equipment was used for 4 columns, while the remaining columns were measured manually. Soil water pressure heads h were obtained by converting θ to h based on the soil water retention characteristics given in Fig. 3.3 and Table 3.2. Salinity of irrigation and drainage waters were measured by a conductivity cell (Digimeter L21; Eijkelkamp, Agrisearch Equipment, The Netherlands).

Actual transpiration T_a measurements were made by suspending the columns and weighing them with a digital balance. The transpiration rate of each column has been measured at least 5 times a day. The transpired waters for each column were related to the surface area of the soil columns, rather than to the plant canopy. Leaf water potentials LWP were measured twice a day at 10.00 am and 2.00 pm with a pressure chamber. All of the LWP data reported here are the mean of at least 5 leaves, which have been taken from the top of each plant. For every treatment, detail LWP measurements were made at 2-hour intervals for one irrigation interval, starting before the lights were turned on until just before they were turned off.

4.3. Experimental data

A summary of all the irrigation intervals, except the first two of phase II (see Table 3.1) with only salinity stress is given in Table 4.1.

Table 4.1. Summary of experimental phase II.

Treatment	Water application	R	S ₁	S ₂	S ₃	S ₄	S ₅	
<i>EC_w</i> (dS/m)		Tap	1.5	2.0	3.0	4.0	5.0	
Target <i>LF</i> (-)		0.5	0.5	0.5	0.5	0.5	0.5	
Irrigation interval (d)		2	2	2	2	2	2	
Applied water (mm)	3	40	40	40	40	40	40	
	4	52	52	52	52	52	52	
	5	52	52	52	52	52	52	
	6	62	62	62	62	62	62	
	7	52	52	52	52	52	52	
	8	62	62	62	62	62	62	
	9	52	52	52	52	52	52	
	10	52	52	52	52	52	52	
	Actual <i>LF</i> (-)	3	0.39	0.44	0.48	0.51	0.59	0.60
		4	0.42	0.44	0.45	0.48	0.51	0.58
5		0.36	0.47	0.50	0.52	0.56	0.61	
6		0.34	0.39	0.40	0.42	0.49	0.58	
7		0.35	0.42	0.47	0.52	0.61	0.68	
8		0.32	0.38	0.43	0.51	0.65	0.67	
9		0.32	0.33	0.43	0.48	0.57	0.51	
10		0.27	0.34	0.41	0.46	0.51	0.56	
Transpired water (mm)		3	24.6	22.4	20.8	19.5	16.5	15.9
		4	26.0	25.4	24.8	21.5	21.3	19.6
	5	33.2	27.4	26.0	25.1	23.1	20.5	
	6	41.0	37.6	37.0	36.1	31.8	26.0	
	7	33.9	30.0	27.4	24.8	20.5	16.8	
	8	41.9	38.7	35.4	30.6	22.0	20.2	
	9	35.4	34.7	29.9	27.2	22.5	18.8	
	10	37.8	34.4	30.9	28.2	25.6	22.7	
	Drainage water (mm)	3	15.4	17.6	19.2	20.5	23.5	24.1
		4	22.0	22.9	23.4	24.9	26.6	30.0
5		18.8	24.6	26.0	26.9	28.9	31.5	
6		21.0	24.4	25.0	25.9	30.2	36.0	
7		18.1	22.0	24.6	27.2	31.5	35.5	
8		20.1	23.3	26.6	31.4	40.0	41.8	
9		16.6	17.3	22.1	24.8	29.5	33.2	
10		14.2	17.6	21.2	23.8	26.4	29.3	
<i>EC</i> of drainage water (dS/m)		3	-	2.35	2.25	2.90	3.10	3.60
		4	-	3.00	2.90	2.50	2.30	2.90
	5	-	3.15	4.05	4.65	4.15	5.25	
	6	-	3.70	4.40	5.30	5.70	7.30	
	7	-	4.50	5.10	7.30	7.80	8.70	
	8	-	4.45	7.65	8.25	8.80	8.50	
	9	-	4.30	8.00	8.40	8.60	9.10	
	10	-	4.60	8.30	8.50	9.10	9.90	

Figure 4.1 presents the water content distribution of all salinity treatments during the fifth irrigation interval. As depicted in these figures, the water content of the most saline treatment (S_5) was higher than the less saline treatment (S_1) as well as R. This indicates that increasing salinity reduces root water uptake. The magnitude of water content decrease due to root water uptake was not necessarily uniform over the root zone for each individual treatment. Most of the water was taken up in the top 25 cm of the root zone. As discussed in Chapter 1, according to ample reports the most active part of alfalfa roots is located in the first 50 cm of the rooting depth and in nonsaline conditions most of the water is taken up from this part. The depth of the experimental columns was 65 cm. Thus, the entire rooting depth can be considered as active, and it was expected that the plants would take up water relatively uniformly from different parts of the root zone. The water content changes over the root zone for the reference treatment (R) clearly indicate, however, that the plants took up water predominantly from the upper part while sufficient water was available everywhere in the soil profile. As depicted in Fig. 4.1, except for S_1 the water content decrease was more or less the same over the root zone. However, it should be noted that EC_{ss} was spatially variable over the root zone (Fig. 4.2). More uptake was expected at depths with lower salinities than the data indicate. Presumably, this is due to the high hydraulic conductivity at high water contents, causing water taken up from one depth to be compensated immediately from another depth. Figure 4.2 illustrates the EC_{ss} distribution of each individual saline treatment over the root zone. Despite applying relatively large leaching fractions and using highly soluble salts, the spatial variability of EC_{ss} over the root zone was still relatively large. In most cases, EC_{ss} increased with time. This implies that the soil solution was concentrated as a result of root water uptake. In most cases, this increase occurred over the whole rooting depth. The corresponding EC_b measurements by TDR for all the treatments are given in Fig. 4.3. These distributions are similar to the EC_{ss} . This suggests that the TDR and the salinity bridge equipment worked satisfactorily.

Figure 4.4 shows the sink term S distributions of all the treatments at the first day after the fifth irrigation interval. The sink terms have been calculated based on the continuity equation (Eq. 2.2) for 10 hour time interval. For the reference treatment R, most water was taken up from depth 10 cm. Figure 4.4 clearly shows that the uptake rate decreased over the root zone with increasing salinity. However, except for S_5 , the trend of uptake changes over the root zone was almost similar to that of R.

Figure 4.5 presents the absolute values of the negative leaf water heads, LWH , as function of time for all the treatments. According to these measurements, the largest change in LWH always happened after switching on the lights (at 6.00 am). This trend continued until 4 pm; after that, the LWH for all the treatments increased due to the lower temperature and higher air circulation in the greenhouse.

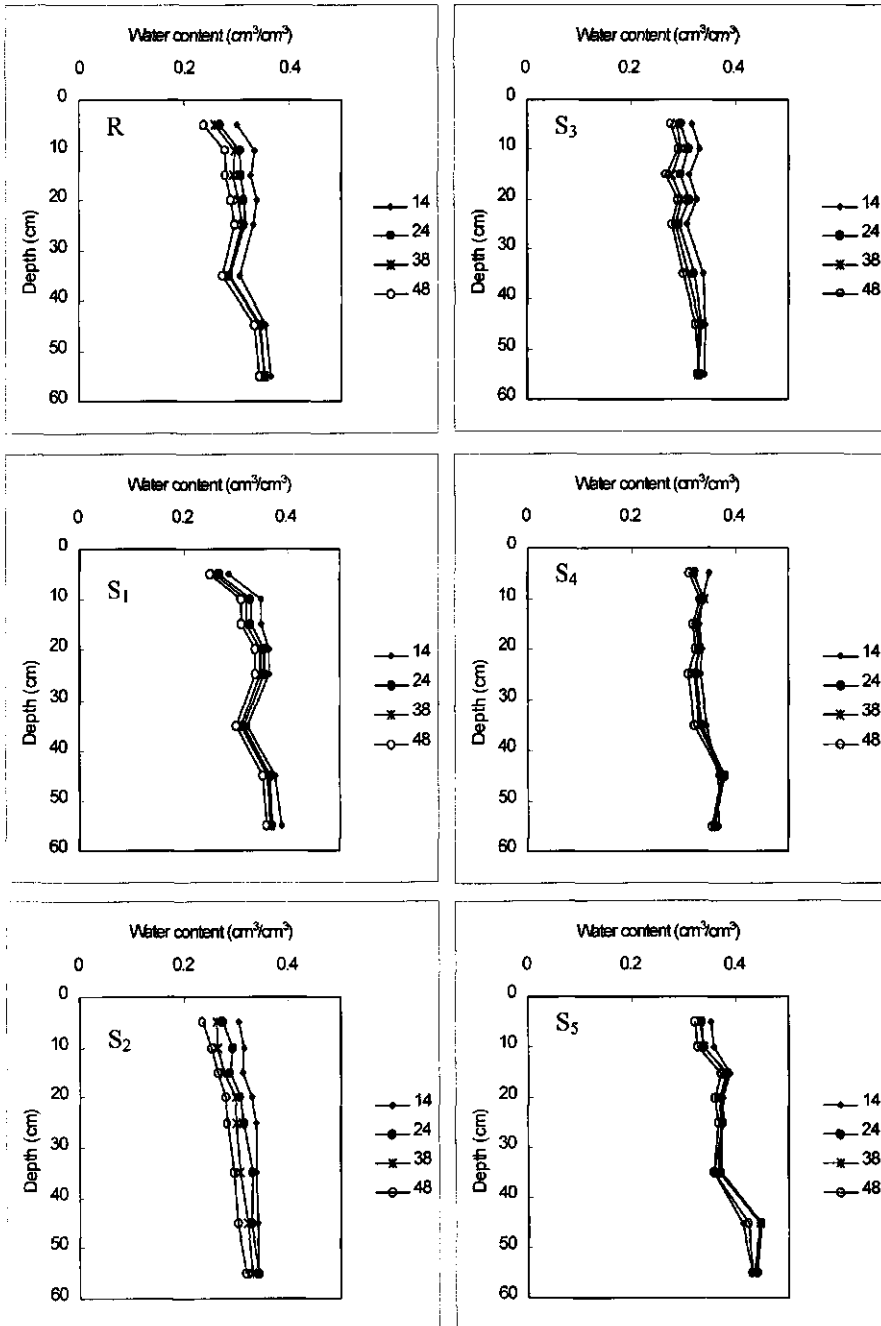


Figure 4.1. Water content distributions of the reference R and salinity treatments S₁, S₂, S₃, S₄ and S₅ at 14, 24, 38 and 48 hours after irrigation.

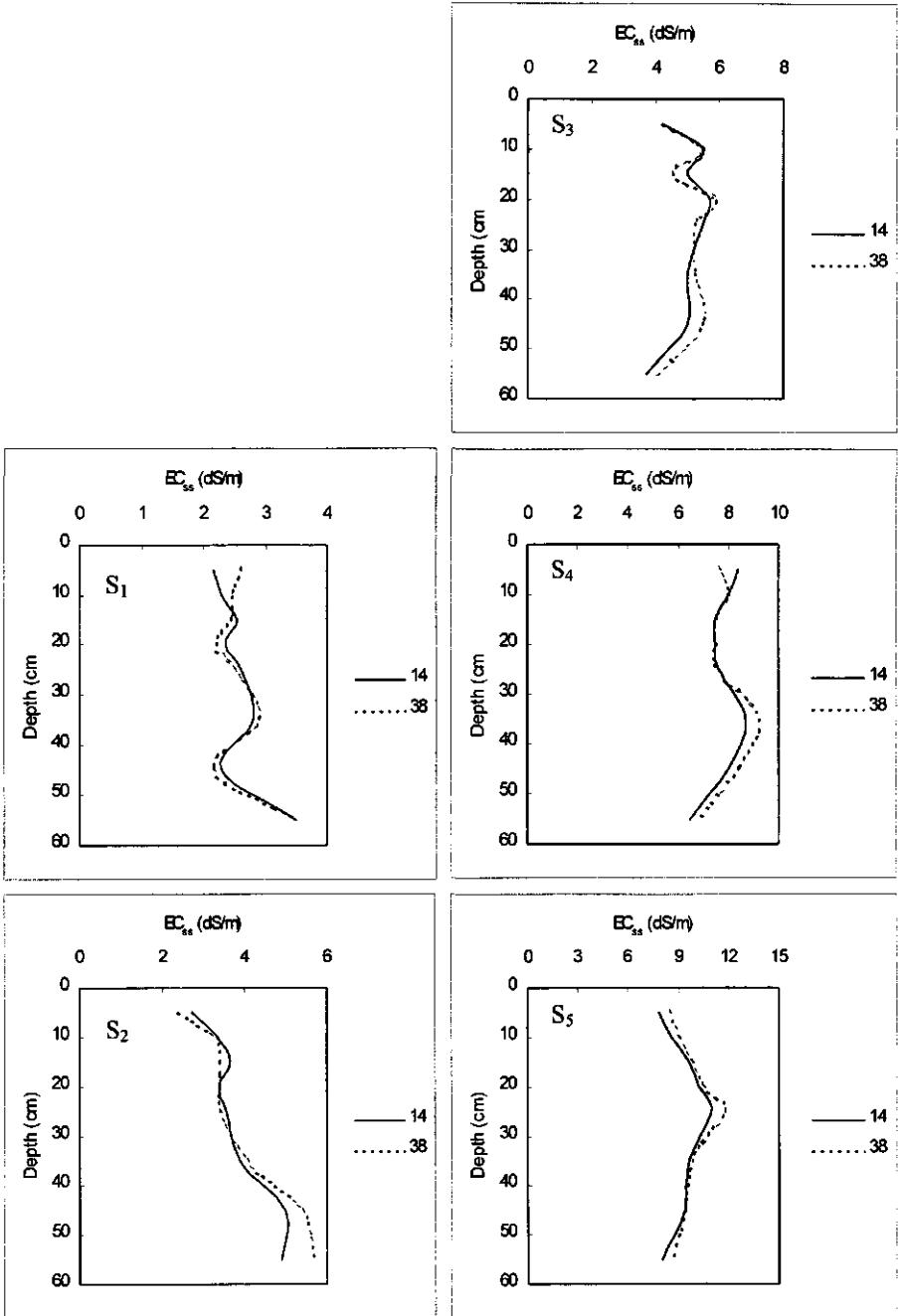


Figure 4.2. Soil solution electrical conductivity EC_{ss} distributions of salinity treatments S₁, S₂, S₃, S₄ and S₅ over the root zone for 14 and 38 hours after the irrigation.

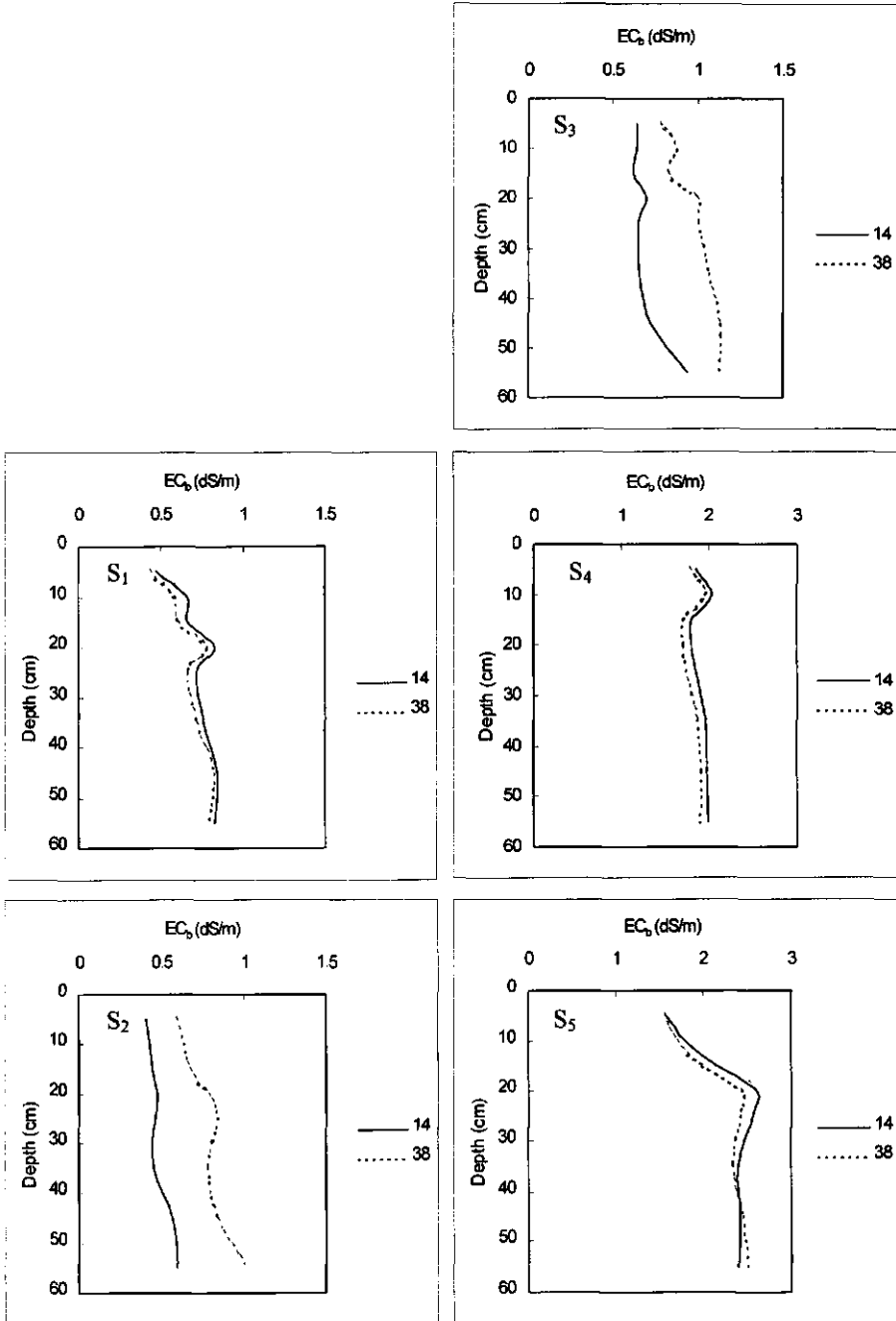


Figure 4.3. Soil bulk electrical conductivity distributions of the salinity treatments S₁, S₂, S₃, S₄ and S₅ at 14 and 48 hours after irrigation.

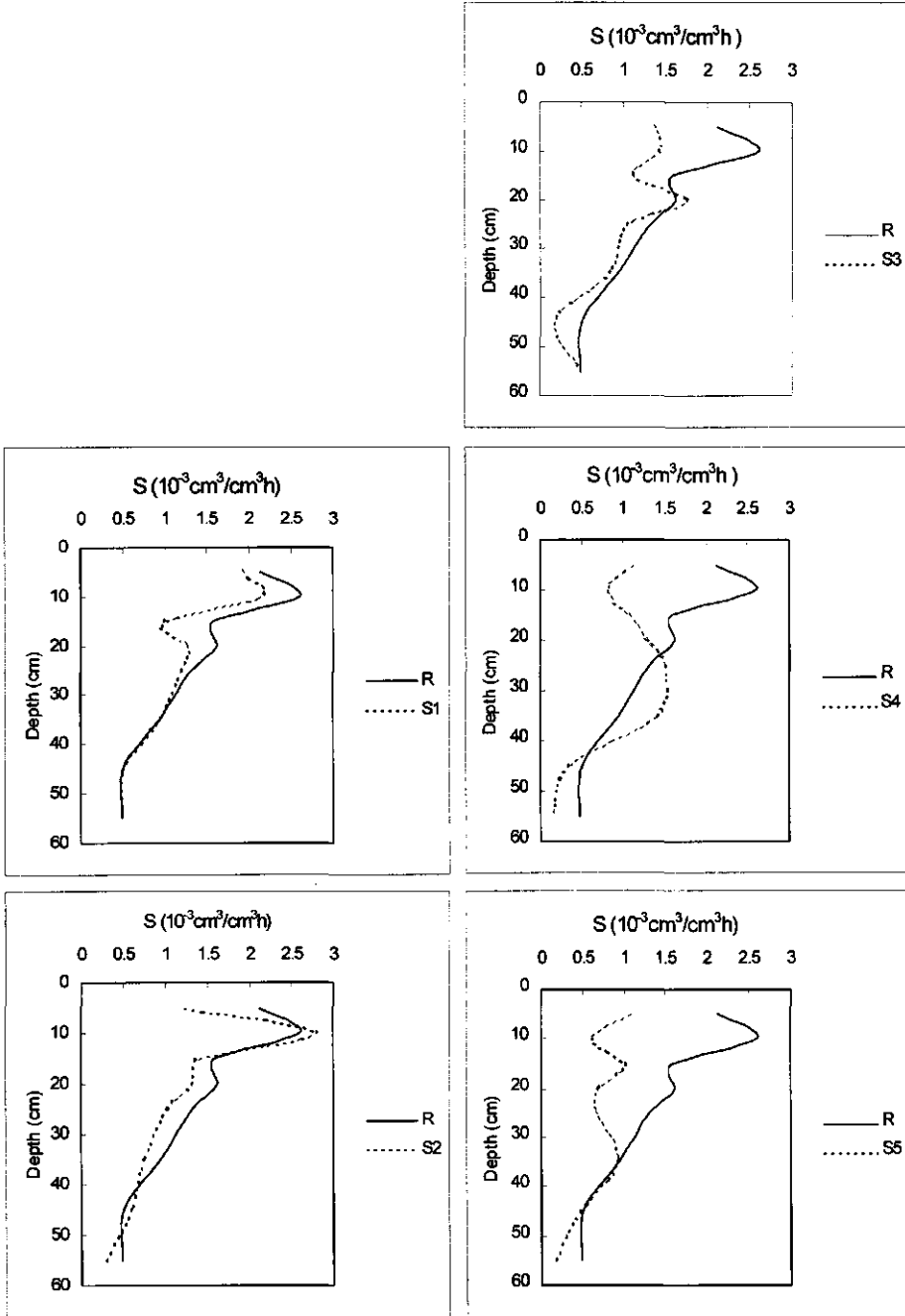


Figure 4.4. Comparison between the sink term distributions of the reference R and salinity treatments S_1, S_2, S_3, S_4 and S_5 at 38 hours after irrigation. Corresponding water content and soil solution salinity distributions are depicted in Figures 4.1 and 4.2, respectively.

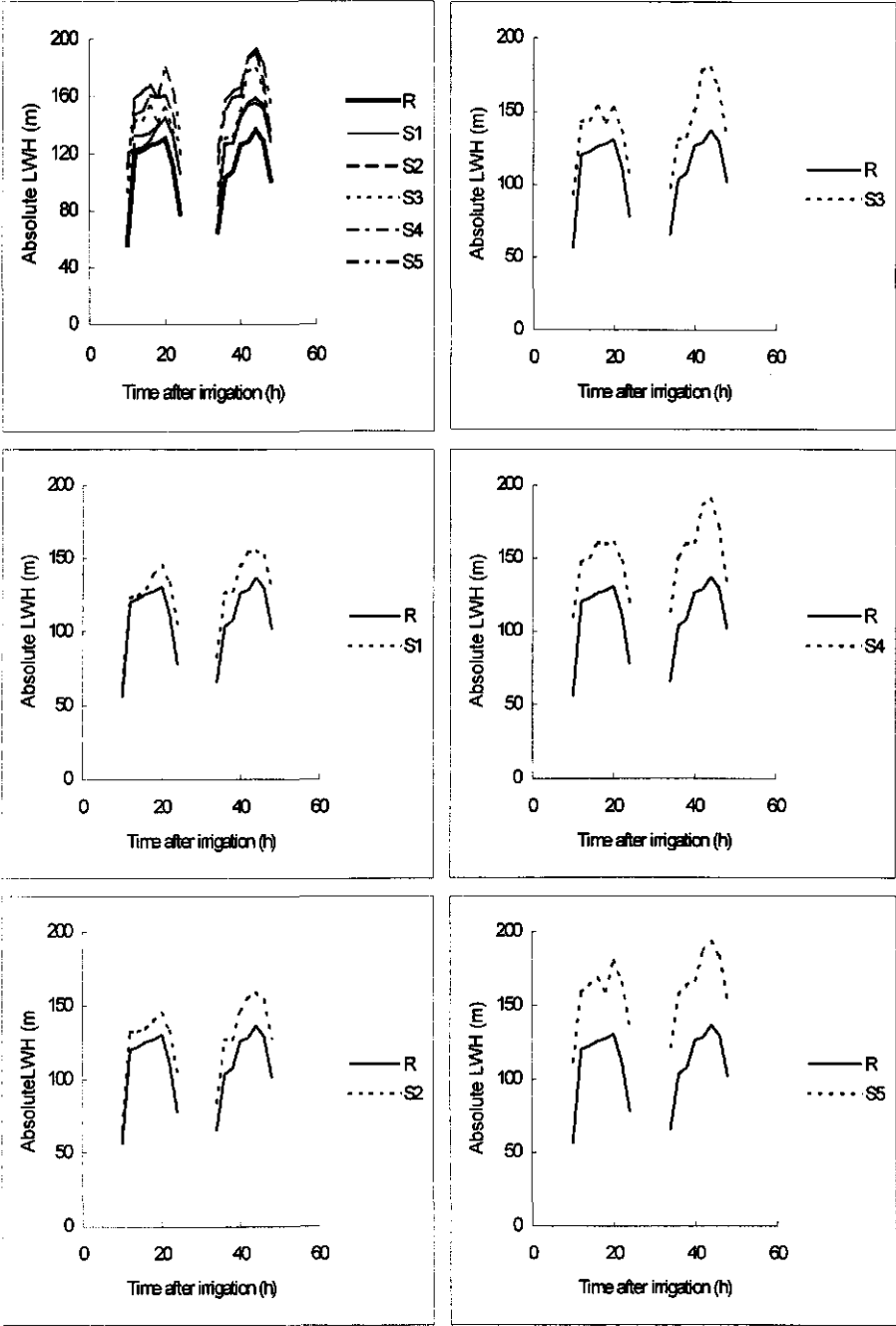


Figure 4.5. Absolute leaf water head *LWH* changes as function of time after the irrigation for the reference *R* and salinity stress treatments *S*₁, *S*₂, *S*₃, *S*₄ and *S*₅. Times 10 and 34 in the figures corresponds to 6.00 am.

The climatic conditions of the greenhouse did not differ sensibly between about 10.00 and 12.00 h; as a result, there was little change in *LWH*. The recovery of *LWH* of the stressed plants during the dark period was enough to survive and tolerate the next stressed day, but the *LWH* did not recover to the value of the previous day.

Cumulative transpired water (mm) for all the treatments is depicted in Fig. 4.6. The total transpired water for R was always higher than that of the saline treatments (with an exception for S_1 at the first irrigation interval). The transpired water of R in some instances was about two times more than that of S_5 . The quantity of water sucked out from R was always less than that of the saline treatments. This can be related to the higher remaining water content just before applying the next irrigation to the soil columns.

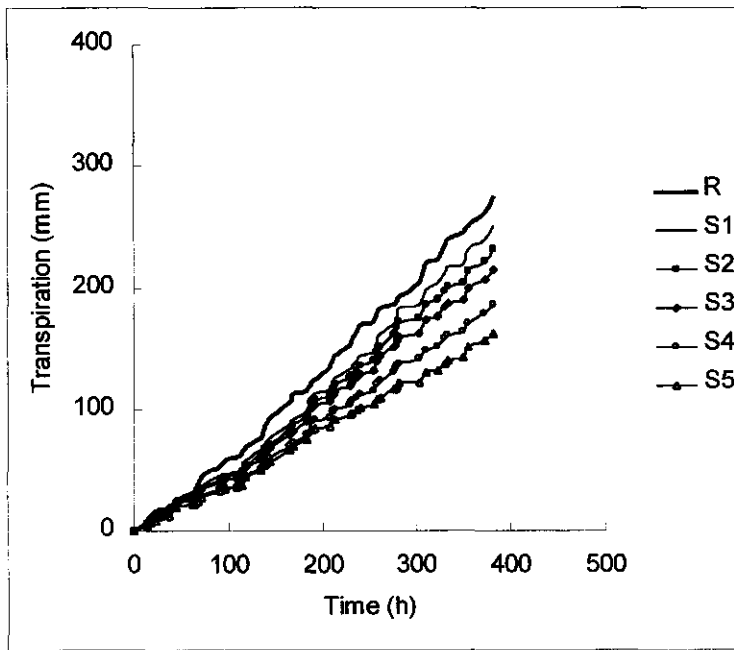


Figure 4.6. Cumulative transpired water of the reference R and salinity treatments S_1 , S_2 , S_3 , S_4 and S_5 for the whole growth period.

4.4. Salt heterogeneity and relative root water uptake

Soil salinity is seldom uniform with depth, and at any given depth it varies with time. The question of how plants integrate this space and time varying salinity is important because by changing management practices it is possible to change both the frequency of salinity fluctuations and the distribution of salinity over the root zone. Increase in soil salinity as a result of evaporation occurs at the soil surface, while the

site of separation of salts from the soil water due to root water uptake takes place at the soil-root interface. The actual distribution of salts over the root zone reflects the water extraction pattern, which depends not only on root distribution, but also upon root activity. Root distribution over the root zone depends to a great extent upon whether the root system developed into a saline or nonsaline profile. In the heterogeneous saline profile, roots do not penetrate readily into highly saline depths, but once established in nonsaline soil, creating salinity does not change the root distribution drastically. In the current study, the root system was well developed before introducing salinity in the root zone. Thus the distribution of soil salinity over the root zone was largely dependent on the root water uptake patterns.

Theoretical concepts of how plants integrate soil salinity have not been fully developed and verified. To avoid difficulties arising from complications of plant integration, many studies have been conducted in uniform soil solution salinities. While studies under such uniform conditions can improve understanding of root water uptake in saline soils, the question still remains unanswered. In the nonuniform salt distribution situation, it is frequently assumed that the plant responds to the average salinity in such circumstances. Concerning this heterogeneity, there are three contradictory ideas in the literature (see Ch. 1). The first states that the relative uptake is strongly affected by the more saline part in the root zone. The second suggests that the water uptake can better be related to the salinity of the upper part of the root zone than that of the deeper part. The third proposed that the plant response can be described better by some weighted mean salinity (*Raats, 1974a; Hoffman and Van Genuchten, 1983; Dirksen, 1985; Dirksen et al., 1994*). *Dirksen (1985)* proposed the following uptake-weighted mean osmotic head:

$$h_o = \frac{\int_0^{\infty} S(z) h_o(z) dz}{\int_0^{\infty} S(z) dz} \quad 4.1$$

The analyses made by *Dirksen (1985)* and *Dirksen et al. (1994)* on the experimentally collected data with Eq. 4.1 indicated satisfactory results. However, investigations on the mentioned controversy are rare and it is not yet clear which one is the closest to reality. The main reason for this scarcity is that required data cannot be obtained easily and the subject should be investigated in fully controlled conditions which is either time consuming and/or expensive.

Probably, the best way to check these contradictory ideas is to create different salt distributions over the root zone in different columns with the same mean salinities. Such conditions occurred in a few of our experimental columns. Table 4.2 represents the data obtained under such conditions. The average EC_{ss} of all columns was about

Table 4.2. Soil water content θ , soil solution salinity EC_{ss} , and water uptake rate S for four soil columns with about the same average EC_{ss} , T_a/T_p , and LWP_R/LWP_{Si} .

Soil Column	Depth cm	EC_{ss} dS/m	θ cm ³ /cm ³	S 10 ⁻³ cm ³ /cm ³ h	T_a/T_p -	LWP_R/LWP_{Si} -
A	5	2.5	0.290	2.34	0.85	0.86
	10	3.3	0.296	0.68		
	15	2.8	0.301	1.46		
	20	2.2	0.317	1.68		
	25	2.2	0.317	1.47		
	35	2.7	0.332	1.87		
	45	2.8	0.338	1.68		
	55	1.8	0.351	2.30		
	Average	2.5	0.320	1.76		
B	5	4.1	0.269	0.72	0.84	0.84
	10	3.6	0.291	0.88		
	15	3.3	0.276	0.91		
	20	3.0	0.280	1.95		
	25	3.4	0.272	1.45		
	35	3.1	0.281	1.68		
	45	2.7	0.336	1.15		
	55	0.3	0.341	2.61		
	Average	2.7	0.300	1.49		
C	5	2.0	0.206	1.65	0.86	0.89
	10	2.2	0.268	2.65		
	15	2.7	0.248	1.08		
	20	2.8	0.284	2.09		
	25	2.6	0.244	0.53		
	35	2.6	0.244	0.81		
	45	2.4	0.296	1.92		
	55	3.3	0.307	0.72		
	Average	2.6	0.270	1.36		
D	5	2.0	0.201	1.05	0.84	0.78
	10	2.1	0.267	1.89		
	15	1.9	0.245	1.76		
	20	2.0	0.281	2.18		
	25	1.9	0.239	0.66		
	35	1.9	0.240	0.64		
	45	2.0	0.291	0.94		
	55	5.6	0.297	0.89		
	Average	2.6	0.260	1.15		

2.6 dS/m. In these experimental columns, the water content distributions over the root zone were not exactly the same for all the columns but they were very close to each other, and were high enough to prevent any water deficit. The interesting observation of these columns was that the relative uptake (T_a/T_p) as well as the relative leaf water head (LWH_R/LWH_{Si}) for all of them were almost the same. The sink term is calculated based on Eq. 2.2.

Root water uptake under heterogeneous soil water osmotic head conditions seems to be a function of several factors such as soil solution electrical conductivity, water content, depth, and root density. Since the plants in each container were treated uniformly before creating any stress, we assume that the root density in all the columns was the same. Table 4.2 will be discussed in the following steps in order to find a conclusion for such heterogeneity:

1. Equal water content and same depth, different salinity

In column A, the water content from 5 to 15 cm was relatively constant. By increasing EC_{ss} from 2.5 to 3.3 dS/m, the uptake rate S decreased sharply from 2.34 to $0.68 \times 10^{-3} \text{ cm}^3/\text{cm}^3 \text{ h}$. Again, by decreasing salinity from 3.3 to 2.8 dS/m at 15 cm depth S increased drastically from 0.68 to $1.46 \times 10^{-3} \text{ cm}^3/\text{cm}^3 \text{ h}$. At the bottom of this column a decrease of salinity from 2.8 to 1.8 dS/m (having the same water content) increased S by the magnitude of $0.62 \times 10^{-3} \text{ cm}^3/\text{cm}^3 \text{ h}$ per 1dS/m. This magnitude is comparable but not equal to that at 5-15 cm depth. In column B, θ is the same at 15 and 20 cm. While salinity decreased from 3.3 to 3.0 dS/m, S increased from 0.91 to $1.95 \times 10^{-3} \text{ cm}^3/\text{cm}^3 \text{ h}$. Again, by a salinity increase from 3.0 to 3.4 dS/m, S changed from 1.95 to $1.45 \times 10^{-3} \text{ cm}^3/\text{cm}^3 \text{ h}$, and by a salinity decrease from 3.4 to 3.1 dS/m, S increased from 1.45 to $1.68 \times 10^{-3} \text{ cm}^3/\text{cm}^3 \text{ h}$. In column C, by a salinity increase from 2.4 to 3.3 dS/m at depths 45 and 55 cm the relative uptake decreased sharply from 1.92 to $0.72 \times 10^{-3} \text{ cm}^3/\text{cm}^3 \text{ h}$. Also in column C, both EC_{ss} and θ are the same at 25 and 35 cm, while S decreased from 0.81 to $0.53 \times 10^{-3} \text{ cm}^3/\text{cm}^3 \text{ h}$. In column D, by a salinity increase from 2.0 dS/m at depth 45 cm to 5.6 dS/m at depth 55 cm, S decreased slightly. Even though the magnitudes of the S changes per unit salinity change is not equal for the reported data, the trend of the S variations support the assumption of Dirksen *et al.* (1994).

2. Equal salinity, different water content

In column D, the salinity of the soil solution is about the same except for the last increment and the main difference is in water content. In the top of the column (5 - 10 cm) the water content is quite different, the soil solution salinity is the same, and the sink term increased from 1.05 to $1.89 \times 10^{-3} \text{ cm}^3/\text{cm}^3 \text{ h}$. At the next depth (15 cm), by

decreasing θ from 0.267 to 0.245 cm^3/cm^3 , the sink term was also decreased from 1.89 to 1.76 $\times 10^{-3}$ cm^3/cm^3 h. At the depths of 20 and 25 cm by decreasing θ from 0.281 to 0.239 cm^3/cm^3 the uptake rate was decreased to 0.66 $\times 10^{-3}$ cm^3/m^3 h. However, having the same EC_{ss} and θ at depths 25 and 35 cm, almost the same S value occurred. These observations suggest that at constant EC_{ss} , higher θ provides higher uptake rate. Note that this conclusion is drawn for low amounts of salinity.

3. Equal salinity and water content, different depth

In column D, at depth 15 and 35 cm with $EC_{ss} = 1.9$ dS/m and $\theta = 0.24$ cm^3/cm^3 , S decreased sharply from 1.76 to 0.64 $\times 10^{-3}$ cm^3/cm^3 h. Further, in column A at depths 20 and 25 cm both θ and EC_{ss} were equal, and S was almost the same. However, S at depth 15 cm was less than that at 5 cm. This can be related to the influence of depth on water uptake rate, in as much as the plants prefer to provide their demand from the upper parts.

These observations indicate that even with this detailed experiment, drawing a clear picture on how plants integrate under heterogeneous salinity conditions is rather complicated, if not impossible. Remains the interesting observation that all the experimental columns depicted in Table 4.2 with about the same mean salinity exhibited almost the same relative transpiration rates and relative leaf water heads. Thus, *leaving all complications behind, we will follow the macroscopic root water uptake under saline conditions based on the soil solution osmotic head averaged over the root zone.*

4.5. Test of theoretical reduction functions against experimental data

In this section, the experimentally collected data are compared with existing salinity reduction functions. These functions were introduced and discussed in chapter 2 (Eq. 2.33, Eq. 2.35, and Eq. 2.36). They are empirical in nature and leave some questions to be answered. First, it is not yet clear if a so-called crop response function (Eq. 2.33) can be used as a reduction term in a macroscopic root water uptake model. If so, it is not clear whether or not the same parameter values can be employed. Furthermore, the linearity of the widely used Eq. 2.33 is questionable and it is now clear that the salinity threshold value varies with climate and soil conditions. For instance, in gypsiferous soils plants can tolerate EC_{ss} about 4 dS/m higher than in other soils (Maas, 1990). Also, by increasing the evaporative demand the salinity threshold value decreases. Equation 2.33 contains two input parameters, the salinity threshold value and the slope. If the threshold value varies due to high evaporative

demand, it is not yet clear whether the slope proposed by *Maas and Hoffman (1977)* is applicable, and if not what modification should be made.

In both equations 2.35 and 2.36 the shape of the function is strongly dominated by the exponent p and $h_{0.50}$, while there is still no physical or empirical definition for the former. It is of most interest to find (at least) an empirical definition for p . Also, it is practically difficult to obtain $h_{0.50}$ as one of the main parameters needed in the equations. An interesting subject is whether the latter can be replaced by a relatively simple parameter. In this section, first the salinity reduction functions will be compared with the experimental data to find out which function can fit the data best, and then will be tried to answer the above mentioned questions. The variability of the experimental *LWP* data as function of different soil solution salinities are also demonstrated and discussed.

In the following comparisons, the data were collected from all the irrigation intervals. The reported EC_{ss} data are the mean values over the root zone. The relative uptake is defined as

$$\frac{\int_0^{z_r} S \, dz}{\int_0^{z_r} S_{\max} \, dz} = \frac{T_a}{T_p} = \alpha(h_0) \tag{4.2}$$

will be compared with the measured T_a/T_p for the corresponding soil solution salinities.

4.5.1. Comparison of conceptual soil salinity reduction functions with experimental data

Figure 4.7a presents the relative transpiration $\alpha = T_a/T_p$ as function of the mean soil solution salinity. Either a linear (Figure 4.7b) or a nonlinear (Fig. 4.7c) shape can be fitted to the experimental data. In Fig. 4.7b the soil solution salinity threshold value EC^* and $h_{0.50}$ value are about 2 dS/m (-720 cm) and -2880 cm (8 dS/m), respectively. The experimental EC^* is half of that reported by *Maas and Hoffman (1977)* for alfalfa and less than that obtained by *Dirksen et al. (1993)*. In the case of linear fitting, the experimental data were compared with the linear Eq. 2.33 as depicted in Fig. 4.7d. In this figure, the originally proposed parameter values for EC^* ($EC_{ss} = 4$ dS/m) and the slope (0.073 m/dS) were compared with the experimentally obtained parameter values and the best linear fitting, respectively. As shown in Fig. 4.7d, most of the experimental data are underestimated if the proposed EC^* by *Maas and Hoffman* is used. On the other hand, using the experimentally obtained EC^* with the same slope of *Maas and Hoffman*, provides almost the same fitting as the best fitted line.

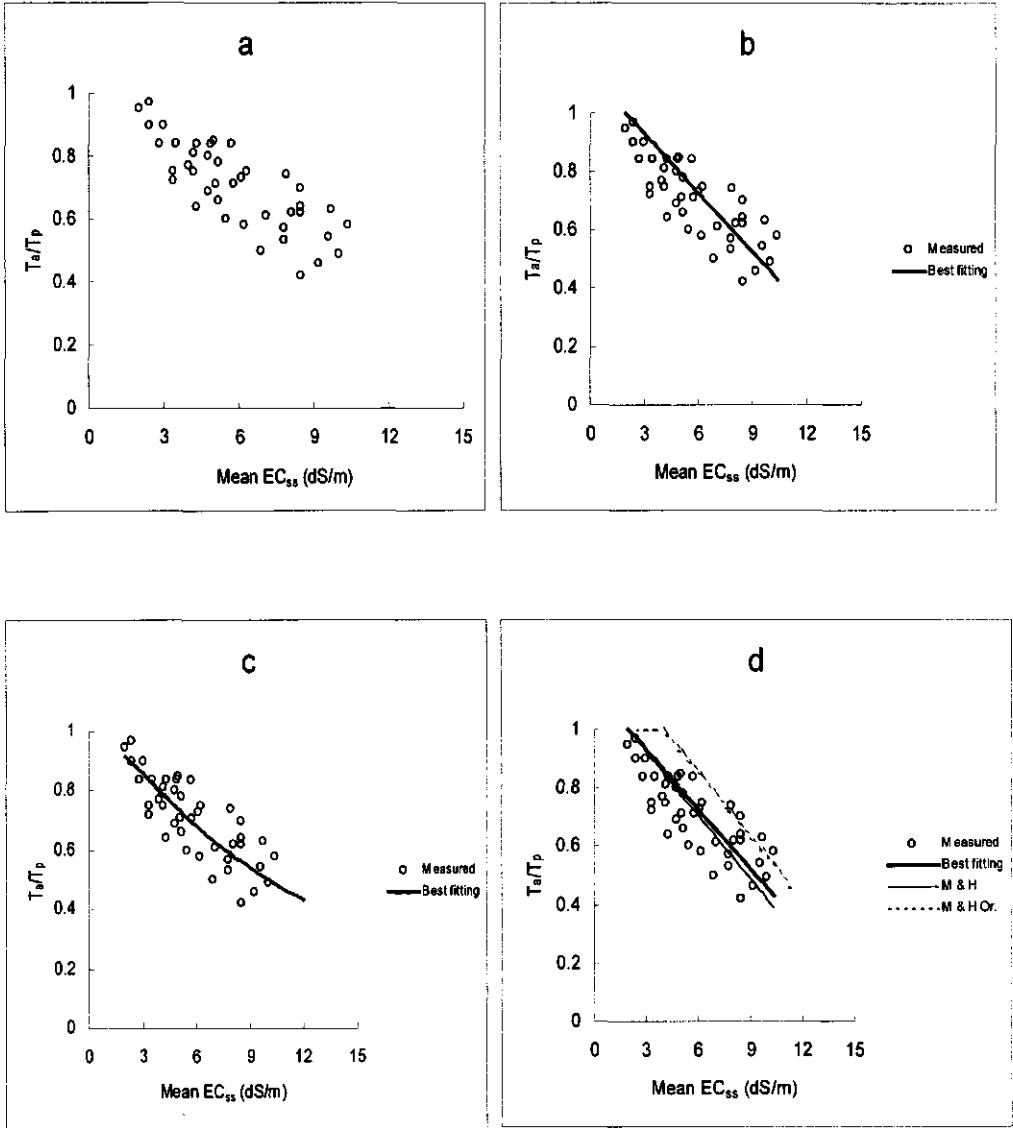


Figure 4.7. The relation between the experimental relative transpiration T_a/T_p and the mean soil solution salinity over the root zone. a: the measured data; b: the best linear fit; c: the best nonlinear fit; d: comparison between the best linear fit, the original *Maas and Hoffman* (1977) parameter values, and the *Maas and Hoffman* function with the experimentally obtained threshold value and slope.

This implies that Eq. 2.33 is more sensitive to its threshold value than the slope. Thus, future investigations may need to be more focused on quantification of EC^* under different soil and climatic conditions.

In the case of nonlinear fitting, the experimental data are compared with Eqs. 2.35 and 2.36 as illustrated in Figs. 4.8a and 4.8b, respectively. *Van Genuchten and Hoffman* (1984), and *Van Genuchten* (1987) fit their data with the dimensionless exponent $p = 3$, while *Dirksen et al.* (1993) obtained the best fit with $p = 1.5$. The latter obtained $h_{0.50} = -3900$ cm and the threshold value $h_o^* = -2800$ cm from the fitted data. *Van Genuchten and Hoffman* (1984) used $h_{0.50} = -6300$ cm from the database of *Maas and Hoffman*. When these values were used in Eqs. 2.35 and 2.36, the agreement between the calculated and experimental data was unsatisfactory. Both equations were sensitive to $h_{0.50}$, while Eq. 2.36 to a lesser extent was sensitive to h_o^* . Thus, in Figs. 4.8a and 4.8b the experimentally obtained values for h_o^* and $h_{0.50}$ with $p = 1.5$ and $p = 3$ were used and compared with the best nonlinear fitted curve and the experimental data. Also, since p in these equations is not yet defined, an alternative is proposed. Indeed, p is a shape parameter, as are h_o^* and $h_{0.50}$, but the influence of $h_{0.50}$ is larger than that of h_o^* . Similar to *Van Genuchten* (1987), I assume that p is crop, soil and climate-specific, and propose that the following ratio be used until further evidence confirms or rejects it:

$$p = \frac{h_{0.50}}{h_{0.50} - h_o^*} \quad 4.3$$

The difficulty of obtaining $h_{0.50}$ remains unsolved.

Figure 4.8a illustrates the agreement between the data obtained and calculated with Eq. 2.35. In this figure the values $p = 3$ (*Van Genuchten*, 1987), $p = 1.5$ (*Dirksen et al.* 1993) and $p = 1.35$ (Eq. 4.3) are used. As expected, the latter in Eq. 2.35 does not provide a satisfactory agreement with the experimental data. The reason is that Eq. 2.35 does not contain a salinity threshold value, while it is a component of Eq. 4.3. Figure 4.8b compares the data obtained and calculated with Eq. 2.36. The same parameter values are used in this figure as for Fig. 4.8a. As can be seen in Fig. 4.8b, the exponent obtained with Eq. 4.3 gives good agreement with the experimental data, and is close to that obtained with $p = 1.5$. An interesting observation about Eq. 4.3 is that it provides about the same value as that derived from the database by *Maas and Hoffman* for alfalfa.

Equation 2.36 ($r = 0.80$) provides better correlation with the experimental data than Eq. 2.35 ($r = 0.75$). This can be related to the salinity threshold parameter in Eq. 2.36, which makes this model more precise.

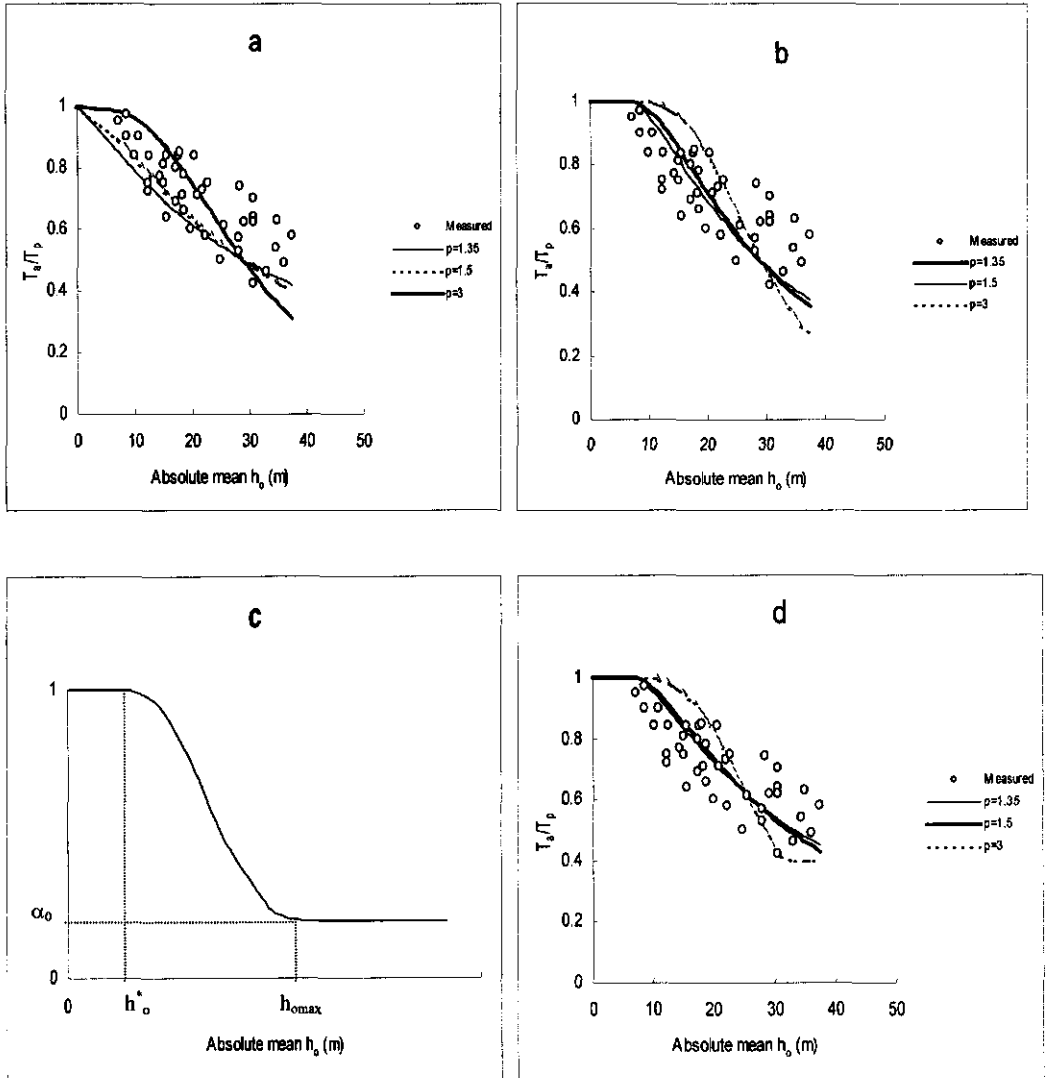


Figure 4.8. The relation between the measured relative transpiration T_a/T_p and mean absolute osmotic head and that calculated with reduction functions. a: Eq. 2.35; b: Eq. 2.36; and d: Eq. 4.4 for different values of the exponent p . Schematic representation of the nonlinear two-threshold reduction function Eq. 4.4 is shown in c.

In conclusion, Eq. 2.33 can be used as a salinity reduction function in the macroscopic root water uptake model of Feddes *et al.* (1978), but it is very sensitive to the salinity threshold value. Secondly, the presented experimental data suggest a nonlinear trend similar to the data reported by Dirksen *et al.* (1993) and some others. Such nonlinearity should be taken into account for detailed and more accurate purposes such as numerical simulation models. Equations 2.35 and 2.36 are more sensitive to p than h_{050} , and therefore, for convenience sake should be defined at least empirically or replaced by simpler parameters. The proposed Eq. 4.3 to determine p empirically is promising, but it still contains h_{050} as an input parameter which is difficult to obtain. Having a salinity threshold parameter, Eq. 2.36 is in principle more reliable than Eq. 2.35. Similarly to Eq. 2.35, an important limitation is the unavailability of h_{050} for a large number of crops, as it is hard to obtain this value even in completely controlled experiments. Equation 4.3 provides almost the same value for p as that which can be derived from the database of Maas and Hoffman for alfalfa. This might be due to the slight nonlinearity of the experimental data. However, it is not yet clear if this observation can be expanded to other plants. If so, the only parameter needed to specify Eq. 4.3 is the salinity threshold value. Thus, the database of Maas and Hoffman can be used to transform their linear function to the nonlinear one.

4.5.2. A nonlinear two-threshold reduction function for salinity stress

The observations reported in the previous subsection clearly imply the need for a simple and nonlinear function with accessible parameters. We have seen that all nonlinear reduction functions are sensitive to their parameter values. As discussed, Eqs. 2.35 and 2.36 could not fit our experimental data if the parameter values proposed by the original authors are used. If for a moment we assume that the definition of p in Eq. 4.3 is accurate enough, at least h_{050} should be replaced by another parameter. Equation 2.35 does not employ the threshold value as an input parameter.

The presented data indicate a smooth nonlinear shape of the reduction term for saline conditions. The low degree of nonlinearity appeared to be the reason for the good agreement between the experimental data and those calculated with Eq. 2.33. This agreement was especially good in the range of $\alpha = 1$ to about $\alpha = 0.6$. For higher salinity, the nonlinearity plays a significant role, which has to be taken into consideration. The advantage of Eq. 2.33 is its simplicity, but it contains the following shortcomings:

- Similar to any other biological system, a linear reduction function is far from reality. There is ample evidence in the literature that a nonlinear function can better fit actual

data. (Van Genuchten and Hoffman, 1984; Dirksen, 1985; Van Genuchten, 1987; Dirksen et al., 1993, 1994).

- At a certain salinity, a linear reduction function becomes zero. For alfalfa this value is about $EC_e = 14$ dS/m (Maas and Hoffman, 1977). Much evidence in the literature does not support this. When the water content is high enough, wilting due to salinity occurs at much higher soil solution salinities than what follows from the linear extrapolation of Eq. 2.33 (for more detail see Ch. 1 and Ch. 2).
- The equation is rather sensitive to the salinity threshold value, while the latter is influenced by the climatic conditions (evaporative demand), soil type, and the kind of soluble salts in the root zone. Because the model contains only two input parameters, by changing the threshold value for one climatic condition to that for another, the accuracy of the model is significantly changed.

The shortcomings of the nonlinear reduction functions Eq. 2.35 and Eq. 2.36 are:

- they are highly sensitive to their exponent, which has not yet been defined.
- both equations employ h_{o50} as an input parameter, which is very difficult to determine.
- it is not clear at which salinity the reduction term approaches a minimum.

Based on the above mentioned points, I suggest as modification for Eq. 2.36:

$$\alpha(h_o) = \frac{1}{1 + \left(\frac{1 - \alpha_o}{\alpha_o} \right) \left[\frac{h_o^* - h_o}{h_o^* - h_{o\max}} \right]^p} \quad 4.4$$

The nonlinear form of Eq. 4.4 is shown in Fig. 4.8c. The osmotic head threshold value h_o^* is the value at which the reduction starts. The reduction in α due to salinity beyond h_o^* continues significantly until a certain degree of salinity ($h_{o\max}$) is reached; beyond $h_{o\max}$ salinity increases do not cause significant further reductions in α . This reflects the fact that at $h_o \leq h_{o\max}$ the plant is still alive but the biological activities are at their minimum rate. α_o is the value of α corresponding to $h_{o\max}$. This model is not very sensitive to its exponent p which similar to Eq. 4.3 can be obtained from:

$$p = \frac{h_{o\max}}{h_{o\max} - h_o^*} \quad 4.5$$

Equation 4.4 is valid for $1 \geq \alpha \geq \alpha_o$. The other general validities are

$$\begin{aligned} \alpha(h_o) &= 1 & \text{if} & & h_o &\geq h_o^* \\ \alpha(h_o) &= \alpha_o & \text{if} & & h_o &\leq h_{o\max} \end{aligned}$$

The agreement between the experimental data and that calculated with Eq. 4.4 is depicted in Fig. 4.8d, using different values for p . The agreement with $p = 1.35$ is almost the same as $p = 1.5$ and that with the best nonlinear fitting.

4.5.3. Leaf water potentials for nonuniform soil solution salinities

Leaf water head can be considered as an indicator for the whole soil-water-plant-climate system. Figure 4.9a represents the measured absolute LWH of all salinity treatments as function of mean EC_{ss} . The trend of the data in this figure is not clear due to the fact that the LWH of the salinity treatments consist of a nonstressed part and a stressed part. For this reason, the net effect of salinity on LWH is shown in Fig. 4.11b. By subtracting the LWH of the reference treatment, LWH_R , from each individual salinity treatment, LWH_{si} , Fig. 4.9b provides a better trend and seems to be nonlinear. Following this normalization, the ratio of LWH_{si}/LWH_R is also depicted in Fig. 4.9c. Similarly to Fig 4.9b, the trend is nonlinear.

Due to the similarity between transpiration and leaf water potential (both represent the whole system), one may expect a relation between them. Figure 4.9d shows that the relative leaf water head LWH_{si}/LWH_R and the relative transpiration T_s/T_p are related to each other, but statistically it is not a 1:1 relation. One may conclude that the LWH data suggest more clearly a nonlinear trend than the relative transpiration data in saline soil.

4.6. Simulation with HYSWASOR

The one-dimensional simulation model for hysteretic water and solute transport in the root zone, HYSWASOR, has been designed particularly to study root water uptake under nonuniform soil water osmotic and pressure heads, making it ideally suitable for use in this study. The governing flow equations and the root extraction term of this model have been discussed in Chapter 2.

In HYSWASOR, the top boundary condition can be specified as head, flux density (evaporation included), water layer applied (controlled by Mariotte head), and free evaporation during light. Required input for the top boundary conditions include solute concentration of the infiltration water, potential transpiration rate, and evaporation rate. The bottom boundary condition can be specified as head, flux density, gravitational flow, and suction candle. The latter was particularly necessary for this part of the study, because the experimental columns were connected to a suction pump to suck out excess water during the night. Required input lower boundary conditions include soil water pressure head and/or soil water content, solute concentration, and hysteresis index for any soil depth. These must be given at least for

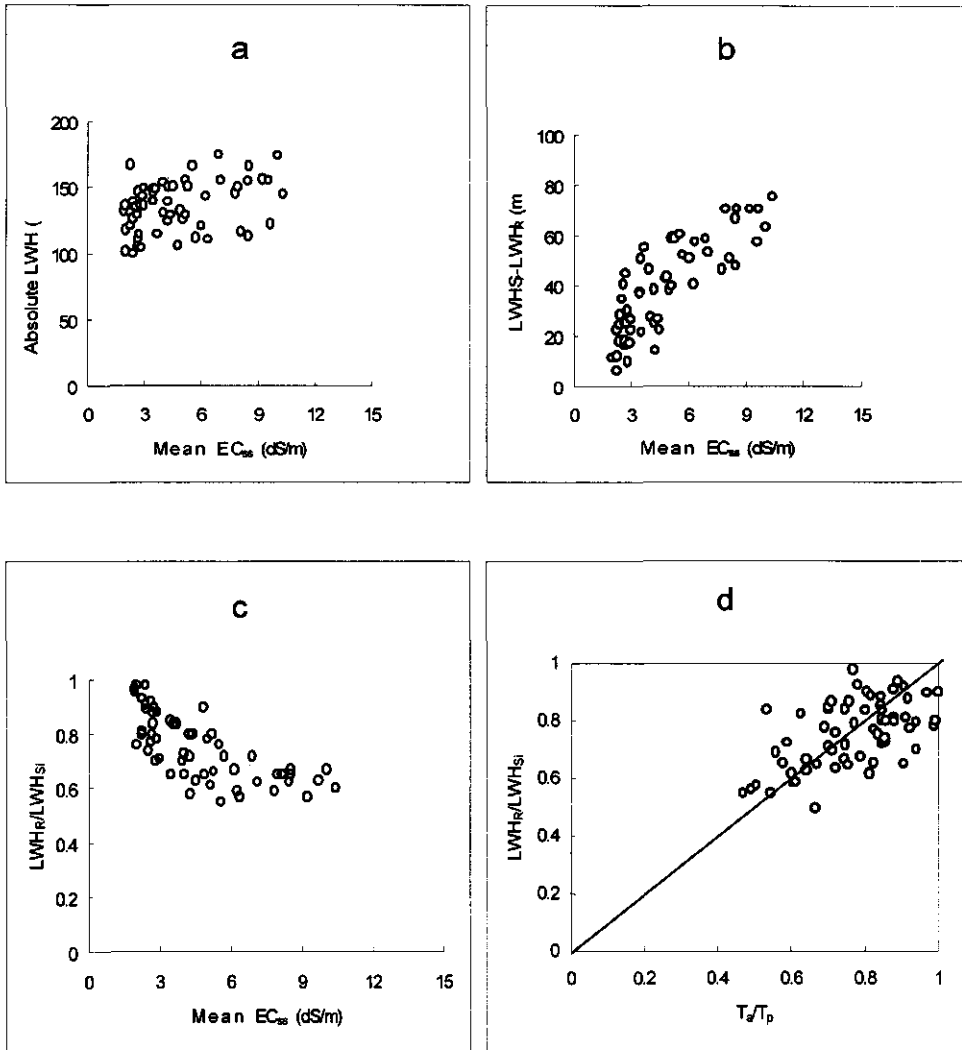


Figure 4.9. Absolute leaf water head LWH (a) and net LWH (b) versus mean soil solution salinity EC_{ss} . Relative leaf water head LWH_R/LWH_{Si} (c) versus mean EC_{ss} , and transpiration T_a/T_p (d).

the top and bottom of a soil column. Root water uptake parameters (constant during the simulation) must be specified as input. Either *Mualem-Van Genuchten* parameters or a K - θ table must be given as soil parameters. The model provides as output volumetric soil water content, soil water pressure head, hydraulic head, soil water flux density, root water uptake rate, and solute concentration at any desired node and time step. Also, cumulative values of infiltrated water, evaporation, drainage, capillary rise,

transpiration, infiltrated and drained solutes are generated by the model. Simulated soil water content, soil water pressure and osmotic heads and water uptake rate distributions are shown on screen, providing a valuable tool to follow the process during the simulation.

HYSWASOR has been developed further such that the sample input file given in *Dirksen et al.* (1993) is no longer current. The input file used in this study for the S₃ treatment is given in Table 4.3 (only a part of the specified boundary conditions and the K - θ table are shown). The water uptake parameters have been derived from the experimental data. The boundary condition times are linked to irrigation intervals and potential transpiration measurements. The latter obtained experimentally from the reference treatment. Soil evaporation is set to zero. Since no reliable soil water pressure heads were obtained during the experiments, initial water contents are specified rather than soil water pressure heads. The initial soil solution concentrations are derived from measured EC_{ss} based on Eq. 3.6.

4.6.1. Calibration

From five experimental treatments, the S₃ treatment was selected for the calibration. This treatment was irrigated every 48 hours with 3 dS/m ($c = 30 \mu\text{mol}/\text{cm}^3$, $h_o = -1080 \text{ cm}$) water. The soil hydraulic functions were obtained from a laboratory experiment with the evaporation method of *Wind* (1966). The influence of hysteresis on the water content simulations was tested by varying the hysteresis code. *Kool and Parker* (1987) proposed that the α parameter in Eq. 2.6 for the wetting soil water retention characteristic is two times that of the drying one. The simulations indicated no significant influence on water contents over the root zone. This is due to the fact that the experimental columns were irrigated with large quantities of water to reach the high target leaching fractions. As a result, the columns were nearly saturated every 48 hours, and the scanning curves always started at the wet end of the retention curve. However, simulations for a dry column (water stress experiment) showed the sensitivity for hysteresis. Therefore, hysteresis was included in all simulations.

The root activity distribution influences the root water uptake pattern significantly. In HYSWASOR, any root activity distribution can be specified. All the root activity patterns proposed in chapter 2 (constant with depth, exponential with a maximum at the soil surface, linear with a maximum at the soil surface and zero for the bottom of the root zone, and stepwise root density distributions) were used to check the difference in the simulated soil water contents and actual transpiration. The simulated water contents as well as the simulated actual transpiration indicated no significant

Table 4.3. Input file for S_3 treatment with reduction function Eq. 2.36. Only part of the specified $K-\theta$ table and boundary conditions are given.

```

=====GeneralData =====
MaxDepth  NrOfElements  ConcGroundWater  MariotteHead  MaxSurfaceDetention
  65          650          0              100              0
HysCode  SolCode  TranspCode  PltCode  PltInt  PltChoice  BCOutCode  LCOutCode
Debug
  1          1          0          1          10          0          0          0
Oneday(1 or 24)  Sunrise  Sunset  DeltMax  Tmax  OutTimesInterval
  24          10.5          0          0.1          480          1
Additional times for output (2 lines; total output times < 500)

Depths in extra plot file (max.: 8):
  5  10  15  20  25  35  45  55
Water uptake parameters (all heads in cm):
  Matric: Threshold  50% Exponent;  Osmotic: Threshold  50% Exponent
          -1e6      -1.1e6      1.5          -720      -2650      1.35
Root activities/densities (incr. depth; min nr. of depths: 0, max. nr.: 20)
  Time \ Depths:  0  5  10  15  20  25  35  45  55  65
                0          1  0.9  0.8  0.65  0.55  0.45  0.35  0.25  0.2
===== Soil parameters ===== line nr. xx = 21  NrOfRootActLines ====
Soil type i:
  ad  nd  md  wcsd  wcrd  aw  nw  mw  wcsw  SatCond  Lk
0.0146  1.386  0.279  0.428  0.01  0.0292  1.386  0.279  0.428  0.84  -1
-----
  CondCode  Rhob  Dfp  Ldis  lamb1  lamb2  FreundK  FreundExp  MinAir
  1          1.42  0.017  1          0          0          0          1          0
-----
k-theta table (increasing order of theta, max. nr.: 20, incl. saturation)
Theta: 0.1844 0.1994 0.2072 0.2121 0.2231 0.2311 0.2407 0.248
k: 0.779e-4 0.198e-3 0.278e-3 0.371e-3 0.621e-3 0.11e-2 0.176e-2 0.26e-2
===== Boundary conditions === line nr. yy = xx + 11*NrOfSoils =====
BCTime  TopCode  TopVal  TopCon  BotCode  BotVal  PotTrans  Evapor
  0          2          3.8          15          3          -50          0          0
  10.5       1          0          0          3          -50          0          0
  10.51      1          0          0          1          0          0.110       0
  15         1          0          0          1          0          0.173       0
  18         1          0          0          1          0          0.116       0
  24         1          0          0          1          0          0.109       0
  38         1          0          0          1          0          0.103       0
  41         1          0          0          1          0          0.115       0
  48         2          3.8          15          3          -50          0.115       0
-----
  428        2          5.2          15          3          -50          0.289       0
  438.5      1          0          0          3          -50          0          0
  438.51     1          0          0          1          0          0.08        0
  446        1          0          0          1          0          0.092       0
  456        1          0          0          1          0          0.118       0
  480        1          0          0          1          0          0.118       0
===== Initial conditions ===== line nr. yy + NrOfBC + 2 =====
depth  soil  kap  hi  wci  ci
  0.0  1  -1  0  .137  30  (at least given)
  5    1  -1  0  .137  30
  10   1  -1  0  .193  33
  15   1  -1  0  .167  25
  20   1  -1  0  .184  27
  25   1  -1  0  .135  23
  35   1  -1  0  .136  16
  45   1  -1  0  .153  15
  55   1  -1  0  .193  15
  65.0 1  -1  0  .233  15  at top and bottom)

```

change due to the different root activity distributions. The simulated total actual transpiration with the different root activity distributions resulted in only about 1mm difference for the whole experimental growth period. This was expected because water contents in the columns were high. Any decrease in water content at a particular depth causes a hydraulic head gradient that moves water from other depths to compensate the water that was taken up. This was checked by means of a modification of the original version of HYSWASOR, such that the water flux density for each node was printed in the output file. For instance, during the daylight the water flux density was even comparable with the root water uptake at the same depth. The simulated salt concentrations are more sensitive to the root activity distributions than the water contents. Water uptake from a particular depth causes an increase in salt concentration due to the water content decrease at that depth. At the same time, water moving through the soil to compensate water taken up by the roots, carries salt along. The best agreement between the simulated and a particular experimental soil solution concentration distribution was obtained when the root activity distribution was set to 1.00, 0.90, 0.80, 0.65, 0.55, 0.45, 0.35, 0.25, 0.20, and 0.20 for the depths of 0.0 (the soil surface), 5, 10, 15, 20, 25, 35, 45, 55, and 65 cm, respectively. Therefore, in all the simulations this root activity distribution was specified. The root activity distribution is automatically normalized such that the integral over depth is unity.

4.6.2. Comparison of experimental and simulated actual transpiration for different soil solution salinities

The main purpose of this part of the study was to find out how the plant roots behave under salinity stress. The final judgment on the agreement between simulated and experimental root water uptake data was based on the actual transpiration. The simulation model was run with the salinity reduction terms of Eqs. 2.33, 2.35, 2.36 and 4.4. The threshold-slope model of Eq. 2.33 is much more sensitive to the salinity threshold value h^* , than to the slope. The experimental threshold value was about half of that of *Maas and Hoffman*, but the slope was almost the same. This indicates that different soil types and different evaporative demands, even different kinds of salt, influence the threshold value. The models employing a salinity threshold value are potentially more accurate than those that do not, but the value of h^* must be determined as accurately as possible. The actual transpiration simulated with Eq. 2.33 for different h^* values indicated that this model is very sensitive to this parameter, while different slopes have less influence on the simulated transpiration. The simulated total actual transpiration changed significantly when h^* was varied between 2 to 4 dS/m. The closest agreement with the experimental data was obtained

for $h_o^* = -600$ cm and the slope of 0.071 m/dS. Therefore, in all simulations these values were used for Eq. 2.33 (Table 4.4).

The sensitivity analysis shows that the actual transpiration simulated with the reduction term of equation 2.35 is highly sensitive to p . By changing p from 3 (*Van Genuchten, 1987*) to 1.35 (about that of the experiments) total actual transpiration changed about 75mm. The model is also sensitive to h_{o50} , but not as much as to p . The best agreement with the experimental data was obtained with $p = 1.72$ and $h_{o50} = -2880$ cm and these values were used in the simulations (Table 4.4).

Equation 2.36 is sensitive to p , but not as much as Eq. 2.35. Equation 2.36 is most sensitive to h_o^* , and less to h_{o50} . The closest agreement between experiments and simulated transpiration with Eq. 2.36 was obtained for $h_o^* = -720$ cm, $h_{o50} = -2650$ cm and $p = 1.35$. These values were used in all simulations with Eq. 2.36 (Table 4.4).

Equation 4.4 is not as sensitive to p and $h_{o\max}$ as to h_o^* and α_0 . The best simulated transpiration with Eq. 4.4 was obtained with the experimental parameter values, only α_0 was changed from 0.25 to 0.40 (Table 4.4).

Table 4.4. Parameter values for Equations 2.33, 2.35, 2.36 and 2.36, originally proposed, experimentally derived, and optimized for S_3 .

Equation	parameter	Original	Experiment	Optimized
2.33	h_o^* (cm)	-1440	-720	-600
	Slope m/dS	0.073	0.071	0.071
2.35	h_{o50} (cm)	-6300	-2880	-2880
	p (-)	3	1.35	1.72
2.36	h_o^* (cm)	-2800	-720	-720
	h_{o50} (cm)	-3900	-2880	-2650
	p (-)	1.5	1.35	1.35
4.4	h_o^* (cm)	-	-720	-720
	$h_{o\max}$ (cm)	-	-5700	-5700
	p (-)	-	1.35	1.35
	α_0	-	0.25	0.40

In section 4.5 the experimental relative transpirations were compared with the calculated values according to reduction functions Eqs. 2.33, 2.35, 2.36, and 4.4, with the conclusion that Eqs. 2.33, 2.35 and 2.36 do not give good agreement if the originally proposed parameter values are used. For the simulated actual transpiration the same comparison is followed. Figure 4.10a shows the comparison between the experimental actual transpiration and those simulated with reduction terms of equations 2.33, 2.35, 2.36 and 4.4, using the parameter values originally proposed by the modelers. These values do not provide a reasonable agreement. Figure 4.10b presents the best agreement between experimental and simulated cumulative actual transpiration for treatment S₃, obtained with the parameter values listed in the last column of Table 4.4. These optimized values differ slightly from the experimentally derived values.

Figures 4.10c, 4.10d, 4.10e, and 4.10f present the comparison between the experimental actual transpiration and that simulated with the optimized parameter values of Eqs. 2.33, 2.35, 2.36 and 4.4 for the treatments S₁, S₂, S₄ and S₅, respectively. The experimental potential transpiration that was obtained from the reference R treatment is also given in these figures, denoted as T_p .

4.6.3. Quantitative comparison of experimental and simulated actual transpiration

Analysis of residual errors, differences between measured and simulated values, can be used to evaluate model performance. *Loague and Green (1991)* used the following statistics to evaluate solute transport models: maximum error ME , root mean square error $RMSE$, coefficient of determination CD , modeling efficiency EF , and coefficient of residual mass CRM . The mathematical expressions of these statistics are:

$$ME = \text{Max } |P_i - O_i|_{i=1}^n \quad 4.6$$

$$RMSE = \left[\frac{\sum_{i=1}^n (P_i - O_i)^2}{n} \right]^{1/2} \frac{100}{\bar{O}} \quad 4.7$$

$$CD = \frac{\sum_{i=1}^n (O_i - \bar{O})^2}{\sum_{i=1}^n (P_i - \bar{O})^2} \quad 4.8$$

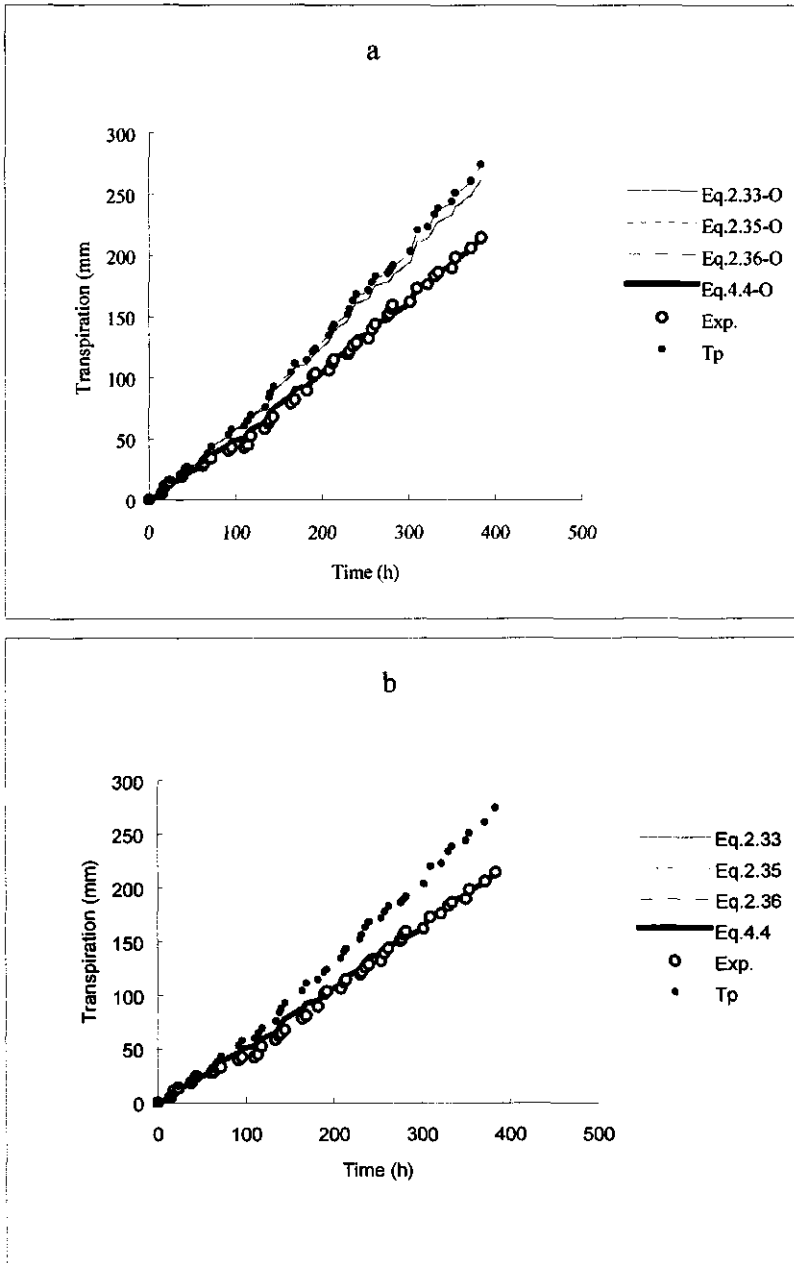


Figure 4.10. Comparison between the experimental (Exp.) and simulated cumulative transpiration of treatment S_3 for the reduction function Eqs. 2.33, 2.35, 2.36 and 4.4, using a: the parameter values originally proposed by the authors (O) and b: the optimized values that yield the best agreement listed in Table 4.4. The potential transpiration T_p is also given.

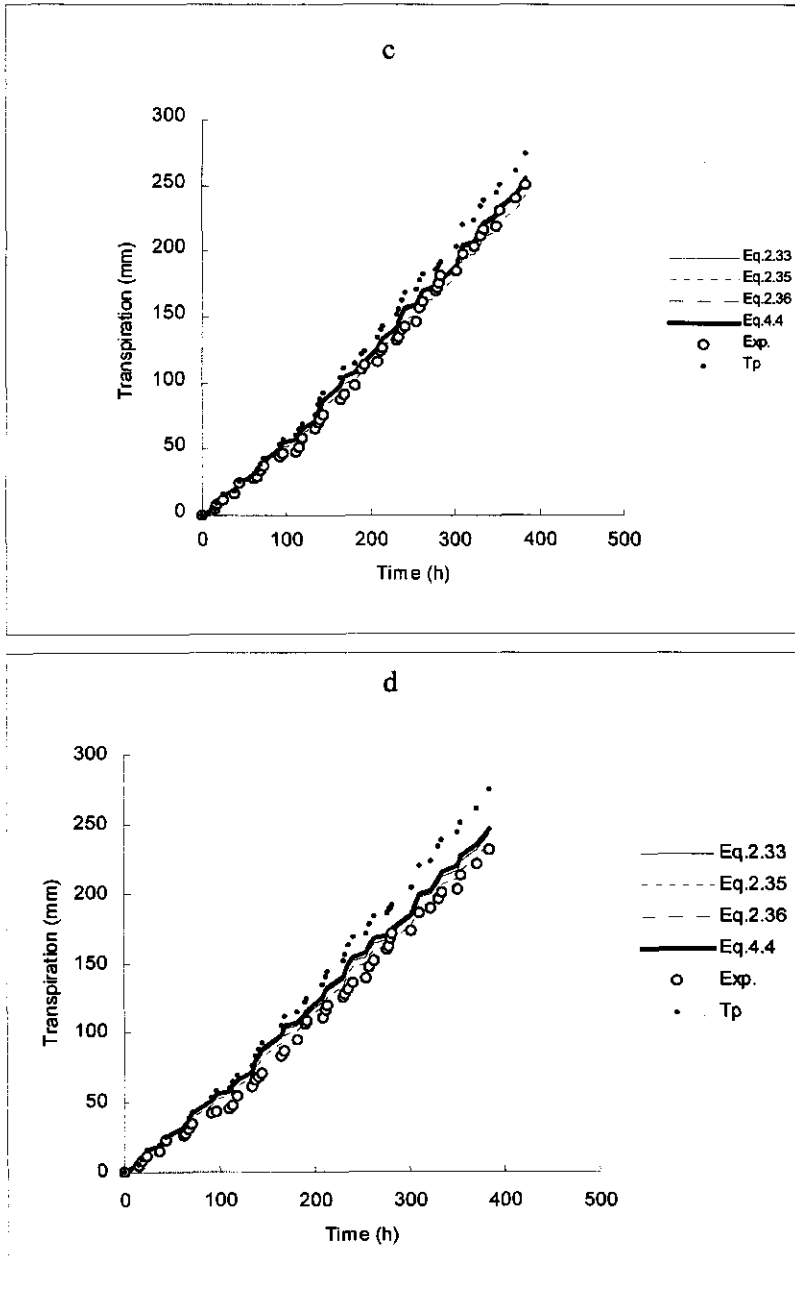


Figure 4.10. Comparison between the experimental (Exp.) and simulated cumulative transpiration with reduction functions Eqs. 2.33, 2.35, 2.36 and 4.4, using the parameter values optimized for treatment S₃. c: S₁ treatment, d: S₂ treatment.

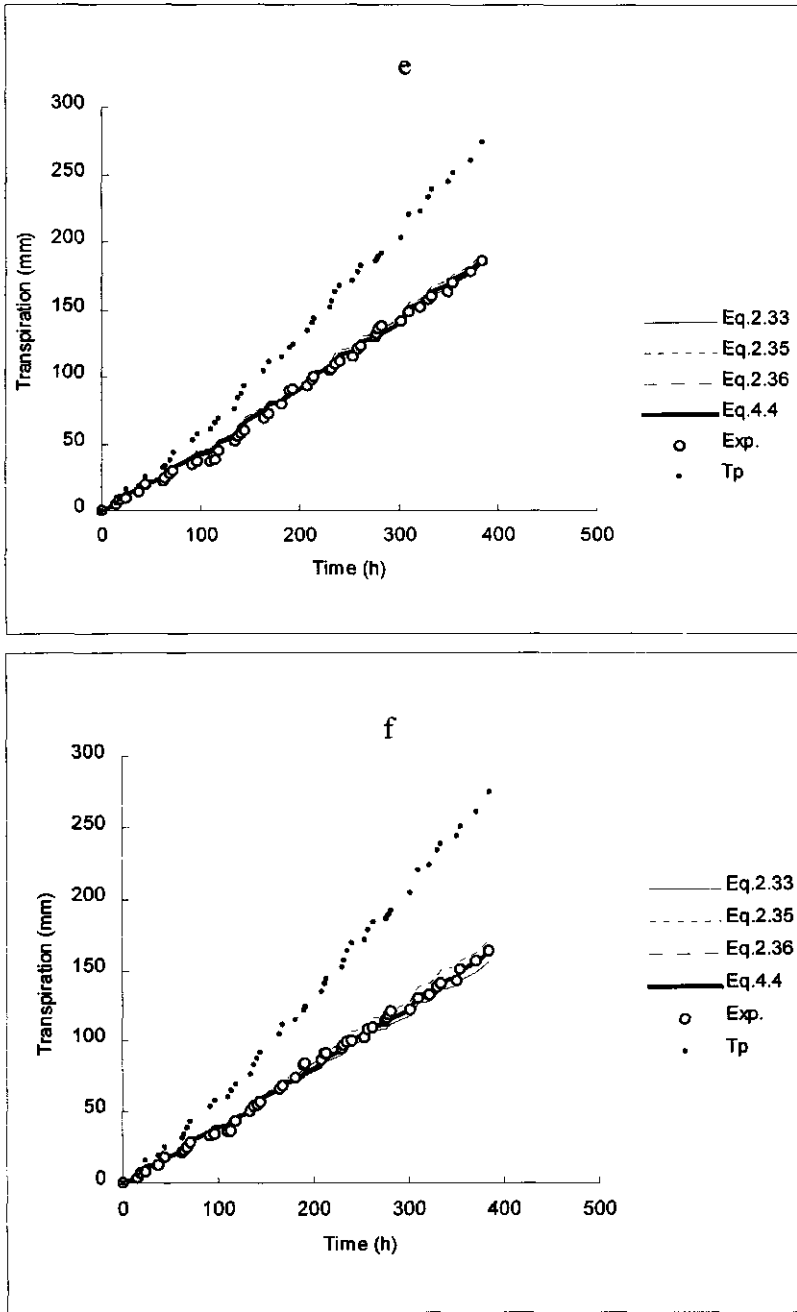


Figure 4.10. Comparison between the experimental (Exp.) and simulated transpiration with reduction functions Eqs. 2.33, 2.35, 2.36 and 4.4, using parameter values optimized for treatment S_3 , e: S_4 , treatment f: S_5 treatment.

$$EF = \frac{\left(\sum_{i=1}^n (O_i - \bar{O})^2 - \sum_{i=1}^n (P_i - O_i)^2 \right)}{\sum_{i=1}^n (O_i - \bar{O})^2} \quad 4.9$$

$$CRM = \frac{\left(\sum_{i=1}^n O_i - \sum_{i=1}^n P_i \right)}{\sum_{i=1}^n O_i} \quad 4.10$$

where P_i are the predicted (simulated) values; O_i are the observed (measured) values; n is the number of samples; and the overlined characters represent mean values. The lower limit for ME , $RMSE$, and CD is zero. The maximum value for EF is one. Both EF and CRM can be negative. The ME value represents the worst case performance of the model while the $RMSE$ value shows how much the simulations overestimate or underestimate the measurements. The CD gives the ratio between the scatter of the simulated values and of the measurements. The EF value compares the simulated values to the averaged measured values. A negative EF value indicates that the averaged measured values give a better estimate than the simulated values. The CRM is a measure of the tendency of the model to overestimate or underestimate the measurements. A negative CRM shows a tendency to overestimate. If all simulated and measured data are the same, the statistics yield: $ME = 0$; $RMSE = 0$; $CD = 1$; $EF = 0$; and $CRM = 0$. Table 4.5 gives the values of the five statistics for the experimental and simulated actual transpiration based on Eqs 2.33, 2.35, 2.36 and 4.44. The performance of all the reduction functions is almost similar. The tendency of the reduction functions to under or overestimate is also similar, but this tendency is not strong because all CRM values are around zero. Furthermore, there is no significant difference in calculated CD among the reduction functions. Most results for Eqs. 2.36 and 4.4 are the same, indicating that the performance of these reduction functions is rather similar. If a nonlinear function is needed, Eq. 4.4 can be used because of its relatively accessible input parameters. In conclusion, these statistics indicate that all the salinity reduction functions perform almost similarly. For simplicity, one may then as well choose Eq. 2.33 with less, and widely available input parameters. However, it should be noted that in all the reduction functions the experimentally obtained parameter values were used rather than those proposed by the modelers.

Table 4.5. Statistical parameters to evaluate the model performance with the reduction functions of Eqs. 2.33, 2.35, 2.36 and 4.4.

Treatment	$\alpha (h_0)$	ME mm	RMSE mm	CD -	EF -	CRM -
S ₁	Eq. 2.33	11.89	30.24	0.954	-0.047	-0.041
	Eq. 2.35	12.16	23.90	0.969	-0.030	0.000
	Eq. 2.36	13.24	37.50	0.930	-0.074	-0.053
	Eq. 4.4	13.19	37.13	0.931	-0.072	-0.052
S ₂	Eq. 2.33	16.00	59.50	0.870	-0.140	-0.086
	Eq. 2.35	11.68	36.76	0.935	0.068	0.050
	Eq. 2.36	18.60	73.19	0.846	-0.181	-0.106
	Eq. 4.4	18.50	72.79	0.847	-0.180	-0.106
S ₃	Eq. 2.33	11.15	26.94	0.969	-0.031	-0.028
	Eq. 2.35	9.85	23.98	0.978	-0.021	-0.018
	Eq. 2.36	11.45	27.73	0.979	-0.021	-0.030
	Eq. 4.4	11.45	27.42	0.979	-0.021	-0.029
S ₄	Eq. 2.33	11.29	28.83	0.991	0.008	0.027
	Eq. 2.35	11.59	39.53	0.922	-0.084	0.055
	Eq. 2.36	11.29	29.53	0.989	-0.010	-0.032
	Eq. 4.4	9.29	25.07	0.989	-0.043	-0.025
S ₅	Eq. 2.33	9.27	31.91	0.944	0.055	0.034
	Eq. 2.35	9.79	32.39	0.871	-0.146	-0.034
	Eq. 2.36	6.65	17.89	0.964	-0.036	0.000
	Eq. 4.4	6.85	17.79	0.970	-0.030	-0.003

4.6.4. Comparison of experimental and simulated water content and salinity distributions

The initial soil water contents and osmotic heads were obtained from the experimental measurements just before the first irrigation after the plants were well developed. The same procedure as described for subsection 4.6.2 was followed to find the best agreement between the simulated and experimental S₃ treatment, using different parameters (Table 4.4) for the different reduction functions. The closest agreement with the experimental data was obtained with the parameter values in the last column of Table 4.4. Figure 4.11 shows the water content distribution with Eq. 2.36 and $p = 1.35$; the results for $p = 1.5$ were slightly different. The simulated water contents in Fig. 4.11 represent almost the best agreement with the experimental data. For other cases, there were discrepancies in different degrees between the simulated and measured water contents. An interesting observation is that in the whole simulation period the simulated and measured *mean* water contents agreed closely.

The corresponding experimental and simulated EC_{ss} distributions are given in Fig. 4.12. The simulated salinities follow about the same trend as the experimental data, but the magnitude of the simulated salinities is unsatisfactory. The simulated *mean* soil solution salinities for the entire simulation period are closer to the real data, similar to the water contents. Generally, the simulated *mean* water contents and *mean* soil solution salinities over the root zone for all the reduction functions were in better agreement with the experimental data than each individual simulated value.

The presented data show that the water contents cannot be simulated precisely. This can be related to the way in which the simulation model calculates water contents. The model distributes the potential transpiration over the root zone according to the specified root activity distribution. The actual transpiration is equal to the potential transpiration until the threshold salinity is reached and the actual transpiration is calculated for every node according to the specified reduction function. The integration of the calculated transpiration over all the nodes gives the actual transpiration for the entire root zone. When the soil salinity differs with depth, the model assumes that water can be taken up independently at every depth according to the specified reduction function and the (relative) root activity. For instance, if the soil solution salinity near the bottom is lower than at the top, the model calculates the higher water uptake at the bottom. The water contents and salinities are then calculated according to the water depletion at each node. This algorithm causes a discrepancy between the simulated and measured water contents and salinities, because under real conditions plants tend to minimize the energy needed to overcome the osmotic head of the soil water. This means that they tend to take up water from the depth with the minimum salinity and stop taking up water from other parts as long as the zone with minimum salinity contains enough water to provide the evaporative demand. When the minimum salinity zone can no longer satisfy the evaporative demand, water will be taken up from the next less saline depth. This process continues until the free energy of the soil water due to high salinity decreases to such an extent that the biological energy of the plants has become insufficient and water uptake stops altogether.

When plants take up water from one depth only (because of lower salinity) the water moves from another depth with higher water content due to the hydraulic head gradient. The soil solution salinity may or may not change due to the transported water at that depth, compared with that before root water uptake. But, the salinity at the depth from which the water was taken up will certainly increase if the water is not replenished from another depth. Thus, at a certain time and depth EC_{ss} may change or remain unchanged due to root water uptake. This process may describe the discrepancy of the experimental and simulated soil solution salinity data.

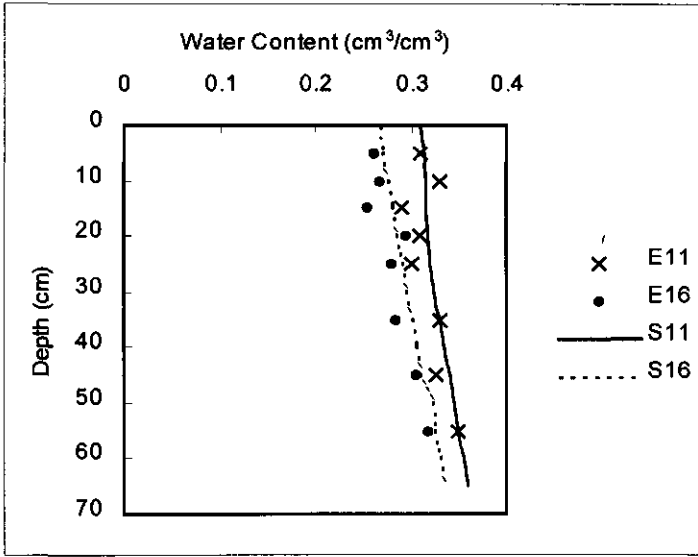


Figure 4.11. Experimental (E) and simulated (S) water content distribution at day 11 and 16 of S_3 treatment, using reduction function Eq. 2.36.

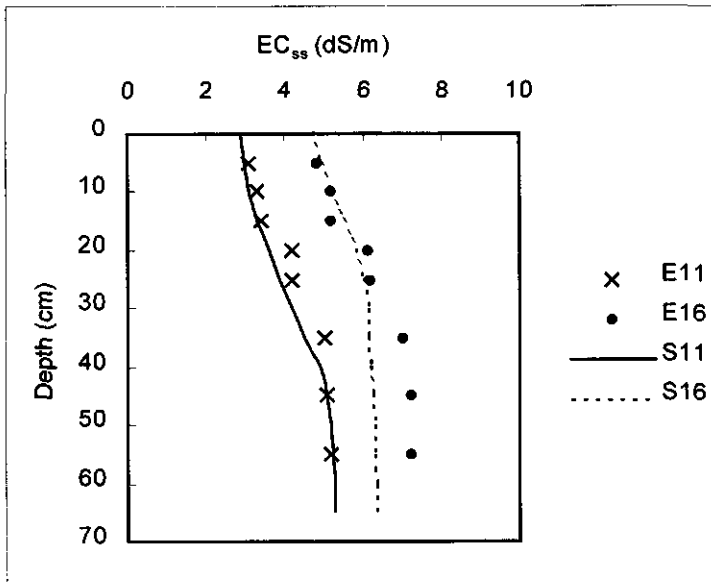


Figure 4.12. Experimental (E) and simulated (S) soil solution salinity EC_{ss} at day 11 and 16 of S_3 treatment, using reduction function Eq. 2.36.

This may also be regarded as a reason for what was found earlier in this study, that different root activity distributions did not influence θ and T_p (but they slightly changed EC_{ss}). Because such a process is not yet well understood, including it in the numerical simulation model is rather difficult. Besides this, the simulated and experimental *mean* θ and EC_{ss} data agree closely. Also, regardless of what kind of salinity reduction function is used the simulations give reasonable actual transpirations compared with the experiments. This implies that the simulation model provides acceptable results if the system in its entirety is regarded.

4.7. Summary and conclusions

Four different salinity reduction functions, Eqs. 2.33, 2.35, 2.36, and 4.4, were tested directly on experimental data and inserted in the numerical simulation model HYSWASOR to check their performance in a macroscopic root water uptake model (Eq. 2.27). Equation 2.33, was used to check if this function originally proposed for the long-term response (yield) can be employed in the macroscopic sink term of Eq. 2.27 as a reduction function. Further, equations 2.35, 2.36 and the newly developed Eq. 4.4 that are originally proposed as salinity reduction functions were tested with the experimental data.

The results indicated that Eq. 2.33, known as the crop response (yield) function, can be used as a reduction function in Eq. 2.27 with the original slope (proposed by the modelers) and a modification in its salinity threshold value. From both the experimental and simulated data it appeared that the most sensitive part of the reduction functions is the threshold value, while for Eq. 2.35 without a threshold the major sensitivity lies in its shape parameter. Equations 2.35 and 4.4 were also sensitive to their shape parameters, but to a lesser degree.

Because most of the parameter values originally proposed by the modelers could not provide good agreement with the experimental data, the values were derived from the experimental data. These experimental values were based on the mean soil solution salinities. Because the simulation model responds to each individual value at each depth, these values were slightly modified (optimized) to reach the best agreement between the simulated and experimental data.

The simulated cumulative actual transpirations were rather close to the experimental values, while the simulated soil water contents and soil solution osmotic head showed some discrepancies with the actual data, but the mean soil solution salinity and water content were very close to the measured data. This implies that the simulation model can provide good agreement with the measured data when the system is regarded in its entirety.

The different salinity reduction functions could provide almost the same results if the parameter values are well specified. This observation suggests the use of the simple linear reduction term Eq. 2.33, although it should be noted that the maximum salinity obtained in the present experiments was about 12 dS/m. In this salinity range, extrapolation of the linear function of Eq. 2.33 does not create a big error, but at higher salinities such extrapolation is not risk-free, because the data appear to have a nonlinear trend. *For practical use, the linear function of Eq. 2.33 may be used in combination with the macroscopic model of Eq. 2.27 to estimate the actual transpiration as well as the root water uptake.*

5. Root water uptake under nonuniform transient water stress

5.1. Introduction

Root water uptake studies generally have one of two purposes. Either they produce estimates of transpirational water losses for water budget models or they provide estimates of plant water status for predicting water stress. Root water uptake is a dynamic process influenced by soil, plant, and climate conditions. It depends on a number of factors such as soil water pressure head, soil hydraulic conductivity, osmotic head (in saline condition), evaporative demand, rooting depth, root density distribution, and plant properties. As discussed in Chapter 2, there are two main approaches to quantifying root water uptake. The so-called microscopic approach considers the root as an infinitely long cylinder of uniform radius and water absorbing properties. The soil water flow equation in this model is written in cylindrical coordinates and solved for the appropriate boundary conditions at the root surface and at some distance from the roots. The most important limitation of this approach in terms of application is the unavailability (if not impossibility to obtain) of the required input parameter values, particularly those at the root surface.

The second, so-called macroscopic approach, is an empirical function that describes plant water uptake based on the observed response to soil water pressure head. In the macroscopic approach, the flow to individual roots is ignored and the overall root system is assumed to extract water from individual increments of the root zone at rates that are related to bulk soil water properties. The most common formulation of this approach is based on the work of *Feddes et al.* (1978) and describes water uptake as the actual transpiration rate over the root zone (Eq. 2.27). The advantage of the macroscopic approach is that it does not require complete insight in the physical process of root water uptake and, therefore, eliminates the need for soil and plant parameters that are difficult to obtain. Such an empirical approach still needs to be calibrated, however, for different plants and probably different climate conditions.

The objective of this part of the study was to investigate the impact of different soil water pressure heads on the root water uptake pattern, and to investigate which pressure head reduction function can provide the best correlation with the experimental data. Since the overall reaction of plants on the heterogeneous soil water pressure head system is of most interest, the actual reaction of plants in terms of transpiration rate was central for this study. Dealing with numerical simulation models, it was also important to check the performance of the pressure head reduction functions of *Feddes et al.* (1978), *Van*

Genuchten (1987) and *Dirksen et al.* (1993) in combination with the macroscopic model of Eq. 2.27. This chapter first compares these reduction functions with the experimental data and then evaluates their performance in the numerical simulation model HYSWASOR.

5.2. Materials and methods

Two water stress treatments (W_1 and W_2) and a reference (R) were established in the greenhouse to investigate the influence of different soil water pressure heads on the root water uptake of alfalfa. The target amount of applied water for the first level of water stress W_1 was 70 percent of the no-stress treatment R, while the second level W_2 received about 50 percent of the irrigation water of R.

The measurements were started after healthy plants developed. Salinity stress was not allowed and hence the irrigation intervals were relatively long (i.e. 4 and 3 days) in order to let the columns dry out as much as possible. Tap water was applied to the soil columns by flood irrigation immediately before turning off the lights in order to allow as much water as possible to move downward at night. To prevent evaporation from the soil surface the top of each column was covered by granules. All measurements (with few exceptions) were started after switching on the lights. The artificial light period was mostly 15 hours per day from 6.00 am (or 6.30) until 9.00 pm.

Some fertilizers in solution form were added to the irrigation water to prevent any possible nutrient deficiency. The electrical conductivity of the applied water with the fertilizers was always less than 0.65 dS/m, thus the salinity caused by these applications was negligible. To verify that, some salinity measurements were made after each irrigation. Until the last application, soil solution salinity was less than the lowest readable value with the Salinity Bridge. For more experimental details, see Chapter 3.

5.3. Experimental data

A summary of experimental phase III (see Table 3.1) is given in Table 5.1. It shows that the transpired amount of water by the stressed treatments W_1 and W_2 was about 66 and 50 percent of the reference treatment R. Total transpired water for W_1 and W_2 was 18 and 40 mm, respectively, higher than the total applied water. Hence, the water storage of the soil columns was partly depleted. Figure 5.1 presents the water content distributions over the root zone for one irrigation interval of the R, W_1 and W_2 treatments. The reference treatment shows an increasing water content with depth, while the water content of the stressed treatments decreases with depth.

Table 5.1. Water budget of experimental phase III.

Treatment	Applied water mm	Transpired water mm	Irrigation interval d
R	585	535	2, 2, 2, 2, 2, 2, 2, 2, 2
W ₁	335	353	4, 4, 3, 3, 3, 3
W ₂	227	267	4, 4, 3, 3, 3, 3

The data of both stress treatments belong to the fifth of six irrigation intervals, while those of R belong to the seventh out of 10. Until 44 hours after the irrigation most of the water of the R treatment was taken from the top 25 cm, while in the period 44-48 hours most of the water was extracted from 30-55 cm depth. This shift occurred when θ had decreased to about $0.17 \text{ cm}^3/\text{cm}^3$. The stressed treatments had been under water stress already for 14 days and the irrigation water was only enough to wet the upper part of the root zone. The corresponding soil water pressure head distributions of all the treatments are also given in Fig. 5.1. These are obtained by converting the experimentally measured water contents according to the analytical expression of *Van Gemuchten* (1980) for the main drying retention curve.

Figure 5.2 shows the *LWH* of all the treatments measured at 2-hour intervals. The treatments received irrigation water on the evening before. The lower left hand value of each set was measured at the end of the dark period (at about 6.00 am) and the lower right hand value just before switching to darkness. The *LWH* of the stressed treatments at the first day after irrigation differed slightly from that of R. This implies that the *LWH* is not sensitive to the water deficit in the lower part of the root zone. As long as the plant is provided with the required transpirational water, the *LWH* behaves about the same as under nonstressed conditions. During the night, plant recovery was the same for all the treatments. In the second day after irrigation, the difference between stressed and nonstressed treatment became larger. The largest difference occurred at the third day after irrigation. Complete recovery did not occur from the second day on for all the treatments. Figure 5.2 also shows the sensitivity of *LWH* to evaporative demand. *LWH* values during daylight hours changed considerably, while the light intensity as well as all other greenhouse conditions except the temperature were constant. Hence, one can argue that *LWH* is too sensitive to be considered as an accurate indicator for deriving the parameter values for the root water uptake reduction functions.

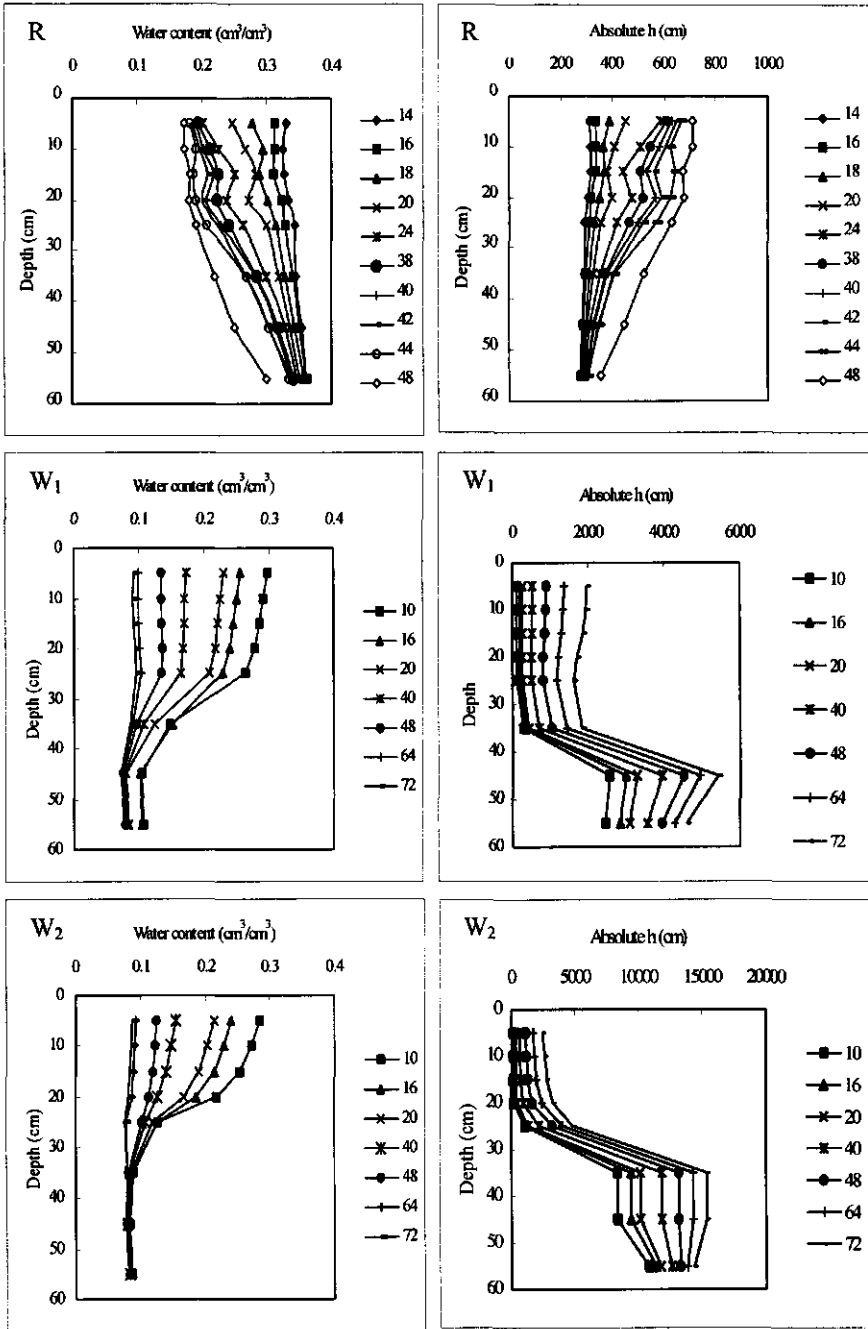


Figure 5.1. Soil water content and corresponding pressure head distributions at 14, 16, 18, 20, 24, 38, 40, 42, 44 and 48 hours after the seventh irrigation of R and at 10, 16, 20, 40, 48, 64, and 72 hours after the fifth irrigation of W₁ and W₂.

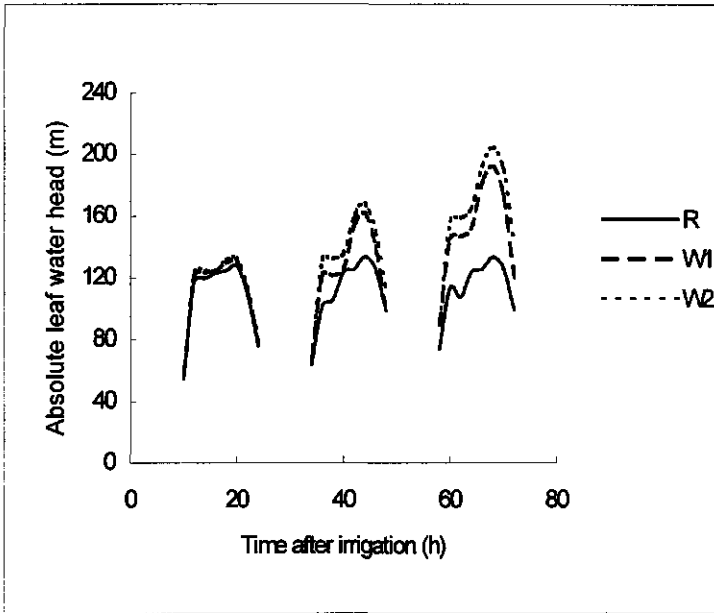


Figure 5.2. Absolute leaf water head versus time after irrigation for reference R and stressed treatments W_1 and W_2 .

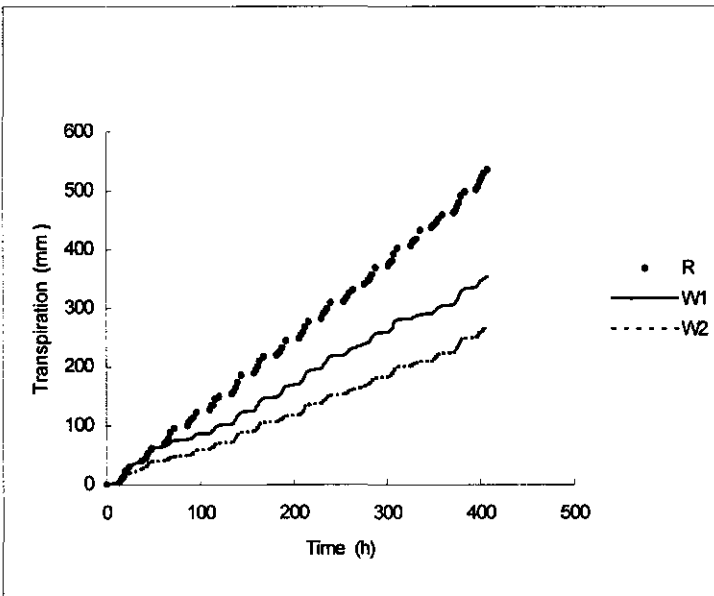


Figure 5.3. Measured cumulative transpiration versus time for reference R and stressed treatments W_1 and W_2 .

Figure 5.3 represents the measured cumulative transpiration for all the treatments. During the first day after irrigation, total transpiration of W_1 and W_2 was nearly the same as that of the R treatment. For W_1 this trend continued until 62 hours after the first irrigation, for W_2 the transpiration started to differ from R immediately after the first day. This indicates that the columns that received less water than R transpired the same amount of water as R in the first day after the irrigation. This trend has been observed for nearly all irrigation intervals. Thus, one may conclude that if part of the root zone can supply all the water needed to satisfy the evaporative demand, it does not matter that other parts of the root zone are very dry. Total available water is more important for the plant than the specific location of the water. Therefore, unlike salt heterogeneity over the root zone, heterogeneity of the soil water pressure head does not play an important role in terms of root water uptake, i.e. the water is taken up from depths with higher water content.

Figure 5.4 shows the measured relative transpiration T_a/T_p as function of the mean soil water content over the root zone. One can fit a linear threshold-slope relationship on the data; the threshold being about $0.15 \text{ cm}^3/\text{cm}^3$. Fig. 5.5 shows the nonlinear relationship between the experimental T_a/T_p and the mean absolute soil water pressure head, $|h|$, derived from the soil water content of each soil increment according to the analytical expression of *Van Genuchten* (1980). The two relatively high T_a/T_p values belong to a short time period in which a sharp decrease of the temperature in the greenhouse diminished the evaporative demand considerably. This observation support the suggestion of *Feddes et al.* (1978) that the reduction term for water stress is evaporative-demand dependent (see Ch. 2, Fig. 2.1a). This observation led us to follow the scatter of the data based on evaporative demand. In Fig. 5.5, the relation between T_a/T_p and mean $|h|$ exhibits the most scatter in the range of $3 \leq |h| \leq 30 \text{ m}$. In all cases at a given $|h|$, T_a/T_p depended considerably on the evaporative demand of the greenhouse. As the evaporative demand increased, mostly between 12.00 and 14.00h, T_a/T_p values shifted down sharply. Based on Fig. 5.5, the h threshold value is about -800 to -1000 cm. This range is within the accuracy of the data of *Dirksen et al.* (1993), and is very close to that proposed by *Feddes et al.* (1996).

The relationship of the absolute LWH (Fig. 5.6a), nor that of the normalized LWH_{W1}/LWH_R (Fig. 5.6b), versus absolute mean h , exhibits any trends. Subtracting $|LWH|$ values of the reference treatment from the stress treatments, $|LWH_{W1} - LWH_R|$, provided a non-linear trend (Fig. 5.6c). The correlation between LWH_{W1}/LWH_R and T_a/T_p in Fig. 5.6d is reasonably good ($r = 0.846$). This appears due to the fact that both T_a/T_p and LWH_{W1}/LWH_R represent the whole system and are evaporative-demand dependent.

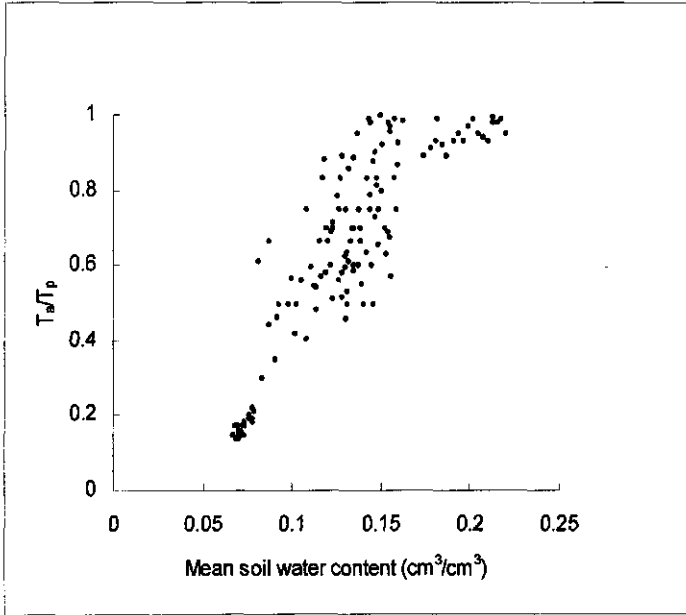


Figure 5.4. Experimental relative transpiration T_s/T_p versus mean soil water content of the root zone for W_1 and W_2 .

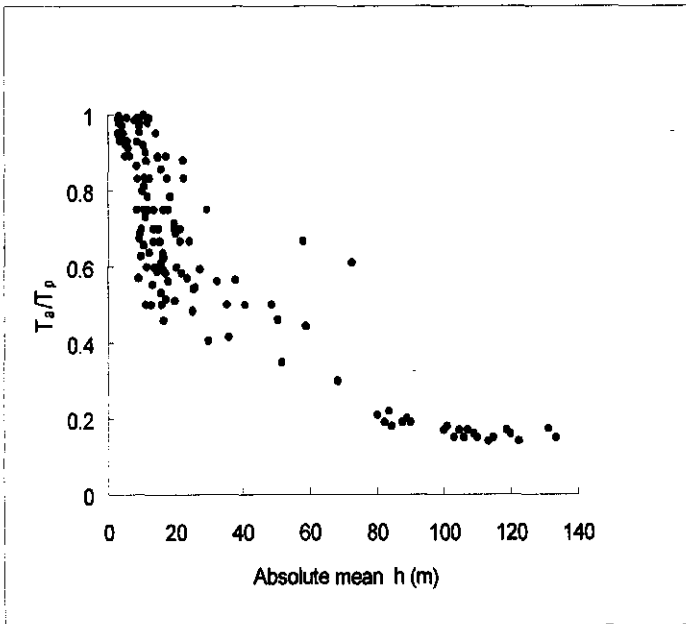


Figure 5.5. Experimental relative transpiration T_s/T_p versus absolute mean soil water pressure head h of W_1 and W_2 .

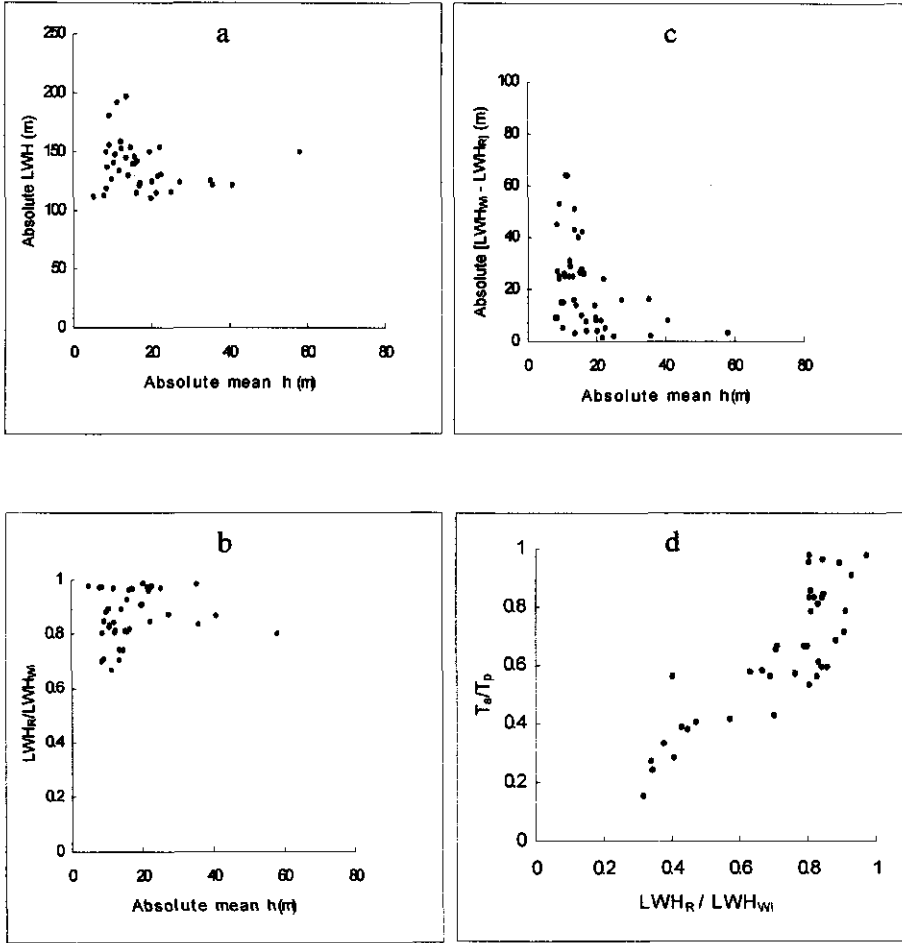


Figure 5.6. a: Absolute leaf water head LWH versus absolute mean soil water pressure head h ; b: relative leaf water head LWH_R/LWH_{WI} versus absolute mean h ; c: absolute net leaf water head $LWH_{WI} - LWH_R$ versus absolute mean h ; d: relative transpiration T_s/T_p versus relative leaf water head LWH_R/LWH_{WI} .

5.4. Test of theoretical reduction functions against experimental data

This section aims to compare the data obtained from the experiments with existing macroscopic reduction functions. Feddes *et al.* (1978) proposed for the stress part of Fig. 2.1a a simple linear function that is controlled by h_3 and h_4 according to:

$$\alpha(h) = \frac{h - h_4}{h_3 - h_4} \quad 5.1$$

in which h is the prevailing soil water pressure head, h_3 is the soil water pressure head threshold value and h_4 is the soil water pressure head at wilting (see Fig. 2.1a).

Alternatively, *Van Genuchten* (1987) proposed, similar to Eq. 2.35, the S-shaped relationship of Eq. 2.38. *Dirksen et al.* (1988,1993) modified Eq. 2.38 by the assumption that root water uptake is not reduced above a threshold value of soil water pressure head h^* , and introduced:

$$\alpha(h) = \frac{I}{I + \left[\frac{h^* - h}{h^* - h_w} \right]^p} \quad 5.2$$

The data presented here are taken from all irrigation intervals. The relative uptake is assumed to be equal to the relative transpiration as:

$$\frac{\int_0^{z_r} S \, dz}{\int_0^{z_r} S_{\max} \, dz} = \frac{T_a}{T_p} = \alpha(h) \quad 5.3$$

Figure 5.7 presents the comparison between the experimental relative transpiration and that calculated with Eq. 5.1 as function of $|h|$. The values $|h_4| = 16000, 9000, 6000, 4000,$ and 3500 cm (Table 5.2) are indicated in Fig. 5.7 as Eqs. 5.1a, b, c, d, e, and f, respectively. The best correlation ($r = 0.64$) was obtained for $|h_3| = 800$ cm and $|h_4| = 3500$ cm. A linear fit is not possible for the whole range of experimental data. From the crop production point of view the most important part of the data is about $|h| < 4000$ cm, and hence, the relative transpiration data for the higher $|h|$ values can be ignored. On the other hand $|h_4| = 4000$ cm or even larger values for the wilting point pressure head make no physical sense; this is a shortcoming of any linear extrapolation. Fig. 5.7 shows that alfalfa can survive even at $|h_4| \approx 13000$ cm. An alternative is to make a two-segment linear fit to the experimental data, as depicted in Fig. 5.8. The break point (second threshold) and slope of the line can as yet not be assigned a physical meaning. To avoid unreasonable extrapolation, an alternative for equation 5.1 is to define a threshold-slope equation similar to that of *Maas & Hoffman* (1977):

$$\alpha(h) = 1 - a'(h_3 - h) \quad 5.4$$

Like any other threshold-dependent model, Eq. 5.1 and Eq. 5.4 are sensitive to the threshold value. *Feddes et al.* (1978) suggested the threshold value to be only evaporative-demand dependent, while it seems to be soil-dependent as well. The water supply by soil to plant roots largely depends on the soil hydraulic conductivity.

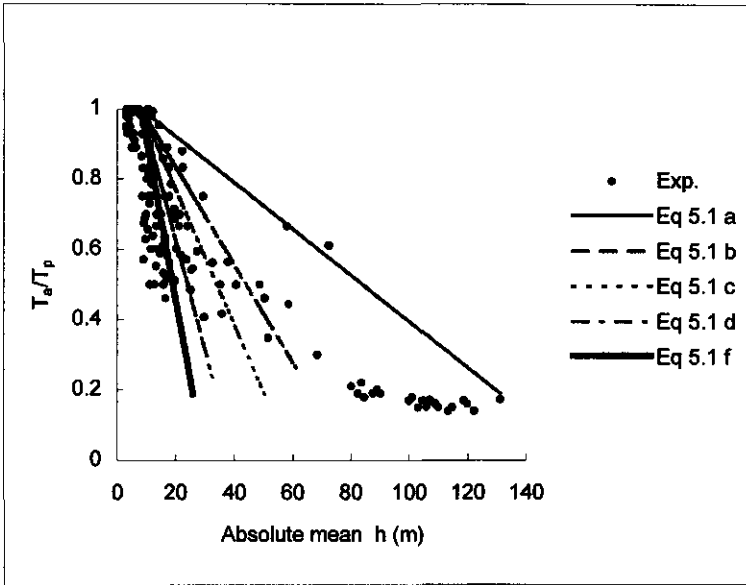


Figure 5.7. Linear fit of experimental relative transpiration T_a/T_p as function of absolute mean pressure head by Eq. 5.1 with the parameter values in Table 5.2.

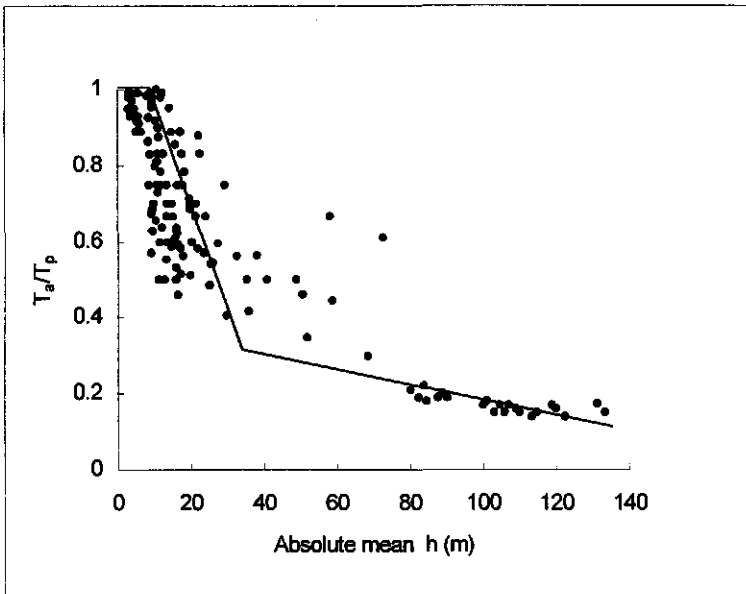


Figure 5.8. Two-piece linear fit of experimental relative transpiration T_a/T_p as function of absolute mean pressure head.

At high water contents, the hydraulic conductivity is large and the soil can quickly provide the requested water to the roots. As the water content/soil water pressure head decreases, the soil hydraulic conductivity sharply decreases nonlinearly, and with it the rate of water movement towards the plant roots. Clearly, the hydraulic properties differ largely from one soil to another and cannot be ignored in root water uptake studies. Thus, it is reasonable to consider h_3 also as a soil-dependent parameter.

Figure 5.9 presents a nonlinear fit of the experimental T_a/T_p versus mean $|h|$ of the root zone by the reduction function of Eq. 2.38, for which several values of h_{50} and p are chosen, as shown in Table 5.2. This includes the h_{50} value proposed by *Dirksen et al.* (1993), as well as the values obtained from the experiments. Also for p , the values originally proposed by *Van Genuchten* ($p = 3$), *Dirksen et. al* ($p = 1.5$), and that derived from salinity stress data ($p = 1.35$) are used. None of these parameter values provides a good fit over the entire experimental range. For instance, the values used in Eq. 2.38b and Eq. 2.38c provide excellent agreement only for $0.5 \leq \alpha(h) \leq 1$. Similarly, parameter values that give the best agreement for the lower mean $|h|$ values give an unsatisfactory fit for the higher soil water pressure heads. Besides the unavailability of the h_{50} and p values, another shortcoming of this nonlinear reduction function is that it does not have a threshold value as input parameter.

Figure 5.10 shows similar nonlinear fits by Eq. 5.2; again the parameter values are summarized in Table 5.2. As discussed for the salinity stress data, this nonlinear reduction function has the advantage of a threshold value as input parameter. The parameter values were taken from *Dirksen et al.* (1993), the current experimental data, and from the salinity stress treatments. Similar to Eq. 2.38, none of the fitted curves covers the whole range of experimental data. For instance, Eq. 5.2b, d, and e provide good agreement only for the first half of the experimental data ($T_a/T_p > 0.5$). As discussed for Eq. 2.38, this limitation was expected because Eq.5.2 does not contain a second threshold value that specifies from which h value on the reduction is less significant.

Similar to the reduction function for salinity proposed in Chapter 4, the following “two-threshold non-linear function” may be used as a pressure head reduction function in the macroscopic sink term of Eq. 2.27:

$$\alpha(h) = \frac{1}{1 + \left(\frac{1 - \alpha_0}{\alpha_0} \right) \left[\frac{h^* - h}{h^* - h_{\max}} \right]^p} \tag{5.5}$$

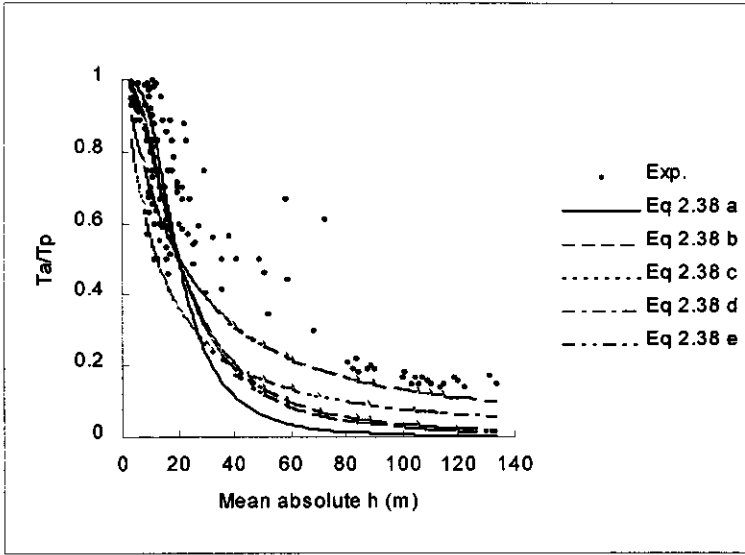


Figure 5.9. Nonlinear fit of experimental T_d/T_p versus mean $|h|$ by Eq. 2.38 with parameter values given in Table 5.2.

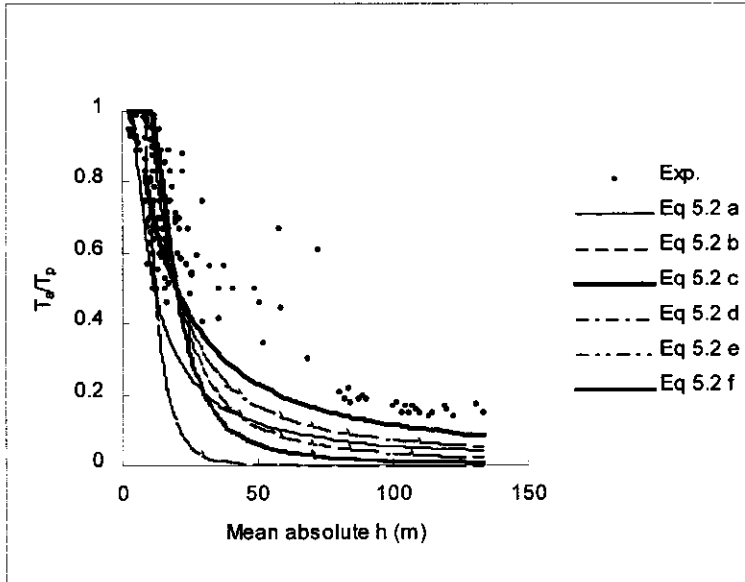


Figure 5.10. Nonlinear fit of experimental T_d/T_p versus mean $|h|$ by Eq. 5.2 with parameter values given in Table 5.2.

Table 5.2. The parameters used in the reduction functions of Eqs. 5.1, 2.38, 5.2, and 5.5. The correlation coefficient r is also given.

Equation	h_3 or h^* cm	h_4 cm	h_{50} cm	h_{max} cm	p -	α_0 -	r -
5.1a	-800	-16000					0.55
5.1b	-800	-8000					0.62
5.1c	-800	-6000					0.60
5.1d	-800	-4000					0.61
5.1e	-800	-3500					0.64
2.38a			-2000		3.00		0.86
2.38b			-2000		2.00		0.88
2.38c			-1200		1.50		0.87
2.38d			-2000		1.35		0.87
2.38e			-2000		1.15		0.89
5.2a	-400		-1200		1.50		0.83
5.2b	-400		-1200		3.00		0.76
5.2c	-400		-2000		1.50		0.85
5.2d	-1000		-2000		1.35		0.84
5.2e	-1000		-2000		1.15		0.88
5.2f	-1000		-2000		2.00		0.83
5.5a	-1000			-9000	1.15	0.20	0.91
5.5b	-1000			-9000	1.35	0.20	0.91
5.5c	-1000			-10000	1.15	0.20	0.91
5.5d	-1000			-12000	1.15	0.20	0.91
5.5e	-800			-9000	1.12	0.20	0.92
5.5f	-1000			-8000	1.12	0.17	0.92

in which h_{max} (the second threshold value) is the soil water pressure head beyond which changes of h no longer influence the relative transpiration significantly, and α_0 is the relative transpiration at h_{max} .

Similarly to Eq. 4.3 the dimensionless exponent p can be obtained from the expression:

$$p = \frac{h_{max}}{h_{max} - h^*} \quad 5.6$$

Compared to Eqs. 2.38 and 5.2, Eq. 5.5 with h^* and h_{max} has the advantage of providing entire coverage of the experimental data. Furthermore, as discussed for the salinity stress experiments, the non-defined p in Eqs. 2.38 and 5.2 can now be defined by Eq. 5.6.

Another limitation of Eqs. 2.38 and 5.2 is that it is difficult to derive h_{50} even from laboratory experiments. For salinity stress, one can use the data collected by *Maas and Hoffman*, but for water stress such data do not exist. It is not yet clear whether h_{50} is soil- and/or plant-specific. Analogous to the conclusion drawn for the pressure head threshold value, one can argue that h_{50} also is soil-dependent. The difference between the reported

value by *Dirksen et al.* ($h_{50} = -1200$ cm) and that of our experiment ($h_{50} = -2000$ cm) could then be explained by the difference in soil types.

In Eq. 5.5, h_{\max} replaces h_{50} . Eq. 5.5 is neither sensitive to p nor to h_{\max} . Since the shape of the function is controlled by three parameters (α_0 , h_{\max} and p), the sensitivity of the model to its shape parameters is decreased considerably compared to Eqs 2.38 and 5.2. Figure 5.11 shows the fit of the experimental data by the reduction function of Eq. 5.5 with the parameter values listed in Table 5.2. This figure shows that the newly proposed reduction function Eq. 5.5 indeed covers the whole range of experimental data.

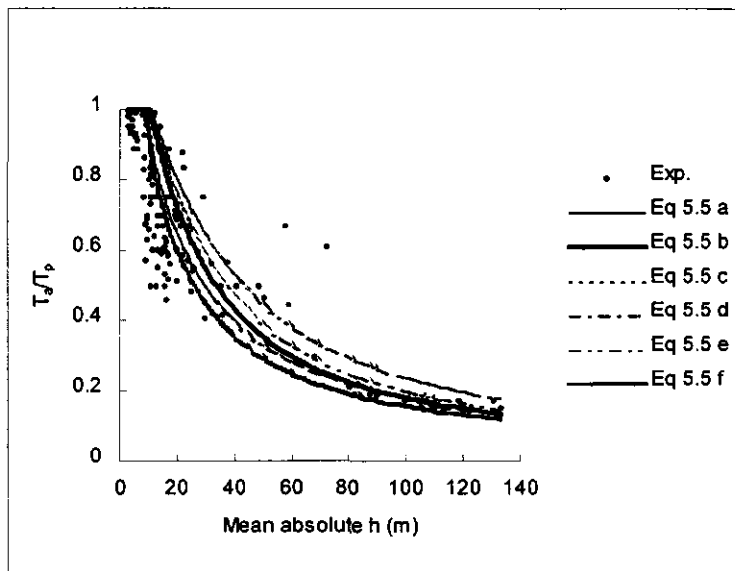


Figure 5.11. Nonlinear fit of experimental T_a/T_p versus mean $|h|$ by Eq. 5.5 with parameter values given in Table 5.2.

5.5. Simulation with HYSWASOR

The one-dimensional simulation model for hysteretic water and solute transport in the root zone, HYSWASOR, its governing flow equations and the original root extraction term used in this model were already discussed in Chapter 2. The required input information is given in Chapter 4. HYSWASOR has been designed to study root water uptake under nonuniform soil water osmotic and pressure heads. The model is flexible to study such system in detail during short time intervals. These features make the model ideally suitable for use in this study. The pressure head reduction functions of Eqs. 5.1, 2.38, 5.2 and 5.5 were used in the simulation model and evaluated against the experimental data. The water uptake parameters were first

taken from the best fits of the experimental data (Table 5.2) and later modified according to the best calibration based on one of the experimental treatments. The boundary condition times were linked to the irrigation intervals and the potential transpiration measurements (reference treatments). Soil evaporation was set to zero. Since no reliable soil water pressure heads were obtained during the experiments, the initial water content distribution was specified.

5.5.1. Calibration

The experimental treatment W_1 was used for the calibration. The soil hydraulic functions were determined by the evaporation method of *Wind* (1966). The influence of hysteresis on the water content simulations has been tested. *Kool and Parker* (1987) proposed that the α parameter in Eq. 2.6 for the wetting soil water retention characteristic (α_w) is two times that of the drying one α_d . To find the best agreement between the experimental and simulated water contents, α_w was changed from 1.75 to 2.25 times α_d . The best agreement was obtained with $\alpha_w = 1.95\alpha_d$. This value was used in all simulations to describe hysteresis.

In HYSWASOR any root activity distribution can be specified in the input file. Simulations with different root density distributions indicated a reasonable influence on the simulated water contents, particularly for the higher water contents. In relatively wet soil, the soil hydraulic conductivity is large enough to allow water to move from one depth to another to compensate the water taken up. Similar to the salinity stress simulations, the closest agreement between the simulated and experimental water content distributions was obtained with an exponential root activity distribution. Accordingly, in all the simulations the following root activity distribution was specified: 1.00, 0.90, 0.80, 0.65, 0.55, 0.45, 0.35, 0.25, 0.20, and 0.20 for the depths of 0, 5, 10, 15, 20, 25, 35, 45, 55, and 65 cm, respectively. Except for the uniform distribution that gave 6 mm difference, the other root activity distributions resulted in only about 1 mm difference between simulated and experimental cumulative actual transpiration for the whole growth period. This can be related to the fact that except the uniform distribution, all the root activity distributions specify the highest activities in the upper 25 cm.

5.5.2. Comparison of experimental and simulated water content distributions

Figure 5.12 shows samples of the experimental and simulated water content distributions obtained with the reduction term Eq.5.5 for one irrigation interval of the W_1 and W_2 treatments. The model simulates the trend of water content changes

reasonably, but there are some discrepancies between the actual values. Irrespective of what reduction function is used, these discrepancies are especially high when the evaporative demand is high. In most cases, the disagreement starts during the second night after irrigation and increases with time. These observations prompted us to follow the water content distributions during the dark period. The column weight remained exactly the same during the dark period, indicating that no water transpired. However, the water content decreased in the top 25 cm of the soil columns, but not in the deeper parts. This always happened between 21.00 to 4.00 h; thereafter, water contents remained unchanged until the lights were turned on at 6.00 am. Thus any uptake due to small natural light intensities between 4.00 and 6.00h is unlikely. Before 4.00h, the plants must have taken up water from the upper part of the soil column and store it in their tissues. This is supported by the recovery of the *LWH* (Fig. 5.2). This process was observed under water stress, but not in the saline treatments (Ch. 4). This may be related to the high soil water contents in these treatments. Typical changes in soil water content over the root zone during the dark period of the stressed treatments are depicted in Fig. 5.13. The integrated amount of depleted water over the night was irregular from day to day, but in most cases depleted water was high when the evaporative demand during the light period was high. More observations are needed to quantify this phenomenon.

5.5.3. Experimental and simulated actual transpiration for different soil water pressure heads

The main purpose of this part of the study was to investigate the influence of different soil water pressure heads on root water uptake using macroscopic root water uptake models. Thus, the final judgement for agreement between simulated and experimental data is actual transpiration. The simulation model was run with the reduction terms of Eqs. 2.38, 5.1, 5.2, and 5.5.

As discussed earlier, the linear model of *Feddes et al* is sensitive to both h_3 and h_4 . Simulation of actual transpiration with Eq. 5.1 for different h_3 values indicated that this model is more sensitive to h_3 than to h_4 , similar to that for salinity stress with the model of *Maas and Hoffman*. For example, simulated actual total transpiration for one growth period changed about 12 mm between $h_3 = -600$ to -400 cm, while decreasing h_4 from -3500 to -5500 changed the transpiration about 5 mm. The closest agreement between simulated actual transpiration and experimental data of W_1 was obtained with $h_3 = -800$ cm and $h_4 = -3500$ cm (Fig. 5.14). These values were used in all following simulations of W_1 and W_2 with the reduction function of Eq. 5.1 (Table 5.3).

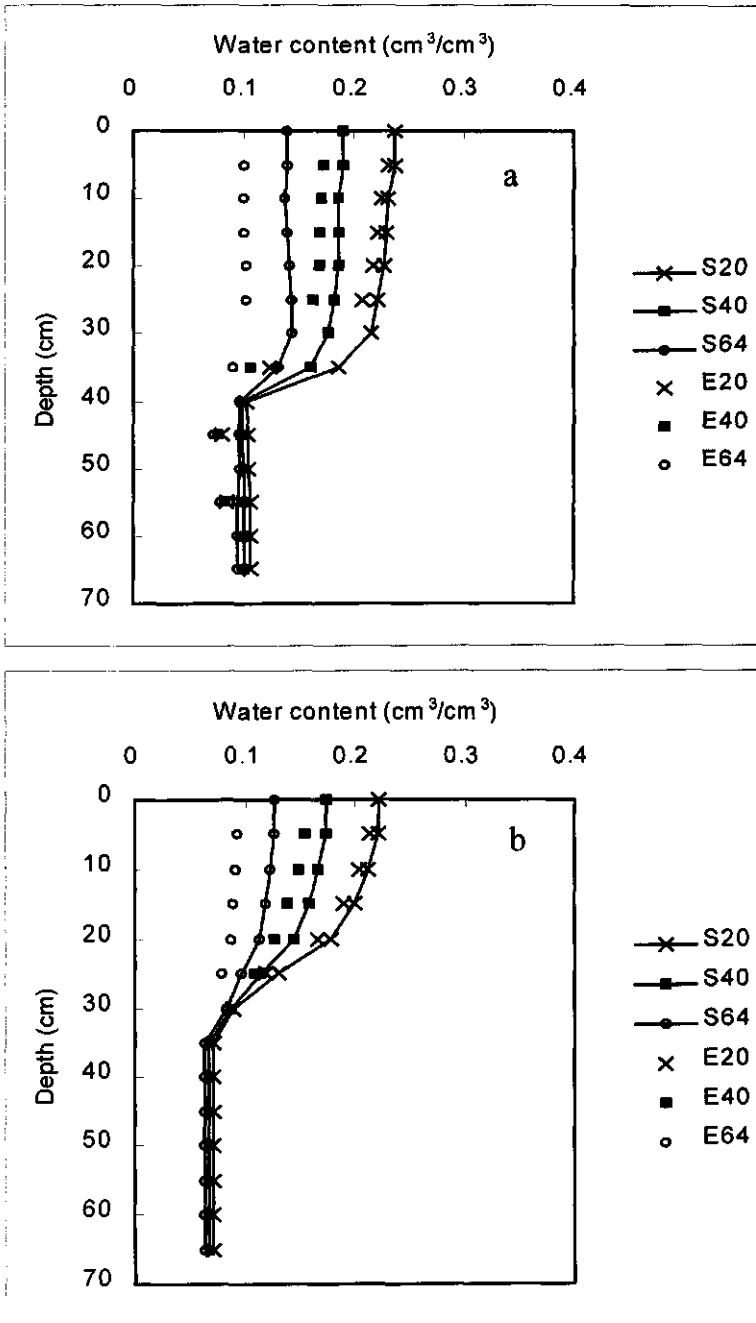


Figure 5.12. Experimental (E) and simulated (S) soil water content distributions with reduction function Eq. 5.5 at 20, 40, and 64 hours after fifth irrigation. a: treatment W₁, b: treatment W₂.

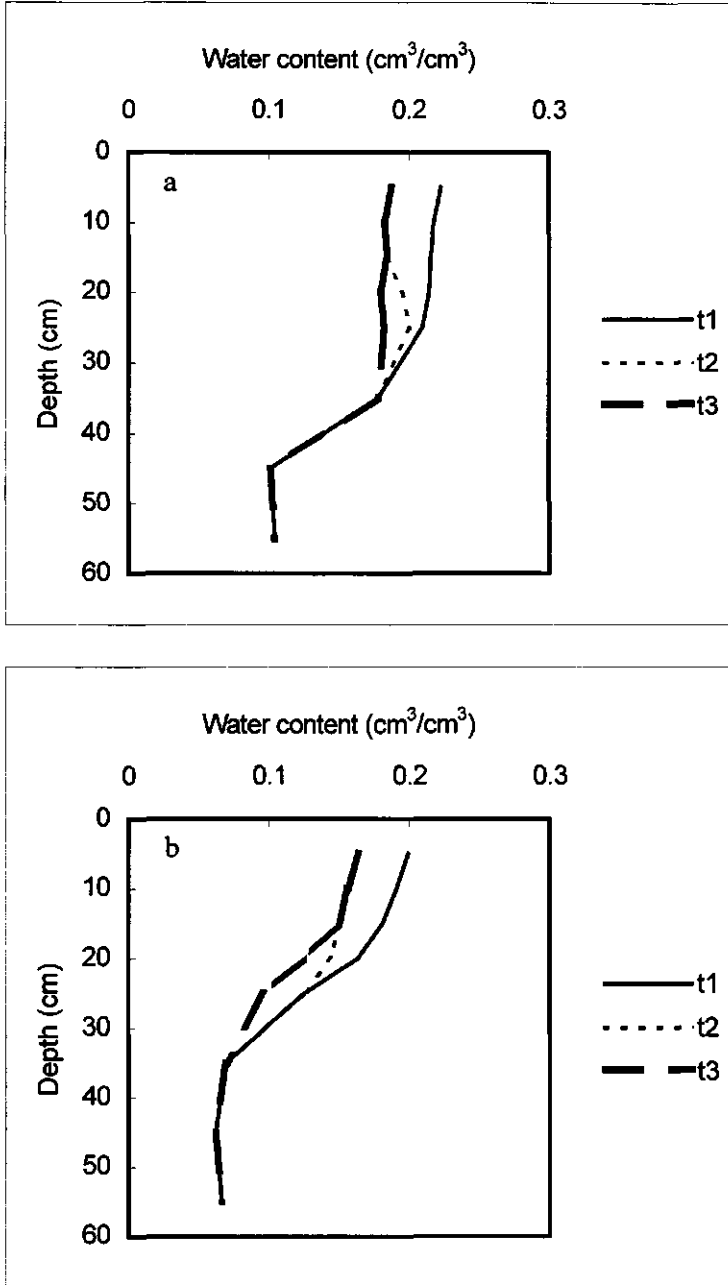


Figure 5.13. Measured soil water content changes during the dark period. t₁: immediately after darkness, t₂: just before turning on the lights and t₃: after 4 hours of light. a: treatment W₁, b: treatment W₂.

The sensitivity analysis shows that the simulated actual transpiration with the reduction term of equation 2.38 is sensitive to h_{50} as well as p , as expected for a nonlinear function. By changing p from 3 (proposed by *Van Gemuchten*) to 1.15 (that of the current experiment) total actual transpiration changed only about 3 mm. The model is more sensitive to h_{50} than p , as the total transpiration changed about 8 mm when h_{50} was decreased from -2000 to -1800 cm. The best fit in Fig. 5.9 was obtained with $p = 1.15$ and $h_{50} = -2000$ cm (Table 5.2), but these parameter values resulted in an overestimation of transpiration. The closest agreement between actual transpiration and experimental data was obtained for $h_{50} = -1800$ cm. These values were used in the following simulations of W_1 and W_2 with Eq. 2.38 (Table 5.3).

Table. 5.3. The parameter values used in the simulations for different reduction functions.

Equation	h_3 or h^* cm	h_4 cm	h_{50} cm	h_{max} cm	p -	α_0 -
5.1	-800	-3500	-	-	-	-
2.38	-	-	-1800	-	1.15	-
5.2	-800	-	-1600	-	1.25	-
5.5	-1000	-	-	-7000	1.15	0.17

Equation 5.2 is sensitive to h_{50} as well as to p and h^* , but not as much as Eq. 2.38. The shape of Eq. 5.2 is dominated by three parameters (p , h^* , h_{50}). The parameter values were first taken from the best experimental fit of Fig. 5.10; i.e. $h^* = -1000$ cm, $h_{50} = -2000$ cm and $p = 1.15$ (Table 5.2). The actual transpiration simulated with these values, however, was slightly overestimated. The closest agreement between the simulated actual total transpiration and experimental data of W_1 was obtained by changing the parameter values to $h^* = -800$ cm, $h_{50} = -1600$ cm and $p = 1.25$. In all following simulation of W_1 and W_2 with Eq. 5.2, these values were used (Table 5.3). The sensitivity analysis indicated that the reduction term of Eq. 5.5 is neither sensitive to p nor to h_{max} , and slightly sensitive to h^* and α_0 . The total actual transpiration changed about 3 mm when h^* was changed from -800 to -600 cm. The same difference of 3 mm was obtained when α_0 was changed from 0.17 to 0.25. The total actual transpiration did not change when h_{max} was changed from -6000 to -12000 cm. The parameter values for Eq. 5.5 were first assumed to be the same as for the best fit in Fig. 5.11, which were $h^* = -1000$ cm, $h_{max} = -8000$ cm, $p = 1.15$ and $\alpha_0 = 0.17$ (Table 5.2). The closest results with the experimental data was obtained by changing only h_{max} from -8000 to -7000 cm. These parameter values were used in all following simulations of W_1 and W_2 with Eq. 5.5 (Table 5.3).

The need for the slight modification of the parameter values obtained from the best fit of the experimental data can be related to the fact that the experimental parameter values were derived from the *mean* soil water pressure head over the root zone, while in the numerical simulation the reduction term is calculated for each node and then integrated over the root zone. The comparison between the experimental cumulative actual transpiration and that simulated with reduction functions of Eqs. 5.1, 2.38, 5.2, and 5.5 and the parameter values listed in Table 5.3 are depicted in Fig. 5.14 for the calibration treatment W_1 and Fig. 5.15 for the validation treatment W_2 . The experimental potential transpiration that was obtained from the reference R is also given in these figures.

5.5.4. Quantitative comparison of the experimental and simulated actual transpiration

Residual errors can be analyzed to compare the simulated and experimental results. *Loague and Green (1991)* used statistics to evaluate solute transport models. These statistics are: maximum error (*ME*), root mean square error (*RMSE*), coefficient of determination (*CD*), modeling efficiency (*EF*), and coefficient of residual mass (*CRM*). The mathematical expressions that describe these measures have been introduced in Chapter 4. Table 5.4 presents these statistics for the actual transpiration simulated with Eqs. 5.1, 2.38, 5.2 and 5.5. This shows that the simulated transpiration for all four equations is almost similar. Similar to what was concluded for the salinity reduction terms, all the pressure head reduction functions appear to lead to about the same result if the required input parameters are specified satisfactorily. In this case, the results were almost identical because the parameter values were primarily obtained from the same experimental conditions. In such a situation, one may as well choose for the simple, less-parameter-needing function of Eq. 5.1, but as was discussed, extrapolation of this linear model is not risk-free.

Table 5.4. Statistical parameters used for comparison of the experimental actual transpiration and the model performance for the calibration (W_1) and validation (W_2) treatments.

Treatment	Equation	<i>ME</i> mm	<i>RMSE</i> mm	<i>CD</i> -	<i>EF</i> -	<i>CRM</i> -
W_1	5.1	31.27	85.65	0.851	-0.174	-0.087
	2.38	18.26	46.07	0.946	0.053	0.037
	5.2	23.56	70.89	0.952	0.047	0.071
	5.5	28.77	70.03	0.952	0.047	0.071
W_2	5.1	36.24	123.84	0.958	0.041	-0.129
	2.38	31.34	146.56	0.870	-0.148	-0.156
	5.2	35.85	139.23	0.940	-0.063	-0.148
	5.5	30.01	140.40	0.904	-0.242	-0.149

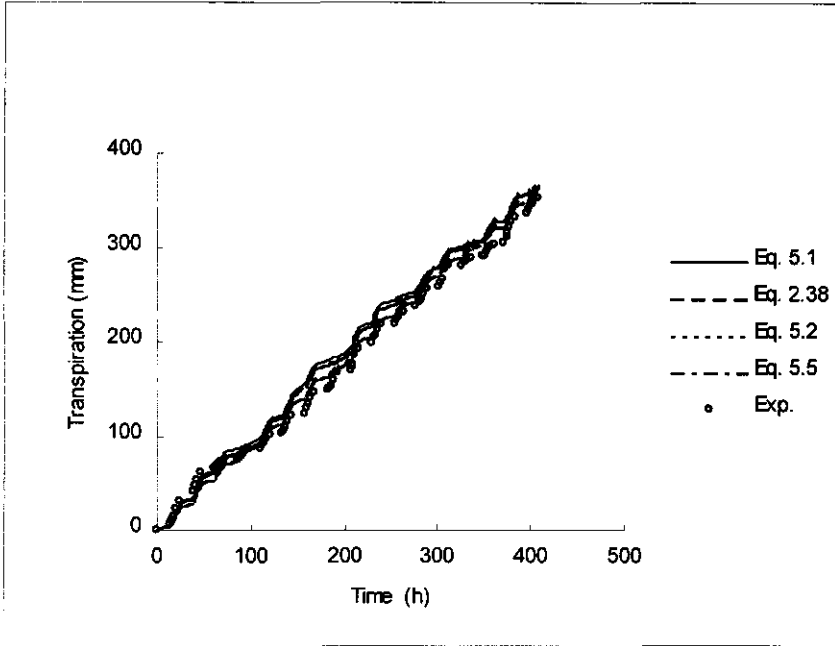


Figure 5.14. Experimental and simulated total actual transpiration for W_1 treatment.

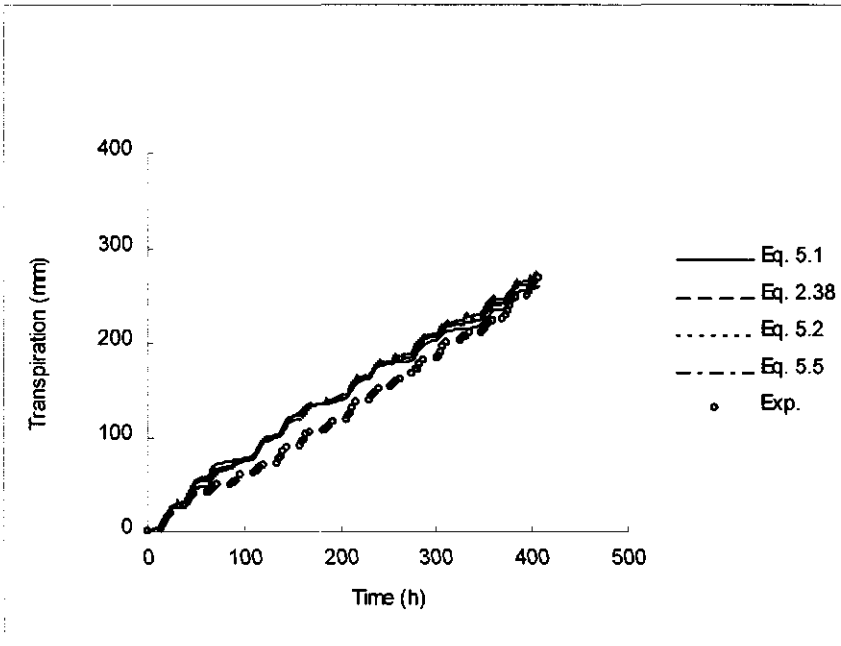


Figure 5.15. Experimental and simulated total actual transpiration for W_2 treatment.

5.6. Summary and conclusions

Four different soil water pressure head reduction functions were used in the macroscopic model of Eq. 2.27. The linear reduction function of Eq. 5.1 did not fit well T_a/T_p as function of mean soil water pressure head. The nonlinear functions of equations 2.38 and 5.2 T_a/T_p could not fit the whole range of T_a/T_p as function of mean soil water pressure head, while the two-threshold function of Eq. 5.5 provided a reasonable fit to all T_a/T_p data as function of mean soil water pressure head. The soil water pressure head heterogeneity over the root zone did not play an important role in water uptake, as long as there is enough water in one part of the root zone. The plants seem to satisfy the evaporative demand from wet parts of the root zone irrespective of the water deficit in drier parts. This conclusion is based upon the observations that on the first day after the irrigations both actual relative transpiration and relative leaf water head were almost the same for the stressed and nonstressed treatments. Some discrepancies were observed between measured and simulated individual water contents, and also for the mean soil water content over the root zone. The main reason for these disagreements appeared to be root water uptake during night. Whereas roots took up water during the dark period, the plants had no possibility to transpire it and hence the plants held the water in their tissues. As a result, leaf water potentials of the stressed treatments recovered reasonably after the dark period. In the simulations, all four reduction functions led to almost the same results when the parameters were primarily derived from the experimental data and slightly modified. However, the reduction function of Eq. 5.5 required very small modification on only one of its parameters, while for the other reduction functions more parameter values had to be modified.

Quantitative comparison between experimental and simulated actual transpiration indicated that all the reduction functions give almost similar results. Besides taking the input parameter values from the experimental data for calibration, the input parameters had to be modified to obtain the best agreement with the experimental data. This can be related to the fact that these values were derived from the experimental mean pressure head over the root zone, while in the simulations the reduction term is calculated for each individual node based on its own soil water pressure head.

Since all the reduction functions led to about the same results, for practical use the most simple Eq. 5.1 is proposed to be used in Eq. 2.27.

6. Root water uptake under joint nonuniform transient salinity and water stress

6.1. Introduction

Most salt tolerance and water stress studies have been carried out separately and many data are available for either water stress or salinity stress only. There are only few publications dealing with root water uptake under joint water and salinity stress conditions. A review of the conceptual models of root water uptake under joint water and salinity stress is given in section 2.5.

It is well known that water uptake is reduced due to salinity. It is not yet clear how plants react when low soil water pressure head h occurs together with low osmotic head h_o . In the earliest studies (see section 2.5) the investigators proposed that joint effect of salinity and water stress on water consumption may be related to the *total* soil water osmotic and pressure heads. The concept of *total* was later designated as the *sum* of these two components, from which the *additivity* concept was born. Some researchers clearly showed that one unit h_o does not influence the water consumption the same as one unit of h . The proponents of additivity suggested that some empirical proportionality coefficients should be included in the linear additivity of h_o and h (see section 2.5). Such empirical coefficients are considered to be plant, soil, and climate specific, but have never been introduced in the literature.

The so-called *multiplicativity* concept is based upon the *product* of the separate *reduction terms* for soil water osmotic and pressure heads. This concept was originally proposed by *Van Genuchten* (1987) and has been used extensively in many numerical simulation models dealing with root water uptake.

The objective of this part of the study was to investigate the joint influence of different levels of h and h_o on root water uptake patterns, and to investigate which concept fits experimental data best, or what adjustments need to be made.

In this chapter all existing concepts were used as reduction functions in the macroscopic Eq. 2.27 and compared with the experimental data. Furthermore, they were incorporated into the simulation model HYSWASOR, and the obtained results compared with experimental data. Since the overall reaction of plants to heterogeneous soil water osmotic and pressure heads was central for this study, the actual transpiration was considered the best indicator for comparing experimental and simulated data.

6.2. Materials and methods

In this part of the study different levels of salinity ($S_1, S_2, S_3, S_4,$ and S_5) and water stresses (W_1, W_2) have been applied to the plants simultaneously, using an individual reference treatment R for each water stress level (see Table 3.1). Water and salinity stresses were applied to the plants after healthy plants had developed. The target water applications were 70 and 50 percent of the reference for W_1 and W_2 , respectively. The irrigation water salinities were 1.5, 2.0, 3.0, 4.0 and 5.0 dS/m for $S_1, S_2, S_3, S_4,$ and S_5 , respectively. All possible combinations of the mentioned water and salinity stresses with their own references were applied. Variations of soil water content, soil water pressure head, and osmotic head distributions in the root zone were obtained by varying the quantity of applied water, irrigation intervals, and irrigation water salinities. At the end of each experimental growth period, plants were harvested and the wet and dry matter of each individual column determined; the latter by drying the plant for 24 hours at 70 °C. More details on materials and methods of this part of the study are reported in Chapter 3.

6.3. Experimental data

The quantities of applied water and transpired water as well as the irrigation intervals of the experimental treatments are given in Table 6.1. The applied water for the reference and the stressed treatments for the first level of water stress (S_iW_1) was less than that of the second level of water stress (S_iW_2). This was due to the higher evaporative demand of the greenhouse at the time that the S_iW_2 treatments were established. Therefore, each level of water stress had its own reference, R_1 , and R_2 , and the applied water for S_iW_1 was $0.52R_1$ and that for S_iW_2 was between $0.29R_2$ to $0.43R_2$. In the $S_1W_1, S_2W_1, S_3W_1,$ and S_4W_1 treatments, more water transpired than was applied. Only in the most saline column (S_5W_1), the applied water could not be taken up totally due to high salinity; this happened only in the last two irrigation intervals. Leaching was not allowed in the treatments, and thus by each water application more salt was introduced in the soil column, increasing the salt concentration in the soil solution particularly in the upper part of the root zone. This resulted in a decrease of transpiration with time.

The S_1W_2, S_2W_2 and S_3W_2 treatments also transpired more water than was applied. For the S_4W_2 and S_5W_2 treatments this was true only in the last two (fifth and sixth) irrigation intervals.

Figure 6.1 shows the soil water content distributions of $R_2, S_1W_2, S_2W_2, S_3W_2, S_4W_2,$ and S_5W_2 at 16, 38, and 62 hours after the first irrigation. The water content of R_2 was always higher than the stress treatments.

Table 6.1. Applied and transpired water (mm), salinity of irrigation water EC_{iw} (dS/m) and irrigation time intervals (d) for joint water and salinity stress treatments.

Treatments	Applied water mm	EC_{iw} dS/m	Transpired water mm	Irrigation interval d
R_1	458.0	Tap	428	2, 2, 2, 2, 2, 2, 2, 2, 2
S_1W_1	237.6	1.5	315	4, 4, 3, 3, 3, 3, 3
S_2W_1	237.6	2.0	307	4, 4, 3, 3, 3, 3, 3
S_3W_1	237.6	3.0	278	4, 4, 3, 3, 3, 3, 3
S_4W_1	237.6	4.0	258	4, 4, 3, 3, 3, 3, 3
S_5W_1	237.6	5.0	212	4, 4, 3, 3, 3, 3, 3
R_2	654	Tap	547	2, 2, 2, 2, 2, 2, 2, 2, 2
S_1W_2	282	1.5	368	4, 4, 3, 3, 3, 3, 3
S_2W_2	266	2.0	350	4, 4, 3, 3, 3, 3, 3
S_3W_2	266	3.0	342	4, 4, 3, 3, 3, 3, 3
S_4W_2	266	4.0	219	4, 4, 3, 3, 3, 3, 3
S_5W_2	188	5.0	144	4, 4, 3, 3, 3, 3, 3

Figure 6.2 shows the soil solution electrical conductivity distributions of S_1W_2 , S_2W_2 , S_3W_2 , S_4W_2 , and S_5W_2 at the same times. There was no leaching applied to the columns. After each irrigation, EC_{ss} increased particularly in the upper parts of the columns. This resulted in a high spatial variability at the end of the experimental growth period.

Figure 6.3a presents the cumulative transpired water (mm) during one experimental growth period for the R_1 , S_1W_1 , S_2W_1 , S_3W_1 , S_4W_1 , and S_5W_1 treatments; Fig. 6.3b shows the same for R_2 , S_1W_2 , S_2W_2 , S_3W_2 , S_4W_2 , and S_5W_2 . The transpiration from R_1 and R_2 was much larger than that from the corresponding stressed treatments. The high transpiration rates are due to the fact that the transpiration is related to the cross sectional area of the soil columns, rather than the plant canopies (see Ch. 3).

The measured absolute leaf water heads $|LWH|$ of all the treatments are given in Fig. 6.4. The measurements were made at 2-hour time intervals, starting just before the end of the darkness periods. The $|LWH|$ values of S_5W_1 in the second day after irrigation were slightly lower than in the first day after irrigation. This is due to the lower evaporative demand in the greenhouse at the second day. The $|LWH|$ of S_5W_2 in the first and second day after irrigation deviated considerably from the other treatments. This reflects the lower amounts of water applied to W_2 compared to W_1 .

Figure 6.5 presents the relationship between the relative leaf water head LWH_R/LWH_{SiW_i} and mean absolute soil water pressure head $|h|$ for different mean EC_{ss} . Except at 3-4 dS/m, the trend of variation is almost linear. The slopes of the lines increase and the intercepts decrease with increasing mean soil solution salinity.

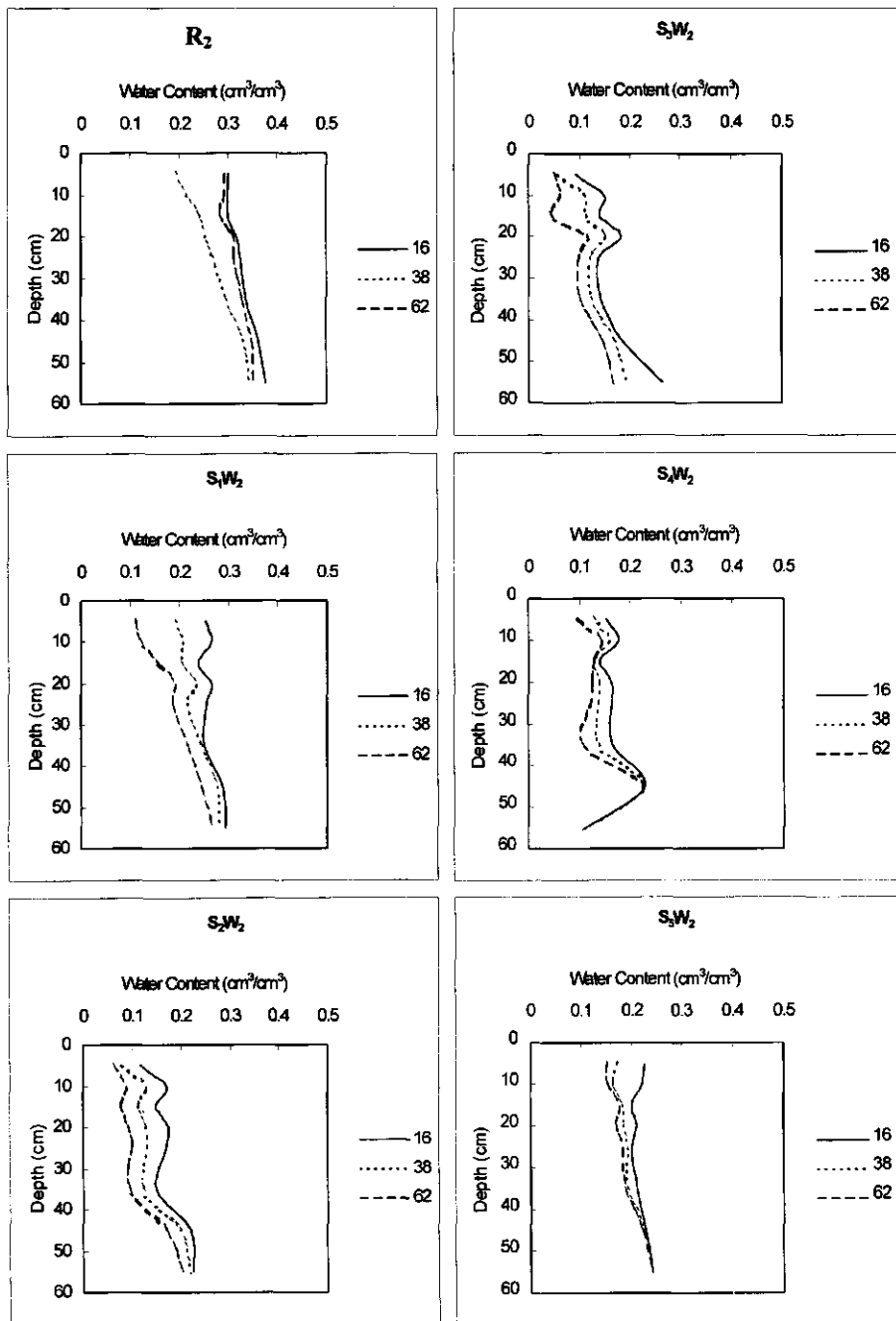


Figure 6.1. Measured soil water content distributions of R , S_1W_2 , S_2W_2 , S_3W_2 , S_4W_2 , and S_5W_2 at 16, 38 and 62 hours after the first irrigation.

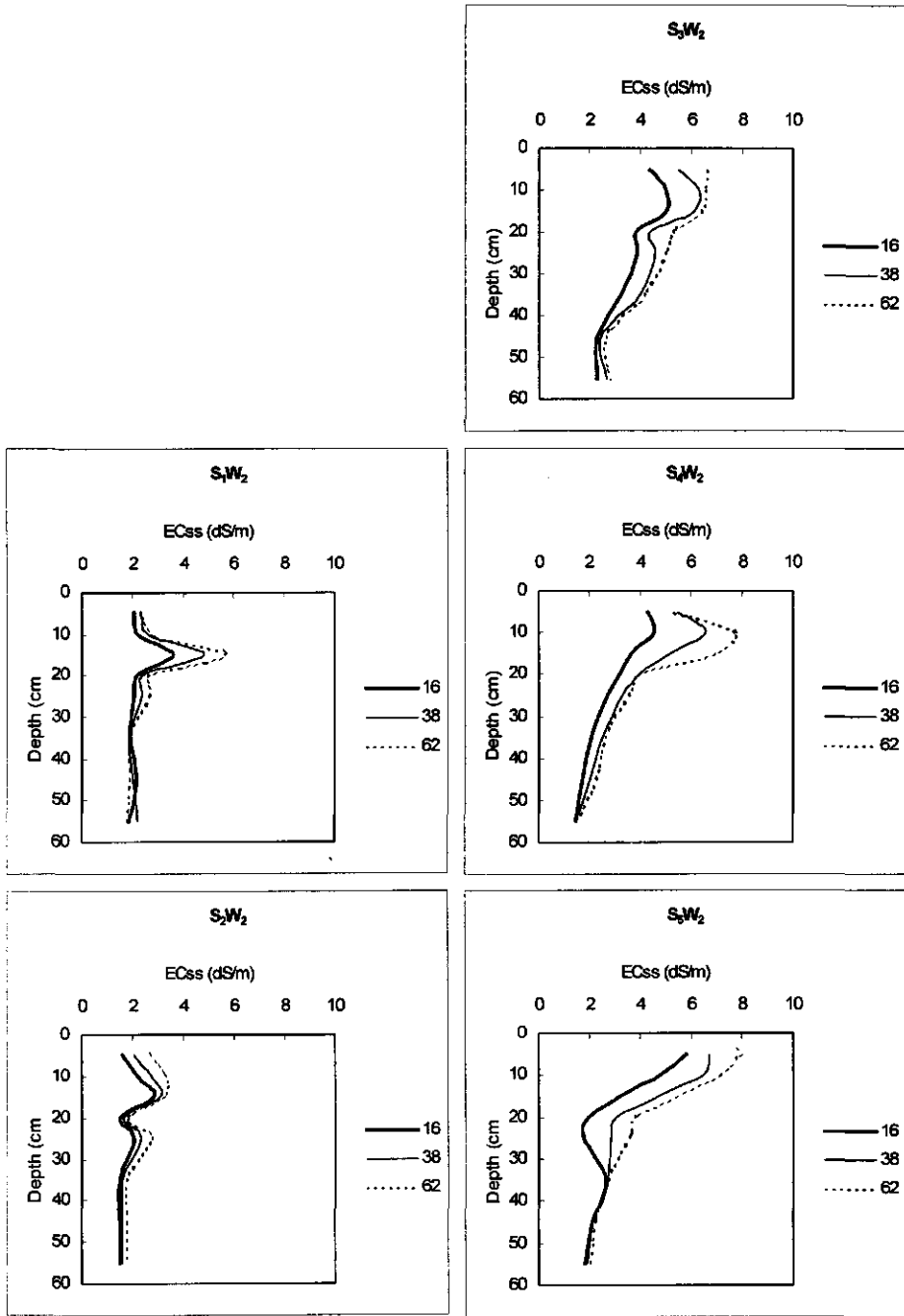


Figure 6.2. Measured soil solution salinity EC_{ss} distributions corresponding with water contents in Fig. 6.1.

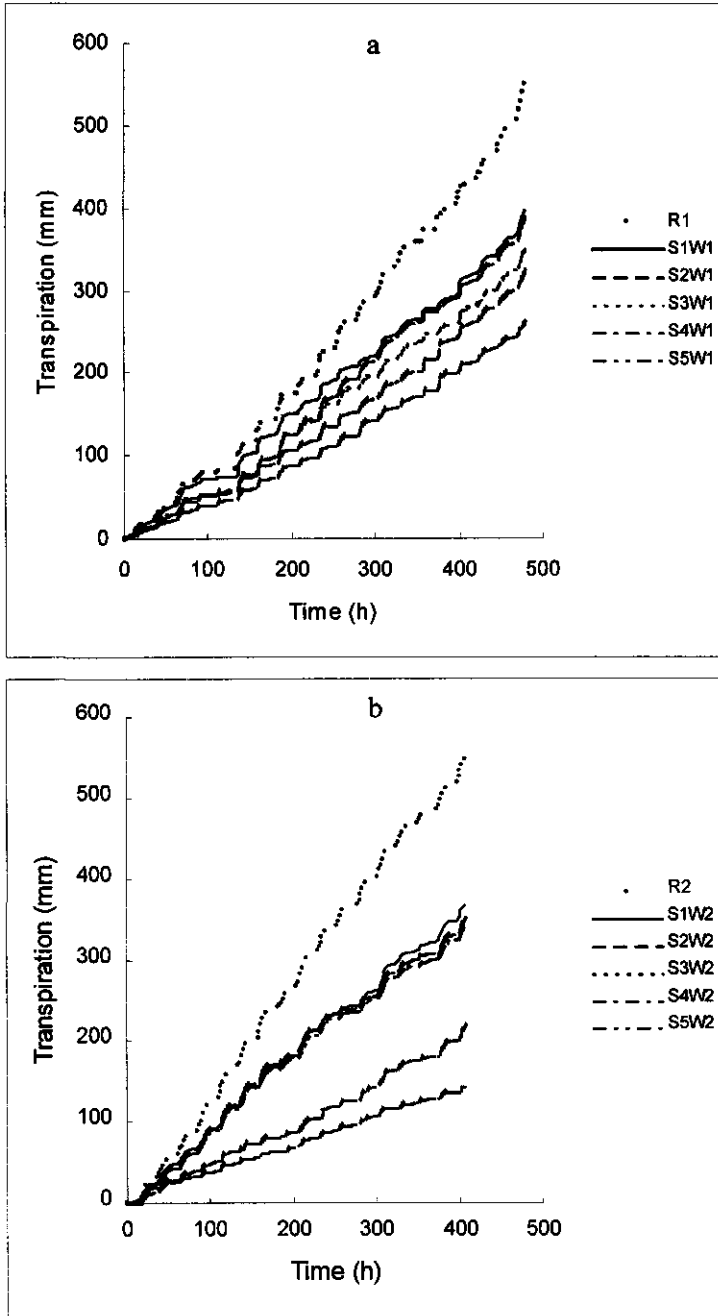


Figure 6.3. Measured cumulative transpiration of R₁, S₁W₁, S₂W₁, S₃W₁, S₄W₁, and S₅W₁ (a) and of R₂, S₁W₂, S₂W₂, S₃W₂, S₄W₂ and S₅W₂ (b).

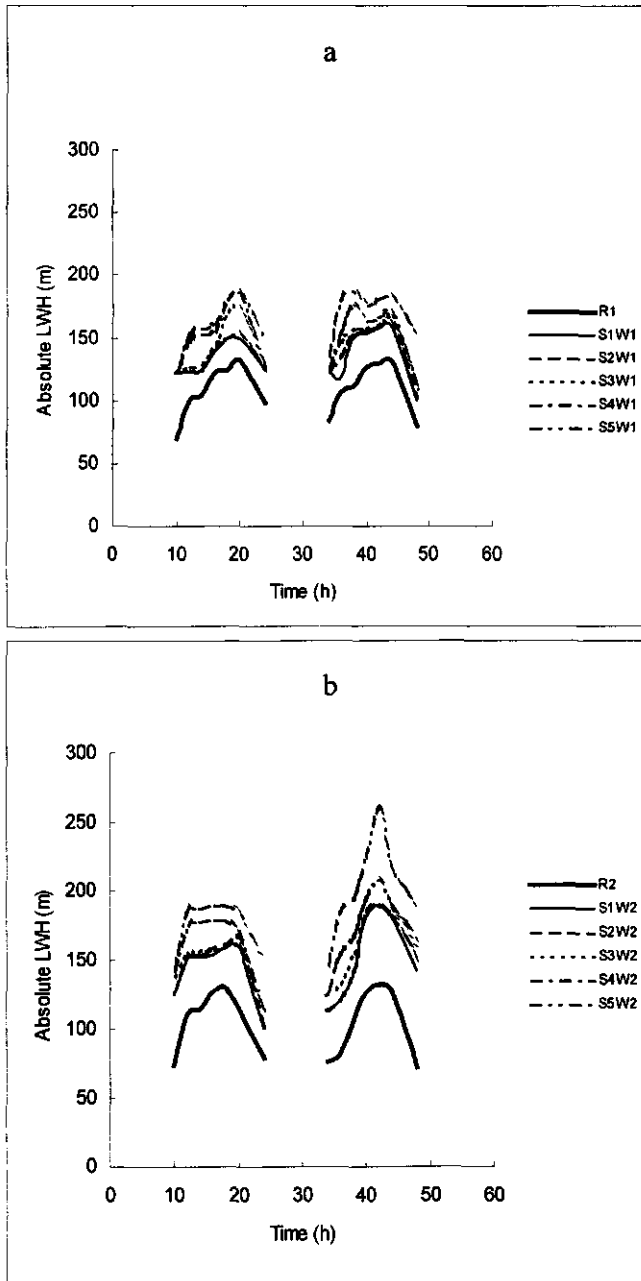


Figure 6.4. Absolute leaf water heads versus time after irrigation for R₁, S₁W₁, S₂W₁, S₃W₁, S₄W₁, and S₅W₁ (a) and for R₂, S₁W₂, S₂W₂, S₃W₂, S₄W₂, and S₅W₂ (b).

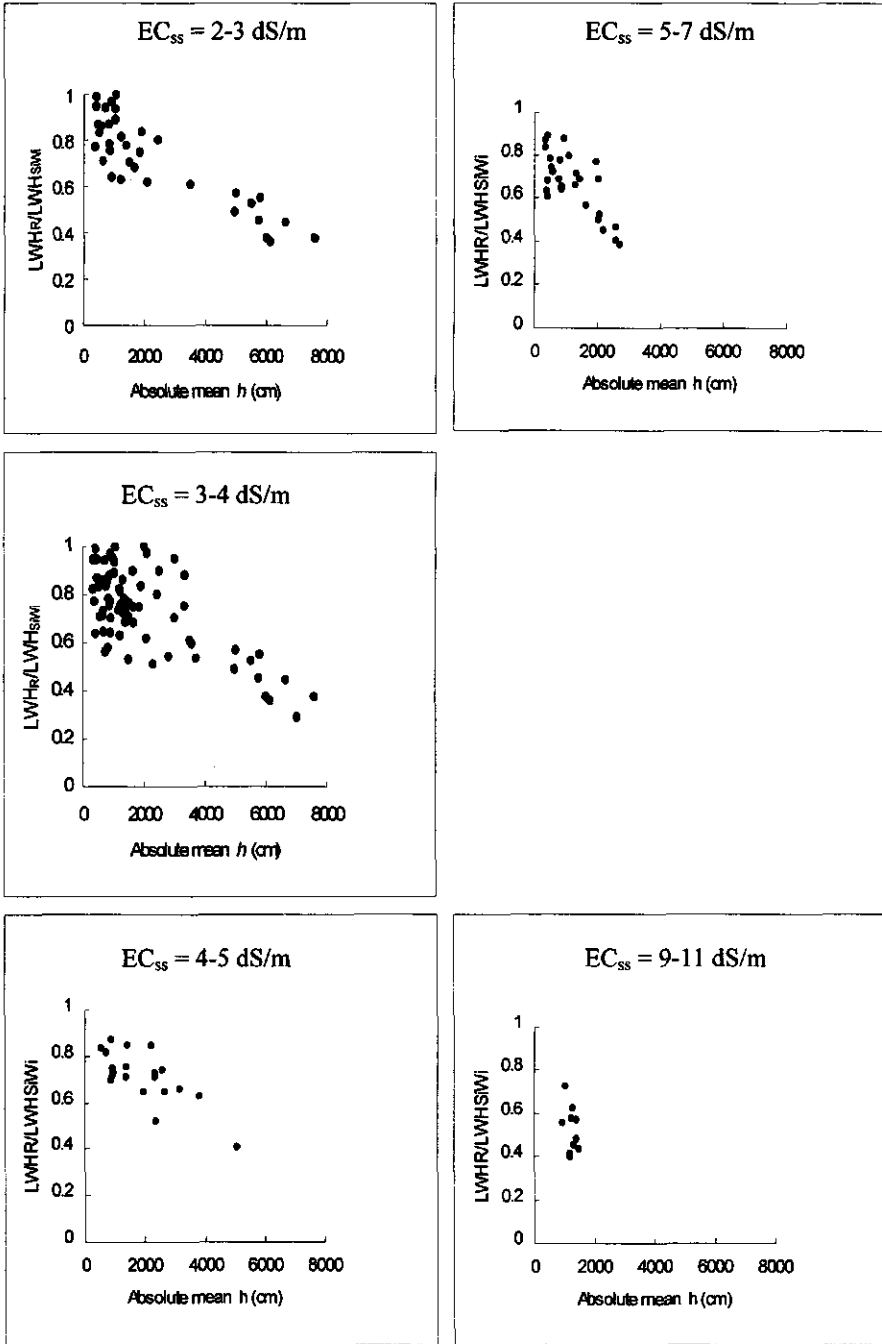


Figure 6.5. Relative leaf water head $LWHR/LWHS_{iWi}$ versus mean $|h|$ for mean EC_{ss} of 2-3 dS/m, 3-4 dS/m, 4-5 dS/m, 5-7 dS/m, and 9-11 dS/m.

Figure 6.6 presents the relationships between the experimental relative transpiration T_d/T_p and the mean $|h|$ for different mean EC_{ss} over the root zone. Either linear or nonlinear fitting can be applied in Fig. 6.6a, but for the other figures the relations become almost linear as the mean EC_{ss} increases. The relative transpiration decreased from 1.00 for mean $EC_{ss} = 2-3$ dS/m to 0.40 for mean $EC_{ss} = 9-11$ dS/m. The mean $|h|$ at which the plant's biological activities become minimal (wilting) changed from -8000 cm for mean $EC_{ss} = 2-3$ dS/m to about -2000 cm for mean $EC_{ss} = 9-11$ dS/m.

At a given soil water pressure head, the relative transpiration decreases with increasing salinity, similar to the relative leaf water head (Fig. 6.5). For the same mean soil solution salinities, neither the slopes nor the intercepts are exactly the same, and extrapolation to $T_d/T_p = 0$ and $LWH_R/LWH_{Si}W_i = 0$, respectively, does not give the same $|h|$ value.

The close similarity of relative LWH and relative transpiration as function of mean $|h|$ for a given EC_{ss} supports the suggestion of Dirksen (1985) that LWH instead of relative transpiration can be used to derive the parameter values for the $\alpha(h, h_0)$ function. One should keep in mind, however, that LWH depends not only on h_0 and h , but also on the time of measurement and evaporative demand. The LWH can change even within short time periods (see Figs. 6.4a and 6.4b). For all the experimental phases, it appears that the relative LWH was more sensitive to evaporative demand than relative transpiration. For instance, at a given h and h_0 the relative LWH could recover from about 0.6 to about 0.9 in the morning. The relative transpiration is also evaporative-demand dependent, but never changed as much. Furthermore, many plants are heterogeneous along their stems and provide different LWH at different locations. When deriving parameter values for reduction functions from LWH , these effects of location and times should be minimized. By doing so, the close agreement between the relative LWH and relative transpiration data in Figs 6.5 and 6.6 was obtained.

6.4. Test of theoretical reduction functions against experimental data

This section aims to compare the data obtained from the experiments with all the existing reduction functions under joint heterogeneous salinity and water stress. First, the existing concepts for joint water and salinity stress will be discussed, followed by introducing a new combination method under joint heterogeneous soil water osmotic and pressure heads. The latter differs conceptually from other approaches. Second, the experimental data under separate and combined stresses are compared and the available concepts are tested with the mean soil solution osmotic and pressure head data.

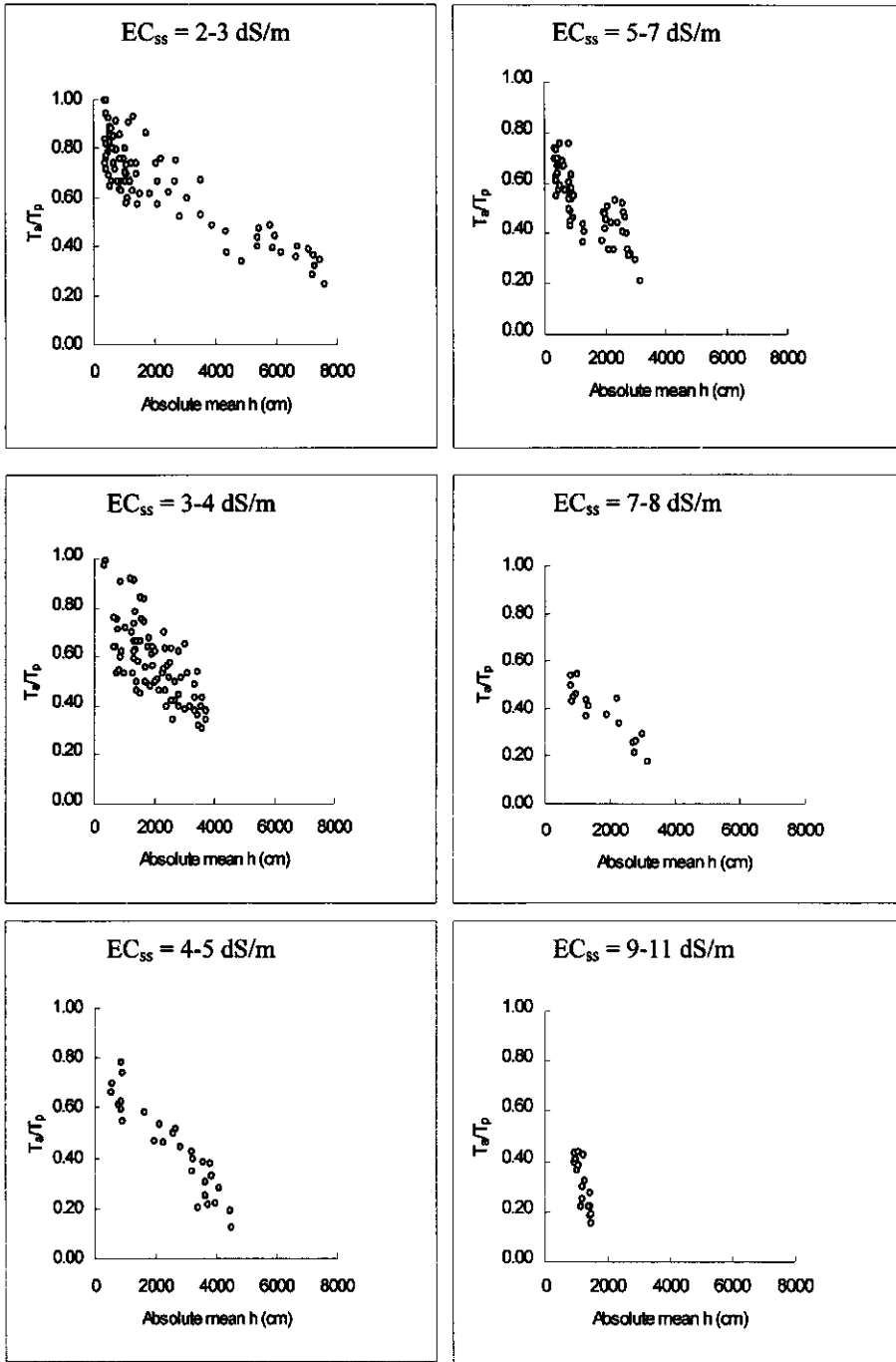


Figure 6.6. Relative transpiration T_s/T_p versus mean $|h|$ for mean EC_{ss} of 2-3 dS/m, 3-4 dS/m, 4-5 dS/m, 5-7 dS/m, 7-8 dS/m, and 9-11 dS/m.

6.4.1. Theoretical concepts

The available reduction functions can be divided into two categories: additive (Eq. 2.39) and multiplicative (Eqs. 2.40 and 2.41). One more multiplicative reduction function has been recently introduced in the latest version of SWAP (Van Dam *et al.*, 1997), the product of Eq. 2.33 and 5.1:

$$\alpha(h, h_o) = \frac{h - h_a}{h_3 - h_a} \times \left[1 - \frac{a}{360} (h_o^* - h_o) \right] \quad 6.1$$

For separate salinity and water stress, I proposed the two-threshold nonlinear functions Eqs. 4.4 and 5.5, respectively, which fit the experimental data satisfactorily. Similar to Eqs. 2.40 and 2.41, one can also take the product of those expressions:

$$\alpha(h, h_o) = \frac{1}{1 + \left(\frac{1 - \alpha_{01}}{\alpha_{01}} \right) \left[\frac{h^* - h}{h^* - h_{\max}} \right]^{p_1}} \times \frac{1}{1 + \left(\frac{1 - \alpha_{02}}{\alpha_{02}} \right) \left[\frac{h_o^* - h_o}{h_o^* - h_{o\max}} \right]^{p_2}} \quad 6.2$$

in which dimensionless p_1 and p_2 can be obtained from Eqs. 5.6 and 4.3, respectively. However, Eq. 6.2 belongs to the multiplicative category. This multiplicative approach, in principal, has no physical basis and cannot discriminate between its components. Different reductions due to osmotic and soil water pressure head produce the same result. For instance, the *joint reduction* $\alpha(h_o, h)$ due to $\alpha(h_o) = 0.25$ and $\alpha(h) = 0.50$ is exactly the same as for $\alpha(h_o) = 0.50$ and $\alpha(h) = 0.25$. From this point of view, multiplicativity can be regarded as an *identical* approach. As for the magnitude of the product, there is no evidence to support that separate reductions of 0.25 and 0.50 due to osmotic head and pressure head cause 0.875 reduction in water uptake.

*In view of these shortcomings, I introduce a new combination of reduction functions of Maas and Hoffman (1977) and Feddes *et al.* (1978) that differs conceptually from the additive and multiplicative approaches.* Figures 6.7a and 6.7b illustrate these reduction functions, respectively.

The reduction function of Fig. 6.7b can be divided into three parts. Part I (triangle h_1Ah_2) represents air deficiency, part II (rectangular h_2ABh_3) is the non-stress part, and part III (triangle h_3Bh_4) represents water stress. The slope of Bh_4 is determined by h_3 and h_4 . The latter (wilting point) is constant for a particular plant and h_3 is assumed to be only evaporative-demand dependent (Feddes *et al.*, 1978). Since this model originally was developed for nonsaline conditions, the slope of Bh_4 is valid for salinities equal to or less than the salinity threshold value EC^* , as shown in Fig. 6.7b.

The database of Maas and Hoffman is collected from nonrestricted water conditions. Taking advantage of this, I apply the reduction of this model directly to the no-water-stress part of Fig. 6.7b, as shown in figure 6.7c for alfalfa. Assuming linear reduction from B to h_4 , I assume further that each dS/m salinity beyond the threshold value shifts the wilting point 360 cm to the left. This is consistent with the observation that plants wilt at higher soil water pressure head in the presence of salinity than without salinity. The magnitude of 360 proposed here is only a preliminary guess coming from the well-known Eq. 3.6 and will be used until further evidence provides a more precise quantity.

The effect of each level of joint water and salinity stress can be obtained as illustrated in figure 6.7d. The general expression for the reduction in root water uptake due to joint soil water osmotic and pressure heads, as depicted in Fig. 6.7d can then finally be written as:

$$\alpha(h, h_0) = \frac{h - (h_4 - h_0)}{h_3 - (h_4 - h_0)} \times \left[1 - \frac{a}{360} (h_0^* - h_0) \right] \quad 6.3$$

This equation is valid for $h_0 \leq h_0^*$ and $(h_4 - h_0) \leq h \leq h_3$, respectively. Other general validities are the same as the original models.

This combination model is flexible to use any other (nonlinear) salinity reduction function instead of the linear function of Maas and Hoffman. Different salinity reduction functions should only change the height of the horizontal non-stress line segment of the Feddes *et al.* reduction function and not influence the slope of the line segment beyond h_3 significantly. The reduction function due to salinity and water stress remains linear, and the right hand side of Eq. 6.3 can be replaced with the appropriate parts of Eqs. 2.40, 2.41 and 6.2, respectively, in the following way:

$$\alpha(h, h_0) = \frac{h - (h_4 - h_0)}{h_3 - (h_4 - h_0)} \times \frac{1}{1 + \left[\frac{h_0}{h_{050}} \right]^{p_2}} \quad 6.4$$

$$\alpha(h, h_0) = \frac{h - (h_4 - h_0)}{h_3 - (h_4 - h_0)} \times \frac{1}{1 + \left[\frac{h_0^* - h_0}{h_0^* - h_{050}} \right]^{p_2}} \quad 6.5$$

$$\alpha(h, h_0) = \frac{h_0 - (h_4 - h_0)}{h_3 - (h_4 - h_0)} \times \frac{1}{1 + \left(\frac{1 - \alpha_{02}}{\alpha_{02}} \right) \left[\frac{h_0^* - h_0}{h^* - h_{0\max}} \right]^{p_2}} \quad 6.6$$

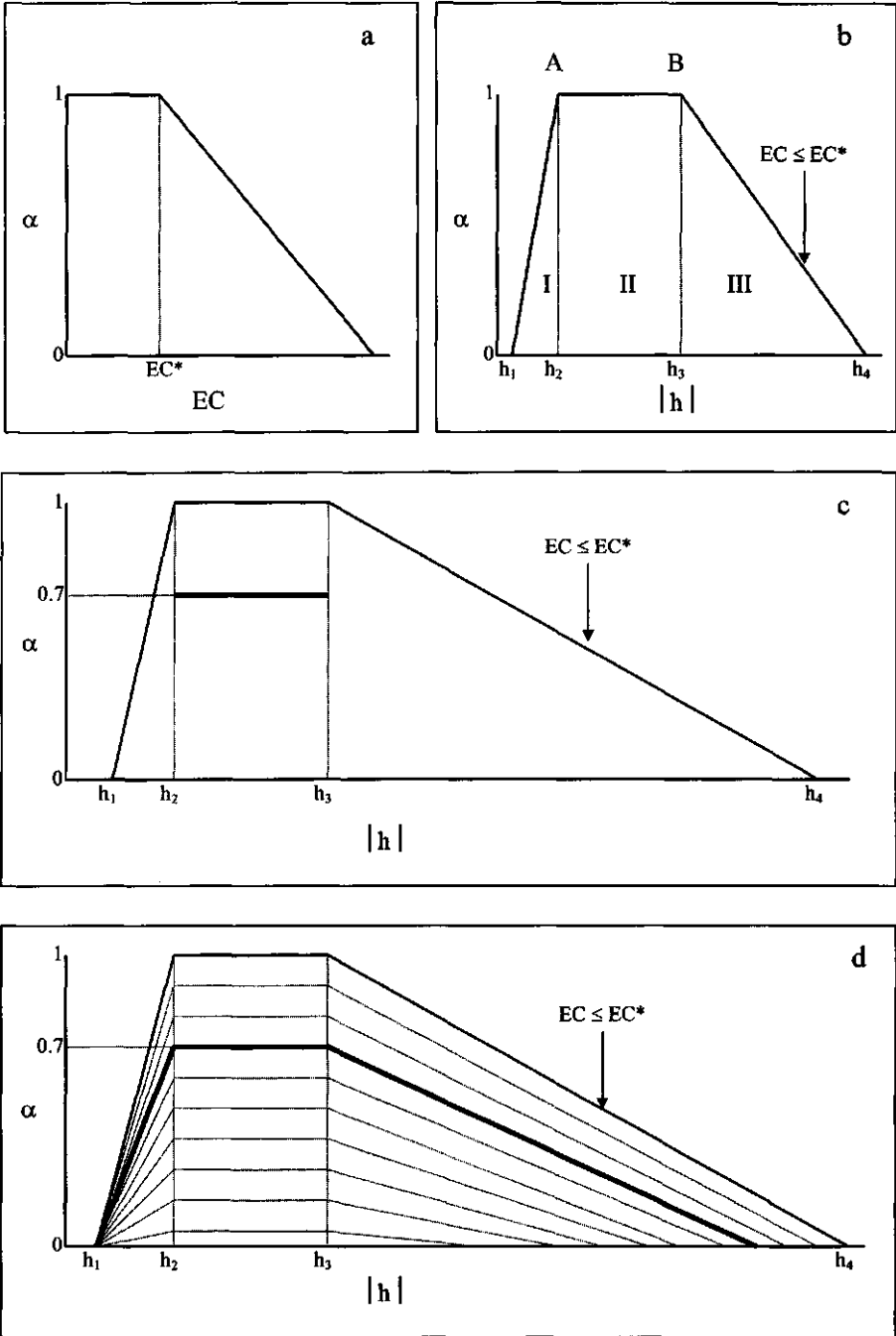


Figure 6.7. Schematic illustration of reduction functions of a: *Maas and Hoffman (1977)*; b: *Feddes et al. (1978)*; c: direct application of salinity reduction of *Maas and Hoffman* model (for $\alpha = 0.7$) into no-stress part of *Feddes et al.*; and d: combined reductions as function of soil salinity and pressure head.

In this section all these equations for joint water and salinity stress are compared with the experimental data. The data presented here belong to all the treatments in Table 6.1. The relative uptake is assumed to be equal to the relative transpiration:

$$\frac{\int_0^{z_r} S dz}{\int_0^{z_r} S_{\max} dz} = \frac{T_a}{T_p} = \alpha(h, h_0) \quad 6.7$$

6.4.2. Comparison of separate stress and combined stress data

Whereas in Chapters 4 and 5 the experimental data for separate salinity and water stress have been reported, this chapter presents the data under joint heterogeneous soil water osmotic and pressure heads. To facilitate discovering any consistent relationship of the separate and combined stresses, various experimental parameters are summarized in Table 6.2. The transpired water in all the salinity stress treatments was less than the applied water, while in the water stress treatments some water was taken up from the soil column in excess of applied water.

For the S_iW_0 treatments, relative transpiration T_a/T_p decreased with increasing salinity. Such a reduction also occurred for the S_iW_1 and S_iW_2 treatments and for the S_0W_i treatments in response to increasing water deficit. In most treatments the relative dry weight $(Y/Y_m)_d$ of the harvested plants was higher than the relative transpiration T_a/T_p . This may be regarded as contrary to the basic assumption made in Eqs. 4.2, 5.3 and 6.7. The most likely reason for this disagreement is that the plants were first allowed to develop into healthy plants before the stresses were introduced. Thus, the dry weight reflects in the first place the mass obtained before stress, and only secondarily the influence of the stress later on. In all the treatments the relative wet weight $(Y/Y_m)_w$ was less than the relative dry weight $(Y/Y_m)_d$.

According to the multiplicative models the separate reductions due to salinity and water stress can simply be multiplied. The data presented in Table 6.2 can potentially confirm or reject this concept. The product of $T_a/T_p = \alpha$ of S_1W_0 and $T_a/T_p = \alpha$ of S_0W_1 is $0.92 \times 0.66 = 0.61$. This product of the reduction terms due to the individual stresses S_1 and W_1 is smaller than the reduction term of the combined stress S_1W_1 , for which $T_a/T_p = \alpha = 0.74$. Similarly, for W_1 and $S_2, S_3, S_4,$ and S_5 this product is 0.56, 0.51, 0.44, and 0.39, respectively, while the reduction term for the combined stresses $S_2W_1, S_3W_1, S_4W_1,$ and S_5W_1 is 0.72, 0.65, 0.60, and 0.50. The same comparison yields $(0.92 \times 0.50 =) 0.46, 0.42, 0.39, 0.33,$ and 0.30 versus 0.67, 0.64, 0.62, 0.40, and 0.26 for $S_1W_2, S_2W_2, S_3W_2, S_4W_2,$ and S_5W_2 , respectively. The multiplicative model underestimates the

actual transpiration, except for S_5W_2 . Thus, the presented experimental data do not confirm the multiplicative concept. This conclusion is drawn irrespective of any functions. This will be evaluated in the next subsection.

Table 6.2. Comparison between relative transpiration T_d/T_p , relative applied water I_w/I_{wR} , ratio of transpired and applied water T_d/I_w , relative wet weight $(Y/Y_m)_w$, and relative dry weight $(Y/Y_m)_d$ of the separate and combined water and salinity stress treatments.

Treatment		T_d/T_p	I_w/I_{wR}	T_d/I_w	$(Y/Y_m)_w$	$(Y/Y_m)_d$
		-	-	-	g	g
S_1W_0	S_1W_0	0.92	1	0.98	0.89	1.00
	S_2W_0	0.85	1	0.98	0.76	0.87
	S_3W_0	0.78	1	0.98	0.56	0.65
	S_4W_0	0.67	1	0.98	0.49	0.58
	S_5W_0	0.59	1	0.98	0.37	0.55
S_0W_1	S_0W_1	0.66	0.57	1.05	0.61	0.87
	S_0W_2	0.50	0.39	1.18	0.56	0.69
S_1W_1	S_1W_1	0.74	0.52	1.33	0.59	0.74
	S_2W_1	0.72	0.52	1.29	0.57	0.70
	S_3W_1	0.65	0.52	1.17	0.48	0.69
	S_4W_1	0.60	0.52	1.08	0.47	0.64
	S_5W_1	0.50	0.52	0.89	0.45	0.55
S_1W_2	S_1W_2	0.67	0.43	1.30	0.52	0.70
	S_2W_2	0.64	0.41	1.30	0.48	0.65
	S_3W_2	0.62	0.41	1.28	0.47	0.59
	S_4W_2	0.40	0.41	0.82	0.45	0.58
	S_5W_2	0.26	0.29	0.76	0.25	0.36

6.4.3. Application of reduction functions to mean soil solution osmotic and pressure heads

Among the introduced reduction functions, Eq. 2.39 represents an additive form of water and salinity stress. As discussed in Chapter 2, values for the proportionality coefficients a_1 and a_2 in Eq. 2.39 are not available and hence Eq. 2.39 is simplified to a simple linear additivity of h and h_o , or $a_1 = a_2 = 1$. Figures 6.8a and 6.8b present the fit of the additive (Eq. 2.39), multiplicative (Eq. 2.40, 2.41, 6.1 and 6.2), and newly proposed combination (Eq. 6.3) reduction functions with the experimental relationship

of T_a/T_p versus mean h , for mean EC_{ss} of 7-8 and 9-11 dS/m, respectively. In both figures, Eq. 6.3 gives the best fit, while the worst agreement belongs to Eq. 2.39.

Equations 6.1 and 6.3 both represent a combination of the Feddes *et al.* (1978) and Maas & Hoffman (1977) models. Figure 6.9a compares the two models against experimental data for a mean EC_{ss} over the root zone of 9-11 dS/m. The simple product of the separate osmotic and pressure head components in Eq. 6.1 keeps h_4 (wilting point) constant in the saline condition. In contrast, Eq. 6.3 follows the experimental trend that with increasing salinity wilting occurs at higher soil water pressure heads. As the salinity increases, the disagreement between the two equations becomes greater. Figure 6.9b compares the new combination model with linear (Eq. 6.3) and nonlinear (Eqs. 6.4, 6.5, and 6.6) reduction due to salinity against the experimental data for mean $EC_{ss} = 9-11$ dS/m. The nonlinear salinity reduction terms influence the height of the horizontal segment only slightly (from 0.42 to 0.45). In view of this small difference, I propose that for practical purposes Eq. 6.3 be used, rather than Eqs. 6.4, 6.5, or 6.6.

These results indicate that neither the multiplicative nor the additive reduction functions fit the experimental data satisfactorily. *The best fits were obtained with Eq. 6.3, which combines the linear salinity reduction function of Maas & Hoffman (1977) with the pressure head reduction function of Feddes et al. (1987).* The additive Eq. 2.39 generally gave the worst agreement with the experimental data. *From a practical point of view, Eq. 6.3 appears to be accurate enough (Fig. 6.9b).* The parameter values for the Maas & Hoffman equation are available for many plants, while those of the nonlinear functions (Eqs. 6.4, 6.5, and 6.6) are difficult to obtain. *I propose, therefore, that Eq. 6.3 be used as a reduction function for joint heterogeneous soil water osmotic and pressure heads in the macroscopic root water uptake equation (Eq. 2.27).*

6.5. Simulation with HYSWASOR

In the simulations with HYSWASOR the input parameter values for the different reduction terms have been obtained from the previously calibrated treatments of separate salinity and water stress. Thus, no calibration was made for the 10 joint water and salinity stress treatments. The parameter values used in the simulations are given in Table 6.3.

Figure 6.10 presents a comparison between the experimental and that simulated with Eq. 6.3 water content distributions of S_1W_1 , S_2W_1 , S_3W_1 , S_4W_1 , and S_5W_1 at 40 and 166 hours after the first irrigation. The simulation model provides reasonably good agreement with the experimental water contents, particularly at relatively wet conditions.

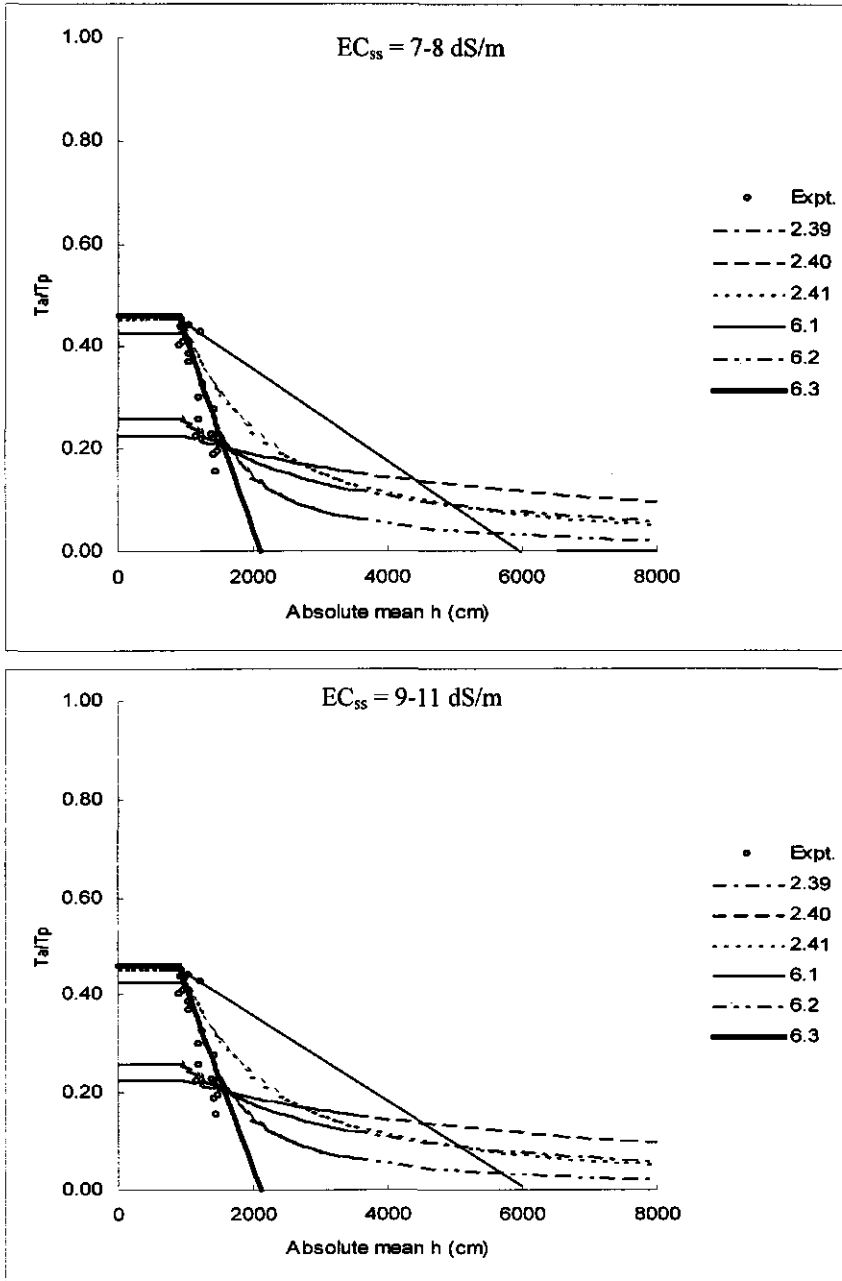


Figure 6.8. Comparison between additive (Eq. 2.39), multiplicative (Eqs. 2.40, 2.41, 6.1, and 6.2) and newly proposed combined reduction function (Eq. 6.3) with the experimental relationship of T_e/T_p versus mean pressure head for mean EC_{ss} of 7-8 dS/m and 9-11 dS/m.

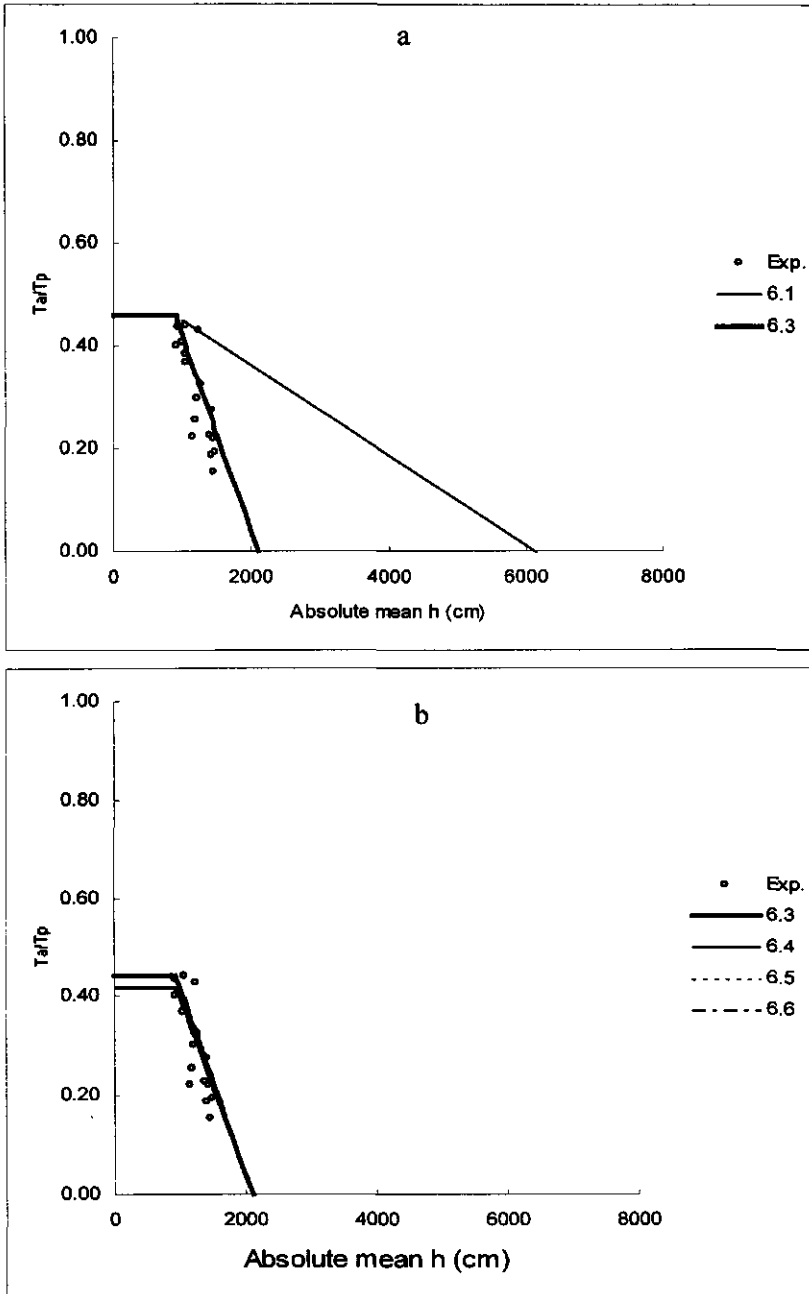


Figure 6.9. a: Comparison of multiplication of Feddes et al. (1978) and Maas and Hoffman (1977) models (Eq. 6.1), and the new combination reduction function (Eq. 6.3), with the experimental data for mean EC_{ss} of 9-11 dS/m; b: comparison between the new combination reduction function with linear (Eq. 6.3) and nonlinear (Eqs. 6.4, 6.5, and 6.6) reductions due to salinity.

Figure 6.11 shows that the corresponding experimental and simulated EC_{ss} distributions agree closer than the water contents. In some treatments and at some depths, the magnitude of the simulated EC_{ss} differs from the experimental values, but the trend is almost the same. The corresponding simulated root water uptake rates are given in Fig. 6.12. The water uptake distribution generally corresponds with the water content and EC_{ss} distributions. The highest water uptake rate occurs with S_1W_1 at 40 hours after the first irrigation in the upper 20 cm of the soil column. This reflects the high water content and low EC_{ss} in that part of the soil profile. The highest simulated salinity occurs after 166 h at 5 cm depth of S_5W_1 , at a water content of about $0.13 \text{ cm}^3/\text{cm}^3$ (Fig. 6.10). The simulated water uptake rate under these conditions is only about $0.002 \text{ cm}^3/\text{cm}^3 \text{ h}$.

Table 6.3. Parameter values used in simulations with various reduction functions.

Eq.	h_3 or h^* cm	h_4 cm	h_{50} cm	h_{max} cm	P_1 -	α_{01} -	h_o^* cm	h_{o50} cm	h_{omax} cm	P_2 -	α_{02} -	a m/dS
2.39	-	-	-1800	-	1.15	-	-	-	-	-	-	-
2.40	-	-	-1800	-	1.15	-	-	-2880	-	1.72	-	-
2.41	-800	-	-1600	-	1.25	-	-720	-2650	-	1.35	-	-
6.1	-1000	-8000	-	-	-	-	-600	-	-	-	-	0.071
6.2	-1000	-	-	-7000	1.15	0.17	-720	-	-5700	1.35	0.4	-
6.3	-1000	-8000	-	-	-	-	-600	-	-	-	-	0.071

Actual transpiration can be considered as the best indicator for the whole soil-plant-climate system under heterogeneous soil water osmotic and pressure head distributions. Thus, the final argument on the simulation performance of the various reduction functions can be based upon the comparison of the measured and simulated actual transpiration. Figures 6.13 to 6.17 give this comparison for S_1W_1 , S_2W_1 , S_3W_1 , S_4W_1 , S_5W_1 , S_1W_2 , S_2W_2 , S_3W_2 , S_4W_2 , and S_5W_2 . Without additional calibration, Eq. 6.3 provides the closest agreement in most treatments. At the lower soil solution salinities, Eq. 6.1 performs very closely to Eq. 6.3. Both equations combine the Feddes *et al.* (1978) and Maas and Hoffman (1977) functions. The main difference between Eqs. 6.1 and 6.3 is the slope of the reduction line due to salinity. Eq. 6.1 keeps h_4 constant at different salinities, and the slope of the line changes with the height of the horizontal segment for no-water-stress. In Eq. 6.3, h_4 decreases with increasing salinity and thus the slope of the line changes little. Since at low salinities the h_4 values in both equations are very close to each other, both equations provide almost similar results. As the soil solution salinity increases the difference between the equations becomes larger. Quantitative comparisons of all the reduction functions are given in the next subsection.

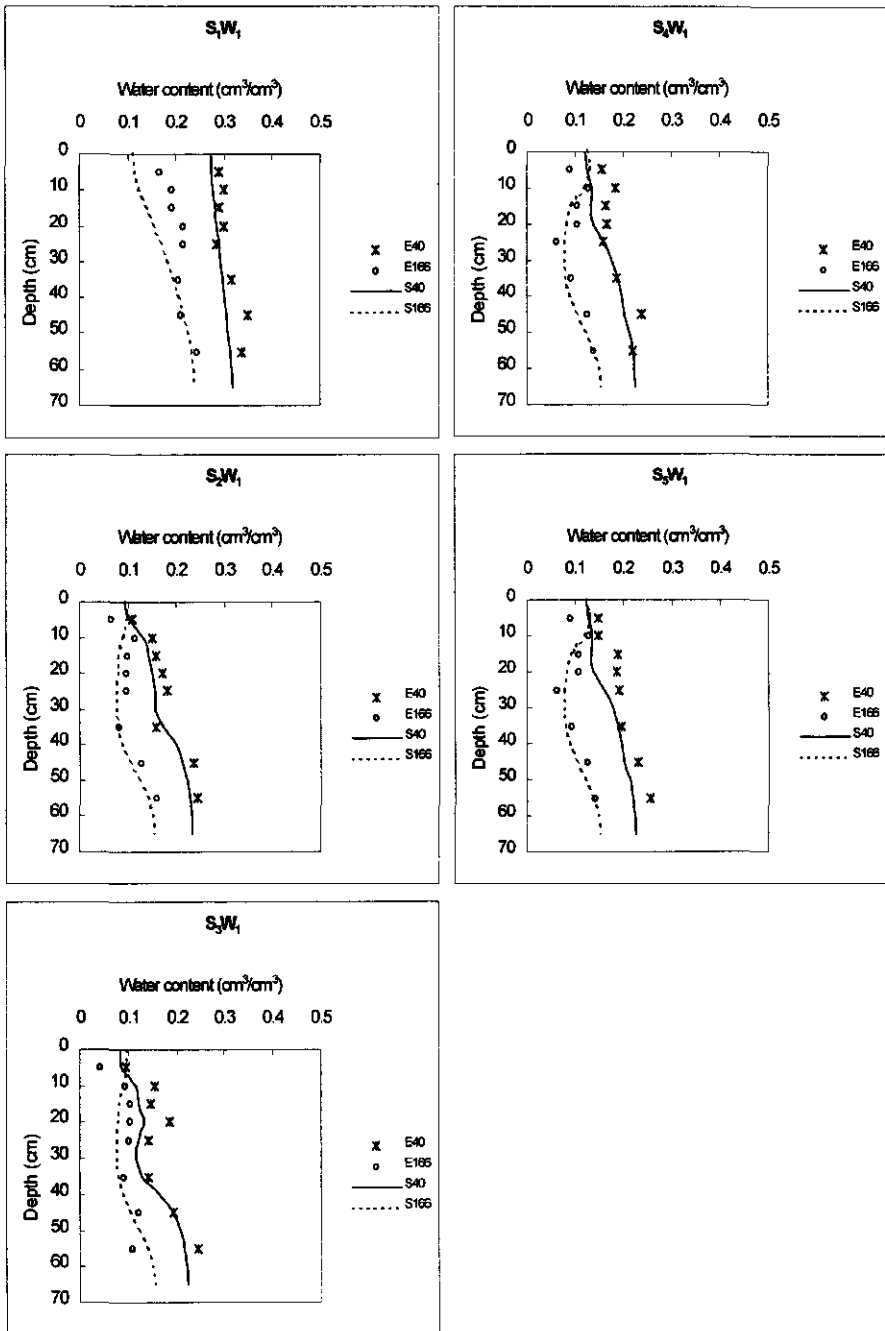


Figure 6.10. Comparison between experimental (E40, E166) and with Eq. 6.3 simulated (S40, S166) soil water content distributions for $S_1 W_1$, $S_2 W_1$, $S_3 W_1$, $S_4 W_1$, and $S_5 W_1$ at 40 and 166 hours after the first irrigation.

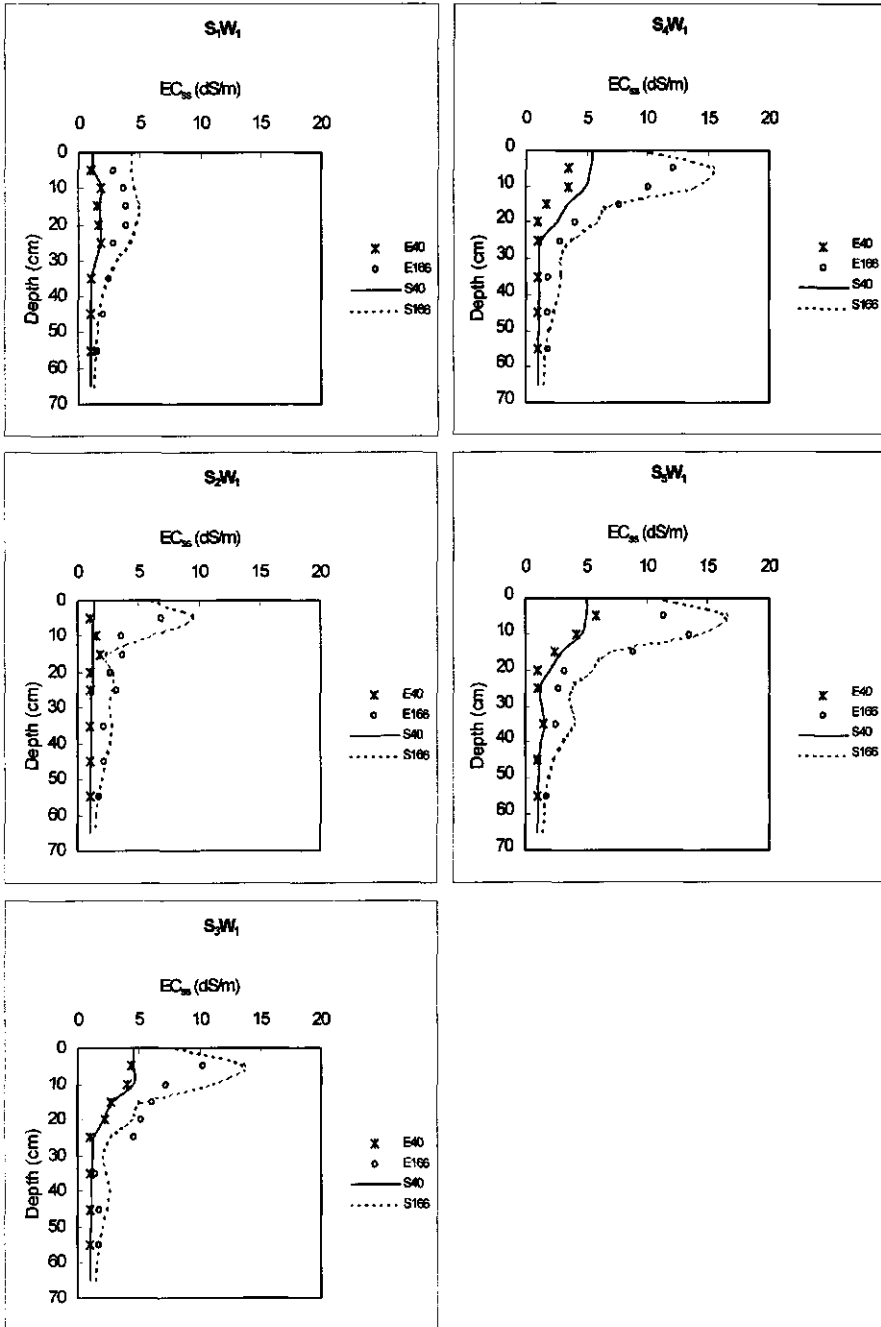


Figure 6.11. Experimental and simulated soil solution salinity EC_{ss} corresponding with water contents in Fig. 6.10.

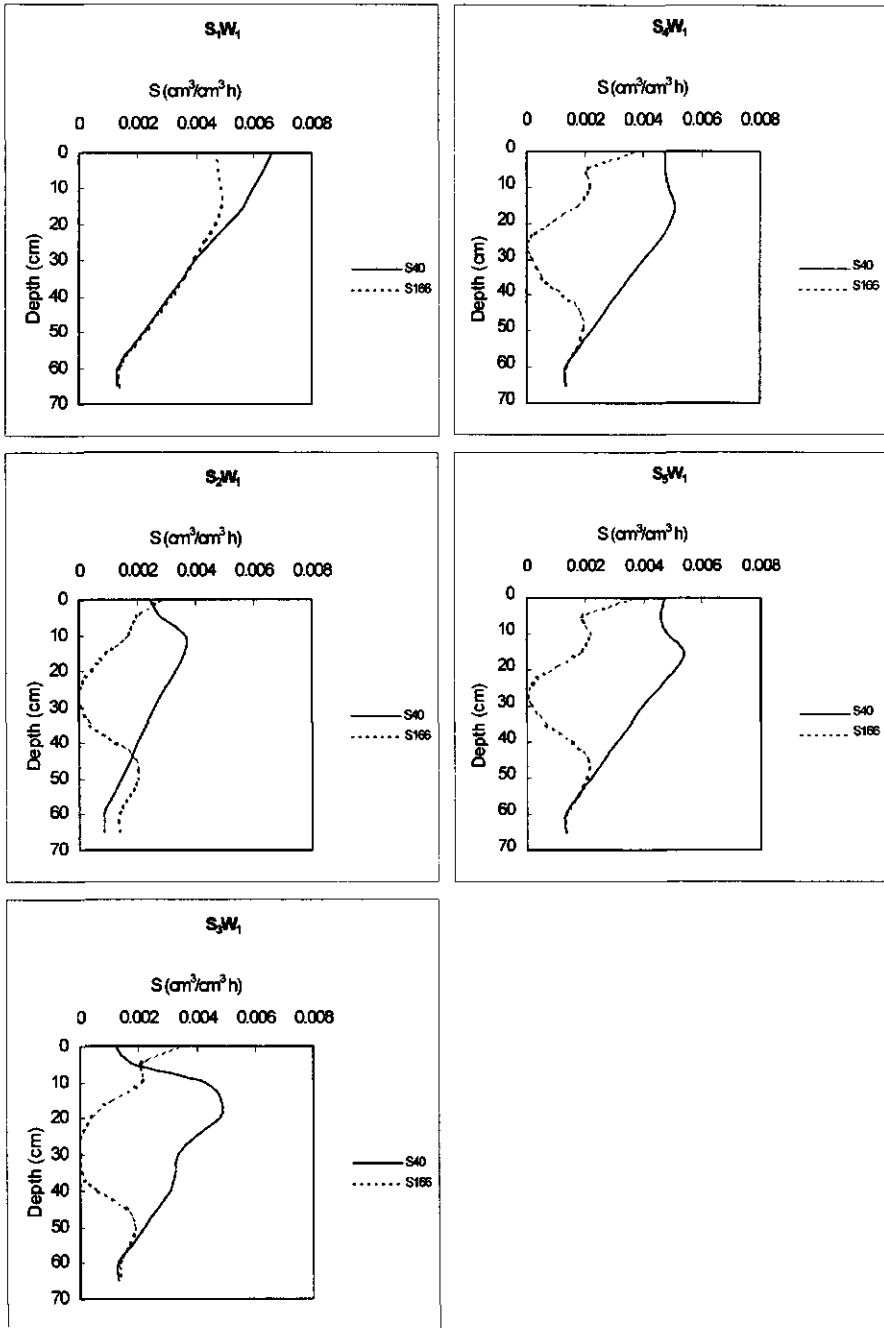


Figure 6.12. Simulated sink term S distributions corresponding with soil water contents and soil solution salinities in Figures 6.10 and 6.11, respectively.

6.5.1. Quantitative comparison of experimental and simulated actual transpiration

In the preceding two chapters, the residual errors between the simulated and experimental results have been analyzed to evaluate the performance of the various reduction functions. The same statistics are employed here, namely maximum error (*ME*), root mean square error (*RMSE*), coefficient of determination (*CD*), modelling efficiency (*EF*), and coefficient of residual mass (*CRM*). The mathematical expressions of these statistics are given in Chapter 4, and the values calculated for the actual transpiration simulated with Eqs. 2.39, 2.40, 2.41, 6.1, 6.2, and 6.3 are given in Tables 6.4 and 6.5.

For all treatments except S_5W_2 , the worst simulation results are obtained with the simple additivity of Eq. 2.39, while Eq. 6.3 performs the best for eight treatments. For S_1W_1 and S_4W_2 , Eq. 6.2 gives a slightly better performance than Eq. 6.3. In most cases, the tendency of Eq. 6.3 to overestimate or underestimate (*CRM*) is less than that of other equations. Tables 6.4 and 6.5 indicate that the root mean square errors with Eq. 6.3 is minimum for 7 of the 10 treatments, which indicates that for these 7 treatments all other equations provide over and/or underestimates of the cumulative actual transpiration. Also, for 7 treatments the simulated transpiration with Eq. 6.3 provides less scatter with the experimental data than the other equations. *In conclusion, for most treatments Eq. 6.3 yields the best agreement with the measured transpiration.*

6.6. Summary and conclusions

Six different reduction functions were used in the macroscopic sink term of Eq. 2.27. The reduction functions are the additive Eq. 2.39, the multiplicative Eqs. 2.40, 2.41, 6.1 and 6.2, and the newly proposed Eq. 6.3 which combines the linear salinity reduction function of *Maas and Hoffman* (1977) and the linear soil water pressure head reduction function of *Feddes et al.* (1978). The parameter values for these reduction functions were first derived from experimental data and then incorporated in the numerical simulation model HYSWASOR. The simulated actual transpiration, water content, and soil solution salinity were compared with the experimental data.

The relation between relative transpiration and mean $|h|$ was more or less linear for all mean EC_{ss} except for the lower level of $EC_{ss} = 2-3$ dS/m (Fig. 6.6). This linearity was also observed for the corresponding relative leaf water head. As the mean soil solution salinity increased the trend became more linear. The linear trend is in agreement with the reported experimental data for the salinity stress treatments (experimental phase II) but not with the nonlinear trend obtained for the water stress treatments (experimental phase III).

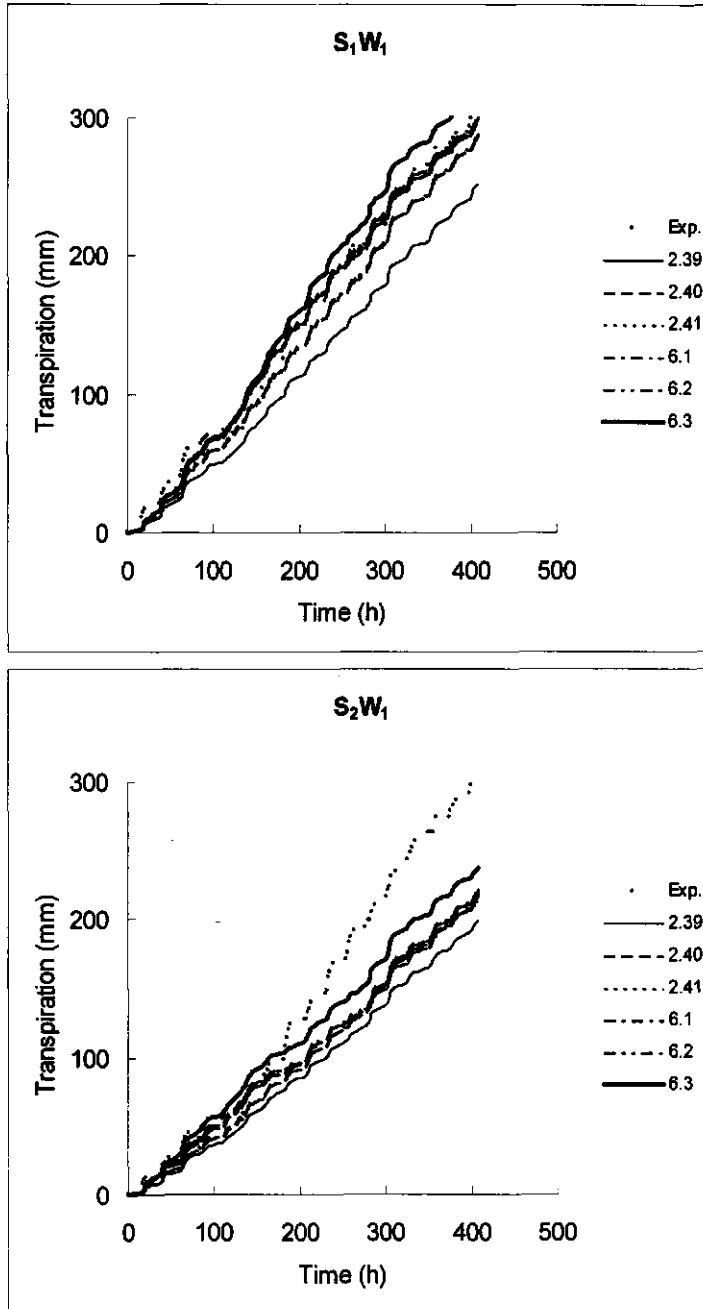


Figure 6.13. Comparison of cumulative actual transpiration simulated with Eqs. 2.39, 2.40, 2.41, 6.1, 6.2, and 6.3 with experimental data for S_1W_1 and S_2W_1 treatments.

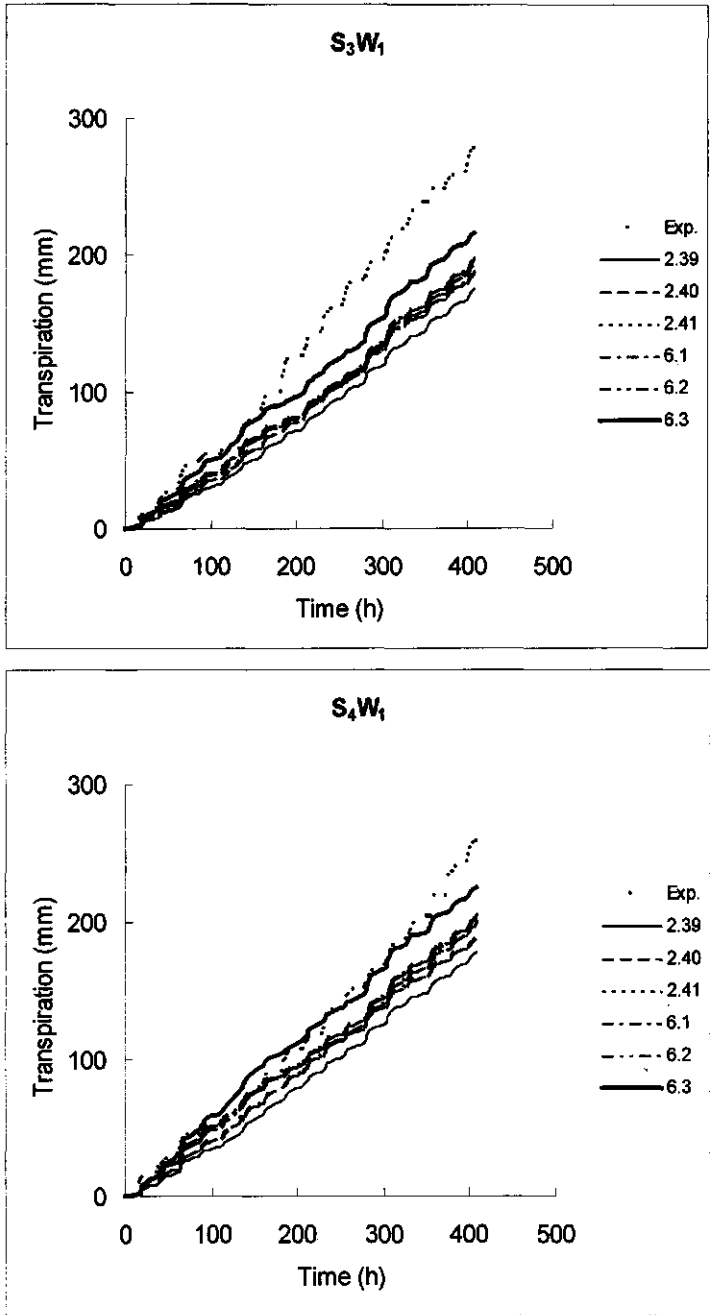


Figure 6.14. Comparison of cumulative actual transpiration simulated with Eqs. 2.39, 2.40, 2.41, 6.1, 6.2, and 6.3 with experimental data for S_3W_1 and S_4W_1 treatments.

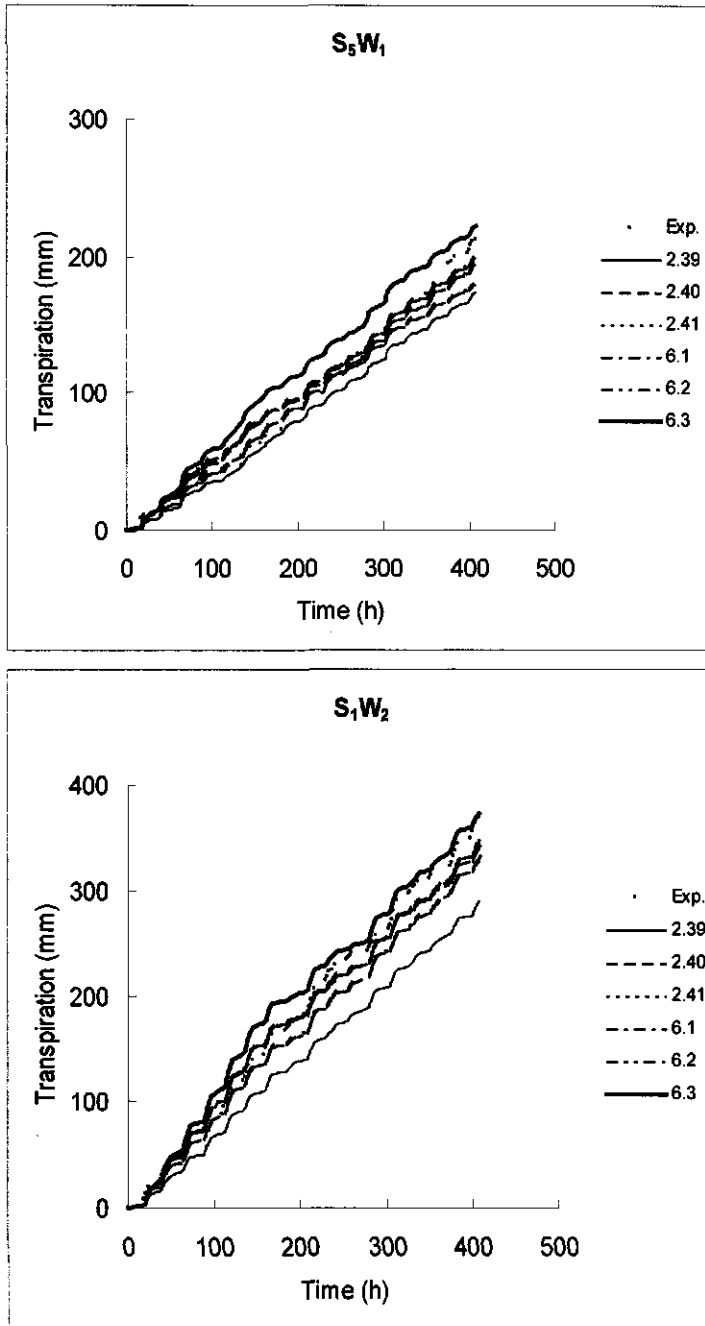


Figure 6.15. Comparison of cumulative actual transpiration simulated with Eqs. 2.39, 2.40, 2.41, 6.1, 6.2, and 6.3 with experimental data for S_5W_1 and S_1W_2 treatments.

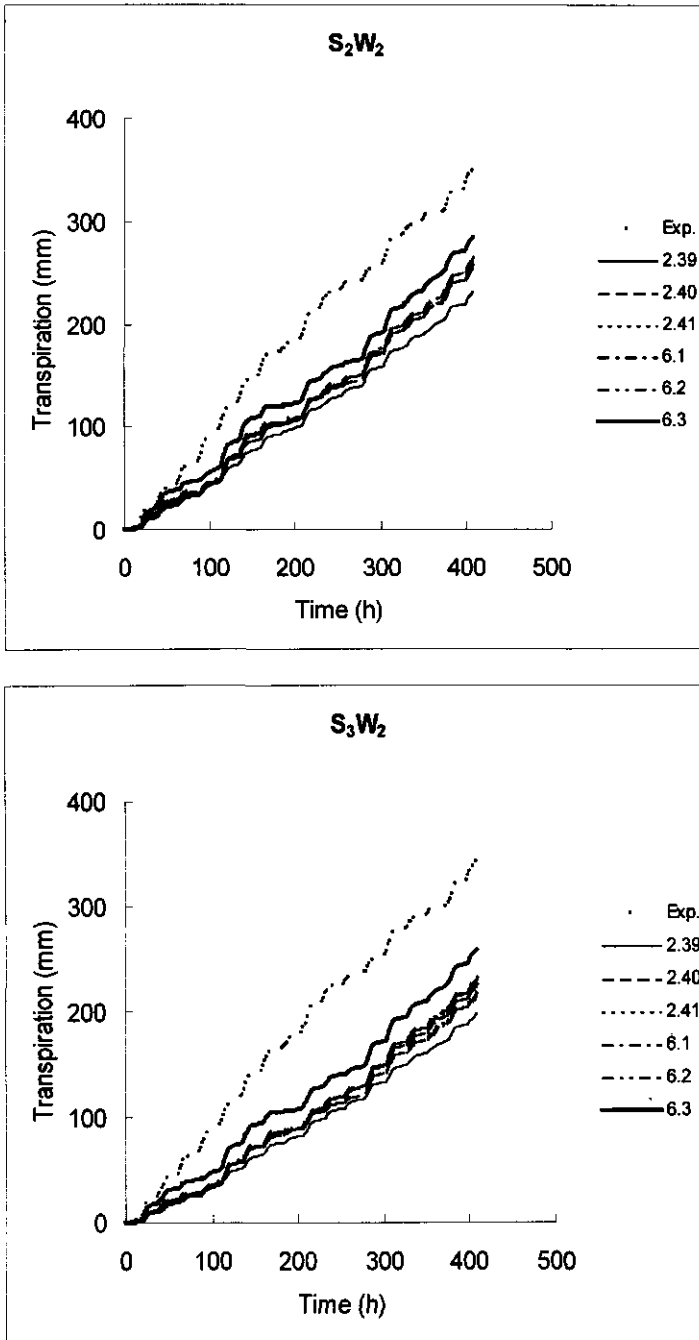


Figure 6.16. Comparison of cumulative actual transpiration simulated with Eqs. 2.39, 2.40, 2.41, 6.1, 6.2, and 6.3 with experimental data for S_2W_2 and S_3W_2 treatments.

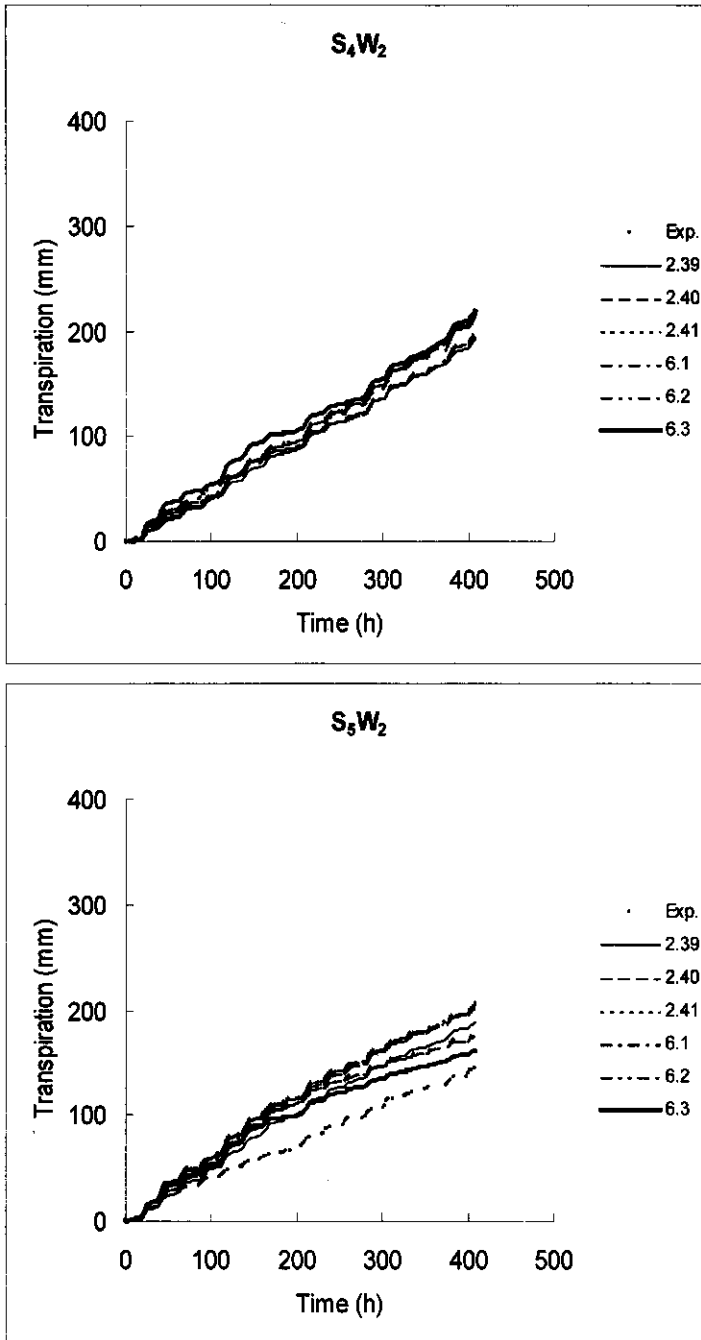


Figure 6.17. Comparison of cumulative actual transpiration simulated with Eqs. 2.39, 2.40, 2.41, 6.1, 6.2, and 6.3 with experimental data for S_4W_2 and S_5W_2 treatments.

Table 6.4. Statistics used to compare the HYSWASOR model performance with different reduction functions for S_1W_1 , S_2W_1 , S_3W_1 , S_4W_1 , and S_5W_1 against the experimental actual transpiration T_a .

Treatments	Equation	ME mm	RMSE mm	CD -	EF -	CRM -	r -
S_1W_1	2.39	63.1	197	0.83	0.165	0.220	0.995
	2.40	29.1	80	0.93	0.066	0.088	0.993
	2.41	17.9	30	0.99	0.002	0.008	0.992
	6.1	17.3	31	0.97	-0.027	0.001	0.980
	6.2	16.5	29	0.99	-0.007	0.006	0.992
	6.3	18.5	74	0.81	-0.229	-0.062	0.983
S_2W_1	2.39	109.4	307	0.67	0.324	0.345	0.998
	2.40	92.5	252	0.65	0.334	0.283	0.998
	2.41	88.3	224	0.61	0.389	0.249	0.997
	6.1	93.7	227	0.58	0.416	0.250	0.997
	6.2	88.3	225	0.61	0.387	0.250	0.997
	6.3	70.7	162	0.60	0.395	0.162	0.998
S_3W_1	2.39	102.6	572	0.82	0.177	0.394	0.997
	2.40	84.7	473	0.78	0.221	0.328	0.997
	2.41	81.2	431	0.73	0.261	0.302	0.994
	6.1	91.6	447	0.70	0.295	0.317	0.992
	6.2	81.2	432	0.74	0.250	0.301	0.994
	6.3	61.7	293	0.68	0.317	0.196	0.998
S_4W_1	2.39	80.7	246	0.73	0.262	0.276	0.998
	2.40	60.2	165	0.75	0.246	0.184	0.997
	2.41	55.5	124	0.70	0.297	0.135	0.996
	6.1	70.7	154	0.618	0.381	0.166	0.995
	6.2	55.6	125	0.70	0.295	0.137	0.996
	6.3	33.8	60	0.81	0.186	0.009	0.996
S_5W_1	2.39	39.3	121	0.77	0.227	0.134	0.996
	2.40	18.2	41	0.90	0.090	0.020	0.996
	2.41	13.2	62	0.90	0.092	-0.043	0.994
	6.1	32.4	90	0.72	0.270	0.007	0.990
	6.2	13.3	61	0.90	0.092	-0.41	0.994
	6.3	9.4	173	0.80	-0.23	-0.194	0.998

Table 6.5. Statistics used to compare the HYSWASOR model performance with different reduction functions for S_1W_2 , S_2W_2 , S_3W_2 , S_4W_2 , and S_5W_2 against the experimental actual transpiration T_a .

Treatments	Equation	<i>ME</i> mm	<i>RMSE</i> mm	<i>CD</i> -	<i>EF</i> -	<i>CRM</i> -	<i>r</i> -
S_1W_2	2.39	76.7	272	0.80	0.197	0.23	0.999
	2.40	34.9	105	0.83	0.160	0.092	0.999
	2.41	20.3	76	0.86	0.130	0.018	0.998
	6.1	24.2	93	0.83	0.140	0.023	0.998
	6.2	20.7	76	0.86	0.133	0.020	0.998
	6.3	16.5	164	0.96	-0.042	-0.070	0.998
S_2W_2	2.39	117.6	370	0.97	-0.022	0.416	0.992
	2.40	94.3	319	0.96	0.036	0.358	0.991
	2.41	93.7	319	0.96	0.036	0.358	0.991
	6.1	96.7	313	0.92	0.070	0.352	0.988
	6.2	88.8	305	0.94	0.056	0.343	0.998
	6.3	77.3	233	0.97	0.152	0.261	0.990
S_3W_2	2.39	143.3	445	0.80	-0.237	0.500	0.991
	2.40	116.5	390	0.88	-0.133	0.438	0.989
	2.41	110.3	381	0.89	-0.121	0.428	0.987
	6.1	125.3	401	0.89	-0.121	0.451	0.989
	6.2	110.5	382	0.89	-0.124	0.429	0.987
	6.3	87.4	290	0.94	-0.064	0.326	0.991
S_4W_2	2.39	23.5	488	0.90	0.09	0.090	0.996
	2.40	9.4	404	0.95	-0.051	-0.006	0.996
	2.41	9.6	395	0.95	-0.053	-0.014	0.997
	6.1	19.9	431	0.83	0.164	0.050	0.997
	6.2	9.5	396	0.95	-0.057	-0.013	0.997
	6.3	20.5	360	0.97	0.033	-0.093	0.997
S_5W_2	2.39	44.8	302	0.44	0.55	-0.333	0.993
	2.40	59.2	424	0.34	0.65	-0.476	0.993
	2.41	60.8	468	0.33	0.66	-0.527	0.995
	6.1	44.6	369	0.48	0.51	-0.416	0.990
	6.2	60.7	466	0.33	0.66	-0.349	0.992
	6.3	34.4	251	0.65	0.34	-0.283	0.998

The experimental results clearly support Eq. 6.3, particularly for the higher soil solution salinities. While Eq. 6.3 contains a linear salinity reduction function, it is still flexible to be used with any nonlinear salinity reduction term, such as Eqs. 6.4, 6.5 and 6.6. However, these expressions give no significant improvement in the comparison with the presented experimental data. *Equation 6.3 has the advantage of simplicity and requires less input values.*

The comparison between the experimental and simulated transpiration indicates that for most treatments Eq. 6.3 provides the best results. Among the multiplicative functions, Eqs. 2.41 and 6.2 provide the better results. Since Eq. 2.41 requires parameter values of h_{50} , h_{050} , p_1 and p_2 that are difficult to obtain, it is more convenient to use Eq. 6.2. The values of p_1 and p_2 can be obtained with Eqs. 5.6 and 4.3, respectively. The simple additivity of Eq. 2.39 always provided the worst agreement with the experimental data. With Eq. 6.3, the simulation model provides reasonably good agreement with the experimental soil water content and even more with the soil solution salinity. Some discrepancies were observed, but the trend of the simulated data was reasonable. The discrepancy between the simulated and experimental water contents is partly due to the way water uptake is calculated. The potential transpiration is distributed equally over each soil increment and the water uptake is calculated according to its own reduction function and root activity, independent of the uptake in other increments. Integration of these uptake increments over the root zone yields the total uptake. In reality, the plant can take up the required water from any depth if there are active roots. Root systems are reasonably flexible to adjust to water uptake at other depths to reach their evaporative demand. Water flow in the soil in compensation of water depletion due to root water uptake at other depths also seems to be an important phenomenon, which has to be taken into account in a proper way. More research is needed to verify and quantify this. The second reason for the disagreement between the simulated and experimental water contents can be attributed to increases in soil hydraulic conductivity in the presence of roots. Soil hydraulic conductivity also increases with increasing salinity (see chapter 1). The input soil hydraulic parameters are obtained from soil samples without roots and salinity and are assumed constant during the simulations.

All observations clearly support the newly proposed Eq. 6.3. The magnitude of the soil water pressure head at which wilting occurs at different salinities needs more investigation.

Summary

Water scarcity and soil salinity are two important limitations for agricultural production in the arid and semi-arid regions. From the point of view of crop production in such areas, it is important to quantify the influence of soil water osmotic and pressure heads under non-optimal conditions. These influences generally appear in the ability of plant roots to take up water from the soil. Root water uptake is a dynamic process influenced by soil, plant, and climate conditions such as soil water pressure head, soil hydraulic conductivity, osmotic head, evaporative demand, rooting depth, root density distribution, and plant hydraulic resistances and other plant properties. To quantify such a process, the major difficulty in solving the *Richards* equation stems from the lack of a sink term function that adequately describes root water uptake.

Historically, both microscopic and macroscopic concepts of water uptake by roots have evolved. The microscopic concept considers the radial flow of soil water towards a representative root of infinite length, uniform thickness, and uniform absorptivity. In microscopic models, the soil water flow equation is usually written in cylindrical coordinates and solved with appropriate boundary conditions at a root surface and at some distance from the root. Since obtaining the required input parameters at the soil-root interface is rather difficult, if not impossible, it has not proven practical to measure the required parameters directly to test the proposed microscopic models. Macroscopic models regard the root system as a whole and the needed parameters can be measured. For this reason, these models are most widely used in numerical simulation studies. The macroscopic concept remains essentially empirical, however, and much research is still needed to be done to derive physically based descriptions.

For the reasons stated above, the empirical macroscopic approach was chosen in this study. All existing reduction functions, as well as those newly developed in this study are used in the macroscopic model and tested against experimental data. The experimental data are used to derive the parameter values needed for the simulation model HYSWASOR. The experiments covered root water uptake by alfalfa under salinity stress, water stress, and combined salinity and water stress. This order is followed with the analysis of the experimental data and the simulations.

The alfalfa was grown in a specifically designed experimental set up with densely instrumented soil columns and harvested at approximately 50-day intervals for one year.

Chapter 2 describes the theory of water flow and solute transport in soil, together with the sink term models. Water flow in the unsaturated zone is described by the *Darcy* equation (Eq. 2.1), together with the soil water retention and hydraulic conductivity characteristics. These soil hydraulic properties are described by the analytical functions of *Van Genuchten* and *Mualem*. Solute transport is described by the convection-dispersion equation (Eq. 2.9). Sink term concepts are reviewed and classified in microscopic and macroscopic models. The existing macroscopic reduction functions for salinity stress, water stress and the combined stress are presented. This theoretical frame work is the basis of HYSWASOR, a one-dimensional finite element model for hysteretic water and solute transport in the root zone.

Chapter 3 describes the experimental materials and methods. The specifically designed set-up and the method used for packing the soil is described in detail. The sequence of the stresses applied to the plants is discussed. The experiments consisted of three phases: salinity stress, water stress, and salinity and water stress. Data analysis and simulation results of each phase are discussed in separate chapters. The standard laboratory method used to determine the soil water retention and hydraulic conductivity characteristics is discussed. The theory of Time Domain Reflectometry (TDR) for indirect measurement of soil water content and bulk electrical conductivity is discussed briefly.

In Chapter 4, existing and a newly developed salinity reduction functions are tested directly on the experimental data and inserted in the numerical simulation model HYSWASOR to check them in a macroscopic root water uptake model (Eq. 2.27). All the experimental and simulated results indicated that the well known so-called crop response function Eq. 2.33 with the slope originally proposed by the modelers and a modified salinity threshold value can be used as a reduction function in Eq. 2.27. The most sensitive part of this reduction function is the threshold value, while for Eq. 2.35 without a threshold the major sensitivity lies in its shape parameter. Because most of the parameter values originally proposed by the modelers do not provide good agreement with the experimental data, the parameter values are derived from the measured mean soil solution salinities. When used in the simulation model, these values still have to be modified slightly to reach the best agreement with the experimental data, because the simulation model calculates the root water uptake independently at individual times and depths. The simulated actual transpirations are rather close to the experimental values, while the simulated soil water contents and soil solution osmotic head indicate some discrepancies with the actual data; the mean values of these variables are very close to the measured data. This implies that the

simulation model can provide good agreement with the measured data when the system is regarded in its entirety. Both the simulated and experimental data indicate that different salinity reduction functions can provide almost the same results if the parameter values are well specified. This observation suggests the use of the simple linear reduction term Eq. 2.33 in the simulation model.

In Chapter 5, four different soil water pressure head reduction functions are used in the macroscopic model of Eq. 2.27. The linear reduction function of Eq. 5.1 can not fit the experimental data well. The nonlinear functions of equations 2.38 and 5.2 do not fit the whole range of the experimental data, while the newly developed two-threshold function of Eq. 5.5 provides a reasonable fit to all the experimental data. The soil water pressure head heterogeneity over the root zone does not play an important role in water uptake as long as there is enough water available in a part of the root zone. The plants can supply the evaporative demand from that part, thus compensating for the water deficit in the drier parts. This conclusion is based upon the observations that on the first day after the irrigations both the actual relative transpiration and the relative leaf water head were almost the same for the stressed and nonstressed treatments. The main reason for the discrepancies between the simulated and measured water contents appears to be *root water uptake during the night*. The water taken up by the roots during the dark period could not be transpired by the plants, and hence it was stored in their tissues. As a result, leaf water potentials of the stressed treatments recovered reasonably well during the dark period. In the simulations, all four reduction functions led to almost the same results when the parameters were primarily derived from the experimental data and slightly modified. Since all the reduction functions lead to about the same results, it is proposed that for practical use the most simple Eq. 5.1 be used in Eq. 2.27.

In Chapter 6, six different reduction functions for combined water and salinity stress are used in the macroscopic sink term of Eq. 2.27. The reduction functions are the additive Eq. 2.39, the multiplicative Eqs. 2.40, 2.41, 6.1 and 6.2, and the *newly developed Eq. 6.3 which combines the linear salinity reduction function of Maas and Hoffman (1977) and the linear soil water pressure head reduction function of Feddes et al. (1978)*. All these reduction functions are compared with the experimental data and have been incorporated in the numerical simulation model HYSWASOR.

The relation between the experimental relative transpiration and the joint soil water osmotic and pressure heads appears to be linear (with an exception for the salinity near the threshold value). This linearity is also observed for the corresponding relative leaf water head. As the mean soil solution salinity increases, the trend becomes more linear. *The presented experimental results support Eq. 6.3, particularly for the higher soil*

solution salinities. The simulations indicated that, for most treatments Eq. 6.3 provides the closest agreement with the experimental transpiration.

Soil water content, and particularly soil solution salinity simulated with Eq. 6.3 agree reasonably with the experimental data: in spite of the observed differences, the trend of the simulated data is good. The discrepancy between the simulated and experimental water contents is partly due to the way in which water uptake is calculated by the simulation model. The potential transpiration is distributed equally over the soil increments and the actual uptake due to the reduction function and root activity is calculated independently for each increment. The integration of these water uptakes over the root zone yields the total uptake. In reality, the plants take the required water from any depth if there are enough active roots. *This means that the root system is reasonably flexible to compensate for lack of water at other depths and satisfy the evaporative demand. Water uptake compensation seems to be an important phenomenon, which has to be taken into account in a proper way.* More investigations are needed to verify and quantify such a phenomenon.

The second reason for the disagreement between the simulated and experimental water contents can be attributed to the influence of roots and the soil concentration on the soil hydraulic conductivity. The input soil hydraulic parameters were obtained from soil samples without roots and salinity and assumed constant during the simulations.

In conclusion, all observations support the proposed Eq. 6.3. The soil water pressure head at which wilting occurs still needs more investigations.

Samenvatting

Watergebrek en verzouting zijn twee belangrijke beperkingen voor de agrarische productie in aride en semi-aride gebieden. Met het oog op de opbrengsten van landbouwgewassen is het belangrijk dat de invloed van de osmotische druk en de drukhoogte van het bodemwater kan worden gekwantificeerd. In het algemeen uiten deze invloeden zich in het vermogen van plantenwortels om water uit de grond op te nemen. Wateropname door plantenwortels is een dynamisch proces dat wordt beïnvloed door bodem, plant en klimatologische omstandigheden, zoals drukhoogte en osmotische druk van het bodemwater, bodemwaterdoorlatendheid, verdampingsvraag, bewortelingsdichtheid en - diepte, hydraulische weerstanden in de plant en andere planteigenschappen. Bij het kwantificeren van dit proces door het oplossen van de *Richards'* vergelijking ligt het grootste probleem in het ontbreken van een onttrekkingsfunctie die de wateropname door wortels adequaat beschrijft.

In de loop der tijd zijn zowel microscopische als macroscopische concepten voor de wateropname door plantenwortels ontwikkeld. Het microscopisch concept beschouwt de radiale stroming van water naar een representatieve wortel van oneindige lengte, uniforme dikte, en uniforme absorptieve eigenschappen. In microscopische modellen wordt de waterstromingsvergelijking gewoonlijk in cilindrische coördinaten geschreven en opgelost met geëigende randvoorwaarden aan het worteloppervlak en op enige afstand van de wortel. Aangezien het erg moeilijk, zo niet onmogelijk is om de vereiste invoerparameters te verkrijgen, is het niet praktisch gebleken om deze parameters direct te meten en daarmee de voorgestelde microscopische modellen te testen. Macroscopische modellen daarentegen beschouwen het wortelstelsel als één geheel, waarbij de benodigde parameters wel kunnen worden gemeten. Om deze reden worden deze modellen het meest gebruikt in numerieke simulatiestudies. Het macroscopisch concept blijft evenwel in essentie empirisch en veel onderzoek is nodig om natuurkundige beschrijvingen af te kunnen leiden.

Vanwege bovengenoemde redenen is in dit onderzoek voor de macroscopische benadering gekozen. Alle bestaande en in deze studie nieuw ontwikkelde wateropname-reductiefuncties zijn in het macroscopisch model gebruikt en getest tegen experimentele data. De experimentele gegevens worden gebruikt om parameterwaarden af te leiden die nodig zijn voor het simulatiemodel HYSWASOR. De experimenten betroffen wateropname door wortels van lucerne onder zoutstress, waterstress, en gecombineerde zout- en waterstress. Dezelfde volgorde is gehandhaafd in de presentatie en analyse van de experimentele resultaten en de simulaties. De lucerne werd gezaaid in intensief

bemeten bodemkolommen met speciaal ontworpen meetapparatuur, waarbij het gewas in een kas gedurende een jaar werd verzorgd en geoogst met intervallen van ongeveer 50 dagen.

Hoofdstuk 2 beschrijft de theorie van water- en zouttransport in de bodem, samen met de wortelopnamemodellen. Water transport in de onverzadigde zone wordt beschreven met de *Darcy* vergelijking (Verg. 2.1), gecombineerd met de bodemwaterretentie- en doorlatendheidskarakteristiek. Deze hydraulische bodemeigenschappen worden beschreven met de analytische functies van *Van Genuchten* en *Mualem*. Transport van opgeloste stoffen wordt beschreven met de convectie-dispersie vergelijking (Verg. 2.9). De wateropnamefuncties worden beoordeeld en ingedeeld volgens microscopische en macroscopische benaderingen. De beschikbare macroscopische reductiefuncties voor zoutstress, waterstress, en gecombineerde zout- en waterstress worden gepresenteerd. Dit theoretische raamwerk vormt de basis van HYSWASOR: een één-dimensionaal, eindige-elementen model voor hysteretisch transport van water en opgeloste stoffen in de wortelzone.

Hoofdstuk 3 beschrijft de experimenten en meetmethoden. De speciaal ontworpen apparatuur en de manier van pakken van de grondkolommen worden in detail beschreven, evenals de volgorde van de aan de planten opgelegde stress. De experimenten waren opgedeeld in drie fasen: zoutstress, waterstress, en zout- en waterstress gecombineerd. De analyse van de resultaten van deze experimenten en die van de simulaties worden voor iedere fase in aparte hoofdstukken besproken. De standaardmethode die is gebruikt voor het bepalen van de bodemwaterretentie- en doorlatendheidskarakteristiek wordt ook uitvoerig besproken. De theorie van de TijdsDomeinReflectometrie (TDR) voor indirecte metingen van het bodemwatergehalte en de elektrische geleidbaarheid worden in het kort besproken.

In Hoofdstuk 4 worden bestaande, alsmede nieuw ontwikkelde reductiefuncties voor zoutstress direct getest aan experimentele resultaten en ingevoerd in het numerieke simulatiemodel HYSWASOR, teneinde ze te verifiëren in een macroscopisch wateropname-model (Verg. 2.27). Alle resultaten van experimenten en simulaties geven aan dat de bekende, zogenoemde gewasopbrengstfunctie (Verg. 2.33) met de oorspronkelijk door de modelmakers voorgestelde helling en een aangepaste waarde voor de zoutdrempel, kan worden gebruikt als reductiefunctie in Verg. 2.27. Het meest gevoelige deel van deze reductiefunctie is de drempelwaarde, terwijl voor Verg. 2.35 zonder drempelwaarde de grootste gevoeligheid huist in de vormparameter. Omdat de meeste parameterwaarden die voorgesteld zijn door de modellenmakers geen goede

overeenstemming met de experimentele resultaten leveren, zijn de parameterwaarden afgeleid van het gemiddelde van de gemeten zoutconcentraties van het bodemwater. Als deze waarden in het simulatiemodel worden gebruikt, moeten ze nog enigszins worden aangepast om de beste overeenstemming met de experimentele resultaten te bereiken. Dit is nodig omdat het simulatiemodel de wateropname afzonderlijk berekent op ieder tijdstip op iedere diepte. De gesimuleerde feitelijke hoeveelheden transpiratie liggen dicht bij de experimentele waarden, terwijl de gesimuleerde bodemwatergehalten en zoutconcentraties van de bodemoplossing enige verschillen vertonen met de experimentele gegevens; de gemiddelden van deze variabelen liggen heel dicht bij de gemiddelde gemeten waarden. Dit betekent dat het simulatiemodel goede overeenstemming kan geven met gemeten resultaten wanneer het systeem in zijn geheel wordt beschouwd. Zowel de gesimuleerde als de experimentele resultaten geven aan dat verschillende zoutreductiefuncties vrijwel dezelfde resultaten kunnen leveren als de parameterwaarden goed zijn gespecificeerd. Deze waarneming suggereert het gebruik van de eenvoudige lineaire reductiefunctie (Verg. 2.33) in het simulatiemodel.

In Hoofdstuk 5 worden vier verschillende reductiefuncties voor de drukhoogte van het bodemwater gebruikt in het macroscopisch model van Verg. 2.27. De lineaire functie van Verg. 5.1 blijkt niet goed bij de experimentele gegevens te passen. De niet-lineaire functies van Verg. 2.38 en 5.2 beslaan niet de gehele rijkwijdte van de experimentele data, terwijl de nieuw ontwikkelde, twee-drempelige functie van Verg. 5.5 alle experimentele resultaten wel redelijk goed dekt. De heterogeniteit van de drukhoogte van het bodemwater over de wortelzone speelt geen belangrijke rol in de wateropname zolang er genoeg water beschikbaar is in een deel van de wortelzone. De planten kunnen vanuit dat deel in de verdampingsvraag voorzien en aldus het watertekort in de drogere gedeelten compenseren. Deze veronderstelling is gebaseerd op de waarneming dat op de eerste dag na de irrigaties zowel de actuele relatieve transpiratie als de relatieve bladwaterdrukhoogte bijna hetzelfde waren voor gestresste en niet-gestresste planten. Het verschil tussen de gesimuleerde en gemeten watergehalten lijkt voornamelijk veroorzaakt te worden door *wateropname door de wortels gedurende de nacht*. Het door de wortels in de donkere periode opgenomen water kon niet door de planten worden verdampt en dus werd het opgeslagen in hun weefsels. Als gevolg daarvan herstelden de bladwaterpotentialen van de gestresste planten zich redelijk in het donker.

In de simulaties geven de vier reductiefuncties vrijwel dezelfde resultaten als de parameterwaarden eerst worden afgeleid van de experimentele resultaten en daarna nog enigszins aangepast. Aangezien alle reductiefuncties ongeveer dezelfde resultaten opleveren, wordt voorgesteld dat voor praktische doeleinden de meest eenvoudige Verg.

5.1 wordt gebruikt.

In Hoofdstuk 6 worden zes verschillende reductiefuncties voor gecombineerde water- en zoutstress gebruikt in de macroscopische opnameterm van Verg. 2.27. De reductiefuncties zijn de additieve Verg. 2.39, de multiplicatieve Verg. 2.40, 2.41, 6.1, en 6.2, en de *nieuw ontwikkelde Verg. 6.3 die de lineaire zoutreductiefunctie van Maas en Hoffman (1977) combineert met de lineaire waterdrukhoogte-reductiefunctie van Feddes et al. (1978)*. Al deze reductiefuncties worden vergeleken met de experimentele data en zijn ingevoerd in het numerieke simulatiemodel HYSWASOR. De relatie tussen de experimentele relatieve transpiratie en de gecombineerde osmotische hoogte en drukhoogte van het bodemwater blijkt lineair te zijn (met een uitzondering voor het zoutgehalte nabij de drempelwaarde). Deze lineariteit wordt ook waargenomen voor de relatieve drukhoogte van het bladwater. Naarmate de gemiddelde zoutconcentratie van de bodemoplossing toeneemt wordt het verband meer lineair. *De gepresenteerde experimentele resultaten ondersteunen Verg. 6.3, in het bijzonder voor de hogere zoutconcentraties van de bodemoplossing. De simulaties geven aan dat Verg. 6.3 voor de meeste stress-behandelingen de beste overeenstemming geeft met de experimentele transpiratie.*

De bodemwatergehalten en in het bijzonder de zoutconcentraties van de bodemoplossing gesimuleerd met Verg. 6.3 komen redelijk overeen met de experimentele data: ondanks de waargenomen afwijkingen is de tendens van de gesimuleerde resultaten goed. De verschillen tussen de gesimuleerde en experimentele watergehalten zijn ten dele het gevolg van de manier waarop wateropname wordt berekend in het simulatiemodel. De potentiële verdamping wordt gelijkmatig verdeeld over de bodemsegmenten en de feitelijke opname als gevolg van de reductiefunctie en de wortelactiviteit wordt onafhankelijk berekend voor ieder segment. De integraal van de wateropnames over de diepte van de wortelzone levert de totale opname. In werkelijkheid neemt de plant het benodigde water op van welke diepte dan ook als daar tenminste voldoende actieve wortels aanwezig zijn. *Dit betekent dat het wortelstelsel redelijk flexibel is om het gebrek aan water op andere diepten te compenseren en aan de verdampingsvraag te voldoen. Wateropname-compensatie lijkt een belangrijk fenomeen te zijn dat op een goede manier in rekening moet worden gebracht.* Meer onderzoek is nodig om dit fenomeen kwantitatief te verifiëren.

De tweede reden voor de verschillen tussen de gesimuleerde en gemeten watergehalten kan worden toegeschreven aan de invloeden van de wortels en de zoutconcentratie op de bodemwaterdoorlatendheid. De ingevoerde waarden van de hydraulische bodemwaterparameters werden namelijk verkregen aan bodemmonsters zonder wortels en zouten en

werden verondersteld constant te zijn gedurende de simulaties.

Concluderend kunnen we stellen dat alle waarnemingen de voorgestelde Verg. 6.3 ondersteunen. De bodemwaterdrukhoogte waarop verwelking optreedt dient echter nog verder te worden onderzocht.

References

- Abrol, I. P., J. S. P. Yadav and F. I. Massoud. 1988. Salt affected soils and their management. FAO Soils Bull. No.39.
- Addiscott, T. M. and R. J. Wagenet. 1985. Concepts of solute leaching in soil: a review of modeling approach. *J. of Soil Sci.*, 36: 411-424.
- Allmaras, R. R., W. W. Nelson, and W. B. Voorhees. 1975. Soybean and corn rooting in southern Minnesota. II. Root distribution and related water flow. *Soil Sci. Soc. Am. J.* 39: 771-777.
- Arkerly, R. J. 1963. Relationships between plant growth and transpiration. *Hilgardia*, 34: 559-584.
- Baker, J. M. and R. R. Allmaras. 1990. System for automating and multiplexing soil moisture measurement by time-domain reflectometry. *Soil Sci. Soc. Am. J.* 54: 1-6.
- Bauder, J. W., J. S. Jacobsen and W. T. Lanier. 1992. Alfalfa emergence and survival response to irrigation water quality and soil series. *Soil Sci. Soc. Am. J.* 56: 890-896.
- Beese, F. and P. J. Wierenga. 1980. Solute transport through soil with adsorption and root water uptake computed with a transient and a constant-flux model. *Soil Sci.* 129(4): 245-252.
- Begg, J. E., and N. C. Turner. 1976. Crop water deficits. *Adv. Agron.* 28: 161-217.
- Belmans, C. J., J. G. Wesseling and R. A. Feddes. 1983. Simulation of the water balance of the cropped soil: SWATRE. *J. of Hyd.* 63: 271-286.
- Bernstein, L. and L. E. Francois. 1973. Leaching requirement studies: Sensitivity of alfalfa to salinity of irrigation waters. *Soil Sci. Soc. Am. Proc.* 37: 931-943.
- Blizzard, W. E. and J. S. Boyer. 1980. Comparative resistance of the soil and plant to water transport. *Plant Physiol.* 66: 809-814.
- Bloom, A. J., F. S. Chapin III, and H. A. Mooney. 1985. Resources limitations in plants: an economic analogy. *Annual review of Ecology and Systematics.* 16: 363-392.
- Bower, C. A., G. Ogata, and J. M. Tucker. 1969. Root zone salt profiles and alfalfa growth as influenced by irrigation water salinity and leaching fraction. *Ag. J.* 61: 783-785.
- Boyer, J. S. 1996. Advances in drought tolerance in plants. *Adv. in Agron.* 56: 187-218.
- Bresler, E., B. L. McNeal and D. L. Carter. 1982. Saline and Sodic soils. *Advanced series in agri. sci.* No.10. pp 236.
- Brown, J. W. and Hayward. 1956. Salt tolerance of alfalfa varieties. *Agron. J.* 48: 12-20.
- Brooks, R.H. and A.T. Corey. 1964. Hydraulic properties of porous media. *Hydrology Paper No. 3, Colorado State Univ., Fort Collins, Colorado.* 27 pp.
- Buckingham, E. 1907. Studies on the movement of soil moisture. *USDA Bur. of Soils. Bull.* 38.
- Caldwell, M. M. and R. A. Virginia. 1989. Root systems. In: R. W. Pearcy, J. R. Ehleringer, H. A. Mooney and P. W. Rundel (eds), *Plant physiological ecology, field methods and instrumentation.* 456pp.

- Cardon G. E. and J. Letty. 1992a. Plant water uptake terms evaluated for soil water and solute movement models. *Soil Sci. Soc. Am. J.* 32: 1876-1880.
- Cardon G. E. and J. Letty. 1992b. Soil-Based irrigation and salinity management model: I. Plant water uptake calculations. *Soil Sci. Soc. Am. J.* 56: 1881-1887.
- Cardon G. E. and J. Letty. 1992c. Soil-Based irrigation and salinity management model: II. Water and solute movement calculation. *Soil Sci. Soc. Am. J.* 56: 1889-1894.
- Chapin, F. S. III, A. J. Bloom, C. B. Field, and R. H. Waring. 1987. Plant response to multiple factors. *Bioscience* 37: 49-57.
- Childs, S. W., and R. J. Hanks. 1975. Model of soil salinity effects on crop growth. *Soil Sci. Soc. Am. J.* 39: 617-622.
- Coelho, E. F. and D. Or. 1996. A parametric model for two-dimensional water uptake by corn roots under drip irrigation. *Soil Sci. Soc. Am. J.* 60: 1039-1049.
- Cowan, I. R. 1965. Transport of water in the soil-plant-atmosphere system. *J. Appl. Ecol.* 22: 221-239.
- Cramer, G. R. 1994. Response of maize (*zea mays L.*) to salinity. In: M. Pessaraki (ed), *Handbook of plant and crop stress*. pp. 449-459. Marcel Dekker, Inc.
- Dalton, F. N., W. N. Herkelrath, D. S. Rawlins, and J. D. Rhoades. 1984. Time domain reflectometry: Simultaneous measurements of soil water content and electrical conductivity with a single probe. *Science (Washington, D.C.)*, 224: 989-990.
- Dalton, F. N., and M. Th. Van Genuchten. 1986. The time-domain reflectometry method for measuring soil water content and salinity. *Geoderma*. 38: 237-250.
- Danielson, R. E. 1967. Root systems in relation to irrigation. In: R. M. Hogan, H. R. Haise and T. W. Edminster (ed.), *Irrigation of agricultural lands*. Am. Soc. Agron. Vol. II, Madison, WI.
- Dasberg, S., and F. N. Dalton. 1985. Time domain reflectometry field measurements of soil water content and electrical conductivity. *Soil Sci. Soc. Am. J.* 49: 293-297.
- De Loor, G. P. 1990. The dielectric properties of wet soils. BCRS (Netherlands Remote Sensing Board) Report No. 90-13. TNO Physics and Electronic Lab., The Hague, The Netherlands. 39 pp.
- Denmead, O. T., and R. H. Shaw. 1962. Availability of soil water to plants as affected by soil moisture content and meteorological conditions. *Ag. J.* 54: 385-390.
- De Wit, C. T. 1958. Transpiration and crop yields. *Versl. Landbouwk. Onderz.*, 64.6. Pudoc, Wageningen. pp. 88.
- Dirksen, C. 1980. The relative speed of wetting and salinity fronts under high-frequency irrigation of alfalfa with saline water. *Int. Symp. Salt-affected soils*, Karnal, India, Feb. 1980. pp. 243-250.
- Dirksen, C. 1985. Relationship between root uptake weighted mean soil water salinity and total leaf water potentials of alfalfa. *Irrig. Sci.* 6:39-40.
- Dirksen, C. 1987. Water and salt transport in daily irrigated root zone. *Neth. J. Agrl. Sci.* 35:395-406.

- Dirksen, C. 1991. Unsaturated hydraulic conductivity. In: K. A. Smith and C. E. Mullins (eds), *Soil analysis, physical methods*. Marcel Dekker, Inc., New York, NY, pp 209-269.
- Dirksen, C. 1996. *Soil physics measurements*. Lecture note. Department of Water Resources. Wageningen Agricultural University. The Netherlands.
- Dirksen, C. and D. C. Augustijn. 1988. Root water uptake function for nonuniform pressure and osmotic potentials. *Agr. Abstracts*. pp. 188.
- Dirksen, C. and S. Dasberg. 1993. Improved calibration of time domain reflectometry, soil water content measurements. *Soil Sci. Soc. Am. J.* 57: 660-667.
- Dirksen, C., M. J. Huber, P. A. C. Raats, S. L. Rawlins, J. Van Schilfgaarde, J. Shalhevet and M. Th. Van Genuchten. 1994. Interaction of alfalfa with transient water and salt transport in the root zone. Research report. No. 135, US Salinity Lab., Riverside, CA., 127 pgs.
- Dirksen, C., J. B. Kool, P. Koorevaar and M. Th. Van Genuchten. 1993b. HYSWASOR - Simulation model of hysteretic water and solute transport in the root zone. In: D. Russo and G. Dagan (eds). *Water flow and solute transport in soils*. Springer Verlag. 99-122.
- Dirksen, C. and P. A. C. Raats. 1985. Water uptake and release by alfalfa roots. *Agronomy J.* 77: 621-626.
- Doorenbos, J. and A. H. Kassam. 1979. Yield response to water. *Irrigation and Drainage Paper 33*. FAO. Rome, 193 pp.
- Doorenbos, J. and W. O. Pruitt. 1977. Guidelines for predicting crop water requirements. *Irrigation and Drainage Paper 24*, 2nd ed., FAO, Rome, 156 pp.
- Faiz, S. M. A. and P. E. Weatherley. 1977a. The location of the resistance to water movement in the soil supplying the roots of transpiring plants. *New Phytol.* 78: 337-347.
- Faiz, S. M. A. and P. E. Weatherley. 1977b. Further investigations into the location and magnitude of hydraulic resistances in the soil: plant system. *New Phytol.* 81: 19-28.
- Feddes, R. A. 1971. Water, heat and crop growth. Ph.D thesis. Wageningen Agric. Univ. 184 pp.
- Feddes, R. A. 1981. Water use models for assessing root zone modification. In: G. F. Arkin and H. M. Taylor (eds), *Modifying the root environment to reduce crop stress*. pp. 347-390. ASAE monograph No. 4.
- Feddes, R. A. 1985. Crop water use and dry matter production: State of the art. In: A. Perrier and C. Riou (eds.). *Proc. Conference internationale de la CIID sur les besoins en eau des cultures*, Paris, 11-14 September 1984. 221-234.
- Feddes, R. A. 1987. Crop factors in relation to Makkink reference crop evapotranspiration. CHO-TNO. The Hague.
- Feddes, R. A. 1995. Remote sensing-inverse modeling approach to determine large scale effective soil hydraulic properties in soil-vegetation-atmosphere system. In: R. A. Feddes (ed), *Space and time scale variability and interdependencies in hydrological processes*. pp. 33-42. Cambridge University Press.

- Feddes, R. A., E. Bresler and S. P. Neuman. 1974. Field test of a modified numerical model for water uptake by root system. *Water Resour. Res.* 10(6):1199-1206.
- Feddes, R. A., P. Kabat, P. J. T. Van Bakel, J. J. B. Bronswijk and J. Halbertsma. 1988. Modeling soil water dynamics in the unsaturated zone: state of the art. *J. of Hydrology.* 100: 69-111.
- Feddes, R. A., R. W. R. Koopmans and J. Van Dam. 1996. *Agrohydrology. Lecture note.* Dept. of Water Resources. WAU.
- Feddes, R. A., P. Kowalik, K. Kolinska-Malinka and H. Zarandy. 1976. Simulation of field water uptake plants using a soil water dependent root extraction function. *J. of Hydrology.* 31:13-26.
- Feddes, R. A., P. Kowalik, and H. Zarandy. 1978. Simulation of field water use and crop yield. *Pudoc. Wageningen.* pp. 189.
- Feddes, R. A. and P. E. Rijtema. 1972. Water withdrawal by plant roots. *J. of Hydrol.* 17: 33-59.
- Fellner-Felldegg, H. 1969. The measurement of dielectrics in time domain. *J. Phys. Chem.* 73: 616.
- Feyen, J., C. Belmans, and D. Hillel. 1980. Comparison between measured and simulated plant water potential during soil water extraction by potted ryegrass. *Soil Sci.* 129: 180-185.
- Francois, L. E. 1981. Alfalfa management under saline condition with zero leaching. *Agronomy J.* 73: 1042-1046.
- Gardner, W. H. 1986. Water Content. In: A. Klute (ed). *Methods of soil analysis. Part I. Physical and mineralogical methods, 2nd edition.* ASA-SSSA, Madison, WI. 493-561.
- Gardner, W. R. 1960. Dynamic aspect of water availability to plants. *Soil Sci.* 89: 63-73.
- Gardner, W. R. 1964. Relation of root distribution to water uptake and availability. *Agro. J.* 56: 41-45.
- Gardner, W. R. and C. F. Ehlig. 1962. Some observations on the movement of water to plant roots. *Agrono. J.* 54: 453-456.
- Gardner, W. R., W. A. Jury., and J. Knight. 1975. Water uptake by vegetation. In: D. A. de Vries and N. H. Afgan (eds). *Heat and mass transfer in the biosphere. I. Transfer processes in plant environment.* pp. 443-456.
- Ghassemi, F., A. J. Jakeman and H. A. Nix. 1995. *Salinisation of land and water resources. Human Causes, Extent, Management and Case Studies.* pp. 526. Univ. New South Wales Press, Sydney, Australia.
- Gradmann, H. 1928. Untersuchungen uber die wasserverhaltnisse des bodens als grundlage des pflanzenwachstums. *Jahrb. Wiss. Bot.* 69(1): 1-100.
- Gupta, R. K., and I. P. Abrol. 1990. Salt-Affected Soils: Their Reclamation and Management for Crop Production. In: *Adv. in Soil Sci.* 11: 223-288.
- Guyen, O. F., F. J. Molz and J. G. Melville. Modeling migration of contaminants in the subsurface environment. In: J. Saxena (ed.), *Hazard Assessment of Chemicals,* pp. 203-282. Hemisphere Publ. Co., New York, NY.

- Halbertsma, J. M., and G. J. Veerman. 1994. A new calculation procedure and simple set-up for the evaporation method to determine soil hydraulic functions. SC-DLO report No. 88. Wageningen. The Netherlands. 25 pp.
- Halbertsma, J. M., and G. J. Veerman. 1997. Determination of the unsaturated conductivity and water retention characteristic using the Wind's evaporation method. In: J. Stole (ed), Manual for soil physical measurements. SC-DLO technical document 37: 47-55. Wageningen, The Netherlands.
- Halvorson, A. D. 1980. Alfalfa for hydrologic control of saline seeps. *Soil Sci. Soc. Am. J.* 44: 370-374.
- Hanks, R. J. 1974. Model for predicting plant growth as influenced by evapotranspiration and soil water. *Agron. J.* 66:660-665.
- Hanks, R. J. 1983. Yield and water use relationships: an overview. In: H. M. Taylor, W. R. Jordan and T. R. Sinclair (eds), *Limitations to efficient water use in crop production*. ASA: 393-411.
- Hanks, R. J. 1984. Predictions of crop yield and water consumption under saline conditions. In: I. Shainberg and J. Shalhevet (eds), *soil salinity under irrigation*. Springer -Verlag. pp. 272-283.
- Hanks, R. J., G. L. Ashcroft, V. P. Rasmussen and G. D. Wilson. 1978. Corn production as influenced by irrigation and salinity - Utah studies. *Irrig. Sci.* 1:47-59.
- Hanks, R. J., H. R. Gardner, and R. L. Florian. 1969. Plant growth-evapotranspiration relations for several crops in the central Great Plains. *Agron. J.* 61: 30-34.
- Hanks, R. J., T. E. Sullivan, and V. E. Hunsaker. 1977. Corn and alfalfa production as influenced by irrigation and salinity. *Soil Sci. Soc. Am. J.* 41: 606-610.
- Hansen, G. K. 1974a. Resistance to water transport in soil and young wheat plants. *Acta. Agric. Scand.* 24:37-48.
- Hansen, G. K. 1974b. Resistance to water flow in soil and plants, plant water status, stomatal resistance and transpiration of Italian ryegrass, as influenced by transpiration demand and soil water depletion. *Acta. Agric. Scand.* 24:83-92.
- Heimovaara, T. J. and W. Bouten. 1990. A computer-controlled 36-channel time-domain reflectometry system for monitoring soil water contents. *Water Resour. Res.* 26: 2311-2316.
- Herkelrath, W. N., E. E. Miller and W. R. Gardner. 1977a. Water uptake by plants: I. Divided root experiments. *Soil Sci. Soc. Am. J.* 41: 1033-1038.
- Herkelrath, W. N., E. E. Miller and W. R. Gardner. 1977b. Water uptake by plant. II: The root contact model. *Soil Sci. Soc. Am. J.* 41: 1039-1043.
- Hillel, D., H. Talpaz and H. Van Keulen. 1976. A macroscopic model of water uptake by a nonuniform root system and of water and salt movement in the soil profile. *Soil Sci.* 121(4): 242-255.
- Hillel, D., C. G. E. M. van Beek, and H. Talpaz. 1975. A microscopic-scale model of soil water uptake and salt movement to plant roots. *Soil Sci.* 120: 385-399.

- Hoffman, G. J. 1981. Alleviating salinity stress. In: G. F. Arkin and H. M. Taylor (eds), *Modifying the root environment to reduce crop stress*. pp. 305-343. ASAE monograph No. 4.
- Hoffman, G. J., and S. L. Rawlins. 1971. Growth and water potential of root crops as influenced by salinity and relative humidity. *Agron. J.* 68: 877-880.
- Hoffman, G. J., J. D. Rhoads, J. Letey, and F. Sheng. 1990. Salinity management. in: Hoffman, G. J., T. A. Howell, and K. H. Solomon (eds), *Management of farm irrigation system*. ASAE. pp. 667-715.
- Hoffman, G. J., and M. Th. Van Genuchten. 1983. Soil properties and efficient water use: Water management for salinity control. In: H. M. Taylor, W. R. Jordan and T. R. Sinclair (eds), *Limitation to efficient water use in crop production*. Am. Soc. Agron., Madison, WI, pp. 73-85.
- Homaee, M. 1991. Effect of saturated and unsaturated flows on leaching. M.Sc. Thesis (in Persian). 178 pp.
- Ingvanson, R. D., J. D. Rhoads, and A. L. Page. 1976. Correlation of alfalfa yield with various index of salinity. *Soil Sci.* 122: 145-153.
- Jarvis, N. J. 1989. A simple empirical model of root water uptake. *J. Hydrol.* 107: 57-72.
- Jarvis, P. G. 1975. Water transfer in plants. In: D. A. de Vries and N. H. Afgan (eds). *Heat and mass transfer in the biosphere. I. Transfer processes in plant environment*. pp. 369-394.
- Jensen, C. R. 1982. Effect of soil water osmotic potential on growth and water relationships of barely during soil water depletion. *Irrig. Sci.* 3:111-121.
- Jury, W. A. 1982. Simulation of solute transport using transfer function model. *Water Resour. Res.* 18(2): 363-368.
- Jury, W. A., W. R. Gardner and W. H. Gardner. 1991. *Soil Physics*. John Wiley. 328 pp.
- Jury, W. A. and K. Roth. 1990. *Transfer function and solute transport through soil: Theory and application*. Berkhauser, Basel. 226 pp.
- Jury, W. A. and G. Sposito. 1985. Field Calibration and Validation of Solute Transport Models for the Unsaturated Zone. *Soil Sci. Soc. Am. J.* 49:1331-1341.
- Jury, W. A., L. H. Stolzy, and P. Shouse. 1982. A Field Test of the Transfer Function Model for Predicting Solute Transport. *Water Resour. res.* 18(2):369-375.
- Kabat, P. and R. A. Feddes. 1995. Modeling soil water dynamics and crop water uptake at the field level. In: P. Kabat., B. Marshall., B. J. Van den Broek., J. Vos and H. Van Keulen (eds), *Modeling and parameterization of the soil-plant-atmosphere system*. pp. 103-133. Wageningen pers.
- Kabat, P., B. J. Van den Broek and R. A. Feddes. 1992. SWACROP: A water management and crop production simulation model. *ICID Bull.* 92, Vol. 41 no. 2. pp. 61-84.
- Katerji, N., J. W. Van Hoorn, A. Hamdy, M. Mastrorilli and F. Karam. 1998. Salinity and draught, a comparison of their effects on the relationship between yield and evapotranspiration. *Agri. Water Manage.* 36: 45-54.

- Kaur, R. 1994. Physics of salt affected soils. In: D. L. N. Rao., N. T. Singh., R. K. Gupta., and N. K. Tyagi (eds). Salinity management for sustainable agriculture. Central soil salinity research Inst., Karnal, India. pp. 1-17.
- Keck, T. J., R. J. Wagenet, W. F. Campbell and R. E. Knighton. 1984. Effect of water and salt stress on growth and acetylene reduction in Alfalfa. *Soil Sci. Soc. Am. J.* 48:1310-1316.
- Kemper, W. D. 1961. Movement of water as affected by free energy and pressure gradients. I. Application of classic equations for viscous and diffusive movements to the liquid phase in finely porous media. *Soil Sci. Soc. Amer. Proc.* 25: 260-265.
- Kemper, W. D., and N. A. Evans, 1963. Movements of water as affected by free energy and pressure gradients. III. Restriction of solute by membranes. *Soil Sci. Soc. Amer. Proc.* 27: 485-490.
- Kemper, W. D., and J. B. Rollins, 1966. Osmotic efficiency coefficients across compacted clays. *Soil Sci. Soc. Amer. Proc.* 30: 529-534.
- Kemper, W. D., and J. C. van Schaik, 1966. Diffusion of salts in clay-water system. *Soil Sci. Soc. Amer. Proc.* 30: 534-540.
- Klute, A. and C. Dirksen. 1986. Hydraulic conductivity and diffusivity: Laboratory methods. in: A. Klute (ed) *Methods of soil analysis, part 1. physical and mineralogical methods*, 2nd ed. Am. Soc. Agron., Madison WI. pp. 789-823.
- Kramer, P. J. and J. S. Boyer. 1995. *Water relations of plants and soils*. Academic Press. 495 pp.
- Larcher, W. 1995. *Physiological plant ecology, ecophysiology and stress physiology of functional groups*. 3rd ed. Springer. 506 pp.
- Lauchli, A., and E. Epstein. 1990. Plant response to saline and sodic conditions. In: K. K. Tanji (ed) *Agricultural salinity assessment and management*. ASCE mogh. 71. pp. 113-137.
- Lascano, R. J. and C. H. M. van Bavel. 1983. Root water uptake and soil water distribution: Test of an availability concept. *Soil Sci. Soc. Am. J.* 48: 233-237.
- Letey, J. 1985. Irrigation uniformity as related to optimum crop production- Additional research is need. *Irrig. Sci.* 6: 253-263.
- Letey, J. and K. C. Knapp. 1990. Crop-water production functions under saline conditions. In: K. K. Tanji (ed) *Agricultural salinity assessment and management*. ASCE mogh. 71. pp. 305-326.
- Letey, J. and K. C. Knapp. 1995. Simulating saline water management strategies with application to arid-region agroforestry. *J. Environ. Qual.* 24:934-940.
- Lipscomb, M. V. 1991. The response of four eicaceous shrubs to multiple environmental resource variation. Ph.D. Diss., Biology Dept., Virginia Polytechnic Inst. and State University, Blacksburg, VA.
- Lonkerd, W. E., C. F. Ehling, and T. J. Donovan. 1979. Salinity profiles and leaching fractions for slowly permeable irrigated field soils. *Soil Sci. Soc. Am. J.* 43: 287-289.
- Lunin, J., M. H. Gallatin, and A. R. Batchelder. 1963. Saline irrigation of several vegetable crops at various growth stages. I. Effect on yield. *Agron. J.* 55: 107-110.

- Maas, E. V. 1986. Salt tolerance of plants. *Appl. Agric. Res.* 1: 12-26.
- Maas, E. V. 1990. Crop salt tolerance. In: K. K. Tanji (ed) *Agricultural salinity assessment and management*. ASCE monograph 71. pp. 262-304.
- Maas, E. V. and G. J. Hoffman. 1977. Crop salt tolerance-current assessment. *J. Irrig. and Drainage Div., ASCE*, 103 (IR2): 115-134.
- Malek, E., G. E. Bingham, G. D. McCarty and R. J. Hanks. 1992. Determination of evapotranspiration from an alfalfa crop irrigated with saline wastewater from an electrical power plant. *Irrig. Sci.* 13:73-80.
- Meiri, A. 1984. Plant response to salinity: Experimental methodology and application to the field. In: I. Shainberg and J. Shalhevet (eds), *soil salinity under irrigation*. Springer-Verlag, pp. 284-297.
- Meiri, A., H. Frenkel, and A. Mantell. 1992. Cotton response to water and salinity under sprinkler and drip Irrigation. *Agron. J.* 84: 44-50.
- Meiri, A., and J. Shalhevet. 1973. Pepper plant response to irrigation water quality and timing of leaching. *Ecological studies*, Vol. IV. Springer. pp 421-429.
- Meyer, W. S., E. L. Greacen and A. M. Alston. 1978. Resistance to water flow in seminal roots of wheat. *J. Exp. Bot.* 29: 1451-1461.
- Maleicki, M. A., R. Plagge, M. Renger and R. T. Walczak. 1992. Application of time domain reflectometry (TDR) soil moisture miniprobe for determination of unsaturated soil water characteristics from undisturbed soil cores. *Irrig. Sci.* 13: 65-72.
- Molz, F. J. 1971. Interaction of water uptake and root distribution. *Agr. J.* 63: 608-610.
- Molz, F. J. 1975. Potential distributions in the soil root system. *Agron. J.* 67: 726-729.
- Molz, F. J. 1981. Models of water transport in the soil-plant system: A review. *Water Resour. Res.* 17(5): 1245-1260.
- Molz, F. J. and I. Remson. 1970. Extraction term models of soil moisture use by transpiring plants. *Water Resour. Res.* 6: 1346-1351.
- Mualem, Y. 1974. A conceptual model of hysteresis. *Water Resour. Res.* 10: 514-520.
- Mualem, Y. 1976. A new model for predicting the hydraulic conductivity of unsaturated porous media. *Water Resour. Res.* 12: 513-522.
- Newman, E. I. 1969. Resistance to water flow in soil and plant. I. Soil resistance in relation to amounts of roots. *J. Applied Ecol.* 16: 1-12.
- Nimah, M. N. and R. J. Hanks. 1973a. Model for estimating soil water, plant, and atmospheric interrelations: I. Description and sensitivity. *Soil Sci. Soc. Am. Proc.* 37: 522-527.
- Nimah, M. N. and R. J. Hanks. 1973b. Model for estimating soil water, plant, and atmospheric interrelations: II. Field tests of model. *Soil Sci. Soc. Am. J.* 37: 528-532.
- Nimmo, J. R. and E. E. Miller. 1986. The temperature dependence of isothermal moisture vs. potential characteristics of soil. *Soil Sci. Soc. Am. J.* 50: 1105-1113.
- Nnyamah, J. U., T. A. Black and C. S. Tan. 1978. Resistance to water uptake in Douglas-Fir forest. *Soil Sci.* 126: 63-79.
- Oliviera, I. B., A. H. Demond, and A. Salehzadeh. 1996. Packing of sands for the production of homogeneous porous media. *Soil Sci. Soc. Am. J.* 60: 49-53.

- Oster, J. D. 1994. Irrigation with poor quality water. A review. *Agricultural Water Management* (25): 271-297.
- Oster, J. D., I. Shainberg and I. P. Abrol. 1996. Reclamation of salt affected soil. in: M. Agassi (ed), *Soil erosion, conservation, and rehabilitation*. Marcel Dekker inc. pp. 315-351.
- Oster, J. D., and W. Schroer. 1979. Infiltration as influenced by irrigation water quality. *Soil Sci. Soc. Am. J.* 43: 444-447.
- Parra, M. A. and G. C. Romero. 1980. On the dependence of salt tolerance of beans (*Phaseolus vulgaris* L) on soil water matric potential. *Plant Soil* 56: 3-16.
- Penman, H. L. 1970. The water cycle. *Sci. Am.* 222: 99-108.
- Pessaraki, M. 1994. Response of green beans (*phaseolus vulgaris* L.) to salt stress. In: M. Pessaraki (ed), *Handbook of plant and crop stress*. pp. 415-430. Marcel Dekker, Inc.
- Philip, J. R. 1957. The physical principles of water movement during the irrigation cycle. *Proc. Int. Congr. Irrig. Drain.*, 8: 124-154.
- Philip, J. R. 1958a. Propagation of turgor and other properties through cell aggregations. *Plant Physiol.* 33: 271-274.
- Philip, J. R. 1958b. Osmosis and diffusion in tissue: Half times and internal gradients. *Plant Physiol.* 33: 275-278.
- Philip, J. R. 1966. Plant water relations: some physical aspects. *Ann. Rev. Plant Physiol.* 17: 245-268.
- Philip, J. R. 1986. Linearized unsteady multidimensional infiltration. *Water Resour. Res.* 12: 1717-1712.
- Porter, L. K., W. D. Kemper., R. D. Jackson, and B. A. Steward, 1960. Chloride diffusion in soils as influenced by moisture content. *Soil Sci. Soc. Am. Proc.* 24: 460-463.
- Prasad, R. 1988. A linear root water uptake model. *J. of Hydrology.* 99: 297-306.
- Prunty, L., B. R. Montgomery and M. D. Sweeney. 1991. Water quality effects on soils and alfalfa. I. Water use, yield, and nutrient concentration. *Soil Sci. Soc. Am. J.* 55(1): 196-202
- Quirk, J. P., and R. K. Schofield. 1955. The effect of electrolyte concentration on soil permeability. *J. of Soil Sci.* 6:163-178.
- Raats, P. A. C. 1974a. Movement of water and salts under high frequency irrigation. *Proc.*, 2nd Int. Drip Irrigation Congress, San Diego, CA., July, 1974. pp. 222-227.
- Raats, P. A. C. 1974b. Steady flows of water and salt in uniform soil profiles with plant roots. *Soil Sci. Soc. Am. Proc.* 38: 717-722.
- Raats, P. A. C. 1977. Convective Transport of Solutes by steady flows. I. General Theory. *Agr. Water Mang.* 1: 201-218.
- Raats, P. A. C. 1990. Characteristic lengths and times associated with processes in the root zone. In: D. Hillel and D. E. Elrick (eds), *Scaling in soil physics: Principles and applications*. SSSA Special publication No. 25. pp. 59-72.
- Rasiah, V., G. C. Carlson and R. A. Kohl. 1992. Assessment of functions and parameter estimation methods in root water uptake simulation. *Soil Sci. Soc. Am. J.* 56:1267-1271.

- Rhoads, J. D. 1990. Overview: Diagnosis of salinity problems and selection of control practices. In: K. K. Tanji (ed) *Agricultural salinity assessment and management*. ASCE monograph 71. pp. 18-41.
- Richards, L. A. 1928. The influence of capillary potential to soil-moisture and plant investigators. *J. Agr. Res.* 37: 719-742.
- Richards, L. A. 1931. Capillary conduction of liquids in porous mediums. *Physics*. 1:318-333.
- Richards, L. A. 1960. Advances in soil physics. *Trans. Intern. Congr. Soil Sci. Madison, 7th I*: 67-69.
- Rowse, H. R., D. A. Stone, and A. Gerwitz. 1978. Simulation of the water distribution in soil. II. The model for cropped soil and its comparison with experiment. *Plant Soil*. 49: 534-550.
- Sardin, M., D. Schweich, F. J. Leij and M. Th. van Genuchten. 1991. Modeling the nonequilibrium transport of linearly interacting solutes in porous media: A review. *Water Resour. Res.*, 27 (9): 2287-2307.
- Schmidhalter, U., H. M. Selim, and J. J. Oertli. 1994. Measuring and modeling root water uptake based on ³⁶-chloride discrimination in a silt loam soil affected by groundwater. *Soil Sci.* 158(2): 97-105.
- Sepaskhah, A. R. and L. Boersma. 1979. Shoot and growth of wheat seedlings exposed to several levels of matric potential and NaCl-induced osmotic potential of soil water. *Agron. J.* 71: 746-752.
- Shalhevet, J. 1984. Management of irrigation with brackish water. In: I. Shainberg and J. Shalhevet (eds), *soil salinity under irrigation*. pp. 298-318. Springer-Verlag.
- Shalhevet, J. 1993. Plants under salt and water stress. In: L. Fowden and T. Mansfield (eds), *Plant adaptation to environmental stress*. Chapman and Hall. pp. 133-154.
- Shalhevet, J. 1994. Using water of marginal quality for crop production. Review article. *Agricultural water management* (25): 233-269.
- Shalhevet, J. and L. Bernstein. 1968. Effect of vertically heterogeneous soil salinity on plant growth and water uptake. *Soil Sci.* 106(2): 85-93.
- Shalhevet, J. and Th. C. Hsiao. 1986. Salinity and drought. A comparison of their effects on osmotic adjustment, assimilation, transpiration and growth. *Irrig. Sci.* 7: 249-264.
- Shalhevet, J., P. Reiniger and D. Shimshi. 1969. Peanut response to uniform and nonuniform soil salinity. *Agron. J.* 61: 384-387.
- Shannon, M. C. 1997. Adaptation of plants to salinity. *Advances in agronomy*. 60: 75-120.
- Simmonds, L. P. and D. S. P. Kurupparachchi. 1995. Dynamics of plant water uptake. In: P. Kabat, B. Marshall, B. J. Van den Broek, J. Vos and H. Van Keulen (eds), *Modeling and parameterization of the soil-plant-atmosphere system*. pp. 77-101. Wageningen pers.
- Slatyer, R. O. 1957. Significance of permanent-wilting percentage in studies of plant and soil water relations. *Bot. Rev.* 23: 552-558.
- Smith, S. E. 1994. Salinity and production of alfalfa. in: M. Pessarakli (ed), *Handbook of Plant and crop stress*. pp. 431-448.

- So, H. B., L. A. G. Aylmore and J. P. Quirk. 1976. The resistance of intact maize roots to water flow. *Soil Sci. Soc. Am. J.* 40: 222-225.
- Stewart, J. I., R. H. Cuenca, W. O. Pruitt, R. M. Hagan, and J. Tosso. 1977. Determination and utilization of water production functions for principal California crops. W-67 Calif. Contrib. Proj. Rep. University of California. Davis.
- Stewart, J. I., R. M. Hagan and W. O. Pruitt. 1974. Functions to predict optimal irrigation programs. *J. Irrig. Drainage Div., ASCE.* 100(IR2): 179-199.
- Stewart, J. I., R. M. Hagan and W. O. Pruitt. 1976. Salinity effects on corn yield, evapotranspiration, leaching fraction, and irrigation efficiency. pp. 316-332, *Proc. Int. Salinity Conf., Lubbock, TX.*
- Sudicky, E. A., and P. S. Huyakorn. 1991. Contaminant migration in imperfectly known heterogeneous groundwater systems. *Rev. of Geophys., Supplement* 29: 238-251.
- Taylor, H. M. and B. Klepper. 1975. Water uptake by cotton root system: an examination of assumptions in the single root model. *Soil Sci.* 120: 57-67.
- Topp, G. C., J. L. Davis, and A. P. Annan. 1980. Electromagnetic determination of soil water content: Measurement in coaxial transmission lines. *Water Resour. Res.* 16: 574-582.
- Topp, G. C. and E. E. Miller. 1966. Hysteretic moisture characteristics and hydraulic conductivities for glass-based media. *Soil Sci. Soc. Am. Proc.* 30:156-162.
- Tseng, P. H., and W. A. Jury. 1994. Comparison of Transfer Function and Deterministic Modeling of Area-Averaged Solute Transport in Heterogeneous field. *Water Resour. Res.* 30(7): 2051-2063.
- Turner, N. C. 1986. Crop water deficits: A decade of progress. *Adv. Agron.* 39: 1-51.
- Turner, N. C. 1997. Further progress in crop water relations. *Adv. Agron.* 58: 293-338.
- U. S. Salinity Laboratory Staff., 1954. Diagnosis and improvement of saline and alkali soils. Handbook 60, U. S. Government printing office. Washington, DC.
- Van Bavel, C. H. M. and J. Ahmed. 1976. Dynamic simulation of water depletion in the root zone. *Eco. Modeling.* 2: 189-212.
- Van Dam, J. C., J. Huygen, J. G. Wesseling, R. A. Feddes, P. Kabat, P. E. V. Van Walsum, P. Groenendijk and C. A. Van Diepen. 1997. Theory of SWAP, version 2.0. Simulation of water flow, solute transport and plant growth in the soil-water-atmosphere-plant environment. Report No. 71. Dept. of Water Resour., Wageningen Agricultural Univ. 167 pp.
- Van den Honert, T. H. 1948. Water transport as a catenary process. *Faraday Soc. Discuss.* 3: 146-153.
- Van Genuchten, M. Th. 1980. A closed form equation for predicting the hydraulic conductivity of unsaturated soils. *Soil Sci. Soc. Am. J.* 44: 892 - 898.
- Van Genuchten, M. Th. 1987. A numerical model for water and solute movement in and below the root zone. Res. Report, U. S. Salinity Lab. Riverside, CA.
- Van Genuchten, M. Th. 1994. New issues and challenges in soil physics research. 15th world congress of soil science. Vol. 1. Inaugural and state of the art conferences, Acapulco, Mexico.

- Van Genuchten, M. Th. and G. J. Hoffman. 1984. Analysis of crop production. In: I. Shainberg and J. Shalhevet (eds), Soil salinity under irrigation. pp. 258-271. Springer-Verlag.
- Van Genuchten, M. Th., F. J. Leij and S. R. Yates, 1991. The *RETCE* code for quantifying the hydraulic functions of unsaturated soils. US Environmental Protection Agency. pp. 85.
- Veihmeyer, F. J. and A. H. Hendrickson. 1927. Soil-moisture conditions in relation to plant growth. *Plant Physiol.* 2: 71-78.
- Veihmeyer, F. J. and A. H. Hendrickson. 1931. The moisture equivalent as a measure of the field capacity of soils. *Soil Sci.* 32: 181-193.
- Veihmeyer, F. J. and A. H. Hendrickson. 1955. Does transpiration decrease as the soil moisture decrease? *Trans. Amer. Geophys. Union.* 36: 425-448.
- Wadleigh, C. H. and A. D. Ayers. 1945. Growth and biochemical composition of bean plants as conditioned by soil moisture tension and salt concentration. *Plant Physiol.* 20, 106-132.
- Wadleigh, C. H., H. G. Gauch, and O. C. Magistad. 1946. Growth and rubber accumulation in guayule as conditioned by soil salinity and irrigation regime. *Tech. Bull. U. S. Dept. Agric.* 925.
- Wadleigh, C. H., H. G. Gauch, and D. G. Strong. 1947. Root penetration and moisture extraction in saline soil by crop plants. *Soil Sci.* 63: 341-349.
- Warrick, A. W. 1974. Solution to the one-dimensional linear moisture flow equation with water extraction. *Soil Sci. Soc. Am. Proc.* 38: 573-576.
- Warrick, A. W., Amoozegar-fard, A. and D. O. Lomen. 1979. Linearized moisture flow from line sources with water extraction. *Trans. ASAE.* 22: 549-553.
- Whisler, F. D., A. Klute and R. J. Millington. 1968. Analysis of steady state evapotranspiration from a soil column. *Soil Sci. Soc. Am. Proc.* 32: 167- 174.
- Wierenga, P. J. 1995. Water and solute transport and storage. In: L. G. Wilson, L. G. Everett and S. J. Cullen (eds), *Handbook of vadose zone characterization and monitoring.* pp. 41-60. Lewis Publisher.
- Wind 1966. Capillary conductivity data estimated by a simple method. *Water in the unsaturated zone, symp. 1966. Proc. UNESCO/IASH,* 181-191. Wageningen, The Netherlands.
- Wosten, J. H. M., G. H. Veerman, and J. Stole. 1994. Water retention and hydraulic conductivity functions of top and subsoils in The Netherlands. The Staring series. Technical Document 18, Winand Staring Centre, Wageningen, The Netherlands, 66p.
- Wraith, J. M. and J. M. Baker. 1991. High-resolution measurement of root water uptake using automated time-domain reflectometry. *Soil Sci. Soc. Am. J.* 55: 928-932.
- Yang, S. J. and E. de Jong. 1971. Effect of soil water potential and bulk density on water uptake patterns and resistance to flow of water in wheat plants. *Can. J. Soil Sci.* 51: 211-220.
- Yanuka, M., G. C. Topp., S. J. Zegelin, and W. D. Zebchuk. 1988. Multiple reflection and attenuation of time domain reflectometry pulses: Theoretical considerations for applications to soil and water. *Water Resour. Res.*, 24: 939-944.

- Yeh, T. C. J. and A. Guzman-Guzman. 1995. Tensiometry. In: L. G. Wilson, L. G. Everett and S. J. Cullen (eds), Handbook of vadose zone characterization and monitoring. pp. 319-328. Lewis Publisher.
- Zegelin, S. J., I. White, and G. F. Russell. 1989. Improved field probes for soil water content and electrical conductivity measurements using time domain reflectometry. *Water Resour. Res.* 25: 2367-2376.

List of main symbols

Symbol	Representation	Dimension	Unit
a	slope in the equation of <i>Maas & Hoffman</i> (Eq. 2.33)	$L^3MT^{-3}I^{-2}$	m/dS
C	differential soil water capacity	L^{-1}	l/cm
c	velocity of light in vacuum (Eq. 3.1)	LT^{-1}	m/s
c	soil solution concentration	ML^{-3}	$\mu\text{mole}/\text{cm}^3$
D	soil water diffusivity; also solute dispersion coefficient	L^2T^{-1}	cm^2/h
E_0	evaporation rate from a free-water surface	LT^{-1}	mm/h
EC	electrical conductivity	$L^{-3}M^{-1}T^3I^2$	dS/m
EC^*	threshold electrical conductivity	$L^{-3}M^{-1}T^3I^2$	dS/m
EC_b	bulk electrical conductivity	$L^{-3}M^{-1}T^3I^2$	dS/m
EC_e	electrical conductivity of saturated extract	$L^{-3}M^{-1}T^3I^2$	dS/m
EC_{iw}	electrical conductivity of irrigation water	$L^{-3}M^{-1}T^3I^2$	dS/m
EC_{ss}	electrical conductivity of soil solution	$L^{-3}M^{-1}T^3I^2$	dS/m
ESP	exchangeable sodium percentage	-	-
ET_a	actual evapotranspiration rate	LT^{-1}	mm/h
ET_p	potential evapotranspiration rate	LT^{-1}	mm/h
h	soil water pressure head	L	cm
h^*	threshold soil water pressure head	L	cm
h_o	soil water osmotic head	L	cm
h_o^*	threshold osmotic head	L	cm
h_{50}	pressure head at which $\alpha(h)$ reduces to 0.50	L	cm
h_{o50}	osmotic head at which $\alpha(h_o)$ reduces to 0.50	L	cm
K	soil hydraulic conductivity	LT^{-1}	cm/h
K_s	saturated hydraulic conductivity	LT^{-1}	cm/h
L	root length per unit volume of soil	LL^{-3}	cm/cm^3
LF	leaching fraction	-	-
LWH	absolute value of leaf water head	L	cm
l	length	L	cm
m	empirical parameter in Eq. 2.6	-	-
n	empirical parameter in Eq. 2.6	-	-
p	empirical exponent in nonlinear reduction functions	LL^{-1}	cm/cm
q	soil water flux density	LT^{-1}	cm/h
S	volumetric root water uptake rate	$L^3L^{-3}T^{-1}$	$\text{cm}^3/\text{cm}^3 \text{ h}$
S_{\max}	maximum volumetric root water uptake rate	$L^3L^{-3}T^{-1}$	$\text{cm}^3/\text{cm}^3 \text{ h}$
SAR	sodium absorption ratio	ML^{-3}	$(\text{meq}/\text{l})^{0.5}$
S_e	degree of saturation	L^3L^{-3}	cm^3/cm^3
T_a	actual transpiration rate	LT^{-1}	mm/h
T_p	potential transpiration rate	LT^{-1}	mm/h
t	time	T	h

List of main symbols

t_s	travel time of TDR pulse in soil	T	s
v	velocity	LT^{-1}	m/s
Y	crop yield	$ML^{-2}T^{-1}$	$kg/m^2 d$
Y_m	maximum crop yield	$ML^{-2}T^{-1}$	$kg/m^2 d$
Z_r	depth of root zone	L	cm
z	gravitational head; also vertical coordinate	L	cm
α	empirical parameter in Eq. 2.6	L^{-1}	1/cm
$\alpha(h)$	pressure head reduction function	-	-
$\alpha(h_o)$	osmotic head reduction function	-	-
$\alpha(h, h_o)$	joint pressure and osmotic head reduction function	-	-
ε	Relative permittivity	-	-
θ	volumetric soil water content	L^3L^{-3}	cm^3/cm^3
θ_r	residual soil water content	L^3L^{-3}	cm^3/cm^3
θ_s	saturated soil water content	L^3L^{-3}	cm^3/cm^3
ρ_d	dry soil bulk density	ML^{-3}	g/cm^3

Curriculum Vitae

Mehdi Homaei was born on 16 November 1961 in Dezful, Iran. In 1988 he received his BSc degree in Soil Science from the Department of Soil Science, University of Tehran, Iran. In 1991 he obtained his MSc in Soil Physics from the Department of Soil Science, Tarbiat Modarres University, Tehran, Iran. After graduation he joined the Department of Soil Science at Tarbiat Modarres University as a lecturer and researcher. Supported by a scholarship awarded by the Ministry of Higher Education of Iran, he was working since March 1995 for his PhD degree at the Department of Water Resources, Wageningen Agricultural University, Wageningen, The Netherlands. He is married and has a daughter.